Evidence-Based Complementary and Alternative Medicine

The Use of Acupuncture for the Treatment of Gastrointestinal Diseases

Lead Guest Editor: Ying Li
Guest Editors: Jianhua Sun, Lizhou Liu, and Mi Liu

The Use of Acupuncture for the Treatment of Gastrointestinal Diseases

Evidence-Based Complementary and Alternative Medicine

The Use of Acupuncture for the Treatment of Gastrointestinal Diseases

Lead Guest Editor: Ying Li
Guest Editors: Jianhua Sun, Lizhou Liu, and Mi Liu

Contents

Hindawi
Evidence-Based Complementary and Alternative Medicine
Volume 2022, Article ID 5814048, 11 pages
https://doi.org/10.1155/2022/5814048

Review Article

Role of Bile Acids and Nuclear Receptors in Acupuncture in Improving Crohn's Disease

Jia-Cheng Shen,[1,2] Qin Qi,[2] Dong Han,[1,2] Shi-min Liu,[1] Rong Huang,[1,2] Yi Zhu,[2] Han-dan Zheng,[2] Kan Gu,[2,3] Huan-gan Wu,[2,3] and Hui-rong Liu[2,3]

[1]*Shanghai University of Traditional Chinese Medicine, Shanghai 201203, China*
[2]*Shanghai Research Institute of Acupuncture and Meridian, Shanghai 200030, China*
[3]*Yueyang Hospital of Integrated Traditional Chinese and Western Medicine, Shanghai University of Traditional Chinese Medicine, Shanghai 200437, China*

Correspondence should be addressed to Huan-gan Wu; wuhuangan@126.com and Hui-rong Liu; lhr_tcm@139.com

Received 15 September 2021; Revised 13 November 2021; Accepted 15 April 2022; Published 13 May 2022

Academic Editor: Md. Areeful Haque

Nuclear receptors (NRs) are ligand-dependent transcription factors that regulate the transcription of target genes. Bile acids (BAs) can be used as effector molecules to regulate physiological processes in the gut, and NRs are important receptors for bile acid signaling. Relevant studies have shown that NRs are closely related to the occurrence of Crohn's disease (CD). Although the mechanism of NRs in CD has not been clarified completely, growing evidence shows that NRs play an important role in regulating intestinal immunity, mucosal barrier, and intestinal flora. NRs can participate in the progress of CD by mediating inflammation, immunity, and autophagy. As the important parts of traditional Chinese medicine (TCM) therapy, acupuncture and moxibustion in the treatment of CD curative mechanism can get a lot of research support. At the same time, acupuncture and moxibustion can regulate the changes of related NRs. Therefore, to explore whether acupuncture can regulate BA circulation and NRs expression and then participate in the disease progression of CD, a new theoretical basis for acupuncture treatment of CD is provided.

1. Introduction

Crohn's disease (CD) is a clinically common inflammatory bowel disease (IBD) whose main clinical manifestations include gastrointestinal symptoms (recurrent abdominal pain, diarrhea, intestinal obstruction, perianal abscess, and anal fistula), fever, anemia, and malnutrition [1]. In recent years, epidemiology shows that the incidence of CD presents an increase in trend, and the highest incidence is mainly in developed countries and cities such as Europe and North America [2]. The acceleration of urbanization will lead to the occurrence of CD, the epidemiology of China shows that the incidence rate of CD is about 1.05 to 1.24/100000 people, and the incidence showed a gradient change from east to west [3]. At present, the exact cause of CD has not been fully revealed, which may be related to diet, environment, heredity, immunity, intestinal flora, and external bacterial and viral infection [1, 4]. Studies have shown that 12% of CD patients have family genetic history [5], and genomics studies have shown that 13.1% of patients are derived from genetic genes [6]. Therefore, genetics alone cannot explain the pathogenesis of CD, which highlights the importance of other nongenetic environmental factors [7]. A study shows that when low-risk countries and regions adopt Western lifestyle, the incidence rate of CD is rising sharply [8]. In addition, study has also shown that smoking increases the prevalence of CD by two times, indicating that smoking is an important inducement [9]. At the same time, the use of drugs such as aspirin and nonsteroidal anti-inflammatory drugs (NSAIDS), the decrease of dietary fiber intake, and the increase of saturated fat will increase the risk of CD [10, 11]. At present, drug is the main treatment method of modern medicine, including induction and maintenance therapy. The choice of drugs depends on the severity of the disease

and the response to the previous treatment; the most widely used drugs for CD include corticosteroids, immunosuppressants such as thiopurine and methotrexate, and biological agents such as anti-TNF drugs (infliximab, adalimumab, and certolizumab pegol) and antiadhesion molecule (vedolizumab) [12].

Although drug treatment has achieved satisfactory results, there are still some disadvantages. For example, long-term use will cause serious side effects such as infection, tumor, and drug tolerance, and some patients have poor curative effect and are difficult to accept [13]. Therefore, a safe and effective complementary replacement therapy is urgently needed. According to statistics, the use of traditional Chinese medicine (TCM) therapy, including acupuncture, moxibustion, and herbal medicine, is increasing in IBD [14]. In Europe and America, about 70% of IBD patients receive complementary and alternative drug treatment [15, 16]. Acupuncture and moxibustion have a long history of clinical use in China and have a unique curative effect in the treatment of IBD [17]. In recent years, the clinical efficacy and mechanism of acupuncture and moxibustion have been widely explored. Clinical studies have shown that acupuncture and moxibustion can significantly improve the symptoms of IBD patients, inhibit intestinal inflammation, and repair intestinal mucosal barrier [18, 19]. Animal experiments show that acupuncture has a positive effect on TNBS-induced CD model rats, such as improving the protein or gene expression of inflammatory factors (TNF-α and IL-1β) [20].

Nuclear receptors (NRs) play an important role in the development of CD; NRs can regulate a wide range of functions in the gut, such as nutrient absorption and transport, gut-liver communication, intestinal flora regulation, and so on [21–23], the signal transduction of NRs is closely related to the immune function of the intestine, and the imbalance of NR signal can cause intestinal immune disorder [24]. As an important signal regulator in the gut-liver circulation, NRs can regulate the absorption of bile acids (BAs) in the gut. BAs can not only promote the absorption of lipids and vitamins, but also regulate a variety of functions in the gut as a signal molecule. Intestine is equipped with a complex BA sensing mechanism to coordinate different intestinal functions and control the communication between the gut and other organs. The pioneering work of some researchers has solved the role of BAs as signaling molecules, which can activate specific receptors to regulate biological processes and trigger cell signaling pathways. BAs can activate NRs and plasma membrane-associated receptors of different cell types and cause physiological effects of BAs [25]. In view of the fact that the complex physiological functions of the intestine and BAs as signaling molecules induce a variety of signal networks, the effect of BAs on intestinal function deserves special attention. Therefore, this review is designed to explore the mechanism of NRs in CD in the gut-liver circulation of BAs and the regulatory effect of acupuncture.

2. BAs Gut-Liver Cycle, NR Family, and IBD

BAs is mainly synthesized in the liver and then reabsorbed via the gut; the reabsorbed BAs are recycled back to the liver that established the gut-liver cycle of BAs [26]. BAs synthesis mainly includes two ways of classic pathways and alternative pathways, wherein the classic pathway is the main pathway, *n* is the passage, and cholesterol is catalyzed by Cholesterol7α-Hydroxylase (CYP7A1) in hepatocytes into primary BAs [27]. In the alternative pathway, cholesterol is catalyzed by cholesterol 27α-hydroxylase to synthesize chenodeoxycholic acid (CDCA). Primary BAs and CDCA combine with glycine or taurine to form conjugated primary BAs [28].

The conjugated primary BAs follow the secretion of bile into the intestine through the bile duct and participate in the absorption of lipids and fat-soluble vitamins. Under the action of intestinal microorganisms, the conjugated primary BAs undergo a series of dehydration and dehydroxylation to form secondary Bas. About 95% of the BAs enter the intestinal mucosal cells through the apical sodium-dependent bile acid transporter (ASBT) in the intestine and combine with ileum bile acid-binding protein (IBABP) to pass through the organic solute transporter α/β enters the portal vein [18], and under the mediation of Na+/taurocholate cotransporting polypeptide (NTCP) and organic anion transporting polypeptides (OATP), it is taken up again by hepatocytes and reentered into the intestine through the bile duct through the action of the bile salt export pump to form a complete BAs gut-liver circulation [29], while the remaining 5% will be excreted with feces (Figure 1) [30, 31].

The gut-liver circulation of BAs plays an important role in maintaining the normal level of BAs and the steady state of intestinal function that can not only increase the utilization of bile acids, promote the absorption of lipids and fat-soluble vitamins, but also inhibit the catalytic effect of CYP7A1 [32]. A large number of studies in the past few decades have shown that BAs not only participate in the absorption of lipids and fat-soluble vitamins in the intestine, but also act as effect molecules to regulate the function of the intestine [25]. As the main place of BAs circulation, the relationship between BAs and intestine has been widely studied. Intestine has a complete and complex response mechanism for BAs that BAs activate specific receptors in the intestine to further initiate intestinal-related signals pathways, including glucose and lipid metabolism and energy balance [33]. Among them, the important receptors that receive BAs activation signals in the intestine are the NR family [34].

NRs are a type of ligand-dependent transcription factors that can be used to activate or inhibit the expression of target genes. So far, 48 NR family members have been found in the human body, which are important transcriptional regulators in the human body [35]. NRs can generally be divided into classic NRs and orphan receptors; about 50% of NRs belong to typical NRs [36]. Classical NRs mainly combine fat-soluble and membrane-permeable ligands and can be activated by endogenous BAs, hormones, or exogenous drugs or intestinal microbes [35, 36]. Classical NRs have similar structures, and

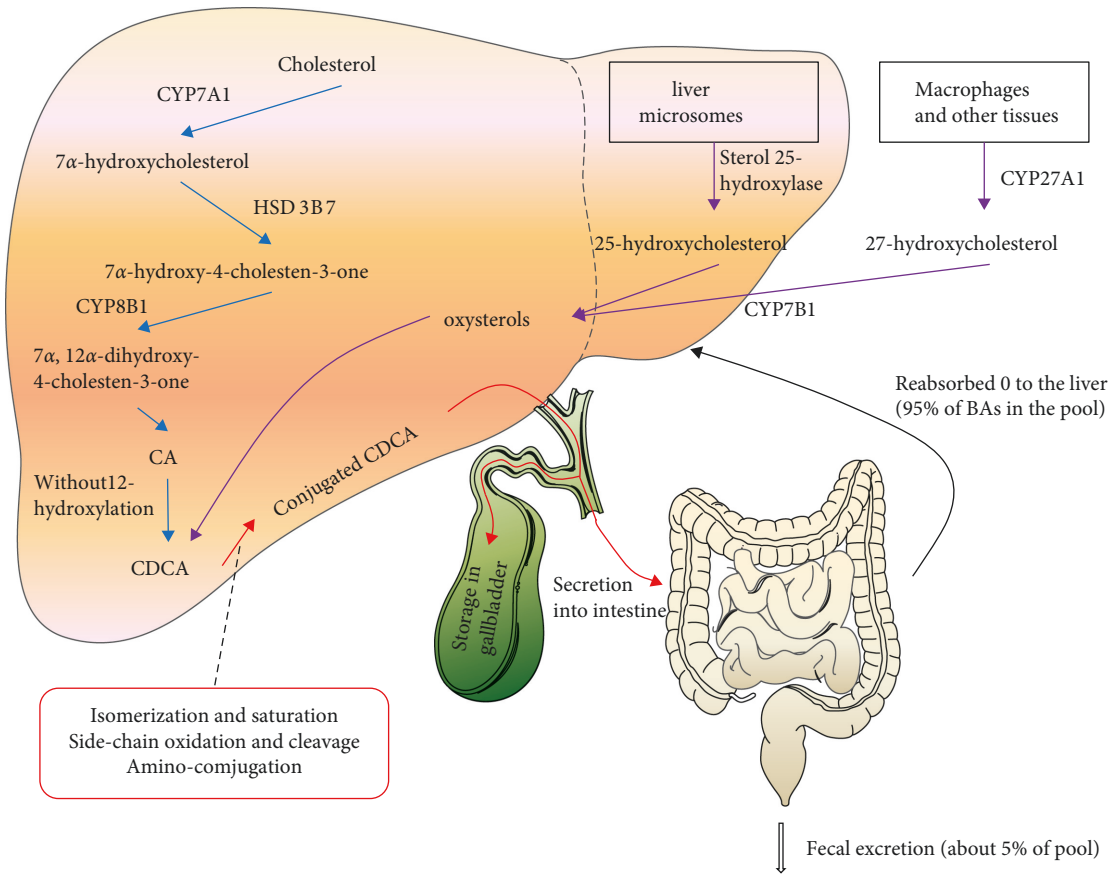

Figure 1: Schematic diagram of bile acid synthesis pathway and gut-liver circulation. The synthesis of BAs is mainly through classical and alternative pathways. The classical pathway is initiated by CYP7A1, and the alternative pathway is initiated by CYP27A1. CDCA is synthesized by cholesterol through a series of enzymatic reactions. CDCA forms conjugated CDCA by binding with glycine or taurine and are secreted into the intestine through bile duct. About 95% of BAs is transported into portal vein by intestinal epithelial cells and reabsorbed by hepatocytes and the remaining 5% will be excreted with feces. CYP7A1: cholesterol 7α-hydroxylase; HSD3B7: 3β-hydroxysteroid dehydrogenase; CYP8B1: sterol 12α-hydroxylase; CA: cholic acid; CDCA: chenodeoxycholic acid; CYP7B1: oxysterol 7α-hydroxylase; and CYP27A1: sterol 27-hydroxylase.

their typical structures mainly include A/B, C, D, E, and F [33], the N-terminal A/B region is composed of active ligand-independent activation domain 1 (AF-1), and the A/B region is highly variable and generally contains at least one AF-1, C region belongs to DNA-binding domain (DBD), which has two zinc finger structures and characterized by being highly conservative [37]. The E region is a ligand-binding domain (LBD), which mainly plays the role of ligand recognition; its sequence is also highly conservative. It contains a ligand-dependent transcriptional activation domain (AF-2). The E region is the largest domain in NRs, which plays an important role in the selective recognition of ligands. There is a short and nonconservative hinge region between regions C and E, namely, region D. The C-terminal also contains a section of F-zone, whose structure height is variable, and the specific structure and function are not fully understood at present (Figure 2(a)) [38, 39]. The structure of orphan receptor is similar to that of classical NRs, but its physiological ligand is not clear at first [40].

Western diet characterized by high sugar, high fat, and low fiber intake is currently considered to be related to the incidence of CD [41]. Enteral nutrition is one of the confirmed induction therapies [42]. BAs are synthesized by the liver and stored in the gallbladder. After eating, they are released into the intestine under the stimulation of food, participating in food digestion and regulating the related functions of the intestine [43]. Studies have shown that CD patients will have poor absorption of bile acids, 95% of which will be recovered by reabsorption, and poor absorption of bile acids will lead to diarrhea and other symptoms [44]. With the abnormal changes of apical sodium dependent bile acid transporter (ASBT), breast cancer-related protein (BCRP), and fibroblast growth factor 19 (FGF-19), the abnormal expression of these factors will lead to increased synthesis, reduced transport and metabolism of bile acids, and excessive accumulation of bile acids in the intestine [45]; the increase of bile acid concentration is related to the structural change and permeability of intestinal mucosal barrier and can cause diarrhea [46]. Relevant studies have also shown that in patients with IBD, abnormal changes will occur in total BAs and other forms of BAs (e.g., combined BAs and glycocombined BAs) [21].

NRs are widely distributed in human body and play an important role in normal physiological functions, such as

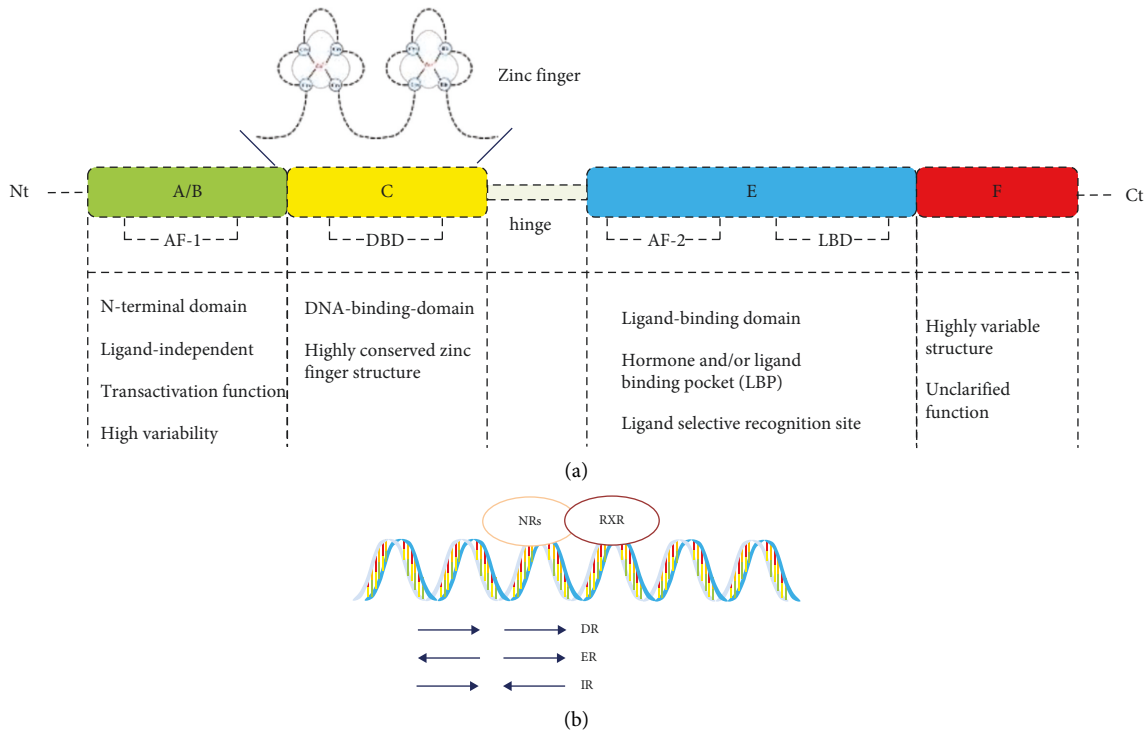

Figure 2: The general structure of nuclear receptors (a) and typical NR dimer (b). The main replication methods of NRs include direct repeat (DR), everted repeat (ER), and inverted repeat (IR). Nt: N-terminal; Ct: C-terminal; AF-1: activation domain 1; DBD: DNA-binding domain; AF-2: transcriptional activation domain; LBD: ligand-binding domain; and RXR: retinoid X receptor.

homeostasis, metabolism, growth, and development [47]. Current thinking suggests that NRs play a role mainly by interacting with other transcription factors and regulating the transcription of target genes [48]. With the development of research, it has been found that NRs, in addition to the above regulatory functions, play an important role in the progress of intestinal inflammation and intestinal mucosal barrier function in IBD [49–51]. At present, in vitro and in vivo models have proved that the expression of PXR and FXR in IBD is reduced, and the upregulation of PXR and FXR expression can improve intestinal inflammatory lesions [52]. Knockout of FXR or PXR promotes intestinal inflammation but does not induce spontaneous colitis [53]. Wilson et al.'s study showed that CD patients had abnormal composition of plasma bile acid spectrum, so PXR and FXR could not be activated normally [52]. Nijmeijer's group demonstrated that the target gene SHP expression of FXR decreased by 50% in CD patients, indicating the decreased activity of FXR [54]. Therefore, it is of great significance to consider the interaction between BAs and NRs in the treatment of CD.

The NRs involved in the progress of gastrointestinal inflammation and intestinal mucosal barrier function mainly include farnesoid X receptor (FXR) [55], pregnane X receptor (PXR) [56], vitamin D receptor (VDR) [57], constitutive androstane receptor (CAR) [58], peroxisome proliferator-activated receptor γ (PPARγ) [59], retinoic acid-related orphan receptor γ (RORγ) [60], and hepatocyte nuclear factor-4α (HNF-4α) [61]. BAs can activate the above NRs, participate in a variety of intestinal signaling pathways, and then regulate the intestinal function.

3. Regulating the Role of Members of NRs Family in CD Disease

Recent studies have shown that the NRs closely related to the progress of intestinal inflammation and intestinal mucosal barrier function of CD mainly include FXR, PXR, VDR, and CAR [62, 63]. FXR is also called bile acid receptor because it was confirmed to be the endogenous receptor of BAs at the beginning of its discovery [34]; it is expressed to varying degrees in tissues and organs such as liver, intestine, heart, blood vessel, kidney, and fat [64]. After FXR binds to the ligand, it can bind to the retinoid X receptor (RXR) to form an FXR/RXR dimer (Figure 2(b)), which can regulate the transcription of target genes [65]. The most important function of FXR is to adjust the balance of BAs [66, 67] and involved in the regulation of a wider range of physiological functions, such as metabolism, growth, and development of the human body [33]. With the development of genetic manipulation techniques, $FXR^{-/-}$ mice have been widely used to study the mechanism of FXR in recent years [68, 69]. In the IBD model induced by dextran sulfate sodium (DSS) or 2,4,6-trinitrobenzene sulfonic acid solution (TNBS), $FXR^{-/-}$ mice are more susceptible to TNBS and DSS [70, 71], and the mRNA expression of inflammatory factors in the colon showed higher level [53]. When FXR agonists such as INT-747 were used, the colitis induced by TNBS or DSS was

significantly inhibited, the inflammatory infiltration was reduced [55], the intestinal permeability was decreased, and the loss of intestinal goblet cells and mucin was restored [72]. Nijmeijer [73] showed that FXR could inhibit the overgrowth of intestinal flora, which protect intestine and maintain functional stability Inagaki [54] showed that the expression of FXR/RXR dimer in CD patients was lower than that in healthy people, which indicated that FXR activity was inhibited in CD patients. FXR regulates intestinal immune function through the expression of immune cells, especially innate immune cells [74]; in addition to the adjustment of the innate immune system, FXR can also protect the intestinal epithelial cell barrier. The research of Gadaleta et al. [49] shows that the activation of FXR in the intestine lowered the expression of associated proinflammatory factors such as IL-6, MCP-1, and IL-1β and retain integrity of intestinal epithelial barrier function. In vitro, FXR agonist INT-747 significantly downregulated expression of TNF-α, IL-17, and IFN-γ in peripheral blood monocytes, CD14+ monocytes, dendritic cells, and lamina propria monocytes of IBD patients; on the other hand, deoxycholic acid and GW4064 can inhibit the healing of intestinal epithelial damage by inducing the nuclear accumulation of FXR [75]. And FXR activator ursodeoxycholic acid (UDCA) promotes damage repair [76]. The above studies can show that in addition to regulating the balance of BAs in the intestinal-hepatic circulation, FXR can inhibit intestinal inflammation and repair the intestinal mucosal barrier during IBD disease.

PXR is highly expressed in the intestinal and liver in the human [77], mainly regulating gene transcription and expression of participating in drug transportation and metabolism [78]. Pregnenolone-16α-carbonitrile (PCN) is a specific PXR agonist in rodents, while rifaximin and rifampicin are PXR agonists in human [40]. Randomized controlled trials (RCT) have shown that rifaximin can effectively improve the 12-week clinical remission rate of CD patients, and its mechanism may be related to rifaximin's activation of PXR to regulate the intestinal symptoms of CD [79, 80]. At the same time, in vivo experiments showed that in PXR knockout mice, T cells were significantly overproliferated and had a higher level of CD25 expression than wild-type mice. The activation of PXR can inhibit T cell proliferation and CD25, IFN-γ expression. PCN activation of PXR can protect DSS-induced colitis that is due to the activation of phase II enzymes and efflux transporters (e.g., GSTa1, MDR1a and MRP2), which can reduce the proinflammatory cytokines IL-6, TNF-α, MCP-1, and IL-1α expression. However, in PXR$^{-/-}$ mice, the protective effect of PCN was abolished. Mechanism, PXR activation inhibits the activation of TNF-α on proinflammatory NF-κB [81]. Mencarelli et al. [82] used primary fetal colonic epithelial cells to find that rifampicin inhibits the expression of IL-6, TNF-α, and IL-8 and promotes the expression of TGF-β by inhibiting lipopolysaccharide- (LPS-) induced NF-κB DNA-binding activity. At the same time, PXR agonists can promote mucosal injury healing and intestinal barrier repair [50, 83, 84].

VDR is a regulatory receptor of 1,25-dihydroxyvitamin D (1,25[OH]2 vitamin D3), which mainly plays a role in regulating metabolism, immunity, and tumor development in the human body [85]. Vitamin D is an important sterol derivative; its deficiency is closely related to the onset of IBD [86]. Studies have shown that decreased expression of vitamin D in plasma will lead to an increase in the recurrence rate of IBD [87]. In IBD, vitamin D plays an important and complex protective role, which can participate in the regulation of the immune system through immune cells such as T cells [86], macrophages [88], and dendritic cells [89], and is considered to be a regulator of the immune system. Animal experiments show that vitamin D deficiency can aggravate the colitis symptoms of IL-10 gene knockout mice. Vitamin D supplementation can improve diarrhea caused by IBD and prevent weight loss [90]. Studies have shown that vitamin D enhances the integrity of the intestinal tract, which is characterized by high expression of tight junction protein and transepithelial resistance, while VDR gene knockout destroys the integrity of the intestinal tract [91]. Intestinal epithelial cells' (IEC) specific VDR knockout mice showed more severe colitis and higher expression of TNF-α, IL-1β, and MCP-1 than wild-type mice. Meanwhile, vitamin D3 inhibited the surface expression of MHC-II complex antigen and costimulatory molecules and downregulated the production of many proinflammatory cytokines [92]. The deficiency of vitamin D can induce the production of IL-22, which is closely related to the occurrence of colitis. In animal experiments, when vitamin D is deficient, mice will have more severe colitis [93]. It has been reported that in VDR knockout mice, the production of IL-22 in innate lymphocytes and antimicrobial peptides is significantly higher than that in wild-type mice, which may be an independent regulatory effect of VDR deficiency [94]. A 3-month RCT study showed that 1,25[OH] D levels were significantly increased in remission IBD patients, while intestinal permeability was maintained [95]. VDR also plays a protective role in colitis by regulating intestinal microbiota. Lack of VDR in intestinal epithelium can lead to autophagy defects and affect microbial aggregation [57]. Clinical studies showed that compared with the healthy control group, the microbial community of CD and UC patients changed significantly after taking vitamin D early [96, 97].

CAR is a kind of exogenous NRs regulated by exogenous, endogenous, and steroid hormones [98]. Its main metabolic function is to remove endogenous and exogenous substances [99]. Its expression in intestine and liver is closely related to intestinal flora [100, 101]. CAR was expressed in healthy intestinal epithelium but decreased in UC and CD patients or DSS mice [58, 102]. In the preclinical DSS mouse model, especially in CAR-deficient mice, wound healing of intestinal epithelial cells was reduced, while the activation of CAR with selective CAR agonist 3,3′,5,5′-tetrachloro-1,4-bis(pyridyloxy)benzene (TCPOBOP) enhanced mucosal healing [58]. In DSS-induced colitis model, CAR agonist decreased the mRNA expression of several proinflammatory cytokines in a CAR-dependent manner. In in vitro cell analysis, CAR inhibited apoptosis by inducing Gadd45b [103].

4. Mechanism of Acupuncture Treatment of CD and Regulation of BAs and NRs

Because the etiology and pathogenesis of IBD are not completely clear, and there is no specific therapy at present, the main clinical treatment methods mainly come from Western medicine, including the traditional sulfasalazine (SASP; 5-aminosalicylic acid (5-ASA)), steroids, immunosuppressants, or biological agents. However, the long-term use of steroids or immunosuppressants will cause serious adverse reactions, and the biological agents are not only expensive so that they lead to a heavy economic burden, but also show unsatisfactory long-term efficacy [104]. As an important part of TCM, acupuncture and moxibustion play an important role in the treatment of many diseases based on the theory of meridians [105]; in clinic, acupuncture is often used to treat CD [106]. According to the theory of TCM, the incidence of CD is closely related to the liver (*Gan*), spleen (*Pi*), and kidney (*Shen*) of viscera. When the external or internal causes affect the viscera, or the spleen and kidney have defects, it will cause the symptoms of CD in the intestine, including damp heat accumulation (*shi re nei yun*), qi fixation and blood stasis (*qi zhi xue yu*), liver stagnation by spleen (*gan yu cheng pi*), spleen deficiency and dampness fixation (*pi xu shi kun*), and spleen and kidney yang deficiency (*pi shen yang xu*). Acupuncture and moxibustion have the functions of dredging meridians, anti-inflammatory and analgesic, warming meridians, warming and dispersing cold evil, eliminating swelling and knot, promoting blood circulation, and removing blood stasis. Clinically, it is commonly used to treat CD acupoints, including Taixi (KI3), Tianshu (ST25), Zhongwan (CV12), Guanyuan (CV4), and Zusanli (ST36) [107]. At present, the recognized mechanism of acupuncture and moxibustion in the treatment of IBD is that the vagus nerve regulates the immune response, mainly including 3 pathways: (1) cholinergic anti-inflammatory pathway (CAP), the stimulation signal of acupuncture and moxibustion reaches the intestinal nerve through the vagus nerve and the intestinal neurons release acetylcholine at the synaptic connection with immune cells α-7-nicotinic acetylcholine receptor binding has been the release of proinflammatory factor (TNF-α); (2) splenic sympathetic anti-inflammatory pathway, the splenic nerve releases norepinephrine after receiving the signal of vagus nerve, which is related to the function of splenic lymphocytes β2 adrenergic receptor binding, and then through α-7-nicotinic Ach receptor inhibits the release of TNF-α from splenic macrophages; (3) the hypothalamus pituitary adrenal (HPA) axis receives vagal stimulation, which causes the adrenal gland to release cortisol [108].

In clinical trials, the expression of tight junction protein in intestinal epithelium was upregulated after receiving mesalazine or acupuncture treatment in CD patients [18]. In another RCT study, the efficacy of acupuncture and moxibustion was compared with that of sham acupuncture, and this experiment showed that the CD activity index score (CDAI) of the acupuncture group was improved; in addition, compared with the sham acupuncture group, the expression level of IL-17 in the acupuncture group was decreased, while the T regulatory cells were increased [19]. In a study using similar sham acupuncture treatment to observe mild-to-moderate CD patients, the levels of CDAI, C-reactive protein, and hemoglobin were significantly improved after acupuncture treatment, but no significant difference was found in endoscopy between the two groups [109]. A study that observed acupuncture alone also showed a significant decrease in CDAI scores compared with the sham acupuncture group [110]. A meta-analysis about the efficacy of acupuncture and moxibustion for IBD, including 43 RCT study, has shown that acupuncture and moxibustion have a significant effect on IBD. 10 studies compared acupuncture and moxibustion with SASP, showing that acupuncture and moxibustion are better than oral SASP in the treatment of IBD [104]. This shows that acupuncture and moxibustion have a significant effect on CD, which is related to the downregulation of intestinal inflammatory indexes.

At the same time, BAs and NRs are closely related to the changes of intestinal immune function. Therefore, it is worth studying whether acupuncture and moxibustion can produce therapeutic effect on CD by regulating the expression of BAs and NRs. At present, the research on the regulation mechanism of acupuncture and moxibustion on BAs and NRs is very limited. Current research shows that acupuncture and moxibustion play a positive role in the regulation of bile acid metabolism. In studying the effect of herb-partitioned moxibustion on metabolites in IBS rats, Lin et al. [111] found that there is an obvious imbalance of bile acid metabolism pathway in IBS rats, mainly manifested in the reduction of bile acid transformation and reabsorption, which can be improved after herb-partitioned moxibustion treatment. Lee et al.'s [112] results also show that manual acupuncture can reduce the deposition of bile acids, which may be related to reducing the activation of spinal microglia. In the study of the regulation of herbs-partition moxibustion on the nuclear receptor LXRα in the reversal of cholesterol transport in atherosclerosis (AS), Wang et al. found that herbs-partition moxibustion can reduce total cholesterol and low-density lipoprotein in serum and liver of AS animal model and promote the synthesis of high-density lipoprotein. At the same time, herbs-partition moxibustion can activate the expression of LXRα protein and mRNA and promote the reverse transport of cholesterol. Cui et al. [113] also obtained similar results in the study of moxibustion in the treatment of ApoE$^{-/-}$ mouse AS model. Moxibustion can regulate lipid metabolism and upregulate the expression of LXRα and ABCA1 to prevent lipid accumulation. The results published by Liu et al. [114] and Li et al. [115] showed that electroacupuncture preconditioning has a protective effect on rats with myocardial ischemia-reperfusion injury, and its mechanism is related to the regulation of FXR/SHP pathway. It is confirmed from the above limited research has confirmed that acupuncture and moxibustion can regulate the liver-intestinal circulation of cholesterol and participate in related pathways mediated by NRs.

Combined with the study of the therapeutic mechanism of acupuncture and moxibustion, and the related role of

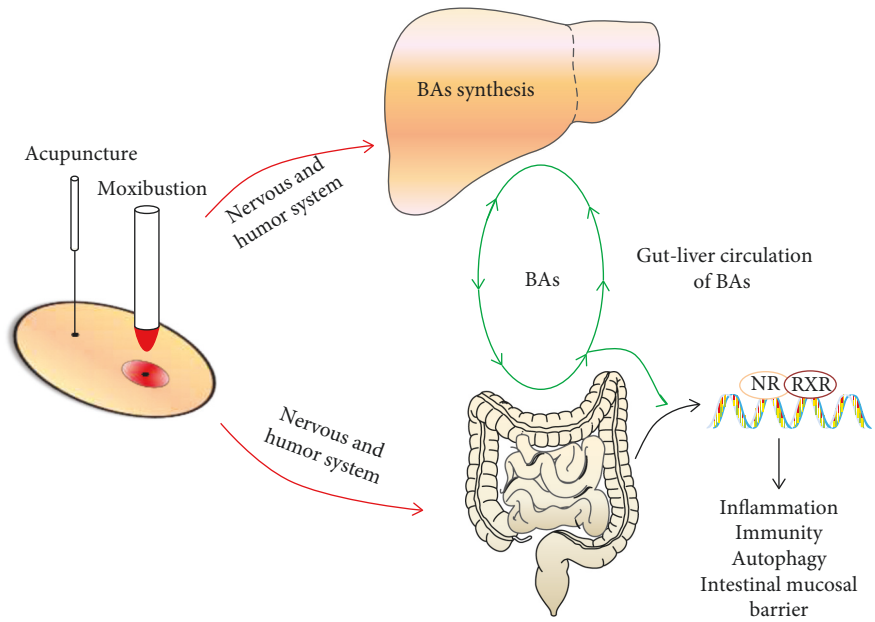

Figure 3: Effects of acupuncture and moxibustion on gut-liver circulation of BAs and the mechanism of regulating NRs.

BAs-NRs in gut-liver circulation, we speculate that in the treatment of CD, acupuncture and moxibustion cause the increase of BAs synthesis in the liver by stimulating local acupoints and through the signal input of nervous and humor system. After BAs are released into the intestine, the NRs were activated and then play a role in intestinal immune regulation and intestinal mucosal barrier repair (Figure 3). The gut-liver circulation of BAs can maintain the balance of BAs and play an important role in promoting the BAs-NRs signal pathway. However, at present, in the treatment of CD, the mechanism on acupuncture and moxibustion of BAs-NRs is very limited, and more basic and clinical research support is needed.

5. Conclusion

CD is currently a refractory gastrointestinal disease in clinical practice, which belongs to one of IBD. Existing research evidence shows that BAs and NRs families play an important role in the progression of CD, which can inhibit the inflammatory progress of CD colon and promote the repair of intestinal mucosal barrier. The NRs involved in the progression of CD disease mainly include FXR, PXR, VDR, CAR, PPARγ, and RORγ. A large number of clinical and animal experiments have shown that NRs can participate in the pathogenesis of CD by regulating related signal pathways such as inflammation, immunity, autophagy, and intestinal mucosal barrier. Acupuncture is an important part of TCM. Both clinical practice and in vivo experiments show that acupuncture has obvious curative effects in the treatment of CD; at the same time, acupuncture can adjust the changes of related NRs. Therefore, exploring whether acupuncture and moxibustion can participate in the disease progression of CD by regulating BA circulation and the expression of NRs can provide a new theoretical basis for acupuncture and moxibustion in the treatment of CD.

Data Availability

The data used to support the findings of this study are available from the corresponding author upon request.

Disclosure

Qin Qi is the co-first author.

Conflicts of Interest

All authors have no conflicts of interest with respect to the publication of this paper.

Acknowledgments

This work was supported by the National Natural Sciences Foundation of China (nos. 81873374 and 82004476), the Science and Technology Commission of Shanghai (no. 21ZR146000), Clinical Research Plan of SHDC (no. SHDC2020CR4042), Shanghai Municipal Health Commission (20184Y0182), and Shanghai Sailing Program (20YF1445400).

References

[1] J. Torres, S. Mehandru, J. F. Colombel, and L. Peyrin-Biroulet, "Crohn's disease," *The Lancet*, vol. 389, no. 10080, pp. 1741–1755, 2017.

[2] N. A. Molodecky, I. S. Soon, D. M. Rabi et al., "Increasing incidence and prevalence of the inflammatory bowel diseases with time, based on systematic review," *Gastroenterology*, vol. 142, no. 1, pp. 46–54, 2012.

[3] Q. Yu, L. Xu, L. Li et al., "Internet and WeChat used by patients with crohn's disease in China: a multi-center questionnaire survey," *BMC Gastroenterology*, vol. 19, no. 1, p. 97, 2019.

[4] J. Mazal, "Crohn disease: pathophysiology, diagnosis, and treatment," *Radiologic Technology*, vol. 85, no. 3, pp. 297–316, 2014.

[5] F. T. Moller, V. Andersen, J. Wohlfahrt, and T. Jess, "Familial risk of inflammatory bowel disease: a population-based cohort study 1977–2011," *American Journal of Gastroenterology*, vol. 110, no. 4, pp. 564–571, 2015.

[6] C. Huang, T. Haritunians, D. T. Okou et al., "Characterization of genetic loci that affect susceptibility to inflammatory bowel diseases in African Americans," *Gastroenterology*, vol. 149, no. 6, pp. 1575–1586, 2015.

[7] J. Torres and J. F. Colombel, "Genetics and phenotypes in inflammatory bowel disease," *The Lancet*, vol. 387, no. 10014, pp. 98–100, 2016.

[8] A. N. Ananthakrishnan, "Epidemiology and risk factors for IBD," *Nature Reviews Gastroenterology and Hepatology*, vol. 12, no. 4, pp. 205–217, 2015.

[9] S. S. Mahid, K. S. Minor, R. E. Soto, C. A. Hornung, and S. Galandiuk, "Smoking and inflammatory bowel disease: a meta-analysis," *Mayo Clinic Proceedings*, vol. 81, no. 11, pp. 1462–1471, 2006.

[10] A. N. Ananthakrishnan, L. M. Higuchi, E. S. Huang et al., "Aspirin, nonsteroidal anti-inflammatory drug use, and risk for crohn disease and ulcerative colitis: a cohort study," *Annals of Internal Medicine*, vol. 156, no. 5, pp. 350–359, 2012.

[11] A. N. Ananthakrishnan, H. Khalili, G. G. Konijeti et al., "Long-term intake of dietary fat and risk of ulcerative colitis and crohn's disease," *Gut*, vol. 63, no. 5, pp. 776–784, 2014.

[12] K. Cushing and P. D. R. Higgins, "Management of crohn disease: a review," *JAMA*, vol. 325, no. 1, pp. 69–80, 2021.

[13] S. Bonovas, G. Fiorino, M. Allocca et al., "Biologic therapies and risk of infection and malignancy in patients with inflammatory bowel disease: a systematic review and network meta-analysis," *Clinical Gastroenterology and Hepatology*, vol. 14, no. 10, pp. 1385–1397, 2016.

[14] P. Esters and A. Dignass, "Complementary therapies in inflammatory bowel diseases," *Current Drug Targets*, vol. 15, no. 11, pp. 1079–1088, 2014.

[15] L. N. Jackson, Y. Zhou, S. Qiu, Q. Wang, and B. Mark Evers, "Alternative medicine products as a novel treatment strategy for inflammatory bowel disease," *American Journal of Chinese Medicine*, vol. 36, no. 05, pp. 953–965, 2008.

[16] S. Danese, "New therapies for inflammatory bowel disease: from the bench to the bedside," *Gut*, vol. 61, no. 6, pp. 918–932, 2012.

[17] D. J. Stein, "Massage acupuncture, moxibustion, and other forms of complementary and alternative medicine in inflammatory bowel disease," *Gastroenterology Clinics of North America*, vol. 46, no. 4, pp. 875–880, 2017.

[18] H. X. Shang, A. Q. Wang, C. H. Bao et al., "Moxibustion combined with acupuncture increases tight junction protein expression in crohn's disease patients," *World Journal of Gastroenterology*, vol. 21, no. 16, pp. 4986–4996, 2015.

[19] C. Zhao, C. Bao, J. Li et al., "Moxibustion and acupuncture ameliorate crohn's disease by regulating the balance between Th17 and treg cells in the intestinal mucosa," *Evidence-Based Complementary and Alternative Medicine*, vol. 2015, Article ID 938054, 11 pages, 2015.

[20] H. Jin, J. Guo, J. Liu et al., "Anti-inflammatory effects and mechanisms of vagal nerve stimulation combined with electroacupuncture in a rodent model of TNBS-induced colitis," *American Journal of Physiology—Gastrointestinal and Liver Physiology*, vol. 313, no. 3, pp. G192–G202, 2017.

[21] E. Tiratterra, P. Franco, E. Porru, K. H. Katsanos, D. K. Christodoulou, and G. Roda, "Role of bile acids in inflammatory bowel disease," *Annals of Gastroenterology*, vol. 31, no. 3, pp. 266–272, 2018.

[22] J. L. Staudinger, S. Woody, M. Sun, and W. Cui, "Nuclear-receptor-mediated regulation of drug- and bile-acid-transporter proteins in gut and liver," *Drug Metabolism Reviews*, vol. 45, no. 1, pp. 48–59, 2013.

[23] S. Fiorucci and E. Distrutti, "Bile acid-activated receptors, intestinal microbiota, and the treatment of metabolic disorders," *Trends in Molecular Medicine*, vol. 21, no. 11, pp. 702–714, 2015.

[24] H. S. Jin, T. S. Kim, and E. K. Jo, "Emerging roles of orphan nuclear receptors in regulation of innate immunity," *Archives of Pharmacal Research*, vol. 39, no. 11, pp. 1491–1502, 2016.

[25] A. L. Ticho, P. Malhotra, P. K. Dudeja, R. K. Gill, and W. A. Alrefai, "Bile acid receptors and gastrointestinal functions," *Liver Research*, vol. 3, no. 1, pp. 31–39, 2019.

[26] N. Keating and S. J. Keely, "Bile acids in regulation of intestinal physiology," *Current Gastroenterology Reports*, vol. 11, no. 5, pp. 375–382, 2009.

[27] H. Jones, G. Alpini, and H. Francis, "Bile acid signaling and biliary functions," *Acta Pharmaceutica Sinica B*, vol. 5, no. 2, pp. 123–128, 2015.

[28] M. Cantore, R. Reinehr, A. Sommerfeld, M. Becker, and D. Häussinger, "The Src family kinase Fyn mediates hyperosmolarity-induced Mrp2 and Bsep retrieval from canalicular membrane," *Journal of Biological Chemistry*, vol. 286, no. 52, pp. 45014–45029, 2011.

[29] P. A. Dawson and S. J. Karpen, "Intestinal transport and metabolism of bile acids," *Journal of Lipid Research*, vol. 56, no. 6, pp. 1085–1099, 2015.

[30] L. Vítek and M. Haluzík, "The role of bile acids in metabolic regulation," *Journal of Endocrinology*, vol. 228, no. 3, pp. R85–R96, 2016.

[31] G. Charach, O. Argov, K. Geiger, L. Charach, O. Rogowski, and I. Grosskopf, "Diminished bile acids excretion is a risk factor for coronary artery disease: 20-year follow up and long-term outcome," *Therapeutic Advances in Gastroenterology*, vol. 11, no. 11, Article ID 1756283X17743420, 2018.

[32] R. M. Gadaleta, S. W. van Mil, B. Oldenburg, P. D. Siersema, L. W. Klomp, and K. J. van Erpecum, "Bile acids and their nuclear receptor FXR: relevance for hepatobiliary and gastrointestinal disease," *Biochimica et Biophysica Acta (BBA)—Molecular and Cell Biology of Lipids*, vol. 1801, no. 7, pp. 683–692, 2010.

[33] L. Ding, L. Yang, Z. Wang, and W. Huang, "Bile acid nuclear receptor FXR and digestive system diseases," *Acta Pharmaceutica Sinica B*, vol. 5, no. 2, pp. 135–144, 2015.

[34] M. Makishima, A. Y. Okamoto, J. J. Repa et al., "Identification of a nuclear receptor for bile acids," *Science*, vol. 284, no. 5418, pp. 1362–1365, 1999.

[35] R. M. Evans and D. J. Mangelsdorf, "Nuclear receptors, RXR, and the big bang," *Cell*, vol. 157, no. 1, pp. 255–266, 2014.

[36] D. J. Mangelsdorf, C. Thummel, M. Beato et al., "The nuclear receptor superfamily: the second decade," *Cell*, vol. 83, no. 6, pp. 835–839, 1995.

[37] A. F. Valledor and M. Ricote, "Nuclear receptor signaling in macrophages," *Biochemical Pharmacology*, vol. 67, no. 2, pp. 201–212, 2004.

[38] E. R. Weikum, X. Liu, and E. A. Ortlund, "The nuclear receptor superfamily: a structural perspective," *Protein Science*, vol. 27, no. 11, pp. 1876–1892, 2018.

[39] G. A. A. Nibourg, M. T. Huisman, T. V. van der Hoeven, T. M. van Gulik, R. A. F. M. Chamuleau, and R. Hoekstra, "Stable overexpression of pregnane X receptor in HepG2 cells increases its potential for bioartificial liver application," *Liver Transplantation*, vol. 16, no. 9, pp. 1075–1085, 2010.

[40] L. Ning, X. Lou, F. Zhang, and G. Xu, "Nuclear receptors in the pathogenesis and management of inflammatory bowel disease," *Mediators of Inflammation*, vol. 2019, Article ID 2624941, 13 pages, 2019.

[41] F. Rizzello, E. Spisni, E. Giovanardi et al., "Implications of the westernized diet in the onset and progression of IBD," *Nutrients*, vol. 11, no. 5, p. 1033, 2019.

[42] F. Ueno, T. Matsui, T. Matsumoto, K. Matsuoka, M. Watanabe, and T. Hibi, "Evidence-based clinical practice guidelines for crohn's disease, integrated with formal consensus of experts in Japan," *Journal of Gastroenterology*, vol. 48, no. 1, pp. 31–72, 2013.

[43] M. Färkkilä and T. A. Miettinen, "Lipid metabolism in bile acid malabsorption," *Annals of Medicine*, vol. 22, no. 1, pp. 5–13, 1990.

[44] O. Martinez-Augustin and F. S. D. Medina, "Intestinal bile acid physiology and pathophysiology," *World Journal of Gastroenterology*, vol. 14, no. 37, pp. 5630–5640, 2008.

[45] J. Jahnel, P. Fickert, A. C. Hauer, C. Högenauer, A. Avian, and M. Trauner, "Inflammatory bowel disease alters intestinal bile acid transporter expression," *Drug Metabolism and Disposition*, vol. 42, no. 9, pp. 1423–1431, 2014.

[46] K. Uchiyama, H. Kishi, W. Komatsu, M. Nagao, S. Ohhira, and G. Kobashi, "Lipid and bile acid dysmetabolism in crohn's disease," *Journal of Immunology Research*, vol. 2018, Article ID 7270486, 6 pages, 2018.

[47] C. M. Leopold Wager, E. Arnett, and L. S. Schlesinger, "Macrophage nuclear receptors: emerging key players in infectious diseases," *PLoS Pathogens*, vol. 15, no. 3, Article ID e1007585, 2019.

[48] M. A. Lazar, "Maturing of the nuclear receptor family," *Journal of Clinical Investigation*, vol. 127, no. 4, pp. 1123–1125, 2017.

[49] R. M. Gadaleta, K. J. van Erpecum, B. Oldenburg et al., "Farnesoid X receptor activation inhibits inflammation and preserves the intestinal barrier in inflammatory bowel disease," *Gut*, vol. 60, no. 4, pp. 463–472, 2011.

[50] A. Garg, A. Zhao, S. L. Erickson et al., "Pregnane X receptor activation attenuates inflammation-associated intestinal epithelial barrier dysfunction by inhibiting cytokine-induced myosin light-chain kinase expression and c-jun N-terminal kinase 1/2 activation," *Journal of Pharmacology and Experimental Therapeutics*, vol. 359, no. 1, pp. 91–101, 2016.

[51] J. Kong, Z. Zhang, M. W. Musch et al., "Novel role of the vitamin D receptor in maintaining the integrity of the intestinal mucosal barrier," *American Journal of Physiology—Gastrointestinal and Liver Physiology*, vol. 294, no. 1, pp. G208–G216, 2008.

[52] A. Wilson, A. Almousa, W. A. Teft, and R. B. Kim, "Attenuation of bile acid-mediated FXR and PXR activation in patients with crohn's disease," *Scientific Reports*, vol. 10, no. 1, p. 1866, 2020.

[53] R. M. Gadaleta, O. Garcia-Irigoyen, M. Cariello et al., "Fibroblast growth factor 19 modulates intestinal microbiota and inflammation in presence of farnesoid X receptor," *EBioMedicine*, vol. 54, Article ID 102719, 2020.

[54] T. Inagaki, A. Moschetta, Y. K. Lee et al., "Regulation of antibacterial defense in the small intestine by the nuclear bile acid receptor," *Proceedings of the National Academy of Sciences*, vol. 103, no. 10, pp. 3920–3925, 2006.

[55] M. S. Mroz, N. Keating, J. B. Ward et al., "Farnesoid X receptor agonists attenuate colonic epithelial secretory function and prevent experimental diarrhoea in vivo," *Gut*, vol. 63, no. 5, pp. 808–817, 2014.

[56] J. Terc, A. Hansen, L. Alston, and S. A. Hirota, "Pregnane X receptor agonists enhance intestinal epithelial wound healing and repair of the intestinal barrier following the induction of experimental colitis," *European Journal of Pharmaceutical Sciences*, vol. 55, pp. 12–19, 2014.

[57] S. Wu, Y. G. Zhang, R. Lu et al., "Intestinal epithelial vitamin D receptor deletion leads to defective autophagy in colitis," *Gut*, vol. 64, no. 7, pp. 1082–1094, 2015.

[58] G. M. Hudson, K. L. Flannigan, S. L. Erickson et al., "Constitutive androstane receptor regulates the intestinal mucosal response to injury," *British Journal of Pharmacology*, vol. 174, no. 12, pp. 1857–1871, 2017.

[59] A. J. Guri, S. K. Mohapatra, W. T. Horne, R. Hontecillas, and J. Bassaganya-Riera, "The role of T cell PPAR gamma in mice with experimental inflammatory bowel disease," *BMC Gastroenterology*, vol. 10, p. 60, 2010.

[60] S. Tani, R. Takano, S. Oishi et al., "Digoxin attenuates murine experimental colitis by downregulating Th17-related cytokines," *Gastroenterology*, vol. 152, no. 5, pp. S573–S738, 2017.

[61] V. Marcil, E. Seidman, D. Sinnett et al., "Modification in oxidative stress, inflammation, and lipoprotein assembly in response to hepatocyte nuclear factor 4α knockdown in intestinal epithelial cells," *Journal of Biological Chemistry*, vol. 285, no. 52, pp. 40448–40460, 2010.

[62] V. Klepsch, A. R. Moschen, H. Tilg, G. Baier, and N. Hermann-Kleiter, "Nuclear receptors regulate intestinal inflammation in the context of IBD," *Frontiers in Immunology*, vol. 10, p. 1070, 2019.

[63] S. Fiorucci, M. Biagioli, A. Zampella, and E. Distrutti, "Bile acids activated receptors regulate innate immunity," *Frontiers in Immunology*, vol. 9, p. 1853, 2018.

[64] M. Boesjes, V. W. Bloks, J. Hageman et al., "Hepatic farnesoid X-receptor isoforms α2 and α4 differentially modulate bile salt and lipoprotein metabolism in mice," *PLoS One*, vol. 9, no. 12, Article ID e115028, 2014.

[65] W. Zheng, Y. Lu, S. Tian et al., "Structural insights into the heterodimeric complex of the nuclear receptors FXR and RXR," *Journal of Biological Chemistry*, vol. 293, no. 32, pp. 12535–12541, 2018.

[66] G. Rizzo, B. Renga, A. Mencarelli, R. Pellicciari, and S. Fiorucci, "Role of FXR in regulating bile acid homeostasis and relevance for human diseases," *Current Drug Targets—Immune, Endocrine and Metabolic Disorders*, vol. 5, no. 3, pp. 289–303, 2005.

[67] F. Kuipers, T. Claudel, E. Sturm, and B. Staels, "The farnesoid X Receptor (FXR) as modulator of bile acid metabolism," *Reviews in Endocrine and Metabolic Disorders*, vol. 5, no. 4, pp. 319–326, 2004.

[68] S. Ducastel, V. Touche, M. S. Trabelsi et al., "The nuclear receptor FXR inhibits glucagon-like peptide-1 secretion in response to microbiota-derived short-chain fatty acids," *Scientific Reports*, vol. 10, no. 1, p. 174, 2020.

[69] S. Seok, H. Sun, Y. C. Kim, B. Kemper, and J. K. Kemper, "Defective FXR-SHP regulation in obesity aberrantly increases miR-802 expression, promoting insulin resistance and fatty liver," *Diabetes*, vol. 70, no. 3, pp. 733–744, 2021.

[70] S. Fiorucci, S. Cipriani, A. Mencarelli, B. Renga, E. Distrutti, and F. Baldelli, "Counter-regulatory role of bile acid

activated receptors in immunity and inflammation," *Current Molecular Medicine*, vol. 10, no. 6, pp. 579–595, 2010.

[71] P. Vavassori, A. Mencarelli, B. Renga, E. Distrutti, and S. Fiorucci, "The bile acid receptor FXR is a modulator of intestinal innate immunity," *The Journal of Immunology*, vol. 183, no. 10, pp. 6251–6261, 2009.

[72] L. Verbeke, R. Farre, B. Verbinnen et al., "The FXR agonist obeticholic acid prevents gut barrier dysfunction and bacterial translocation in cholestatic rats," *American Journal Of Pathology*, vol. 185, no. 2, pp. 409–419, 2015.

[73] R. M. Nijmeijer, R. M. Gadaleta, S. W. C. van Mil et al., "Farnesoid X receptor (FXR) activation and FXR genetic variation in inflammatory bowel disease," *PLoS One*, vol. 6, no. 8, Article ID e23745, 2011.

[74] W. You, L. Li, D. Sun et al., "Farnesoid X receptor constructs an immunosuppressive microenvironment and sensitizes FXR (high) PD-L1 (low) NSCLC to anti-PD-1 immunotherapy," *Cancer Immunology Research*, vol. 7, no. 6, pp. 990–1000, 2019.

[75] M. S. Mroz, N. K. Lajczak, B. J. Goggins, S. Keely, and S. J. Keely, "The bile acids, deoxycholic acid and ursodeoxycholic acid, regulate colonic epithelial wound healing," *American Journal of Physiology—Gastrointestinal and Liver Physiology*, vol. 314, no. 3, pp. G378–G387, 2018.

[76] J. L. Lew, A. Zhao, J. Yu et al., "The farnesoid X receptor controls gene expression in a ligand-and promoter-selective fashion," *Journal of Biological Chemistry*, vol. 279, no. 10, pp. 8856–8861, 2004.

[77] B. Zhang, W. Xie, and M. D. Krasowski, "PXR: a xenobiotic receptor of diverse function implicated in pharmacogenetics," *Pharmacogenomics*, vol. 9, no. 11, pp. 1695–1709, 2008.

[78] J. Gao and W. Xie, "Pregnane X receptor and constitutive androstane receptor at the crossroads of drug metabolism and energy metabolism," *Drug Metabolism and Disposition*, vol. 38, no. 12, pp. 2091–2095, 2010.

[79] C. Prantera, H. Lochs, M. Campieri et al., "Antibiotic treatment of crohn's disease: results of a multicentre, double blind, randomized, placebo-controlled trial with rifaximin," *Alimentary Pharmacology and Therapeutics*, vol. 23, no. 8, pp. 1117–1125, 2006.

[80] C. Prantera, H. Lochs, M. Grimaldi, S. Danese, M. L. Scribano, and P. Gionchetti, "Rifaximin-extended intestinal release induces remission in patients with moderately active crohn's disease," *Gastroenterology*, vol. 142, no. 3, pp. 473–481, 2012.

[81] Y. M. Shah, X. Ma, K. Morimura, I. Kim, and F. J. Gonzalez, "Pregnane X receptor activation ameliorates DSS-induced inflammatory bowel disease via inhibition of NF-κB target gene expression," *American Journal of Physiology—Gastrointestinal and Liver Physiology*, vol. 292, no. 4, pp. G1114–G1122, 2007.

[82] A. Mencarelli, B. Renga, G. Palladino et al., "Inhibition of NF-κB by a PXR-dependent pathway mediates counter-regulatory activities of rifaximin on innate immunity in intestinal epithelial cells," *European Journal of Pharmacology*, vol. 668, no. 1-2, pp. 317–324, 2011.

[83] J. Zhang, L. Ding, B. Wang et al., "Notoginsenoside R1 attenuates experimental inflammatory bowel disease via pregnane X receptor activation," *Journal of Pharmacology and Experimental Therapeutics*, vol. 352, no. 2, pp. 315–324, 2015.

[84] X. Zhang, Y. Gao, Z. Ma et al., "Tanshinone IIA ameliorates dextran sulfate sodium-induced inflammatory bowel disease via the pregnane X receptor," *Drug Design, Development and Therapy*, vol. 9, p. 6343, 2015.

[85] B. Bandera Merchan, S. Morcillo, G. Martin-Nunez, F. J. Tinahones, and M. Macias-Gonzalez, "The role of vitamin D and VDR in carcinogenesis: through epidemiology and basic sciences," *The Journal of Steroid Biochemistry and Molecular Biology*, vol. 167, no. 1, pp. 203–218, 2017.

[86] R. Del Pinto, D. Pietropaoli, A. K. Chandar, C. Ferri, and F. Cominelli, "Association between inflammatory bowel disease and vitamin D deficiency: a systematic review and meta-analysis," *Inflammatory Bowel Diseases*, vol. 21, no. 11, pp. 2708–2717, 2015.

[87] J. Gubatan, S. Mitsuhashi, T. Zenlea, L. Rosenberg, S. Robson, and A. C. Moss, "Low serum vitamin D during remission increases risk of clinical relapse in patients with ulcerative colitis," *Clinical Gastroenterology and Hepatology*, vol. 15, no. 2, pp. 240–246, 2017.

[88] M. T. Cantorna, L. Snyder, Y. D. Lin, and L. Yang, "Vitamin D and 1,25(OH)2D regulation of T cells," *Nutrients*, vol. 7, no. 4, pp. 3011–3021, 2015.

[89] L. M. Das, A. M. Binko, Z. P. Traylor, H. Peng, and K. Q. Lu, "Vitamin D improves sunburns by increasing autophagy in M2 macrophages," *Autophagy*, vol. 15, no. 5, pp. 813–826, 2019.

[90] M. Hewison, "Vitamin D and immune function: an overview," *Proceedings of the Nutrition Society*, vol. 71, no. 1, pp. 50–61, 2012.

[91] M. Froicu and M. T. Cantorna, "Vitamin D and the vitamin D receptor are critical for control of the innate immune response to colonic injury," *BMC Immunology*, vol. 8, p. 5, 2007.

[92] J. Sun, "Vitamin D and mucosal immune function," *Current Opinion in Gastroenterology*, vol. 26, no. 6, pp. 591–595, 2010.

[93] Y. D. Lin, J. Arora, K. Diehl, S. A. Bora, and M. T. Cantorna, "Vitamin D is required for ILC3 derived IL-22 and protection from *Citrobacter rodentium* infection," *Frontiers in Immunology*, vol. 10, p. 1, 2019.

[94] J. Chen, A. Waddell, Y. D. Lin, and M. T. Cantorna, "Dysbiosis caused by vitamin D receptor deficiency confers colonization resistance to *Citrobacter rodentium* through modulation of innate lymphoid cells," *Mucosal Immunology*, vol. 8, no. 3, pp. 618–626, 2015.

[95] T. Raftery, A. R. Martineau, C. L. Greiller et al., "Effects of vitamin D supplementation on intestinal permeability, cathelicidin and disease markers in crohn's disease: results from a randomised double-blind placebo-controlled study," *United European Gastroenterology Journal*, vol. 3, no. 3, pp. 294–302, 2015.

[96] H. Schäffler, D. P. Herlemann, P. Klinitzke et al., "Vitamin D administration leads to a shift of the intestinal bacterial composition in crohn's disease patients, but not in healthy controls," *Journal of Digestive Diseases*, vol. 19, no. 4, pp. 225–234, 2018.

[97] M. Garg, P. Hendy, J. N. Ding, S. Shaw, G. Hold, and A. Hart, "The effect of vitamin D on intestinal inflammation and faecal microbiota in patients with ulcerative colitis," *Journal of crohn's and colitis*, vol. 12, no. 8, pp. 963–972, 2018.

[98] P. Wei, J. Zhang, M. Egan-Hafley, S. Liang, and D. D. Moore, "The nuclear receptor CAR mediates specific xenobiotic induction of drug metabolism," *Nature*, vol. 407, no. 6806, pp. 920–923, 2000.

[99] W. Huang, J. Zhang, S. S. Chua et al., "Induction of bilirubin clearance by the constitutive androstane receptor (CAR),"

Proceedings of the National Academy of Sciences, vol. 100, no. 7, pp. 4156–4161, 2003.

[100] A. Lundin, C. M. Bok, L. Aronsson et al., "Gut flora, toll-like receptors and nuclear receptors: a tripartite communication that tunes innate immunity in large intestine," *Cellular Microbiology*, vol. 10, no. 5, pp. 1093–1103, 2008.

[101] B. Björkholm, C. M. Bok, A. Lundin, J. Rafter, M. L. Hibberd, and S. Pettersson, "Intestinal microbiota regulate xenobiotic metabolism in the liver," *PLoS One*, vol. 4, no. 9, Article ID e6958, 2009.

[102] P. Martin, R. Riley, D. J. Back, and A. Owen, "Comparison of the induction profile for drug disposition proteins by typical nuclear receptor activators in human hepatic and intestinal cells," *British Journal of Pharmacology*, vol. 153, no. 4, pp. 805–819, 2008.

[103] D. Uehara, H. Tojima, S. Kakizaki et al., "Constitutive androstane receptor and pregnane X receptor cooperatively ameliorate DSS-induced colitis," *Digestive and Liver Disease*, vol. 51, no. 2, pp. 226–235, 2019.

[104] J. Ji, Y. Lu, H. Liu et al., "Acupuncture and moxibustion for inflammatory bowel diseases: a systematic review and meta-analysis of randomized controlled trials," *Evidence-Based Complementary and Alternative Medicine*, vol. 2013, Article ID 158352, 11 pages, 2013.

[105] H. V. Acar, "Acupuncture and related techniques during perioperative period: a literature review," *Complementary Therapies in Medicine*, vol. 29, pp. 48–55, 2016.

[106] Y. Wang, M. Li, and A. S. Zha, "Adjuvant treatment of crohn's disease with traditional Chinese medicine: a meta-analysis," *Evidence-Based Complementary and Alternative Medicine*, vol. 2019, p. 8, 2019.

[107] T. J. Kaptchuk, "Acupuncture: theory, efficacy, and practice," *Annals of Internal Medicine*, vol. 136, no. 5, pp. 374–383, 2002.

[108] G. Song, C. Fiocchi, and J. P. Achkar, "Acupuncture in inflammatory bowel disease," *Inflammatory Bowel Diseases*, vol. 25, no. 7, pp. 1129–1139, 2019.

[109] C. H. Bao, J. M. Zhao, H. R. Liu et al., "Randomized controlled trial: moxibustion and acupuncture for the treatment of crohn's disease," *World Journal of Gastroenterology*, vol. 20, no. 31, pp. 11000–11011, 2014.

[110] S. Joos, B. Brinkhaus, C. Maluche et al., "Acupuncture and moxibustion in the treatment of active crohn's disease: a randomized controlled study," *Digestion*, vol. 69, no. 3, pp. 131–139, 2004.

[111] X. Lin, X. Liu, J. Xu et al., "Metabolomics analysis of herb-partitioned moxibustion treatment on rats with diarrhea-predominant irritable bowel syndrome," *Chinese Medicine*, vol. 14, no. 1, 2019.

[112] Y. C. Lee, C. H. Lin, S. Y. Hung et al., "Manual acupuncture relieves bile acid-induced itch in mice: the role of microglia and TNF-α," *International Journal of Medical Sciences*, vol. 15, no. 9, pp. 953–960, 2018.

[113] Y. Cui, J. Liu, C. Huang, and B. Zhao, "Moxibustion at CV4 alleviates atherosclerotic lesions through activation of the LXRα/ABCA1 pathway in apolipoprotein-E-deficient mice," *Acupuncture in Medicine*, vol. 37, no. 4, pp. 237–243, 2019.

[114] Z. Z. Liu, W. Huang, L. L. Xiang et al., "Effect of electro-acupuncture preconditioning on myocyte apoptosis in myocardial ischemia-reperfusion injury rats based on FXR/SHP pathway," *Zhen Ci Yan Jiu*, vol. 46, no. 5, pp. 368–374, 2021.

[115] C. Li, X. L. Zhang, Y. X. Xue et al., "Protective effect and regulating effect on FXR/SHP gene of electroacupuncture preconditioning on myocardial ischemia-reperfusion injury in rats," *Zhongguo Zhen Jiu*, vol. 39, no. 8, pp. 861–866, 2019.

Hindawi
Evidence-Based Complementary and Alternative Medicine
Volume 2022, Article ID 8362892, 16 pages
https://doi.org/10.1155/2022/8362892

Review Article

The Influence of Acupuncture Parameters on Efficacy and the Possible Use of Acupuncture in Combination with or as a Substitute for Drug Therapy in Patients with Ulcerative Colitis

Min'an Chen, Sisi Zhao, Yu Guo, Luxi Cao, Hai Zeng, Zhuowen Lin, Shiqi Wang, Yimin Zhang, and Mingmin Zhu

School of Traditional Chinese Medicine, Jinan University, Guangzhou 510632, China

Correspondence should be addressed to Yimin Zhang; zhangymjnu@163.com and Mingmin Zhu; jnuzmm@jnu.edu.cn

Received 16 September 2021; Revised 13 November 2021; Accepted 25 February 2022; Published 22 March 2022

Academic Editor: Talha Bin Emran

Background. Ulcerative colitis (UC) is an inflammatory disease of the colonic mucosa, which is accompanied by chronic, idiopathic characteristics. Acupuncture may be an effective therapy for UC. Here we focused on manual acupuncture and electroacupuncture (MA/EA), two widely used and studied acupuncture interventions, to probe the effects of acupuncture parameters on clinical efficacy in patients with UC and the use of MA/EA alone or with other drugs to support their wider adoption in clinical practice. *Methods*. The PubMed, Cochrane Library, Web of Science, Embase, China National Knowledge Infrastructure Database, and Wanfang databases were searched from inception to April 27, 2021. Randomized clinical trials (RCTs) published in Chinese or English were included, and subgroup analyses were performed according to acupuncture parameter, acupuncture type, and control medicine type. The risk of bias was assessed using the Cochrane Risk of Bias tool and modified Jadad scale, and Review Manager 5.4 and Stata 14.0 were used to perform a meta-analysis. Sources of heterogeneity were explored; sensitivity analysis was performed; and the GRADE methodology was used to assess the evidence level. *Results*. Sixteen studies (1454 individuals) were included. Retention of the needle [10–30 minutes (RR 1.18, 95% CI [1.11, 1.26], $P < 0.01$; heterogeneity: $\chi^2 = 6.25$, df = 6 ($P = 0.40$), $I^2 = 4\%$)], the frequency of MA [once every other day (RR 1.21, 95% CI [1.08, 1.35], $P < 0.01$; heterogeneity: $\chi^2 = 0.80$, df = 1 ($P = 0.37$), $I^2 = 0\%$)], and the length of treatment [8 weeks (RR 1.35, 95% CI [1.01, 1.81], $P = 0.04$)] improved clinical efficacy at the end of treatment compared with medications alone. MA (RR 1.18, 95% CI [1.11, 1.25], $P < 0.01$; heterogeneity: $\chi^2 = 6.19$, df = 7 ($P = 0.52$), $I^2 = 0\%$) increased clinical efficacy compared with medications. Furthermore, MA plus medications (RR 1.26, 95% CI [1.13, 1.40], $P < 0.01$; heterogeneity: $\chi^2 = 0.95$, df = 2 ($P = 0.62$), $I^2 = 0\%$) and EA plus medications (RR 1.36, 95% CI [1.13, 1.63], $P < 0.01$; heterogeneity: $\chi^2 = 0.13$, df = 1 ($P = 0.72$), $I^2 = 0\%$) both dramatically improved clinical efficacy. The clinical efficacy of MA plus mesalazine or MA plus metronidazole and sulfasalazine was greater than with mesalazine or metronidazole and sulfasalazine alone. Similarly, EA plus sulfasalazine was more effective than sulfasalazine alone. MA/EA resulted in fewer adverse reactions than medical therapies. The use of MA plus medications significantly reduced Baron scores. GRADE evaluations indicated that the evidence strength was moderate to low but mostly low. *Conclusions*. Our study provides the latest evidence to allow us to speculate about the possible optimal MA parameters to treat patients with UC. The low number of adverse reactions and high efficacy make MA/EA a possible supplement to or replacement for traditional UC drugs. The variable parameter settings preferred by patients and acupuncturists may be an important factor limiting the wider clinical deployment of acupuncture as a potential UC therapy.

1. Introduction

Ulcerative colitis (UC) is a chronic, idiopathic inflammatory disease occurring on the colonic mucosa [1], with a global incidence between 0.5 and 24.5 per 100,000 people [2]. The etiopathogenesis of UC remains unclear, but it manifests clinically with abdominal pain, diarrhea, tenesmus, and rectal bleeding [1, 3]. Patients with UC require continuous care and medication [2] due to the persistent and chronic nature of the disease [4]. Furthermore, UC patients are more likely to develop colorectal cancer than the general population [1]. As a result, UC incurs a massive burden on body and mind, quality of life, and healthcare resources.

5-ASA and corticosteroids are common first-line therapies [2] for patients with mild to moderate UC [5]. However, these drugs are associated with side effects, some of which can be severe [6, 7]. Despite their benefit, poor drug compliance can result in patients discontinuing treatment and ultimately poor disease control.

Therefore, there has been increasing interest in complementary and alternative medicines (CAMs) for the treatment of UC, of which traditional Chinese medicine (TCM) is one. [8]. As a natural CAM with an excellent safety profile and few side effects, acupuncture is increasingly recognized as a viable adjunct to other management strategies in many Western countries [9, 10]. The Chinese have used acupuncture to treat UC since ancient times, and it has been revealed to be effective in clinical trials [11–13]. However, the mechanism underpinning the clinical effectiveness of acupuncture in UC patients is still not completely understood, although proposed mechanisms include modulation of gastrointestinal motility, visceral sensitivity, the neuro-endocrine-immune axis, inflammation, and the brain-gut axis [14].

Previous reviews [15] and meta-analyses [16, 17] have focused on the clinical efficacy and adverse reactions of comprehensive acupuncture for UC and confirmed the benign effect of acupuncture for UC, but none of them specifically studied the influence of acupuncture parameters on clinical efficacy, despite them playing an important role in clinical efficacy. In a review, Zhang et al. noted that most current acupuncture studies do not meet dose and quality adequacy criteria for optimal clinical efficacy, including acupuncture manipulation, acupuncture time, frequency, waveform, and other parameters [18]. The acupuncture dosage has always been of importance in TCM, but acupuncture is often practiced based on the beliefs and habits of acupuncturists or even patient preference, significantly restricting the robust exploration and standardization of acupuncture dosage. Nevertheless, scientific advances have allowed in-depth studies of acupuncture dosages and their effect using modern techniques such as the combination of imaging with biochemistry, physiology, and data mining analysis, and animal and clinical studies have also been conducted [19–21]. Fang et al. showed that the differential effects of electroacupuncture (EA) on NTS neuron excitability in normal rats may be caused by different combinations of acupoint and frequency selection [22]. Furthermore, different effects on gastric electrical frequency and amplitude in bradygastria rabbits were related to different manual acupuncture (MA) manipulations of acupoint ST36 [23]. In their in vivo studies, Yang et al. showed that not only needle retention, but also treatment frequency and needle manipulation, were significant determinants of hippocampal learning, memory, and neuron damage in VD rats [24]. In their clinical trial, Xu et al. showed that different acupuncture stimulus techniques had different effects on blood flow perfusion at acupoints in normal adults [25], and in another clinical trial MA stimulation at different acupoints caused different depressor and bradycardic responses [26]. All these data indicate that different acupuncture parameters can produce different clinical effects [27], and acupuncture parameters may be the main factor affecting acupuncture efficacy [28, 29]. Although a growing number of studies have focused on the influence of acupuncture parameters on clinical efficacy [30–32], acupuncture parameters have yet to be thoroughly studied in the clinical management of UC, relevant UC guidelines do not provide detailed acupuncture programs and parameters, and there is still no meta-analysis of the specific clinical impact of acupuncture parameters on UC. Hence, we conducted this systematic evaluation and meta-analysis to probe the optimal MA/EA parameters for the treatment of UC to provide a reference for improvements in the clinical management of UC with MA/EA.

2. Materials and Methods

This systematic review and meta-analysis were registered in the International Platform of Registered Systematic Review and Meta-analysis Protocols (INPLASY202190041). The meta-analysis was conducted according to the PRISMA 2020 statement [33].

2.1. Eligibility Criteria. To ensure the quality of the meta-analysis, participants, interventions, comparisons, outcomes, and study design (PICOS) approach was adopted.

2.1.1. Inclusion Criteria

P: The diagnosis of UC was established on the basis of the internationally or nationally recognized diagnostic guideline, which was not less than one (guidelines). Such as the American Gastroenterological Association Clinical Practice Guidelines on the Management of Ulcerative Colitis [34, 35] or the Consensus on TCM Diagnosis and Treatment of Ulcerative Colitis [36]. Participants were 18 years old or older and were not limited by race, gender, geographic location, or disease course.

I: Manual acupuncture or electroacupuncture (any acupuncture needle specification, acupoint, duration of acupuncture, treatment frequency, period of treatment, and stimulation method) alone or combined with medicines for UC.

C: Do not treat or wait for treatment, conventional drugs, sham acupuncture, or placebo. When a

combination of acupuncture and drugs was used, the drugs in the control group were the same as those in the corresponding experimental group.

O: The primary outcome was the effective ratio. Secondary outcomes included the adverse effects, Baron scores.

S: Only randomized controlled trials were eligible.

2.1.2. Exclusion Criteria. The following conditions were not eligible for inclusion: head needle, abdominal needle, ear needle, eye needle, and other non-traditional manual needle therapy; pregnant or lactating patients or those about to become pregnant; patients with mental illness; severe adverse effects of acupuncture (e.g., fear of acupuncture, fainting during acupuncture); animal experiments, case reports, review articles and repeated publications.

2.2. Information Sources and Search Strategy. PubMed, Cochrane, Web of Science, Embase, China National Knowledge Infrastructure Database, and Wanfang were searched for all relevant literature from database inception to April 27, 2021. The search strategy was divided into clinical status (UC), intervention (MA/EA), and study type (RCT). We combine Medical Subject Headings (MeSH) and related free text words to search. Differences were resolved through discussion between investigators to reach an agreement. The search details for each database are detailed in Supplementary S1. Moreover, additional publications were identified, which were achieved through manual searching of previously published studies and the reference lists of the included studies.

2.3. Data Extraction and Collection. In this process, the duplicates were first removed by two investigators (Min'an Chen and Sisi Zhao) by reading the titles and abstracts. Then, the titles, abstracts, and keywords of the remaining articles were selected and recorded by each investigator individually, according to the inclusion and exclusion criteria. A standardized data extraction form was used to extract general information independently. Missing data or parts related to missing data were removed and not included in the analysis. Furthermore, any differences arising during this process were resolved through negotiation between two investigators (Min'an Chen and Sisi Zhao). If no agreement was reached, a third investigator (Yu Guo) made the final choice to resolve the disagreement.

If different publications included the same participants, the article with the most complete information and the longest follow-up period was selected.

2.4. Risk of Bias Assessment. Two authors (Min'an Chen and Sisi Zhao) independently provided an assessment of the risk of bias using the Cochrane Handbook v.5.3.0-recommended Cochrane Risk of Bias assessment (RoB) tool and the modified Jadad quality scale. The RoB assessment tool has six components: random sequence generation, allocation concealment, blinding of participants and personnel, blinding of outcome assessment, incomplete outcome data, selective reporting, and other biases. Risk grade consists of three parts: low bias risk, unclear bias risk, and high bias risk. The modified Jadad quality scale is scored between 1 and 7, with low quality indicated by 1 to 3 and high quality from 4 to 7. Disagreements were resolved by a third investigator (Yu Guo) to reach a consensus.

2.5. Statistical Analysis. We analyzed and consolidated the data using the Cochrane Collaboration's Review Manager 5.4 software and Stata 14.0. Two-sided tests were used, and a P value <0.05 was considered statistically significant [37, 38]. Relative risk ratios (RR) and corresponding 95% confidence intervals (CIs) were calculated for dichotomous variables. For continuous variables, standard mean differences (SMD) were used to represent the corresponding 95%CIs. Statistical heterogeneity of each trial was evaluated by Cochran's Q statistic and its associated P value. In addition, according to the Cochrane Handbook, the I^2 statistic was selected to test heterogeneity, where a $P < 0.1$ and $I^2 \geq 50\%$ were regarded as high heterogeneity and a random-effects model was used. A $P < 0.1$ and $I^2 < 50\%$ were regarded as some heterogeneity and a $P \geq 0.1$ and $I^2 < 50\%$ were considered homogeneous, in which cases fixed-effects models were adopted.

2.6. Subgroup Analysis and Sensitivity Analysis. Subgroup analyses of MA/EA parameters, acupuncture type, medicine type in the control group, adverse events, and Baron score were conducted. The robustness of the results was assessed by sensitivity analysis.

2.7. Reporting Bias Assessment. The reporting bias was assessed by RevMan version 5.4 and STATA 14.0, which was accomplished by using Funnel plots [39] and Egger's test [40]. If $P > 0.05$ on both sides, there was no reporting bias according to Egger's test.

2.8. Confidence Assessment. The evidence level of the outcomes was assessed, which used the Grading of Recommendations Assessment, Development and Evaluation (GRADE) framework [41] by two independent authors (Min'an Chen and Sisi Zhao) (Supplementary S3). The third investigator (Yu Guo) resolved the disagreements to reach a consensus.

3. Results

3.1. Literature Search. According to the search strategy, 3280 references were identified and 723 duplicates were excluded. After title and abstract screening, 2108 non-clinical studies and literature unrelated to UC and MA/EA were excluded. Further evaluation of this literature was carried out, and non-RCTs, duplicate publications, non-English papers, and non-Chinese papers were removed, leaving 16 papers for study inclusion after reading the full text. Figure 1 summarizes the study details, which relate to the selection process.

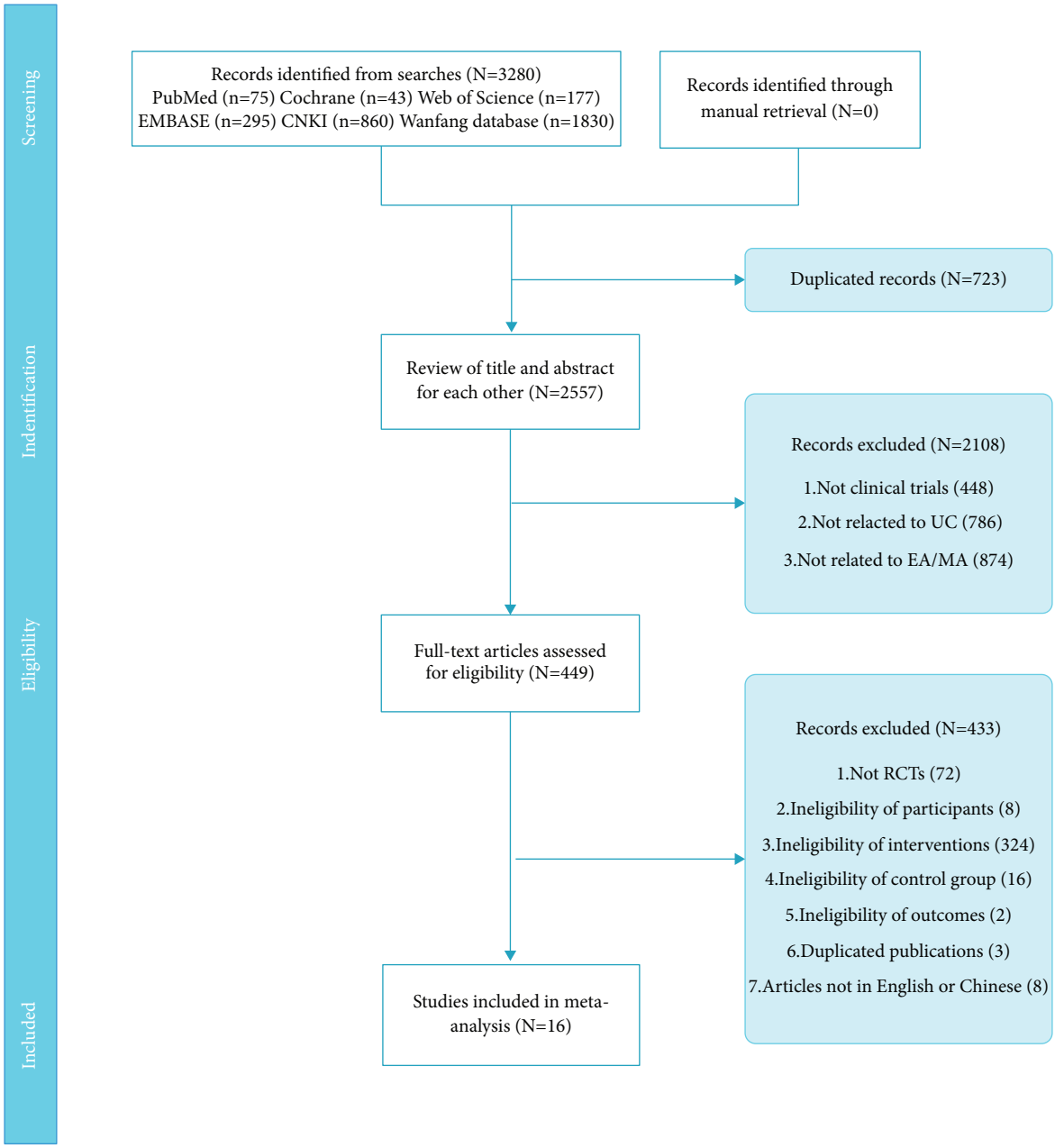

Figure 1: The study selection process.

3.2. Study Characteristics. Participants who met the diagnostic criteria for UC were recruited. Sample sizes ranged from 50 [42, 43] to 196 [44]. Table 1 shows the characteristics of the included studies, which included diagnostic criteria, experimental groups, and control groups.

In the experimental group, MA/EA was slightly different with respect to acupoint selection and operation parameters. Thirteen [42–54] trials used a standardized treatment regimen, each with fixed points selected, mainly on the abdomen, back, and lower limbs. Three [49, 55, 56] used semi-standardized treatment schemes, and acupoints were selected according to diagnosis and symptom differentiation using the main acupoints. Among the 14 standardized treatment plans, the main acupoints were Tianshu (ST25), Qihai (RN6), Guanyuan (RN4), Shangjuxu (ST37), and Dachangshu (BL25). Twelve [43–46, 48, 49, 52–57] trials used MA and four [42, 47, 50, 51] used EA. The acupuncture retention time was between 10 min [52, 54] and 60 min [42, 47, 50], and the most common retention time was 30 min [43, 45, 46, 48, 53, 56]. Acupuncture was administered once a day in nine studies [42, 43, 47–50, 53, 55, 56] , five times a week in three studies [42, 47, 50], and every other day in four studies [46, 51, 52, 54]. The total duration of acupuncture treatment ranged from 10 days [49] to 2 months [42, 45, 47, 50], and the median duration of treatment was 30 days [51, 54, 56].

Table 1: The main characteristics of the included studies.

Author, Year, Country	Diagnostic criteria	Experimental group										Control group								Outcomes
		Sample size (in each group)	Gender (M/F)	Age (years)	Course of disease	Intervention	Treatment duration					Sample size	Gender (M/F)	Age (years)	Course of disease	Intervention	Treatment duration			
				Mean	Mean		Main acupoints	Duration of acupuncture	Acupuncture frequency	Medication frequency	Total period			Mean	Mean		Medication frequency	Total period		
Cao 2019, China	Diagnosis of chronic UC	49	25/24	28–75 41.4 ± 12.8	NR NR	MA	RN12, RN4, DU1, ST25, BL25	20 min	Q.d	NR	2 w	49	26/23	30–75 40.6 ± 13.2	NR NR	Metronidazole + SASP	Metronidazole: 0.2 g p.o. T.i.d; SASP: 0.2 g p.o. T.i.d	2 w	ER, AR
Ge 2012, China	Clinical diagnosis and treatment guide	30	31/29 (tot)	19–58 (tot) 31.7 ± 4.5 (tot)	2 m–7 y (tot) (3.8 ± 2.1) *y* (tot)	EA + SASP	ST25, RN6, RN4, ST37, SP6, LR3; BL18, BL20, BL25, BL23, BL32 (alternate)	60 min	Q.d	The first month: 0.5 g p.o. Q.i.d; the next month: 1.5 g/d	2 m	30	31/29 (tot)	19–58 (tot) 31.7 ± 4.5 (tot)	2 m–7 y (tot) (3.8 ± 2.1) *y* (tot)	SASP	The first month: 0.5 g p.o. Q.i.d; the next month: 1.5 g/d	2 m	AR
Ge 2014, China	Clinical diagnosis and treatment guide	31	16/15	26–71 35.6 ± 7.5	4 m–7 y (3.7 ± 2.8) y	EA + SASP	BL18, BL20, BL25, BL23, BL32, ST25, RN6, RN4, ST37, SP6, LR3 (alternate)	60 min	Q.d	The first month: 1 g p.o. Q.i.d; the next month: 2 g/d	2 m	31	17/14	25–73 38.4 ± 7.8	5 m–8 y (4.0 ± 2.5) y	SASP	The first month: 1 g p.o. Q.i.d; the next month: 2 g/d	2m	ER, AR, ACTH
Ge 2015, China	Clinical diagnosis and treatment guide	25	27/23 (tot)	27–71 (tot) 38.5 ± 6.5 (tot)	5 m–8 y (tot) (4.1 ± 2.7) *y* (tot)	EA + SASP	BL18, BL23, BL20, BL25, BL32, ST25, ST37, RN4, RN6, LR3, SP6 (alternate)	60 min	Q.d	The first month: 1 g p.o. Q.i.d; the next month: 2 g/d	2 m	25	27/23 (tot)	27–71 (tot) 38.5 ± 6.5 (tot)	5 m–8 y (tot) (4.1 ± 2.7) *y* (tot)	SASP	The first month: 1 g p.o. Q.i.d; the next month: 2 g/d	2m	ER, AR
Lin 2020, China	Diagnosis of chronic UC	30	8/22	21–77 NR	3 m–13 y NR	EA	RN12, ST36, ST37, LI11, BL23, BL25	40 min	Q.o.d	NR	30 d	30	11/19	20–73 NR	3 m–15 y NR	Diphenoxylate Co. + norfloxacin + berberine Co	Diphenoxylate Co.: 2# p.o. T.i.d, norfloxacin: 0.2 g 2# p.o. T.i.d,; berberine: 3# p.o. T.i.d	30 d	ER, SE
Liu 2016, China	Diagnosis of chronic UC	62	29/33	23–76 50.67 ± 6.82	(9–19) m (13.63 ± 5.16) m	MA	RN4, RN6, ST25, BL25, DU1	10–30 min	Q.o.d	NR	NR	62	30/32	24–74 51.14 ± 5.46	(9–20) m (14.10 ± 5.22) m	Metronidazole + SASP	Metronidazole: 2#-3# , T.i.d p.o. SASP: 2-3 g/d T.i.d p.o.	NR	ER, AR
Luan 2016, China	Diagnosis of chronic UC	25	13/12	26–42 34 ± 5.75	NR NR	MA	SP4, KI3, ST36, RN4, ST25 , BL16, BL20, BL21, BL22, BL25; DU2, DU6	30 min	Q.d	NR	8 w	25	14/11	23–43 31.28 ± 6.13	NR NR	Mesalazine	1 g p.o. Q.i.d	8 w	ER, AR
Luan 2020, China	Diagnosis of chronic UC	75	40/35	24–76 NR	(9–17) m NR	MA	ST25, RN4, RN6, BL25	30 min	Q.d	NR	NR	75	45/30	25–75 NR	(9–18) m NR	Metronidazole + SASP	Metronidazole: 0.2 g p.o. T.i.d,; SASP: 2.0 g p.o. T.i.d	NR	ER
Pang 2019, China	Consensus opinions on the diagnosis and treatment of inflammatory bowel disease	30	16/14	20–67 41.63 ± 12.86	(4–68) m (36.90 ± 20.94) m	MA + mesalazine	BL31, BL32, BL33, BL34	30 min	Q.o.d	1.0 g p.o. Q.i.d	1 m	30	19/11	20–64 43.33 ± 15.51	(4–66) m (38.03 ± 18.42) m	Mesalazine	1.0 g p.o. Q.i.d	1 m	ER, baron score; serum TNF-α, IL-6, IL-8, IL-10

Table 1: Continued.

Author, Year, Country	Diagnostic criteria	Experimental group										Control group							Outcomes
		Sample size (in each group)	Gender (M/F)	Age (years)	Course of disease	Intervention	Treatment duration					Sample size	Gender (M/F)	Age (years)	Course of disease	Intervention	Treatment duration		
				Mean	Mean		Main acupoints	Duration of acupuncture	Acupuncture frequency	Medication frequency	Total period			Mean	Mean		Medication frequency	Total period	
Sun 2015, China	Consensus opinions on the diagnosis and treatment of inflammatory bowel disease	32	16/16	28–60	≤8 y	MA + mesalazine	RN3, RN4, RN6; ST25, SP15; BL25; ST36, ST37, SP6; LR3	30 min	NR	1 g p.o. Q.i.d	2 m	32	18/14	24–57	≤7 y	Mesalazine	1 g p.o. Q.i.d	2 m	ER, T cell subsets
Wang 2017, China	World gastroenterology organization practice guidelines for the diagnosis and management of IBD in 2010	35	NR	NR	NR	MA	RN12, ST25, RN6, ST36, SP6	30 min	Q.d	NR	4 w	35	NR	NR	NR	SASP	500 mg p.o. Q.i.d	4 w	ER, serum IL-6, IL-8, AR
Wang 2020, China	Diagnosis of chronic UC	39	22/17	44–54 49.27 ± 5.17	NR NR	MA + aminosalicylic acid	Sibian, ST25, RN4, RN6	15–20 min	NR	1-2# p.o. T.i.d	NR	39	25/14	45–61 53.13 ± 8.23	NR NR	Aminosalicylic acid	1-2# p.o. T.i.d	NR	Mayo score, AR
Wang 2021, China	Consensus opinions on the diagnosis and treatment of inflammatory bowel disease	98	46/52	– 37.32 ± 8.16	NR (13.14 ± 5.46) m	MA + mesalazine + flupentixton melitoxin	Guiyan (LU11, SP1)	20 min	NR	Mesalazine, 500 g p.o. T.i.d; flupentixton melitoxin (0.5 mg/10 mg), 1# p.o. Q.d	1 m	98	44/54	NR 38.16 ± 9.52	NR (13.62 ± 6.58) m	Mesalazine + flupentixton melitoxin	Mesalazine: 500 g p.o. T.i.d; flupentixton melitoxin (0. 5 mg/10 mg): 1# p.o. q.d.	1 m	ER, baron score, HADS scale, serum MMP –9, TMAO
Yan 2019, China	Diagnosis of chronic UC	41	25/16	24–61 42.5 ± 4.4	NR NR	MA	ST25, LR13, LI4, BL20, ST37	30 min	Q.d	NR	30 d	41	27/14	25–63 44.3 ± 4.6	NR NR	Mesalazine	1 g p.o. Q.i.d	30 d	ER
Zhang 2018, China	Diagnosis of chronic UC	50	26/24	35–69 45.6 ± 0.01	10 d–3 y (2.1 ± 0.01) y	MA	RN4, RN6, ST25, DU1, BL25	10–30 min	Q.o.d	NR	30 d	50	30/20	34–70 46.5 ± 0.5	9 d–2 y (1.2 ± 0.01) y	Metronidazole	0.2 g p.o. T.i.d	30 d	ER, AR
Zhao 2020, China	Diagnosis of chronic UC	75	35/40	NR	NR	MA	ST36, ST37, ST25, DU1, ST36, SP6, ST25	NR	Q.d	NR	10 d	75	42/33	NR	NR	Mesalazine	p.o. T.i.d	10 d	ER, AR, SF-36

3.3. Outcomes Evaluated. Fourteen of 16 trials evaluated clinical efficacy [42–49, 51–56], and 11 studies reported adverse reactions [42, 43, 46–50, 52, 54, 55, 57]. One trial [47] measured ACTH levels, and the other [51] conducted a patient satisfaction survey. One [43] recorded colonoscopic changes, one [46] collected the levels of TNF-α and IL-10, and one [45] measured T cell subsets (CD3, CD4, CD8, CD4/CD8). One trial [44] used the Hospital Anxiety and Depression Scale (HADS) scale and measured the disease activity index and serum matrix metalloproteinase (MMP)-9 and trimethylamine N-oxide (TMAO) levels. One trial [57] used Mayo scoring and two trials [44, 46] used Baron scoring to assess disease severity. Two trials [46, 48] measured serum IL-6 and IL-8 levels. Sixteen trials gathered data at the beginning and end of the intervention, and only one [49] collected data only at the end of the intervention. Curiously, none of the trials collected follow-up data after treatment.

3.4. Risk of Bias. Graphical summaries of the risk of bias in the included studies are shown in Figure 2.

3.4.1. Cochrane RoB Tool. The main source of bias risk was related to allocation concealment, blinding of participants and personnel, blinding of outcome assessment, and others. A low risk of bias was not present in any of the areas assessed in all trials. Twelve trials [42, 43, 45–49, 52–55, 57] were low risk in three bias risk areas. No item was mentioned for allocation concealment, blinding of outcome assessment, and other bias (Figures 2(a) and 2(b)).

(1) Random sequence generation. Thirteen trials had a low risk of randomization bias, and the remaining three trials [44, 51, 56] did not describe the randomization method.

(2) Allocation concealment. None of the trials reported assigning hidden methods, so we assessed their risk as "unclear."

(3) Blinding of participants and personnel and outcome assessment. Four trials [44–46, 55] mentioned that patients were informed of treatment, which we assessed as "high risk." The remaining 12 trials did not mention the blinding of patients and participants and were therefore assessed as "unclear risk." No trial described whether the outcome assessment was blind and were assessed as "unclear risk."

(4) Incomplete outcome data. One trial [50] had incomplete results, so it was assessed as "high risk."

(5) Selective reporting. Fifteen trials reported all data included in the results and had a low risk of bias. Only one [50] failed to report all pre-stated outcomes and were assessed as "high risk."

(6) Other potential sources. All trials did not describe other potential bias risks and were assessed as "one-sided risk."

3.4.2. Modified Jadad Scale. Thirteen studies [42, 43, 45–50, 52–55, 57] were of low quality and three were rated 0 [44, 51, 56] (Figure 2(c)).

3.5. Primary Outcome

3.5.1. Acupuncture Parameters. The pooled results shown in Figure 3 show the impact of MA parameters on efficacy.

(1) Duration of acupuncture. The pooled results shown in Figure 3(a) show that, using a fixed-effects model, retention of the needle for 10–30 minutes (RR 1.18, 95% CI [1.11, 1.26], $P < 0.01$; heterogeneity: $\chi^2 = 6.25$, df = 6 ($P = 0.40$), $I^2 = 4\%$) improved clinical efficacy at the end of treatment compared with medication.

(2) Acupuncture frequency. The pooled results shown in Figure 3(b) demonstrate that, using a fixed-effects model, compared with the control group, the frequency of MA [once a day (RR 1.18, 95% CI [1.10, 1.26], $P < 0.01$; heterogeneity: $\chi^2 = 6.94$, df = 5 ($P = 0.23$), $I^2 = 28\%$) or once every other day (RR 1.21, 95% CI [1.08, 1.35], $P < 0.01$; heterogeneity: $\chi^2 = 0.80$, df = 1 ($P = 0.37$), $I^2 = 0\%$)] both improved clinical efficacy at the end of treatment.

(3) Period of treatment. As shown in Figure 3(c), using a fixed-effects model, compared with the control group, the period of treatment [2 weeks (RR 1.17, 95% CI [1.06, 1.29], $P < 0.01$; heterogeneity: $\chi^2 = 0.24$, df = 1 ($P = 0.63$), $I^2 = 0\%$), 4 weeks (RR 1.25, 95% CI [1.11, 1.41], $P < 0.01$; heterogeneity: $\chi^2 = 0.16$, df = 2 ($P = 0.92$), $I^2 = 0\%$), and 8 weeks (RR 1.35, 95% CI [1.01, 1.81], $P = 0.04$)] all improved clinical efficacy at the end of treatment.

3.5.2. Acupuncture Type. As shown in Figure 4, using a fixed-effects model, MA (RR 1.18, 95% CI [1.11, 1.25], $P < 0.01$; heterogeneity: $\chi^2 = 6.19$, df = 7 ($P = 0.52$), $I^2 = 0\%$) increased clinical efficacy compared with medicines alone (Figure 4(a)). Furthermore, MA plus medicines (RR 1.26, 95% CI [1.13, 1.40], $P < 0.01$; heterogeneity: $\chi^2 = 0.95$, df = 2 ($P = 0.62$), $I^2 = 0\%$) and EA plus medicines (RR 1.36, 95% CI [1.13, 1.63], $P < 0.01$; heterogeneity: $\chi^2 = 0.13$, df = 1 ($P = 0.72$), $I^2 = 0\%$) both dramatically improved clinical efficacy (Figure 4(b)).

3.5.3. Type of Medical Therapy. As shown in Figure 5, using a fixed-effects model, the clinical efficacy of MA (RR 1.20, 95% CI [1.09, 1.32], $P < 0.01$; heterogeneity: $\chi^2 = 1.17$, df = 2 ($P = 0.56$), $I^2 = 0\%$) alone was greater than oral mesalazine at the end of the intervention (Figure 5(a)). MA plus mesalazine (RR 1.27, 95% CI [1.07, 1.50], $P < 0.01$; heterogeneity: $\chi^2 = 0.94$, df = 1 ($P = 0.33$), $I^2 = 0\%$) increased clinical efficacy compared with oral mesalazine (Figure 5(b)). MA plus metronidazole and sulfasalazine (RR 1.13, 95% CI [1.05, 1.21], $P < 0.01$; heterogeneity: $\chi^2 = 2.24$, df = 2 ($P = 0.33$), $I^2 = 11\%$) increased clinical efficacy compared with oral metronidazole and sulfasalazine

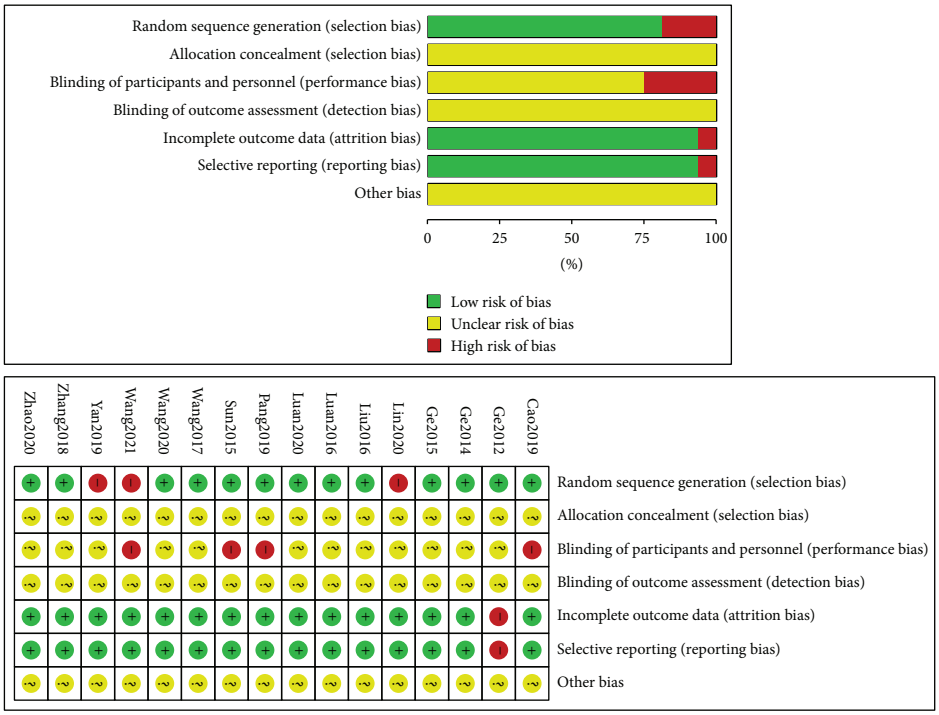

Author,Year	Modified Jadad scale Described as randomized:appropriate (+2) unclear (+1) inappropriate (0)	Method of randomization:appropriate (+2) unclear (+1) inappropriate (0)	Method of blinding:appropriate (+2) unclear (+1) inappropriate (0)	Description of withdrawals and dropouts : yes (+1) no(0)	Final Jadad score (maximum of 7)
Cao 2019	1	1	0	0	2
Ge 2012	1	1	0	0	2
Ge 2014	1	1	0	0	2
Ge 2015	1	1	0	0	2
Lin 2020	0	0	0	0	0
Liu 2016	1	1	0	0	2
Luan 2016	1	1	0	0	2
Luan 2020	1	1	0	0	2
Pang 2019	1	1	0	0	2
Sun 2015	1	1	0	0	2
Wang 2017	1	1	0	0	2
Wang 2020	1	1	0	0	2
Wang 2021	0	0	0	0	0
Yan 2019	0	0	0	0	0
Zhang 2018	1	1	0	0	2
Zhao 2020	1	1	0	0	2

Figure 2: Risk of bias in the included studies.

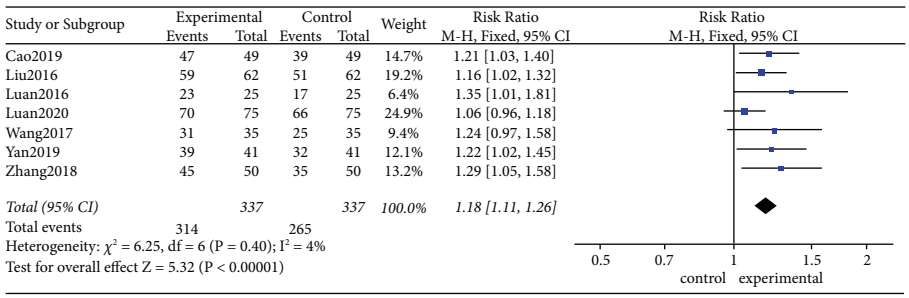

(a)

Figure 3: Continued.

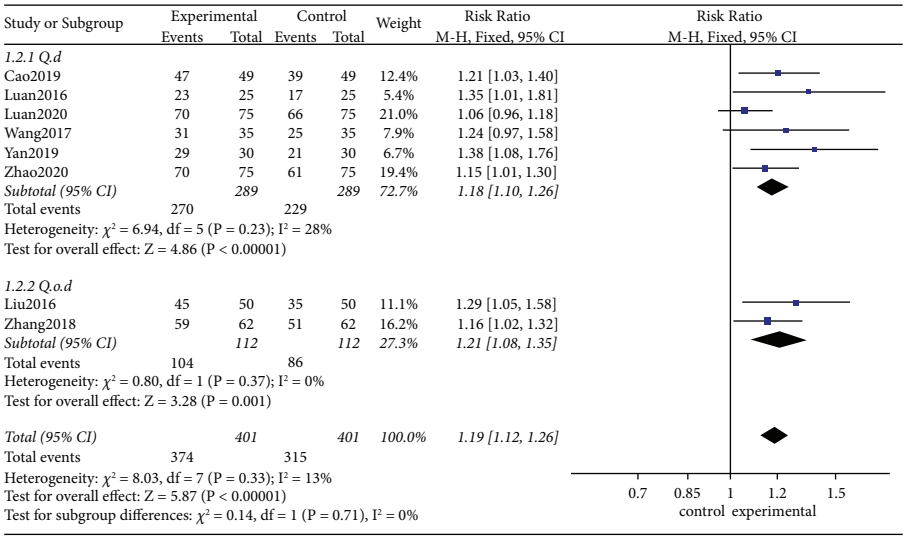

(b)

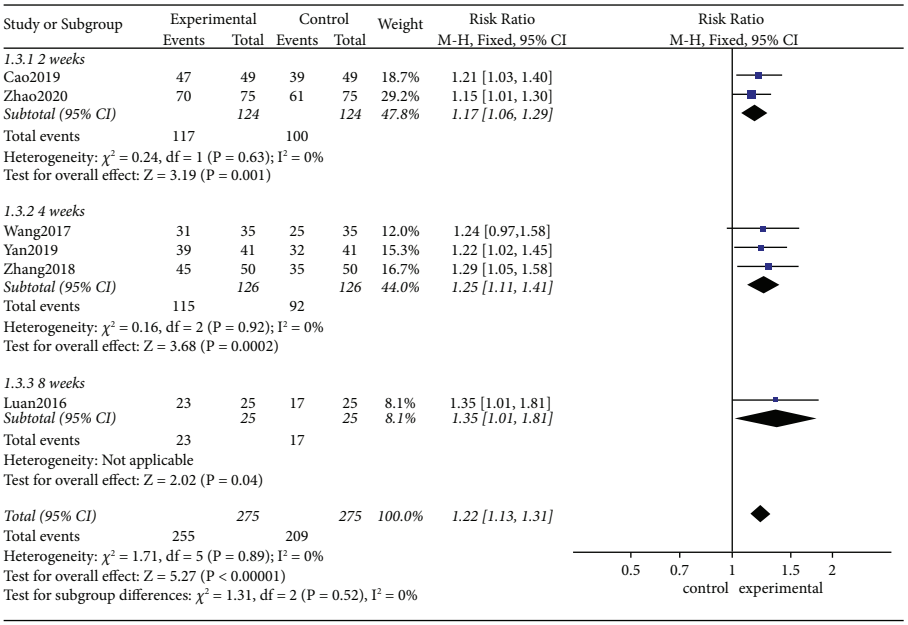

(c)

Figure 3: Impact of MA on clinical efficacy. (a) Effects of 10–30 minutes of acupuncture. (b) Effects of acupuncture frequency (once a day and once every other day). (c) Effects of a period of treatment (2 weeks, 4 weeks, and 8 weeks).

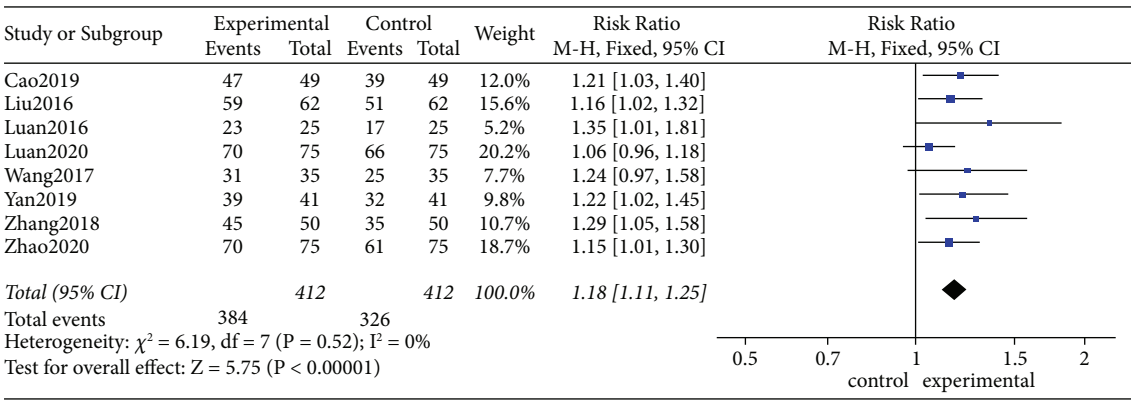

(a)

Figure 4: Continued.

Study or Subgroup	Experimental Events	Experimental Total	Control Events	Control Total	Weight	Risk Ratio M-H, Fixed 95% CI
2.3.1 MA + medicine versus medicine						
Pang2019	29	30	21	30	13.5%	1.38 [1.08, 1.76]
Sun2015	28	32	24	32	15.4%	1.17 [0.92, 1.48]
Wang2021	90	98	72	98	46.2%	1.25 [1.09, 1.43]
Subtotal (95% CI)		*160*		*160*	*75.0%*	*1.26 [1.13, 1.40]*
Total events	147		117			
Heterogeneity: $\chi^2 = 0.95$, df = 2 (P = 0.62); $I^2 = 0\%$						
Test for overall effect: Z = 4.27 (P < 0.0001)						
2.3.2 EA + medicine versus medicine						
Ge2014	29	31	22	31	14.1%	1.32 [1.03, 1.68]
Ge2015	24	25	17	25	10.9%	1.41 [1.07, 1.87]
Subtotal (95% CI)		*56*		*56*	*25.0%*	*1.36 [1.13, 1.63]*
Total events	53		39			
Heterogeneity: $\chi^2 = 0.13$, df = 1 (P = 0.72); $I^2 = 0\%$						
Test for overall effect: Z = 3.27 (P = 0.001)						
Total (95% CI)		*216*		*216*	*100.0%*	*1.28 [1.17, 1.40]*
Total events	200		156			
Heterogeneity: $\chi^2 = 1.60$, df = 4 (P = 0.81); $I^2 = 0\%$						
Test for overall effect: Z = 5.35 (P < 0.00001)						
Test for subgroup differences: $\chi^2 = 0.53$, df = 1 (P = 0.47), $I^2 = 0\%$						

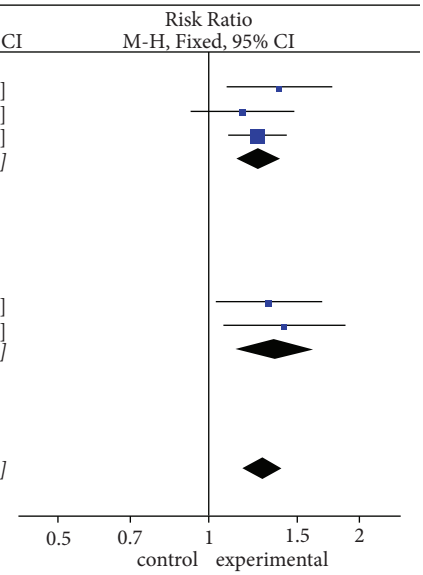

(b)

Figure 4: (a) Effects of MA versus medicines on clinical efficacy. (b) Effects of MA plus medicines versus medicines and EA plus medicines versus medicines on clinical efficacy.

Study or Subgroup	Experimental Events	Experimental Total	Control Events	Control Total	Weight	Risk Ratio M-H, Fixed, 95% CI
Luan2016	23	25	17	25	15.5%	1.35 [1.01, 1.81]
Yan2019	39	41	32	41	29.1%	1.22 [1.02, 1.45]
Zhao2020	70	75	61	75	55.5%	1.15 [1.01, 1.30]
Total (95% CI)		*141*		*141*	*100.0%*	*1.20 [1.09, 1.32]*
Total events	132		110			
Heterogeneity: $\chi^2 = 1.17$, df = 2 (P = 0.56); $I^2 = 0\%$						
Test for overall effect: Z = 3.66 (P = 0.0002)						

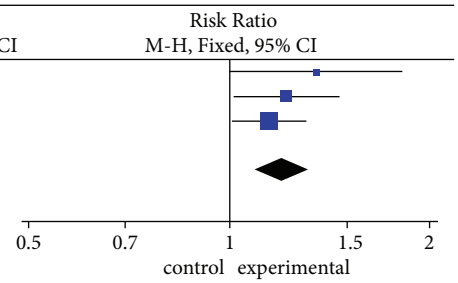

(a)

Study or Subgroup	Experimental Events	Experimental Total	Control Events	Control Total	Weight	Risk Ratio M-H, Fixed, 95% CI
Pang2019	29	30	21	30	46.7%	1.38 [1.08, 1.76]
Sun2015	28	32	24	32	53.3%	1.17 [0.92, 1.48]
Total (95% CI)		*62*		*62*	*100.0%*	*12.7 [1.07, 1.50]*
Total events	57		45			
Heterogeneity: $\chi^2 = 0.94$, df = 1 (P = 0.33); $I^2 = 0\%$						
Test for overall effect: Z = 2.72 (P = 0.007)						

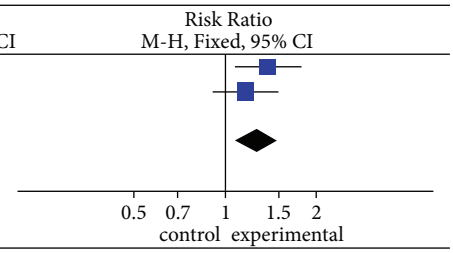

(b)

Study or Subgroup	Experimental Events	Experimental Total	Control Events	Control Total	Weight	Risk Ratio M-H, Fixed, 95% CI
Cao2019	47	49	39	49	25.0%	1.21 [1.03, 1.40]
Liu2016	59	62	51	62	32.7%	1.16 [1.02, 1.32]
Luan2020	70	75	66	75	42.3%	1.06 [0.96, 1.18]
Total (95% CI)		*186*		*186*	*100.0%*	*1.13 [1.05, 1.21]*
Total events	176		156			
Heterogeneity: $\chi^2 = 2.24$, df = 2 (P = 0.33); $I^2 = 11\%$						
Test for overall effect: Z = 3.29 (P = 0.001)						

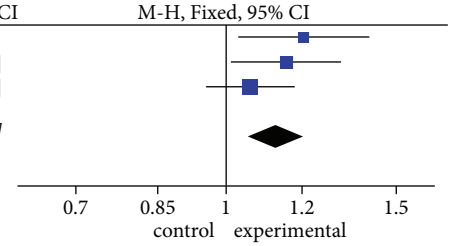

(c)

Figure 5: Continued.

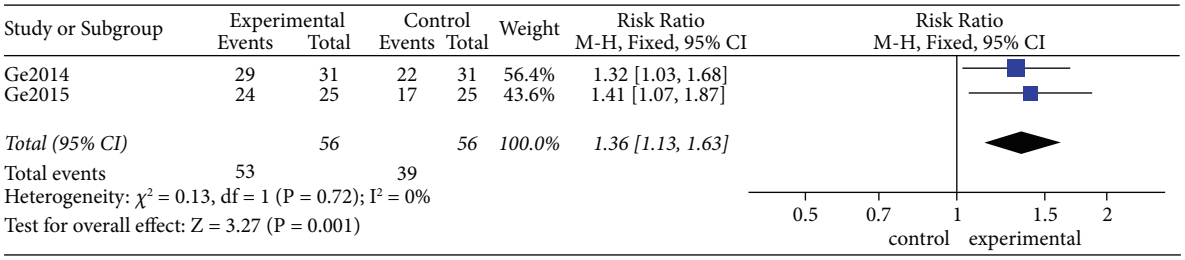

(d)

Figure 5: (a) Effects of MA versus mesalazine on clinical efficacy. (b) Effects of MA plus mesalazine versus mesalazine on clinical efficacy. (c) Effects of MA plus (metronidazole + sulfasalazine) versus metronidazole + sulfasalazine on clinical efficacy. (d) Effects of EA plus sulfasalazine versus sulfasalazine on clinical efficacy.

(Figure 5(c)). Similarly, EA plus sulfasalazine (RR 1.36, 95% CI [1.13, 1.63], $P < 0.01$; heterogeneity: $\chi^2 = 0.13$, df = 1 ($P = 0.72$), $I^2 = 0\%$) was more effective than oral sulfasalazine (Figure 5(d)).

3.6. Secondary Outcomes

3.6.1. Adverse Events. As shown in Figure 6(a), using a fixed-effects model, use of MA/EA (RR 0.33, 95% CI [0.18, 0.59], $P < 0.01$; heterogeneity: $\chi^2 = 0.43$, df = 4 ($P = 0.98$), $I^2 = 0\%$) resulted in fewer adverse reactions than medical therapies. However, in the pooled random-effects model results shown in Figure 6(b), compared with medicines, MA/EA plus medicines (RR 0.72, 95% CI [0.35, 1.49], $P = 0.38$; heterogeneity: $\chi^2 = 10.82$, df = 4 ($P = 0.03$), $I^2 = 63\%$) had no significant impact on adverse events.

3.6.2. Baron Scores. As shown in Figure 7, using a fixed-effects model, use of MA plus medicines (RR 1.31, 95% CI [1.03, 1.58], $P < 0.01$; heterogeneity: $\chi^2 = 0.51$, df = 1 ($P = 0.48$), $I^2 = 0\%$) significantly reduced Baron scores.

3.7. Publication Bias. The pooled results shown in Supplementary S2: Figures S1–S5 show an asymmetrical funnel plot and significant Egger's test (10–30 minutes: $P = 0.008$; once a day: $P = 0.013$) for acupuncture parameters, suggesting that there may be reporting bias, perhaps through the publication of positive results and small sample sizes.

The pooled results shown in Supplementary S2: Figures S6–S8 show an asymmetrical funnel plot and significant Egger's test ($P = 0.005$) for acupuncture type with respect to clinical efficacy.

The pooled results shown in Supplementary S2: Figures S9-S10 show a symmetric funnel plot and non-significant Egger's test ($P = 0.801$) for the adverse events of MA/EA versus medicines, suggesting no obvious publication bias. Nevertheless, the small amount of included studies may have reduced the accuracy of the results.

By reason of the limited amount of studies included, publication bias for other outcomes was not assessed.

3.8. Sensitivity Analysis. The robustness of the combined results of MA/EA plus medicines vs medicines alone on adverse events was verified by sensitivity analysis (Figure 8), with each included study excluded in sequence. When the study by Wang et al. [47] was excluded (Figure 9), the combined results of MA/EA plus medicines vs medicines on adverse events was not significant (RR 1.06, 95% CI [0.64, 1.73], $P = 0.83$; heterogeneity: $\chi^2 = 0.82$, df = 3 ($P = 0.84$), $I^2 = 0\%$), suggesting imbalance from this study.

4. Discussion

Here we focused on MA/EA, two widely used acupuncture interventions across the world, to explore the influence of their administration parameters on clinical efficacy in patients with UC and the advantage of using them with the usual standard of care drugs to support the promotion and application of MA/EA in clinical practice.

4.1. Outcomes

4.1.1. Primary Outcomes. Our study suggests that the impact of MA/EA in patients with UC may be related to the operation parameters used. We therefore explored the impact of the duration of acupuncture retention, frequency of treatment, and duration of treatment in subgroup analyses. With respect to the duration of acupuncture retention, 10–30 minutes significantly enhanced the clinical effect. One treatment every other day seemed to have a slight advantage over daily treatment, and 8 weeks of acupuncture had a slight advantage over shorter treatments in improving the clinical symptoms of UC. Therefore, we hypothesize that 10–30 minutes of acupuncture retention, every other day for 8 weeks, probably represents the optimal protocol informed by existing evidence for the application of MA to patients with UC. In addition, only one study [51] used EA alone as an intervention, with a frequency of 4 times per second, a retention time of 20 minutes, and a treatment course of 30 days once every other day. The results showed clinical efficacy was superior in the acupuncture group than in the medicine group ($P < 0.01$).

Both MA and EA further improved the clinical symptoms and clinical efficacy in UC patients taking pharmaceutical therapies. Furthermore, EA appears to have a

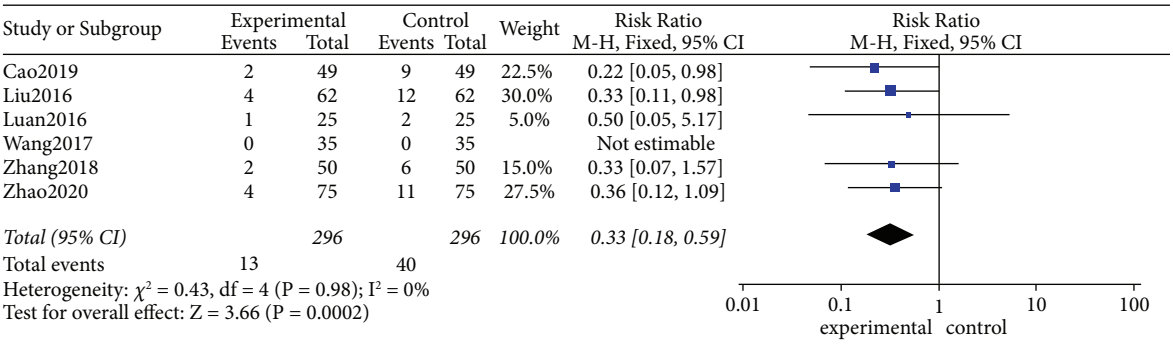

(a)

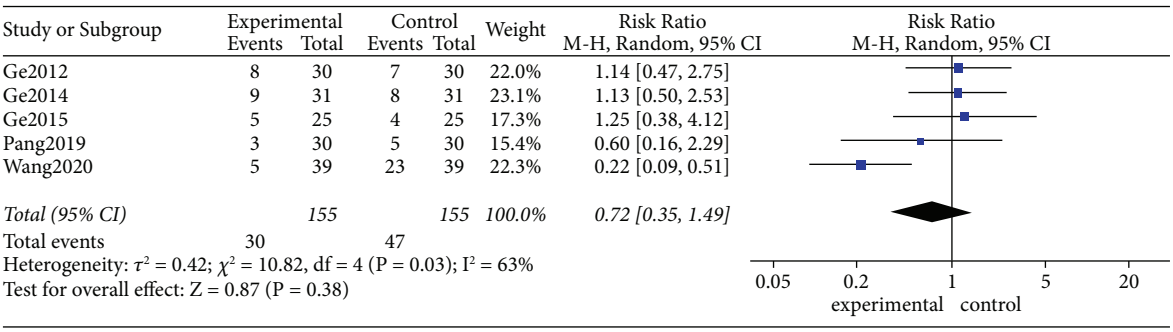

(b)

Figure 6: (a) Effects of MA/EA versus medicines on adverse events. (b) Effects of MA/EA plus medicines versus medicines on adverse events.

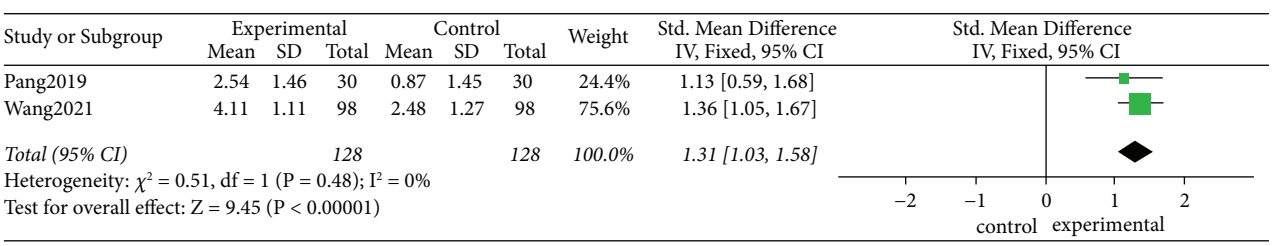

Figure 7: Effects of MA plus medicines versus medicines on baron scores.

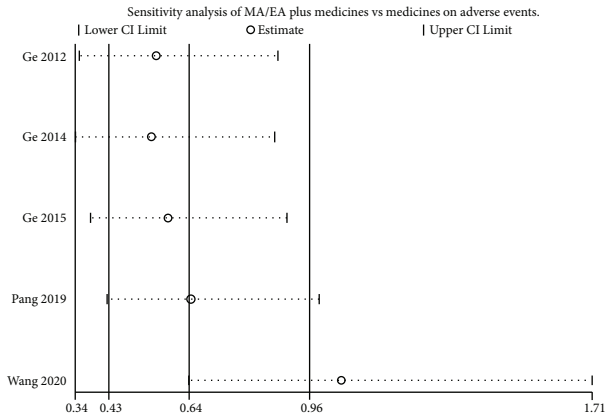

Figure 8: Sensitivity analysis of MA/EA plus medicines vs medicines on adverse events.

Study or subgroup	Experimental Events	Experimental Total	Control Events	Control Total	Weight	Risk Ratio M-H, Random, 95% CI
Ge 2012	8	30	7	30	31.8%	1.14 [0.47, 2.75]
Ge 2014	9	31	8	31	37.3%	1.13 [0.50, 2.53]
Ge 2015	5	25	4	25	17.3%	1.25 [0.38, 4.12]
Pang 2019	3	30	5	30	13.7%	0.60 [0.16, 2.29]
Wang 2020	5	39	23	39	0.0%	0.22 [0.09, 0.51]
Total (95% CI)		116		116	100.0%	1.06 [0.64, 1.73]
Total events	25		24			

Heterogeneity: $\tau^2 = 0.00$; $\chi^2 = 0.82$, df = 3 (P = 0.84); $I^2 = 0\%$
Test for overall effect: Z = 0.22 (P = 0.83)

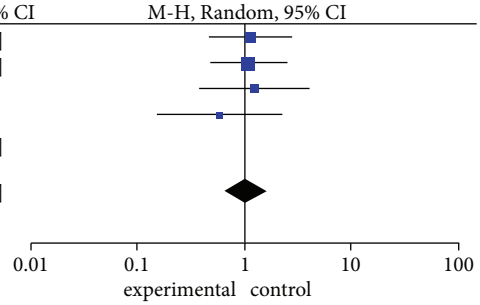

Figure 9: Effects of MA/EA plus medicines versus medicines on adverse events (excluded the study by Wang et al.).

therapeutic advantage over MA. In addition, MA/EA combined with medicine appears to be effective in UC as a combined approach. In subgroup analyses, MA plus metronidazole and sulfasalazine was more effective than metronidazole and sulfasalazine; EA plus sulfasalazine was more effective than sulfasalazine; and MA was more effective than mesalazine either alone or in combination.

4.1.2. Secondary Outcomes. In the subgroup analysis, MA/EA more effectively reduced adverse reactions than the control group and there was no statistically significant difference in the combined MA/EA plus medicine subgroup. Considering the small sample size and high risk of bias, the subgroup analysis of MA/EA plus medicine needs interpreting with caution.

In terms of endoscope-related index scores, Baron scores for endoscopic severity changed more after MA was given with pharmaceuticals, suggesting a synergistic effect of MA plus pharmaceutical therapies in treating UC.

4.2. Strengths of this Review. First, this study was carried out according to PRISMA 2020 guidelines [33] and, using the PICOS framework, we strictly regulated study inclusion to ensure the quality of assessed RCTs. Second, our study focused on acupuncture parameters. Like the dose of a medicine, acupuncture parameters play an important role in the therapeutic outcome. Our results provide a first step towards the standardization of acupuncture protocols and the motivation to ensure uniformity of acupuncture treatment effects, which would help in the application and promotion of acupuncture therapy. Therefore, we focused on the influence of acupuncture parameters on clinical outcomes in patients with UC. Third, we discussed the additive effects of MA/EA when administered with some medicines and their adverse events to explore the potential of acupuncture as combined therapy with regular, standard of care medications. Fourth, we also included the evaluation of endoscopic symptoms, since endoscopy is central to disease monitoring via changes in intestinal mucosa and plays a very important role in the treatment of UC. Fifth, the heterogeneity of the results was "low", and we included a comprehensive assessment of reporting bias. Finally, the GRADE framework was used to evaluate the overall quality of evidence [41].

4.3. Limitations of this Review. Several limitations were found in this meta-analysis. First, the inclusion criteria were strict and the number and sample size of included RCTs were small, which may have biased the results. Second, none of the included trials were conducted outside China, so there was significant publication bias. Nevertheless, this also highlights that acupuncture treatment for UC has not received due attention in clinical practice in other countries and contexts. Third, the included literature was deficient in blinding. At present, due to the way in which acupuncture is administered, blinding is difficult in practice in most studies. Fourth, the acupuncture parameters included in the literature were not comprehensive, which may be related to the subjective nature of treatment by acupuncturists and/or patients resulting in clinical differences in acupuncture parameters. Therefore, only the parameters available in the relevant literature were tentatively analyzed in our study. Fifth, the included literature generally paid little attention to endoscopic features or effects, which might be overcome with further developments in endoscopy. Finally, no study included extended follow-up, so the long-term effects of MA/EA and its parameters on UC are unclear.

4.4. Implications for Practice. We found differences in acupuncture parameters between different studies. Previous studies have shown that a satisfactory therapeutic outcome is inseparable from the acupuncture parameters used, and different acupuncture frequencies, waveforms, intensities [58], and durations play an important role in treatment [2, 59, 60]. Although we provide a set of optimal parameters for acupuncture treatment of UC, this can only be considered a preliminary estimate on the strength of a small amount of low quality and biased studies. We suggest that there is a need for MA/EA studies to examine acupuncture methods and techniques [61] including comprehensive evaluations of manipulation, frequency, current intensity, wave pattern, duration of acupuncture, period of treatment, and needle characteristics. Such studies would help to reduce the variable impact of subjective acupuncture factors on clinical outcomes, thus improving clinical efficacy and promoting the development of highly reproducible, evidence-based acupuncture for UC.

Our results suggest that MA/EA is an effective monotherapy, with fewer adverse reactions than conventional

drugs. We found that EA has a slight advantage over MA. In addition, MA/EA may be a good complement to, or even a possible replacement for, mesalazine and SASP, which provides the potential for reducing UC drug therapy for UC patients. There are few reports on the use of MA/EA alone in UC, and areas that would benefit from high-quality clinical studies.

MA appears to improve the features of intestinal mucosa inflammation as seen with endoscopy, but further high-quality evidence would be useful. Therefore, we suggest that colonoscopy with the histopathological evaluation of the intestinal mucosa should be included in any study of acupuncture treatment for UC.

4.5. Implications for Research. Given the above clinical implications, there is a crying need to improve the quality of clinical trials studying the acupuncture treatment of UC. We therefore provide the following recommendations. First, any RCT should report according to the CONSORT statement [62] and the reporting standards of acupuncture clinical trials [63]. Second, there needs to be a focus on the operating parameters of acupuncture to establish optimal parameter protocols for clinical deployment. Third, the diagnosis, grading, and inclusion of UC patients should be unified according to common standards, preferably using the endoscopic examination. Fourth, trials must be multi-center, adequately powered, include longer-term follow-up, and actively include non-Chinese institutions to promote the generalizability of results. Finally, it is recommended that clinicians, acupuncturists, endoscopists, examiners, and other stakeholders be consulted during the study design phase to select the best practice plan and reduce the impact of subjective differences on the results.

5. Conclusions

In conclusion, our study provides the latest evidence to guide possible optimal parameters for MA: 10–30 min retention, every other day, for 8 weeks. The low number of adverse reactions and high efficacy means that MA/EA can be used as a supplement or even replacement for SASP and mesalazine. Uncertainty over the administration parameters of acupuncture may be an important factor limiting the promotion of acupuncture as a potential UC treatment in clinical practice despite overall evidence of efficacy.

Abbreviations

M/F: Male/female
y: Year
m: Month
w: Week
d: Day
UC: Ulcerative colitis
tot: Total
MA: Manual acupuncture
EA: Electroacupuncture
SASP: Sulfasalazine
Q.D: Quaque die
T.I.D: Third in die
Q.I.D: Quarter in die
Q.O.D: Quaque omni die
CW: Continuous wave
P.O: Per os
NR: Not reported
ER: Effective rate
AR: Adverse reaction.

Conflicts of Interest

The authors declare that they have no conflicts of interest.

Authors' Contributions

Min'an Chen and Sisi Zhao contributed equally to this work. Min'an Chen and Sisi Zhao conceived the study and performed the English searches, search screening, data extraction, and risk of bias assessment on English language papers as well as data entry, meta-analysis, and drafting the manuscript. Yu Guo helped conceptualize the study and perform risk of bias assessments of the included papers. Luxi Cao helped with data extraction and provided input into the manuscript. Hai Zeng helped perform risk of bias assessments. Zhuowen Lin and Shiqi Wang assisted with screening, data extraction, and risk of bias assessments and provided input into the manuscript. Min'an Chen and Sisi Zhao contributed equally to this work.

Acknowledgments

This work was supported by the National Natural Science Foundation of China (nos. 81873362 and 82174483), the Natural Science Foundation of Guangdong Province, China (no. 2114050002002), and the Regional Joint Foundation of Guangdong province (no. 32221048).

Supplementary Materials

Supplementary S1: search strategy for different databases. Supplementary S2: funnel plot and Egger's test graphs of outcomes. Supplementary S3: GRADE Quality evaluation form. Supplementary S4: PRISMA_2020_checklist. (*Supplementary Materials*)

References

[1] I. Ordás, L. Eckmann, M. Talamini, D. C. Baumgart, and W. J. Sandborn, "Ulcerative colitis," *Lancet*, vol. 380, no. 9853, pp. 1606–1619, 2012.
[2] Y. Zhang, S. Yang, X. Fan et al., "Orthogonal design to sift the optimal parameter of neiguan acupuncture for cerebral infarction," *Neural Regeneration Research*, vol. 8, no. 28, pp. 2641–2648, 2013.
[3] T. Kobayashi, B. Siegmund, C. Le Berre et al., "Ulcerative colitis," *Nature Reviews Disease Primers*, vol. 6, no. 1, p. 74, 2020.
[4] J. Cosnes, C. Gower-Rousseau, P. Seksik, and A. Cortot, "Epidemiology and natural history of inflammatory bowel diseases," *Gastroenterology*, vol. 140, no. 6, pp. 1785–1794, 2011.

[5] A. Murray, T. M. Nguyen, C. E. Parker, B. G. Feagan, and J. K. MacDonald, "Oral 5-aminosalicylic acid for maintenance of remission in ulcerative colitis," *Cochrane Database of Systematic Reviews*, vol. 8, no. 8, Article ID Cd000544, 2020.

[6] M. Salice, F. Rizzello, C. Calabrese, L. Calandrini, and P. Gionchetti, "A current overview of corticosteroid use in active ulcerative colitis," *Expert Review of Gastroenterology & Hepatology*, vol. 13, no. 6, pp. 557–561, 2019.

[7] P. Sehgal, J.-F. Colombel, A. Aboubakr, and N. Narula, "Systematic review: safety of mesalazine in ulcerative colitis," *Alimentary Pharmacology & Therapeutics*, vol. 47, no. 12, pp. 1597–1609, 2018.

[8] J. Langhorst, H. Wulfert, R. Lauche et al., "Systematic review of complementary and alternative medicine treatments in inflammatory bowel diseases," *Journal of Crohn's and Colitis*, vol. 9, no. 1, pp. 86–106, 2015.

[9] World Health Organization, *WHO Traditional medicine strategy: 2014-2023*, World Health Organization, Geneva, Switzerland, 2013.

[10] C. M. Witt, D. Pach, B. Brinkhaus et al., "Safety of acupuncture: results of a prospective observational study with 229, 230 patients and introduction of a medical information and consent form," *Complementary Medicine Research*, vol. 16, no. 2, pp. 91–97, 2009.

[11] S. Joos, N. Wildau, R. Kohnen et al., "Acupuncture and moxibustion in the treatment of ulcerative colitis: a randomized controlled study," *Scandinavian Journal of Gastroenterology*, vol. 41, no. 9, pp. 1056–1063, 2006.

[12] C. Zhang, M. Jiang, and A. Lu, "Considerations of traditional chinese medicine as adjunct therapy in the management of ulcerative colitis," *Clinical Reviews in Allergy and Immunology*, vol. 44, no. 3, pp. 274–283, 2013.

[13] C. Yang and H. Yan, "Observation of the efficacy of acupuncture and moxibustion in 62 cases of chronic colitis," *Journal of traditional Chinese Medicine*, vol. 19, no. 2, pp. 111–114, 1999.

[14] H. Li, T. He, Q. Xu et al., "Acupuncture and regulation of gastrointestinal function," *World Journal of Gastroenterology*, vol. 21, no. 27, pp. 8304–8313, 2015.

[15] J. Ji, Y. Lu, H. Liu et al., "Acupuncture and moxibustion for inflammatory bowel diseases: a systematic review and meta-analysis of randomized controlled trials," *Evidence-Based Complementary and Alternative Medicine*, vol. 2013, Article ID 158352, 11 pages, 2013.

[16] X. Wang, N.-Q. Zhao, Y.-X. Sun et al., "Acupuncture for ulcerative colitis: a systematic review and meta-analysis of randomized clinical trials," *BMC Complementary Medicine and Therapies*, vol. 20, no. 1, p. 309, 2020.

[17] T. Zhang, "Meta-analysis and trial sequential analysis of acupuncture combined with moxibustion in the treatment of ulcerative colitis," *World Journal of Integrated Traditional and Western Medicine*, vol. 16, no. 04, pp. 599–606, 2021.

[18] L.-l. Zhang, Q. Chu, S. Wang, H. Lai, and B.-B. Xie, "Is sham acupuncture as effective as traditional Chinese acupuncture? It's too early to say," *Chinese Journal of Integrative Medicine*, vol. 22, no. 7, pp. 483–489, 2016.

[19] G. Xu, "Current status and progress of quantitative research on acupuncture manipulation parameters," *Chinese Archives of Traditional Chinese Medicine*, vol. 35, no. 09, pp. 2255–2258, 2017.

[20] Y. P. Wang, "Research progress in quantification of acupuncture manipulation stimulation," *Shanghai Journal of Acupuncture and Moxibustion*, vol. 25, no. 04, pp. 47–50, 2006.

[21] S. li, "Research progress on quantification of acupuncture manipulative stimulation based on kinematics and dynamics," *Chinese Medicine Modern Distance Education of China*, vol. 19, no. 14, pp. 204–208, 2021.

[22] J.-F. Fang, J.-Y. Du, X.-M. Shao, J.-Q. Fang, and Z. Liu, "Effect of electroacupuncture on the NTS is modulated primarily by acupuncture point selection and stimulation frequency in normal rats," *BMC Complementary and Alternative Medicine*, vol. 17, no. 1, p. 182, 2017.

[23] K. Wang, Y. Xu, Y. Niu et al., "Effects of varying acupuncture manipulations at ST36 (zusanli) on gastric electrical frequency and amplitude in bradygastria rabbits," *Evidence-Based Complementary and Alternative Medicine: eCAM*, vol. 2020, Article ID 9357120, 9 pages, 2020.

[24] N. N. Yang, S. M. Ma, J. W. Yang, T. R. Li, and C. Z. Liu, "Standardizing therapeutic parameters of acupuncture in vascular dementia rats," *Brain and Behavior*, vol. 10, no. 10, Article ID e01781, 2020.

[25] G. Xu, Q. Xi, W. Tang et al., "Effect of different twirling and rotating acupuncture manipulation techniques on the blood flow perfusion at acupoints," *Journal of Traditional Chinese Medicine*, vol. 39, no. 5, pp. 730–739, 2019.

[26] H. Nakahara, T. Kawada, S.-Y. Ueda et al., "Acupoint dependence of depressor and bradycardic responses elicited by manual acupuncture stimulation in humans," *Journal of Physiological Sciences*, vol. 69, no. 6, pp. 1077–1084, 2019.

[27] R. Lyu, M. Gao, H. Yang, Z. Wen, and W. Tang, "Stimulation parameters of manual acupuncture and their measurement." *Evidence-Based Complementary and Alternative Medicine*, vol. 2019, Article ID 1725936, 10 pages, 2019.

[28] X.-B. Chang, S. Wang, Z.-H. Meng, X.-N. Fan, X. Yang, and X.-M. Shi, "Study on acupuncture parameters impacting on the acupuncture effect using cluster analysis in a rat model with middle cerebral artery occlusion," *Chinese Journal of Integrative Medicine*, vol. 20, no. 2, pp. 130–135, 2014.

[29] C. Zheng, G. Huang, X. Xu et al., "Electro-acupuncture with different current intensities to treat functional constipation: a study protocol for a randomized controlled trial," *Trials*, vol. 14, no. 1, p. 344, 2013.

[30] Y. J. Park and J. M. Lee, "Effect of acupuncture intervention and manipulation types on poststroke dysarthria: a systematic review and meta-analysis," *Evidence-Based Complementary and Alternative Medicine*, vol. 2020, Article ID 4981945, 17 pages, 2020.

[31] H. MacPherson, E. A. Vertosick, N. E. Foster et al., "The persistence of the effects of acupuncture after a course of treatment: a meta-analysis of patients with chronic pain," *Pain*, vol. 158, no. 5, pp. 784–793, 2017.

[32] C. Li, Q. Pei, Y. Chen et al., "The response-time relationship and covariate effects of acupuncture for chronic pain: a systematic review and model-based longitudinal meta-analysis," *European Journal of Pain*, vol. 24, no. 9, pp. 1653–1665, 2020.

[33] M. J. Page, J. E. McKenzie, P. M. Bossuyt et al., "The PRISMA 2020 statement: an updated guideline for reporting systematic reviews," *BMJ*, vol. 372, p. n71, 2021.

[34] J. D. Feuerstein, K. L. Isaacs, Y. Schneider et al., "AGA clinical practice guidelines on the management of moderate to severe ulcerative colitis," *Gastroenterology*, vol. 158, no. 5, pp. 1450–1461, 2020.

[35] C. W. Ko, S. Singh, J. D. Feuerstein et al., "AGA clinical practice guidelines on the management of mild-to-moderate ulcerative colitis," *Gastroenterology*, vol. 156, no. 3, pp. 748–764, 2019.

[36] Spleen and Stomach Diseases Branch of China Association of Chinese Medicine, "Consensus on TCM diagnosis and treatment of ulcerative colitis (2009)," *Chinese Journal of Integrated Traditional and Western Medicine*, vol. 30, no. 5, pp. 527–532, 2010.

[37] A. P. Siddaway, A. M. Wood, and L. V. Hedges, "How to do a systematic review: a best practice guide for conducting and reporting narrative reviews, meta-analyses, and meta-syntheses," *Annual Review of Psychology*, vol. 70, no. 1, pp. 747–770, 2019.

[38] M. W.-L. Cheung and R. Vijayakumar, "A guide to conducting a meta-analysis," *Neuropsychology Review*, vol. 26, no. 2, pp. 121–128, 2016.

[39] J. L. Peters, A. J. Sutton, D. R. Jones, K. R. Abrams, and L. Rushton, "Contour-enhanced meta-analysis funnel plots help distinguish publication bias from other causes of asymmetry," *Journal of Clinical Epidemiology*, vol. 61, no. 10, pp. 991–996, 2008.

[40] J. A. C. Sterne, D. Gavaghan, and M. Egger, "Publication and related bias in meta-analysis," *Journal of Clinical Epidemiology*, vol. 53, no. 11, pp. 1119–1129, 2000.

[41] G. H. Guyatt, A. D. Oxman, G. E. Vist et al., "GRADE: an emerging consensus on rating quality of evidence and strength of recommendations," *BMJ*, vol. 336, no. 7650, pp. 924–926, 2008.

[42] F. Ge, Y. Ji, and X. P. Ma, "Clinical effect observation of electroacupuncture combined with medicine in the treatment of ulcerative colitis," *China Modern Medicine*, vol. 22, no. 06, pp. 164–168, 2015.

[43] B. Y. Luan, "Clinical effect of acupuncture in the treatment of ulcerative colitis," *Asia-Pacific Traditional Medicine*, vol. 12, no. 20, pp. 90-91, 2016.

[44] Y. Wang, "Efficacy analysis of mesalazine and flupentixol melitoxin combined with acupuncture at Guiyan point in the treatment of ulcerative colitis," *Journal of Aerospace Medicine*, vol. 32, no. 01, pp. 78–80, 2021.

[45] B. Sun, "Effect of acupuncture on T cell subsets in patients with ulcerative colitis," *Asia-Pacific Traditional Medicine*, vol. 11, no. 24, pp. 104-105, 2015.

[46] H. M. Pang, "Clinical study on regulating qi needling method at baliao point combined with mesalazine for ulcerative colitis at active stage," *Journal of New Chinese Medicine*, vol. 51, no. 11, pp. 209–213, 2019.

[47] F. Ge, "Study of the mechanism of electroacupuncture combined with drugs in treating UC on the brain gut axis--31 cases," *Jiangsu Journal of Traditional Chinese Medicine*, vol. 46, no. 12, pp. 65–67, 2014.

[48] Y. N. Wang and L. L. Qiu, "Clinical effect of wentong acupuncture on ulcerative colitis with deficiency of spleen and kidney yang," *Inner Mongolia Journal of Traditional Chinese Medicine*, vol. 36, no. Z2, pp. 140-141, 2017.

[49] L. Zhao, "Therapeutic effect of acupuncture of traditional Chinese medicine on chronic ulcerative colitis," *China Health Care Nut*, vol. 30, no. 13, p. 1, 2020.

[50] F. Ge, X. P. Ma, and M. B. Xiao, "Effect of electroacupuncture combined with sulfasyridine salazide on ulcerative colitis," *Medical Journal of Communications*, vol. 26, no. 2, pp. 173-174, 2012.

[51] H. Lin, "30 cases of ulcerative colitis were treated with "tong" technique," *Diet Health*, no. 43, p. 102, 2020.

[52] X. H. Liu, "Clinical effect of acupuncture and moxibustion of traditional chinese medicine in the treatment chronic ulcerative colitis," *Guangming Journal of Chinese Medicine*, vol. 31, no. 21, pp. 3173-3174, 2016.

[53] N. Luan and Q. Wang, "Observation of effect on acupuncture of traditional Chinese medicine in the treatment chronic ulcerative colitis," *Psychological Monthly*, vol. 15, no. 11, p. 190, 2020.

[54] C. Y. Zhang, "Therapeutic effect of acupuncture on chronic ulcerative colitis," *Diet Health*, vol. 5, no. 2, pp. 110-111, 2018.

[55] H. Y. Cao, "Therapeutic effect of acupuncture and moxibustion on chronic ulcerative colitis," *Chinese Baby*, no. 9, p. 61, 2019.

[56] W. C. Yan, "Clinical observation of acupuncture in the treatment of ulcerative colitis," *Our Health*, no. 1, p. 15, 2019.

[57] R. M. Wang, "Therapeutic effect of acupuncture on patients with chronic ulcerative colitis," *Diet Health*, no. 50, p. 94, 2020.

[58] Y. Y. Zhang, Q. L. Chen, Q. Wang et al., "Role of parameter setting in electroacupuncture: current scenario and future prospects," *Chinese Journal of Integrative Medicine*, 2020.

[59] L. Zhang, H. Lai, L. Li et al., "Effects of acupuncture with needle manipulation at different frequencies for patients with hypertension: result of a 24- week clinical observation," *Complementary Therapies in Medicine*, vol. 45, pp. 142–148, 2019.

[60] L.-L. Gao, Y. Guo, T. Sha et al., "Differential effects of variable frequencies of manual acupuncture at ST36 in rats with atropine-induced inhibition of gastric motility," *Acupuncture in Medicine*, vol. 34, no. 1, pp. 33–39, 2016.

[61] W. L. Liu and W. F. Zhu, "Standardization of acupuncture and moxibustion methods and techniques," *Journal of Clinical Acupuncture and Moxibustion*, vol. 15, no. 11, pp. 4-5, 1999.

[62] K. F. Schulz, D. G. Altman, D. Moher, and CONSORT Group, "CONSORT 2010 statement: updated guidelines for reporting parallel group randomized trials," *Annals of Internal Medicine*, vol. 152, no. 11, pp. 726–732, 2010.

[63] H. MacPherson, D. G. Altman, R. Hammerschlag et al., "Revised standards for reporting interventions in clinical trials of acupuncture (STRICTA): extending the CONSORT statement," *PLoS Medicine*, vol. 7, no. 6, Article ID e1000261, 2010.

Hindawi
Evidence-Based Complementary and Alternative Medicine
Volume 2022, Article ID 2497430, 11 pages
https://doi.org/10.1155/2022/2497430

Research Article

Electroacupuncture Alleviates Visceral Hypersensitivity in IBS-D Rats by Inhibiting EGCs Activity through Regulating BDNF/TrkB Signaling Pathway

Ying Zhao,[1] Hui-ling Jiang,[1] Yu Shi,[2] Wei Zhang,[3] Lei-xiao Zhang,[4] Yu-jun Hou,[1] Zuo-qin Yang,[5] Bao-yu He,[2] Fan-rong Liang,[1] and Qian-hua Zheng[1]

[1]*Acupuncture and Tuina School of Chengdu University of Traditional Chinese Medicine, Chengdu, Sichuan 610075, China*
[2]*Department of Chongqing Beibei Traditional Chinese Medical Hospital, Chongqing, China*
[3]*Department of Traditional Chinese Medicine, The People's Hospital of Shifang, Shifang, China*
[4]*Department of Integrated Traditional and Western Medicine, West China Hospital, Sichuan University, Chengdu 610041, China*
[5]*Department of Acupuncture and Moxibustion, Chengdu Pidu District Hospital of Traditional Chinese Medicine, Chengdu, China*

Correspondence should be addressed to Qian-hua Zheng; zhengqianhua@cdutcm.edu.cn

Received 10 September 2021; Accepted 17 January 2022; Published 14 February 2022

Academic Editor: Swee Keong Yeap

Objective. To determine whether electroacupuncture (EA) could alleviate visceral hypersensitivity in diarrhea-predominant irritable bowel syndrome (IBS-D) rats by inhibiting EGCs activity via the BDNF/TrkB signaling pathway. *Methods.* Sprague Dawley rats were randomly divided to a control group ($n = 8$) and a model preparation group ($n = 32$), which received Senna solution by gavage and CUMS (chronic unpredictable mild stress) for 14 consecutive days and was further divided to a Model group, an EA group (only electroacupuncture), an EA + TrkB agonist group (electroacupuncture and TrkB), and an EA + DMSO group (electroacupuncture and DMSO, $n = 8$ for each). Rats in the three EA groups were acupunctured at ST25, ST36, and LR3 for 20 min every day for 14 days. Abdominal withdrawal reflex (AWR) was used to quantify visceral sensitivity; reverse transcription polymerase chain reaction (RT-PCR) and double immunofluorescent staining were used to detect the colocalized expression of GFAP/BDNF and GFAP/TrkB. Western Blot (WB) was used to detect the expression of PLC and SP in the colon. Flow cytometry was used to detect the expression of Ca^{2+}. *Results.* EA effectively alleviated visceral hypersensitivity in IBS-D rats ($P < 0.05$). Compared to the control group, the expression of BDNF, TrkB, PLC, SP, and Ca^{2+} and the colocalized expression of GFAP/BDNF and GFAP/TrkB increased in the Model group ($P < 0.05$), while all these parameters decreased in the EA group following EA intervention ($P < 0.05$). In addition, no significant difference was found between the EA + TrkB agonist group and the control group ($P > 0.05$). *Conclusions.* EA alleviates visceral hypersensitivity of IBS-D rats possibly by inhibiting the activity of EGCs through the BDNF/TrkB-PLC-Ca^{2+} signaling pathway in the colon.

1. Introduction

Irritable bowel syndrome (IBS) is a chronic functional gastrointestinal disorder with persistent or recurrent episodes of intestinal disorder [1]. It is characterized by abdominal pain, abdominal distension, altered bowel habits, and/or character of stool that severely affect the quality of patients' life [2]. A wide spectrum of clinical manifestations and a lack of a specific diagnostic basis [2] make it difficult to treat. Although medication, nutritional support, and psychotherapy are currently in use, few drugs are available for effective treatment [3]. Acupuncture therapy has received increasing attention, as numerous clinical studies have shown that it is safe and effective for the treatment of IBS. For instance, a recent trial showed that acupuncture was more effective than PEG 4000 or pinaverium bromide for the treatment of IBS and the sustained effect of acupuncture was up to 12 weeks in a large sample cohort [4]. In addition,

electroacupuncture (EA) had been shown to alleviate abdominal pain in IBS-D patients [5]. However, the mode of action of EA for ISD-D treatment remains unclear.

Extensive studies had shown that an altered visceral sensitivity is associated with the development of IBS [1]. Enteric glial cells (EGCs) play a critical role in supporting and nourishing the enteric nervous system and the development of visceral hypersensitivity in IBS [6, 7], suggesting EGCs as a potential therapeutic target for gastrointestinal disease [8]. Indeed, alterations in EGCs structure and function are associated with IBS pathogenesis [9]. For instance, intestinal EGCs in IBS patients exhibit an activated state, which releases SP substances [9] that continuously excite intestinal sensory neurons and maintain intestinal visceral hypersensitivity. EGCs can be activated through Brain-derived Neurotrophic Factor (BDNF)-related signaling pathways. With a large amount of BDNF being present in the intestinal mucosa of IBS patients, BDNF has been shown to be involved in the production and maintenance of pain in IBS [10]. It has also been shown that BDNF specifically binds to and thus activates the submucosal EGCs surface tyrosine kinase receptor B (TrkB) in the intestinal mucosa [9], which in turn activates the phospholipase C (PLC)-inositol triphosphate (IP3) [11] signaling pathway. Then, the activated signaling pathway upregulates intracellular Ca^{2+} levels with the rapid increase of extracellular Ca^{2+} levels, eventually leading to the activation of EGCs [12, 13].

Accordingly, acupuncture had been shown to alleviate visceral hypersensitive symptoms by reducing serum BDNF level in IBS-D patients [14]. Interestingly, it was found that EA could exert analgesic effects by modulating spinal microglia and spinal astrocytes activation [15, 16]. Moreover, the similarity of EGCs to central nervous system (CNS) astrocytes has been demonstrated. Thus, these studies provided strong evidence on the molecular basis of EA-included alleviation of IBS-D symptoms.

In this study, we speculated that EGCs are a possible target for acupuncture treatment of IBS-D and that BDNF signaling pathway is the key pathway of EGCs activation. Specifically, we hypothesized that EA regulates the activation of EGCs cells by downregulating the BDNF/TrkB pathway, thereby alleviating visceral hypersensitivity in IBS-D rats. To test this hypothesis, we used an IBS-D rat model (Model group) and treated these rats with EA only (EA group), EA with TrkB (EA + TrkB agonist group), or EA with DMSO (EA + DMSO group). Analyses on several parameters including SP levels, BDNF and TrKB protein abundances, and PLC/Ca^{2+} pathways were performed to test our hypothesis (Figure 1).

2. Materials and Methods

2.1. Animals. A total of 40 female Sprague Dawley rats (7-week-old and weighing 180–220 g) were obtained from Chengdu Dasuo Experimental Animals Co. (Chengdu, China). Animals were maintained in the Key Laboratory of Sichuan Province, China, where the temperature was kept at 18–24°C, with 50–70% humidity and a 12 h/12 h light/dark cycle. Animals were allowed to eat and drink freely. This experiment has been approved by the animal ethics committee of Chengdu University of Traditional Chinese Medicine (approval no. 2019–06), and all the disposal of animals conforms to the National Guideline for the Care and Use of Laboratory Animals.

2.2. Rat Model of IBS-D. An IBS-D rat model was established by gavage and CUMS for 14 consecutive days as previously described [17]. Briefly, 32 rats were randomly selected for one of the following CUMS types [18, 19]: 24 h in solitary (one cage), restraint for 2 h, crowding for 24 h (more than 6 in one cage), swimming at 45°C for 5 min, tail clamping for 20 min, or oscillation for 1 h (240 Hz). Each rat received discontinuous CUMS at least twice. Half an hour after each CUMS, rats were given 0.3 g/mL of Senna solution by gavage (10 mL/kg). Abdominal withdrawal reflex (AWR) was used to measure the visceral hypersensitivity. Successfully modeled rats were randomly divided into a Model group, an EA group, an EA + TrkB agonist group, and an EA + DMSO group, with 8 rats in each group. The remaining rats were assigned as a Control group, which was given distilled water by gavage at 10 mL/kg daily.

2.3. EA Treatment. Electroacupuncture was performed in rats after meal. Rats in the EA group, EA + TrkB agonist group, and EA + DMSO group received EA for 20 min once per day for 14 days. After being immobilized on a self-made fixator and disinfection of the skin area at the acupoints with 75% alcohol, the rats were treated with EA. The acupoints were ST25 (*Tianshu*, located in the abdomen; the middle side of the umbilicus is opened about 5 mm), ST36 (*Zusanli*, the posterolateral side of the knee joint, about 5 mm under the fibula head), and LR3 (*Taichong*, located at the tibial side of the second toe of the foot, the posterior depression of the metatarsal bone). Stainless steel acupuncture needles (Huatuo, Suzhou Medical Supplies Co., Ltd., $\Phi 0.16 \times 13$ mm) were inserted into the three acupoints at a depth of 1-2 mm and connected to an EA apparatus (HANS-200A, Nanjing, China). The lateral/dilatational waves were set to a frequency of 2/15 Hz and an intensity of 1.5 mA. Rats in the EA + TrkB agonist group were intraperitoneally injected with a TrkB receptor agonist 7,8-dihydroxyflavone (MedChemExpress, USA) one hour before EA. The 7,8-dihydroxyflavone (7,8-DHF) was dissolved in 10% DMSO administered at a dose of 5 mg/kg through intraperitoneal injection. And the EA + DMSO group was injected with the same dose of DMSO solution, while the control group was only bound on fixator for 20 minutes without EA intervention.

2.4. Abdominal Withdrawal Reflex (AWR) Score. AWR was assessed after 24 h fasting as previously described [20]. A balloon of 5 cm in length and a catheter of 4 mm in diameter were used to make a colorectal tension balloon, and the catheter was connected to a sphygmomanometer via a three-way tube. Following anesthesia and being transferred to an

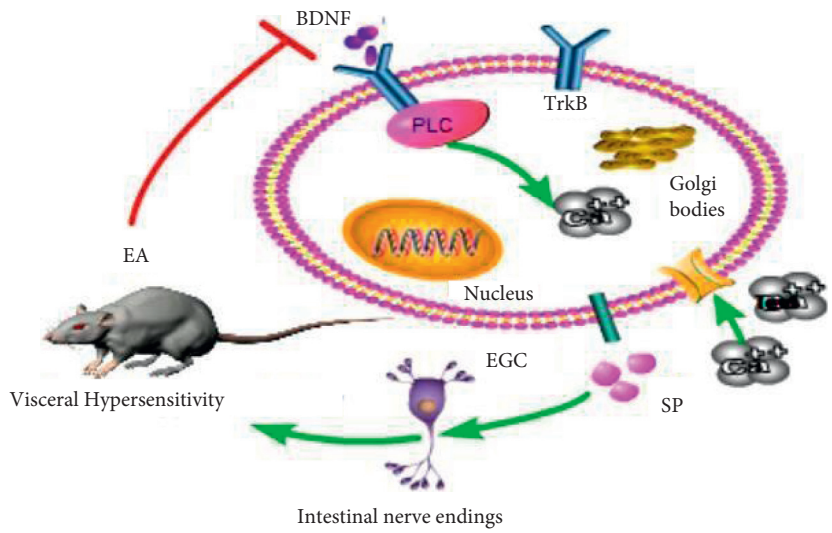

Figure 1: Schematic diagram of the mechanism of acupuncture treatment of IBS in rats. Brain-Derived Neurotrophic Factor (BDNF) specifically binds to and thus activates the enteric glial cells (EGCs) surface tyrosine kinase receptor B (TrkB), which in turn activates the phospholipase C (PLC) signaling pathway. Then, the activated signaling pathway upregulates intracellular Ca^{2+} levels with the rapid increase of extracellular Ca^{2+} levels, eventually leading to the activation of EGCs.

acrylic fixed box (18 × 7 × 6 cm) in which the rats cannot turn around, a colorectal dilatation balloon was inserted to the descending colon and a pressure of 20, 40, 60, or 80 mmHg was applied for colorectal dilatation (CRD). AWD scores, blindly evaluated by two trained researchers who did not know the groups' information, were used to assess the degree of visceral sensitivity during rectal dilation in rats [20, 21] with the following scale: AWR0: no response to CRD; AWR1: slight head rotation; AWR2: abdominal muscle contraction; AWR3: abdomen raised; and AWR4: body arched and pelvis raised. After each 20-second CRD, AWR scores were measured three times, and an average value was recorded as the AWR score.

2.5. Sample Collection. After EA intervention, rats were intraperitoneally injected with pentobarbital sodium (40 mg/kg). Following anesthesia, the abdominal cavity was opened and the colon tissue was collected. The colon tissues were washed with 0.9% saline and then placed in 4% paraformaldehyde for immunofluorescence detection, 3% glutaraldehyde for transmission electron microscopy detection, and liquid nitrogen at −196°C for WB and RT-PCR detection. After the experiment, rats were killed by cervical dislocation.

2.6. Histological Assessment. Colon tissues were fixed in a 10% neutral formaldehyde, dehydrated with 100% alcohol in an automatic dehydrator, embedded in paraffin, and stained with hematoxylin and eosin (H&E). After sectioning, the colon tissue was observed under a light microscope (Jinan Tangier Electronics Co., LTD, China).

2.7. Western Blot (WB). The protein abundance of PLC and SP was quantified by WB in colon tissues. First, total proteins were extracted in RIPA lysis buffer (Beyotime, China) and quantified with the BCA protein quantification kit (Beyotime, China). Samples were separated by electrophoresis, transferred to a PVDF membrane (Sigma-Aldrich, USA), and blocked with 5% skimmed milk. The membrane was incubated with primary antibodies (anti-PLC antibody, 1 : 1000 dilution, rabbit clonal antibody, Abcam, UK; anti-SP antibody, 1 : 1000 dilution, rabbit clonal antibody, Affinity, USA; anti-β-actin antibody, 1 : 100000 dilution, rabbit clonal antibody, ABclonal, China). After washing, the membrane was incubated with a secondary antibody (Biotinylated Goat anti-rabbit IgG (H + L), 1 : 5000 dilution, Abcam, UK). Relative expression of the target protein was obtained by normalization against actin.

2.8. Real-Time PCR (RT-PCR). RT-PCR was used to quantify *BDNF* and *TrkB* expression. First, colon tissues were ground in liquid nitrogen for RNA extraction. For each sample, 50–100 mg tissue was extracted with 1 mL of RNA Trizol Reagent (Hefei Bomei Biotechnology Co., Ltd., China). The total RNA was used to synthesize cDNA. Primers (Shanghai SANGON Biotech Co., Ltd., China) are shown in Table 1. PCR reactions were performed on a real-time fluorescence quantitative instrument (QuantStudio TM3, Thermofisher, USA) with a total of 45 cycles. In this study, the relative expression levels of *BDNF* mRNA and *TrkB* mRNA were calculated by $2^{-\triangle\triangle CT}$.

2.9. Immunofluorescence. Double immunofluorescence labeling was performed to determine the expression patterns of GFAP-BDNF and GFAP-TrkB complexes in colon. Tissue was fixed and dehydrated as described above. After being embedded using BMJ-III, samples were sliced by a rotary slicer (Leica-2016, Germany). Slices were immersed in 0.01 M citrate buffer (pH 6.0), heated in a microwave oven at medium-high heat until boiling with an interval of

Table 1: PCR primers.

Contents	Forward	Reverse
BDNF	GAGCTTTGTGGACCCCTGAGTTC	CCGTGGACGTTTGCTTCTTTCATG
TrkB	GGTCTATGCGTGGTGTGTGTTG	ATGTCTCGCCAACTTGAGCAGAAG
β-Actin	GAAGATCAGATTGCTCC	TACTCCTGCTTGCTGATCCA

5 min. Samples were first rinsed with PBS and then blocked with 10% serum (Zhejiang Tianhang Biotechnology Co., Ltd., China) at room temperature for 30 min. Primary antibodies (anti-GFAP, mouse monoclonal antibody, concentration: 1 : 100, Abcam, UK; anti-TrkB, Rabbit polyclonal antibody, 1 : 100, Affinity Biosciences, OH, USA; anti-BDNF, rabbit polyclonal antibody, 1 : 100, Bioss, China) were added to the samples separately. After rinsing the samples with PBS for 30 min at 37°C, a secondary antibody (FITC labeled goat anti-rabbit IgG, ServiceBio, China; Cy3-labeled goat anti-mouse IgG, ServiceBio, China) was added. The samples were dripped with nuclear dye, washed with PBS, and sealed with an antifluorescence attenuation sealing agent. A fluorescence scanning microscope camera system (Jinan Tangier Electronics Co., LTD, China) was used for image acquisition.

2.10. Flow Cytometry (FCM). The content of Ca^{2+} was measured by FCM. Colon tissues were washed with PBS at 4°C and ground. The resulting suspension was extracted, sieved, and centrifuged for 5 minutes to obtain cell precipitations. Cells were resuspended in 500 μL of diluted Fluo 3-AM (Sigma-Aldrich, USA), followed by washing twice with 500 μL of PBS and reloading 300 μL of Fluo 3-AM. Finally, Ca^{2+} was detected and analyzed by a Cytoflex flow analyzer (Beckman, USA).

2.11. Statistical Analysis. Statistical analysis was performed using SPSS21.0. After normal test and homogeneity analysis of variance, multiple groups comparison and one-way analysis of variance were used. Post hoc test was performed for pair comparison with the least significant difference (LSD) method. In cases where there were no variances among groups, Tamhane's T2 test was used. $P < 0.05$ and $P < 0.01$ were considered as statistically significant and extremely significant, respectively.

3. Results

3.1. Effect of EA on Visceral Hypersensitivity. AWR score is an important index to evaluate visceral hypersensitivity. As shown in Figure 2(a), there was no significant difference in the AWR score of rats among groups with a CRD of 20 mmHg ($P > 0.05$). As the CRD increased to 40, 60, and 80 mmHg, AWR scores of IBS-D rats were significantly increased compared to the control group ($P < 0.05$). Importantly, the AWR score of IBS-D rats showed a significant decrease after EA treatment ($P < 0.05$), while there was no significant change in the EA + TrkB agonist group ($P > 0.05$).

3.2. Histological Assessment. Histological assessment showed that the colon tissue structure of the control group was complete and normal (Figure 3(a)). By contrast, the Model group showed stratification in the colonic tissue without hyperplasia or ulceration (Figure 3(b)). For the EA group, the tissue was completely stratified (Figure 3(c)). For the EA + TrkB agonist group, the tissue was clear without any obvious degeneration and necrosis (Figure 3(d)). Lastly, the colon of the EA + DMSO group was similar to that of the control group (Figure 3(e)). In addition, the mucosa, submucosa, muscle layer, and outer membrane structure of colon tissue were clear for all groups without any obvious pathological changes.

3.3. EGCs Inactivation in Analgesia Effect of EA in IBS-D

3.3.1. Effect of EA on the Structure and Morphology of EGCs. Normal EGCs morphology and structure were observed for the control group with major organelles observed (Figure 4(a)). By contrast, the Model group showed nuclear chromatin edge concentration, widened perinuclear space, more abundant Golgi bodies, and expansion and cystic characters for most of the rough endoplasmic reticulum (rER, Figure 4(b)). For the EA group, a small number of mitochondria in the EGCs cytoplasm showed mild swelling, and a large number of dilated, cystic rER were observed (Figure 4(c)). Although EA promoted EGCs morphologic repair, the effect was not observed in the EA + TrkB agonist group, in which EGCs showed mitochondrial swelling, crest fracture, dissolution, and even disappearance (Figure 4(d)). In the EA + DMSO group, a small number of mitochondria were slightly swollen, and a small part of rER expanded into cystic forms (Figure 4(e)).

3.3.2. Effects of EA on SP. After modeling, the colon SP content in IBS-D rats increased significantly ($P < 0.01$, Figure 5(d)). Compared to the Model group, EA resulted in a significant decrease in SP content ($P < 0.01$). As expected, there was no significant change in the EA + TrkB agonist group ($P > 0.05$).

3.4. Effect of EA on BDNF/TrkB Signaling Pathway

3.4.1. mRNA Expression of BDNF and TrkB in the Colon. Senna solution by gavage and CUMS resulted in an increase in the expression of *BDNF* and *TrkB* compared to the control group (Figures 6(c) and 7(c)). In addition, EA stimulation led to a significant decrease in the expression of both genes. Moreover, there was no significant difference between the Model group and the EA + TrkB agonist group.

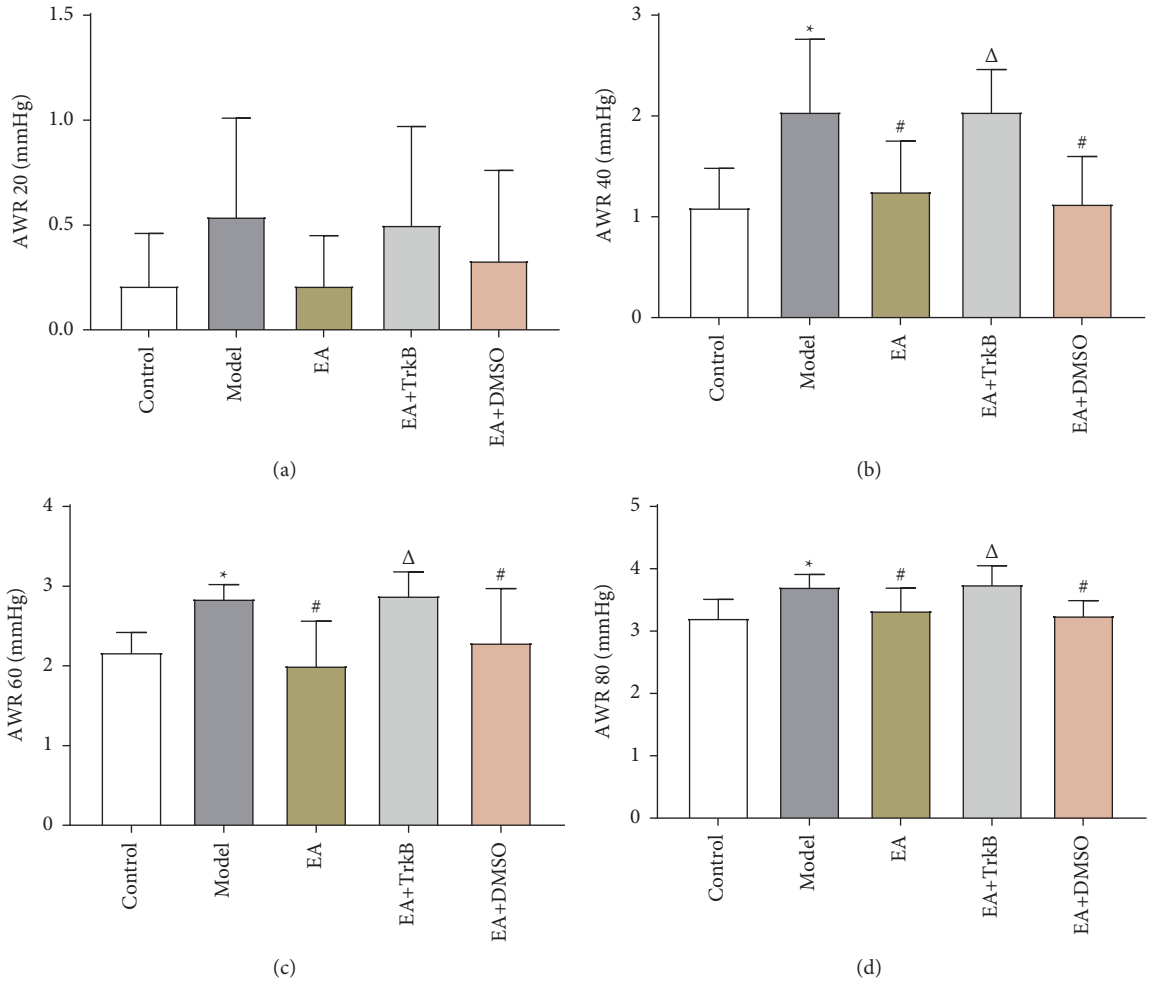

Figure 2: AWR score and SP expression and effect of EA on visceral hypersensitivity. (a) AWR scores with a CRD of 20 mmHg; (b) AWR scores with a CRD of 40 mmHg; (c) AWR scores with a CRD of 60 mmHg; (d) AWR scores with a CRD of 80 mmHg; $^{*}P < 0.05$, versus the blank control group; $^{\#}P < 0.05$ and $^{\Delta}P < 0.05$, versus the model group.

3.4.2. TrkB-Mediated PLC/Ca^{2+} Signaling Pathway in EGCs Was Activated by EA Stimulation. To further determine whether the upregulation of the PLC-Ca^{2+} pathway was mediated by TrkB, the TrkB agonist 7,8-dihydroxyflavone was used prior to the quantification of PLC protein and Ca^{2+} in colon. Our data showed that the protein abundance of PLC increased after modeling (Figure 5(b)). Compared to the Model group, EA intervention led to a significant decrease of PLC protein abundance in the EA and EA + DMSO groups, but not in the EA + TrkB agonist group. A similar trend was found for Ca^{2+} (Figure 5(e)), where modeling caused an increase in Ca^{2+} content and EA restored the level.

3.4.3. Colocalization of GFAP and BDNF and of GFAP and TrkB in the Colon. To explore whether BDNF in IBS-D rat colon specifically binds to TrkB receptor on EGCs and determine selective inactivation of TrkB in colon by EA, a double-label immunofluorescence assay was performed to assess the colocalization between BDNF and GFAP, as well as between TrkB and GFAP. Our data showed a significant increase in colocalized expression of GFAP and BDNF after modeling (Figure 6(a)). Compared to the Model group, a significant decrease was observed in the EA group and the EA + DMSO group ($P < 0.05$), while no significant change was found in the EA + TrkB agonist group (Figure 6). Similar results are also observed in Figure 7, where the fluorescence intensities for GFAP (red) and BDNF (green) increased in the Model group compared to the control group. In addition, EA led to a decrease in the fluorescence intensity compared to the Model group.

Compared to the control group, EGCs in the Model group showed a strong colocalization with TrkB and exhibited high TrkB fluorescence intensity (Figure 7(b)). Significantly, EA led to a decrease in the colocalized expression of GFAP and TrkB, as evidenced by the observation that EA at ST25, ST36, and LR3 was sufficient to inhibit the expression of TrkB in colon ($P < 0.05$). In addition, there was no significant change in the EA + TrkB agonist group ($P > 0.05$). In line with the GFAP/BDNF results, GFAP/TrkB showed an increase in the Model group, which led to a decrease in the fluorescence intensity compared to the EA group (Figure 7).

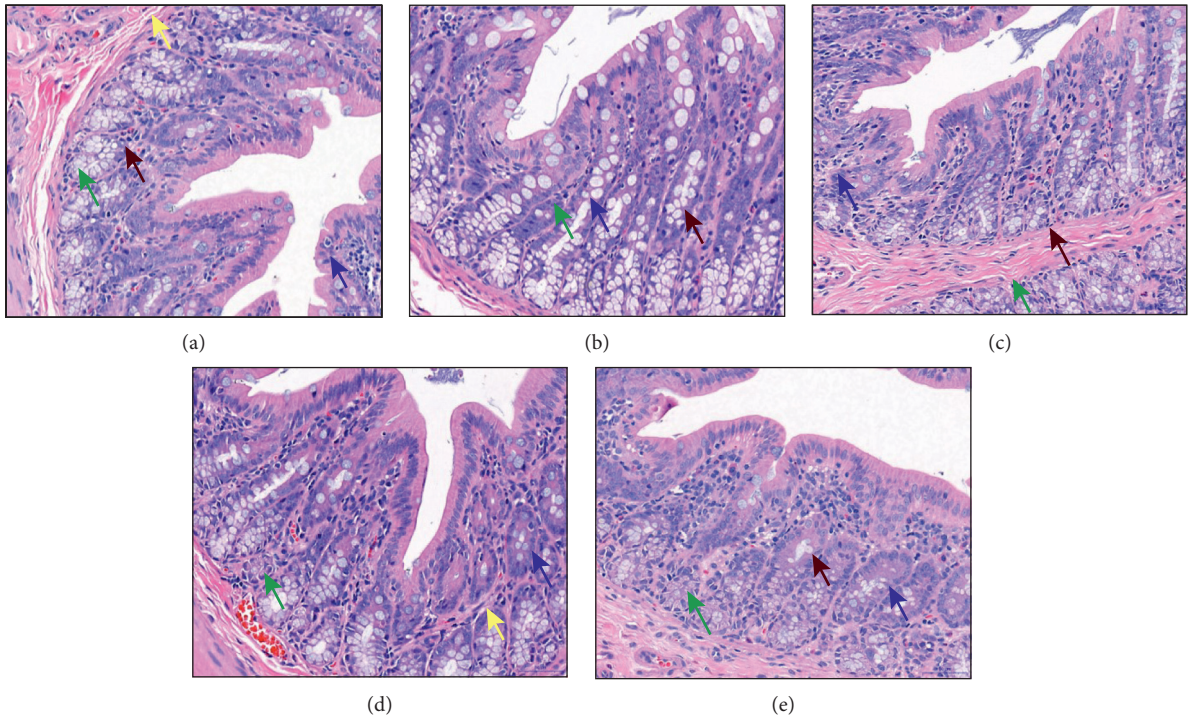

Figure 3: Histological assessment of colon tissues. (a) The control group; (b) the Model group; (c) the EA group; (d) the EA + TrkB agonist group; (e) the EA + DMSO group. Images were taken under a light microscope (×400); goblet cell (↑), lymphocytes (↑), eosinophils (↑), and neutrophils (↑).

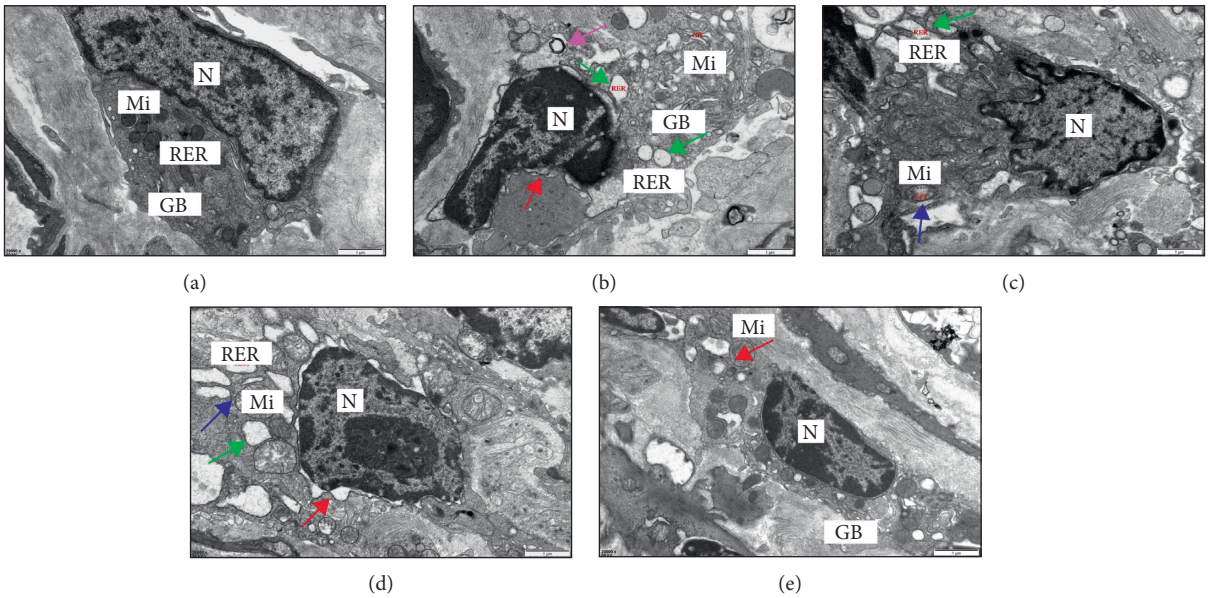

Figure 4: Structure and morphology of EGCs. (a) EGCs of the blank control group; (b) EGCs of the Model group; (c) EGCs of the EA group; (d) EGCs of the EA + TrkB agonist group; (e) EGCs of the EA + DMSO group. Images of EGCs were obtained under TEM (×20000). N, nucleus; Mi, mitochondria; RER, rough endoplasmic reticulum; and GB, Golgi apparatus; widened perinuclear space (↑), mitochondria slightly swollen (↑), dilated rough endoplasmic reticulum (↑), and autophagy (↑).

4. Discussion

The clinical symptoms of IBS are mostly manifested as abdominal pain and bloating, which are typical features of visceral hypersensitivity and an important clinical marker to distinguish IBS from other functional gastrointestinal diseases [22]. A dysregulation in the communication between the gut and brain has also been confirmed for IBS [23]. The cerebral nervous system and the central nervous system are known to share many similarities [24]. While many studies

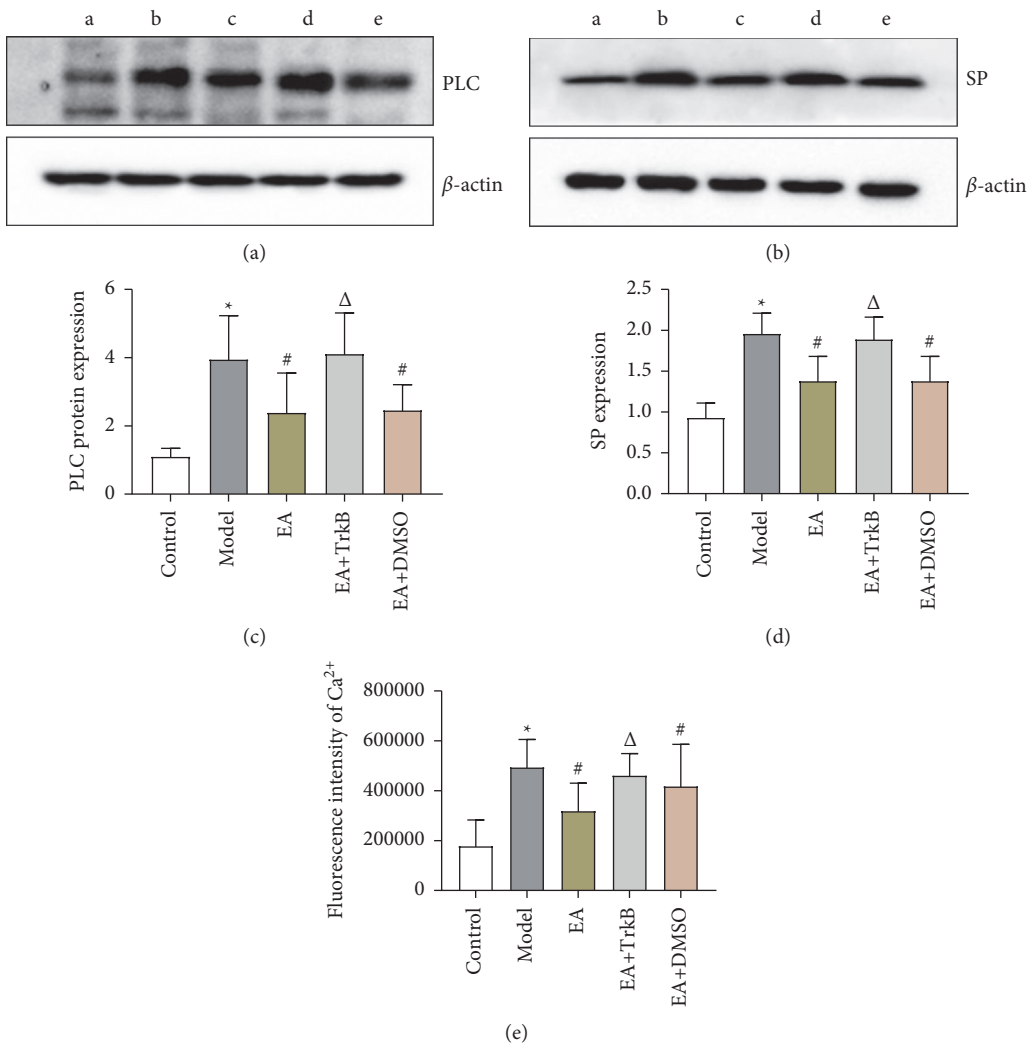

Figure 5: (a–d) The expression of PLC and SP in the colon of each group of rats (a: control group, b: Model group, c: EA group, d: EA + TrkB agonist group, and e: EA + DMSO group). (e) Mean fluorescence intensity of Ca^{2+} in the colon. $^{*}P < 0.01$, versus the blank control group; $^{\#}P < 0.05$ and $^{\Delta}P > 0.05$, versus the model group.

focused on central nervous system such as the central [25] and spinal cord [26], few had explored the enteric nervous system. Mounting evidence has shown that IBS is associated with an increased excitability of sensory neurons in the gut, manifested as hypersensitivity of intestinal receptors to various stimuli and hyperalgesia and allodynia [27]. EA alleviates visceral hypersensitivity in IBS at multiple levels by regulating intestinal dynamics [28], visceral receptor sensitivity [20], intestinal flora [29], and the brain-gut axis [30, 31]. Therefore, this study explored the peripheral mechanism of EA in IBS-D rats. We found that EA resulted in downregulation of the BDNF/TrkB signaling pathway, decreased EGC activity, and lower AWR scores.

In this study, we quantified visceral hypersensitivity using AWR scores, an important index for intestinal sensitivity [32], and found a significant increase with higher CRD pressure in the Model group. The fact that no pathological changes were found in the colon of the Model rats validated the establishment of the model and further confirmed that IBS-D is a functional gastrointestinal disease [33]. More importantly, EA stimulation caused a significant drop in the visceral hypersensitivity of the IBS-D model rats, consistent with a previous report [20]. In addition, a higher CRD pressure was correlated with an enhanced alleviation effect. Furthermore, the alleviation on visceral hypersensitivity by EA was abolished in the EA + TrkB agonist group, suggesting that the modulation of visceral hypersensitivity by acupuncture may be mediated through TrkB receptors.

Glial cells and nerve cells constitute the nervous system, and enteric glial cells (EGCs) belong to the glial cells distributed in the periphery. In the intestine, EGCs are mainly distributed in the submucosal enteric ganglia and enteric myenteric plexus of the enteric nervous system, and GFAP is a biomarker for the activation of EGCs. Under physiological states, EGCs play key roles in maintaining intestinal homeostasis, regulating the intestinal epithelial barrier, and promoting the development of the nervous system [34, 35]. Under pathological states, such as in IBS-D, EGCs can be abnormally activated and secrete substances such as SP to regulate the excitability of intestinal sensory neurons and

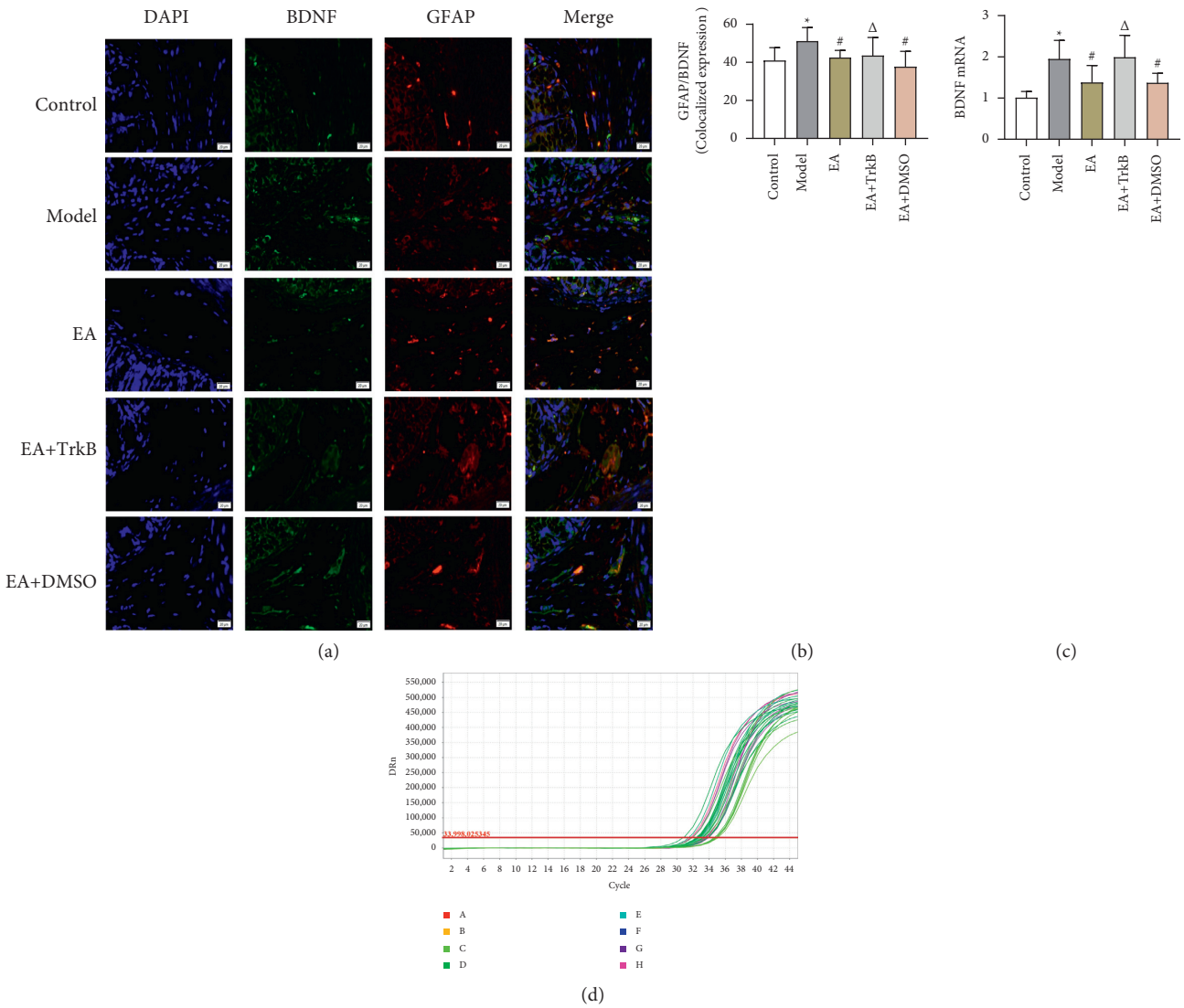

Figure 6: (a) GFAP and BDNF fluorescence in different groups. Green indicates BDNF, red indicates GFAP, and blue indicates DAPI-stained nucleus. (b) Colocalization of GFAP and BDNF. (c) mRNA expression of BDNF in the colon. $^{*}P < 0.05$, versus the blank control group; $^{\#}P < 0.05$ and $^{\Delta}P > 0.05$, versus the Model group.

maintain the visceral hypersensitivity of IBS-D [7, 9]. Previous studies have shown that EGC activation is closely associated with visceral hypersensitivity in IBS [6, 7, 36].

Due to the critical role of EGC in IBS-D visceral hypersensitivity, we observed the morphological and structural changes of submucosal EGCs in the colonic mucosa by using TEM. Compared to the control group, the EA group showed ER expansion, perinuclear gap, and slight swelling of the mitochondria. We thus speculate that the ultrastructure of EGCs in the IBS-D state is altered, and EA may reverse the alteration to some extent. EGCs are also known to secrete SP to stimulate intestinal primary neurons and maintain visceral hypersensitivity. Consistent with previous studies [37], we found that colonic SP substance expression was significantly increased in IBS-D rats and significantly decreased after EA. In addition, our immunofluorescence results showed that GFAP in the Model group was significantly increased compared to the control group, suggesting that the EGCs were in an activated state. On the other hand, EGC inhibitors can alleviate visceral hypersensitivity in IBS rats [9]. Our results showed that EA may alleviate visceral hypersensitivity of IBS-D rats by inhibiting EGC activity as a significant decrease of GFAP was found in the EA and EA + DMSO groups.

Previous studies of IBS-D have shown an increase in the intestinal BDNF, which binds to the TrkB receptor on the submucosal EGC surface of the intestine and activates the PLC-IP3 signaling pathway, triggering a dramatic increase in the intracellular Ca^{2+} level of EGCs and contributing to EGC hyperactivation [9–11, 37, 38]. In line with this, we found that colonic BDNF and TrkB receptors were significantly increased in IBS-D rats. It had been suggested that the increased BDNF in the pathological state of IBS-D specifically binds to the TrkB receptor on the surface of EGCs and activates EGCs. This was assessed by immunofluorescence double staining, in which GFAP was included as a marker of

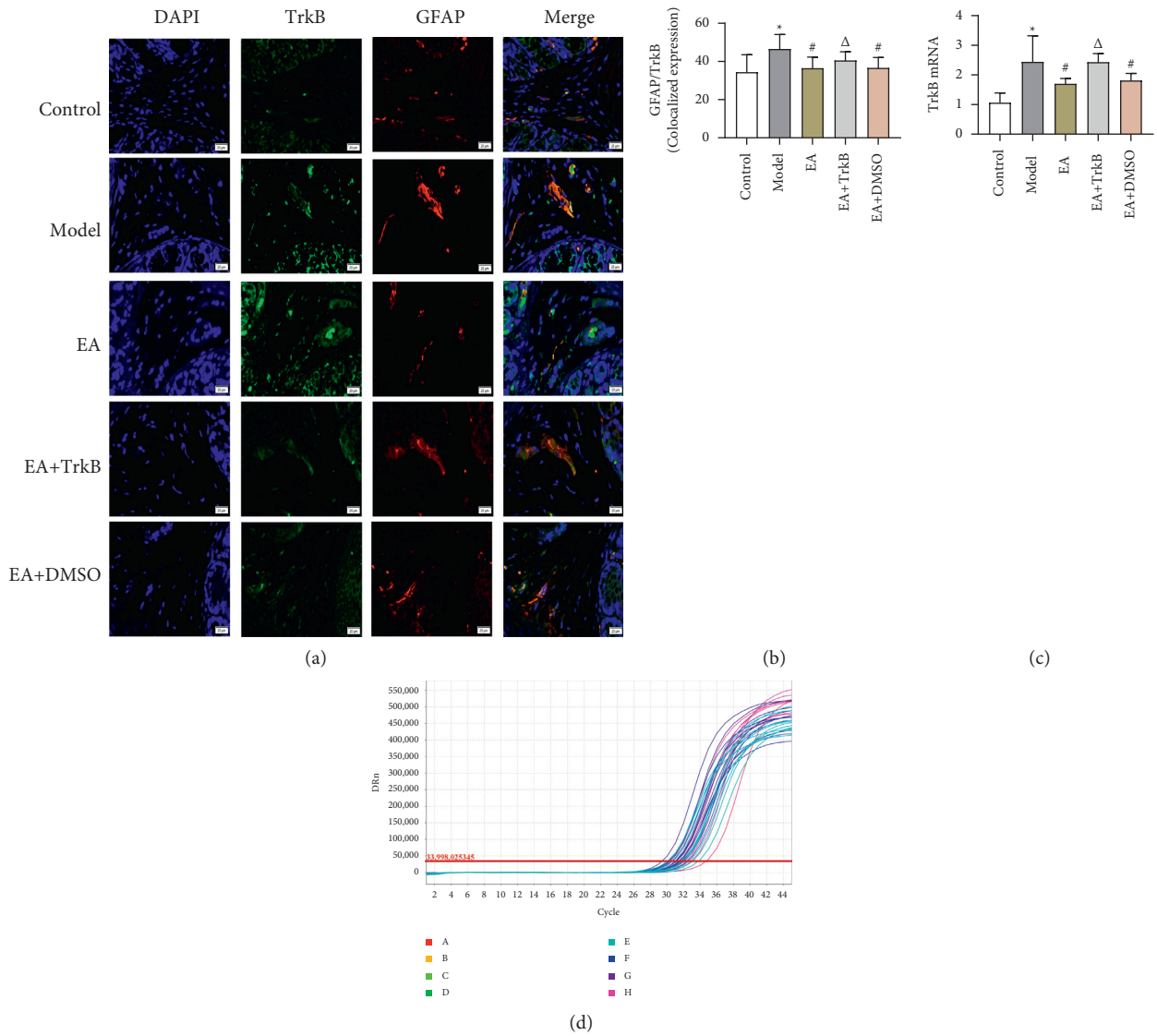

Figure 7: (a) GFAP and TrkB fluorescence in different groups. Green indicates TrkB, red indicates GFAP, and blue indicates DAPI-stained nucleus. (b) Colocalization of GFAP and TrkB. (c) mRNA expression of TrkB mRNA in the colon. $^{*}P < 0.05$, versus the blank control group; $^{\#}P < 0.05$ and $^{\Delta}P > 0.05$, versus the Model group.

EGCs activation [39]. Our results showed an increase in the colocalized expression of GFAP/BDNF and GFAP/TrkB in IBS-D rats compared to the control group. In addition, we found an increase in PLC protein abundance and Ca^{2+} level along with the activation of the BDNF/TrkB pathway, consistent with previous reports.

Compared to the Model group, EA resulted in a decrease in the colocalized expression of GFAP/BDNF and GFAP/TrkB. Additionally, the levels of colonic BDNF and TrkB receptors, PLC protein, and Ca^{2+} were also decreased. Thus, it is possible that EA reduces PLC and Ca^{2+} content, inhibits EGCs activity, and alleviates visceral hypersensitivity of IBS-D rats by inhibiting the binding of BDNF and TrkB receptors on EGCs. To confirm the mode of action, we injected a TrkB agonist intraperitoneally into IBS-D rats before EA. As expected, no difference was found compared to the Model group with regard to all parameters measured (colocalized expression of GFAP/BDNF and GFAP/TrkB, colonic PLC protein abundance, and Ca^{2+} level). Because DMSO was used as the solvent for the EA + TrkB agonist group, the EA + DMSO group was also included as a control. Importantly, the EA + DMSO indeed showed significant changes for all parameters quantified here. Thus, we conclude that the EA effect was attributable to TrkB receptor but not to DMSO. Taken together, EA alleviated visceral hypersensitivity in IBS-D rats by modulating the BDNF/TrkB-PLC-Ca^{2+} signaling pathway.

5. Conclusions

EA improves visceral hypersensitivity of IBS-D rats possibly by inhibiting the activity of EGCs through the BDNF/TrkB-PLC-Ca^{2+} signaling pathway in the colon.

Data Availability

All data included in this study are available upon request to the corresponding author.

Conflicts of Interest

The authors declare no conflicts of interest.

Authors' Contributions

YZ, HLJ, and YS contributed equally to this work. QHZ and FRL designed the animal experiment. YZ and HLJ completed the entire experimental operation. YZ, HLJ, and YS completed the first draft of the manuscript, and YS was also responsible for the data analysis. YJH, WZ, and BYH were in charge of reviewing the final draft. LXZ and ZQY were in charge of consulting and extracting the literature, and QHZ was responsible for quality control. All authors participated in the revision, reading, and approval of the submitted version.

Acknowledgments

The authors are grateful to Professor Ding-jun Cai and Associate Professor Si-yuan Zhou of Chengdu University of Traditional Chinese Medicine for their technical support in animal experiments. The study was supported by National Natural Science Fund of China Youth Foundation Project (81804207) and Project of *Xinglin Scholar* Discipline Talent Scientific Research Promotion Program of Chengdu University of Traditional Chinese Medicine (BSH2018015).

References

[1] P. Enck, Q. Aziz, G. Barbara et al., "Irritable bowel syndrome," *Nature Reviews Disease Primers*, vol. 2, no. 1, p. 16014, 2016.

[2] B. Li, X. F. Luo, S. W. Liu et al., "Abdominal massage reduces visceral hypersensitivity via regulating GDNF and PI3K/AKT signal pathway in a rat model of irritable bowel syndrome," *Evidence-based Complementary and Alternative Medicine: eCAM*, vol. 2020, Article ID 3912931, 13 pages, 2020.

[3] K. Barshop and K. Staller, "Eluxadoline in irritable bowel syndrome with diarrhea: rationale, evidence and place in therapy," *Therapeutic advances in chronic disease*, vol. 8, no. 11, pp. 153–160, 2017.

[4] L. Pei, H. Geng, J. Guo et al., "Effect of acupuncture in patients with irritable bowel syndrome: a randomized controlled trial," *Mayo Clinic Proceedings*, vol. 95, no. 8, pp. 1671–1683, 2020.

[5] L. Zhenzhong, Y. Xiaojun, T. Weijun et al., "Comparative effect of electroacupuncture and moxibustion on the expression of substance P and vasoactive intestinal peptide in patients with irritable bowel syndrome," *Journal of Traditional Chinese Medicine*, vol. 35, no. 4, pp. 402–410, 2015.

[6] S. Xu, B. Qin, A. Shi, J. Zhao, X. Guo, and L. Dong, "Oxytocin inhibited stress induced visceral hypersensitivity, enteric glial cells activation, and release of proinflammatory cytokines in maternal separated rats," *European Journal of Pharmacology*, vol. 818, pp. 578–584, 2018.

[7] X. Long, M. Li, L.-X. Li et al., "Butyrate promotes visceral hypersensitivity in an IBS-like model via enteric glial cell-derived nerve growth factor," *Neuro-Gastroenterology and Motility*, vol. 30, no. 4, Article ID e13227, 2018.

[8] F. Ochoa-Cortes, F. Turco, A. Linan-Rico et al., "Enteric glial cells," *Inflammatory Bowel Diseases*, vol. 22, no. 2, pp. 433–449, 2016.

[9] P. Wang, C. Du, F.-X. Chen et al., "BDNF contributes to IBS-like colonic hypersensitivity via activating the enteroglia-nerve unit," *Scientific Reports*, vol. 6, no. 1, Article ID 20320, 2016.

[10] Y. Zhang, G. Qin, D.-R. Liu, Y. Wang, and S.-K. Yao, "Increased expression of brain-derived neurotrophic factor is correlated with visceral hypersensitivity in patients with diarrhea-predominant irritable bowel syndrome," *World Journal of Gastroenterology*, vol. 25, no. 2, pp. 269–281, 2019.

[11] G. Leal, D. Comprido, and C. B. Duarte, "BDNF-induced local protein synthesis and synaptic plasticity," *Neuropharmacology*, vol. 76, no. C, pp. 639–656, 2014.

[12] M. J. Broadhead, P. O. Bayguinov, T. Okamoto, D. J. Heredia, and T. K. Smith, "Ca2+transients in myenteric glial cells during the colonic migrating motor complex in the isolated murine large intestine," *The Journal of Physiology*, vol. 590, no. 2, pp. 335–350, 2012.

[13] A. Gärtner, D. G. Polnau, V Staiger et al., "Hippocampal long-term potentiation is supported by presynaptic and postsynaptic tyrosine receptor kinase B-mediated phospholipase Cgamma signaling," *Journal of Neuroscience: The Official Journal of the Society for Neuroscience*, vol. 26, no. 13, pp. 3496–3504, 2006.

[14] X. Chen, "The acupuncture treatment of regulating the mind and tonifying the spleen method on diarrhea predominant irritable bowel syndrome patients' status of anxiety and serum BDNF level changes," Master Thesis, Nanjing University of Chinese Medicine, Nanjing, China, 2016.

[15] T. Chen, W. W. Zhang, Y. X. Chu, and Y. Q. Wang, "Acupuncture for pain management: molecular mechanisms of action," *The American Journal of Chinese Medicine*, vol. 48, no. 4, pp. 793–811, 2020.

[16] Y. Li, C. Yin, X. Li et al., "Electroacupuncture alleviates paclitaxel-induced peripheral neuropathic pain in rats via suppressing TLR4 signaling and TRPV1 upregulation in sensory neurons," *International Journal of Molecular Sciences*, vol. 20, no. 23, 2019.

[17] Y. Zhao, D.-N. Luo, Y. Chen, C. Huang, and S.-Y. Zhou, "Dose-effect and time-effect relationship of chronic restraint stress combined with senna extract gavage in inducing diarrhea-predominant irritable bowel syndrome in rats," *World Chinese Journal of Digestology*, vol. 25, no. 15, pp. 1360–1367, 2017.

[18] J. Ma, J. Li, M. Qian et al., "The comprehensive pathophysiological changes in a novel rat model of postinflammatory visceral hypersensitivity," *The FASEB Journal*, vol. 33, no. 12, pp. 13560–13571, 2019.

[19] J. C. Garza, M. Guo, W. Zhang, and X.-Y. Lu, "Leptin restores adult hippocampal neurogenesis in a chronic unpredictable stress model of depression and reverses glucocorticoid-induced inhibition of GSK-3β/β-catenin signaling," *Molecular Psychiatry*, vol. 17, no. 8, pp. 790–808, 2012.

[20] Y. Chen, Y. Zhao, D. N. Luo, H. Zheng, Y. Li, and S. Y. Zhou, "Electroacupuncture regulates disorders of gut-brain interaction by decreasing corticotropin-releasing factor in a rat model of IBS," *Gastroenterology research and practice*, vol. 2019, Article ID 1759842, 23 pages, 2019.

[21] E. D. Al-Chaer, M. Kawasaki, and P. J. Pasricha, "A new model of chronic visceral hypersensitivity in adult rats induced by

colon irritation during postnatal development," *Gastroenterology*, vol. 119, no. 5, pp. 1276–1285, 2000.

[22] Q. Zhou and G. N. Verne, "New insights into visceral hypersensitivity-clinical implications in IBS," *Nature Reviews Gastroenterology & Hepatology*, vol. 8, no. 6, pp. 349–355, 2011.

[23] A. C. Ford, A. D. Sperber, M. Corsetti, and M. Camilleri, "Irritable bowel syndrome," *The Lancet*, vol. 396, no. 10263, pp. 1675–1688, 2020.

[24] A. Chalazonitis and M. Rao, "Enteric nervous system manifestations of neurodegenerative disease," *Brain Research*, vol. 1693, no. Pt B, pp. 207–213, 2018.

[25] L. M. Adams and D. C. Turk, "Psychosocial factors and central sensitivity syndromes," *Current Rheumatology Reviews*, vol. 11, no. 2, pp. 96–108, 2015.

[26] J.-y. Wang, Y.-h. Gao, L.-n. Qiao, J.-l. Zhang, and C.-L. Duanmu, X. Y. Ya, Y.-x. Yan, S.-p. Chen, and J.-l. Liu, Repeated electroacupuncture treatment attenuated hyperalgesia through suppression of spinal glial activation in chronic neuropathic pain rats," *BMC Complementary and Alternative Medicine*, vol. 18, no. 1, p. 74, 2018.

[27] E. Perna, J. Aguilera-Lizarraga, M. V. Florens et al., "Effect of resolvins on sensitisation of TRPV1 and visceral hypersensitivity in IBS," *Gut*, vol. 70, no. 7, pp. 1275–1286, 2021.

[28] X.-P. Ma, J. Hong, An Cai-Ping et al., "Acupuncture-moxibustion in treating irritable bowel syndrome: how does it work?" *World Journal of Gastroenterology*, vol. 20, no. 20, pp. 6044–6054, 2014.

[29] Y. F. Song, L. X. Pei, L. Chen et al., "Electroacupuncture relieves irritable bowel syndrome by regulating IL-18 and gut microbial dysbiosis in a trinitrobenzene sulfonic acid-induced post-inflammatory animal model," *The American Journal of Chinese Medicine*, vol. 48, no. 1, pp. 77–90, 2020.

[30] J.-m. Zhao, J.-h. Lu, X.-j. Yin et al., "Comparison of electroacupuncture and mild-warm moxibustion on brain-gut function in patients with constipation-predominant irritable bowel syndrome: a randomized controlled trial," *Chinese Journal of Integrative Medicine*, vol. 24, no. 5, pp. 328–335, 2018.

[31] F. Zhang, L. Wu, J. Zhao et al., "Neurobiological mechanism of acupuncture for relieving visceral pain of gastrointestinal origin," *Gastroenterology research and practice*, vol. 2017, Article ID 5687496, 13 pages, 2017.

[32] C. Zhao, M. Lin, Y. Pan, and B. Yu, "Blockage of high-affinity choline transporter increases visceral hypersensitivity in rats with chronic stress," *Gastroenterology research and practice*, vol. 2018, Article ID 9252984, 8 pages, 2018.

[33] D. A. Drossman and D. L. Dumitrascu, "Rome III: new standard for functional gastrointestinal disorders," *Journal of gastrointestinal and liver diseases: JGLD*, vol. 15, no. 3, pp. 237–241, 2006.

[34] K. R. Jessen, "Glial cells," *The International Journal of Biochemistry & Cell Biology*, vol. 36, no. 10, pp. 1861–1867, 2004.

[35] Y.-B. Yu and Y.-Q. Li, "Enteric glial cells and their role in the intestinal epithelial barrier," *World Journal of Gastroenterology*, vol. 20, no. 32, pp. 11273–11280, 2014.

[36] G. Burnstock, K. A. Jacobson, and F. L. Christofi, "Purinergic drug targets for gastrointestinal disorders," *Current Opinion in Pharmacology*, vol. 37, pp. 131–141, 2017.

[37] W. J. Liang, G. Zhang, H. S. Luo, L. X. Liang, D. Huang, and F. C. Zhang, "Tryptase and protease-activated receptor 2 expression levels in irritable bowel syndrome," *Gut and liver*, vol. 10, no. 3, pp. 382–390, 2016.

[38] G. Chao, Z. Wang, and S. Zhang, "Research on correlation between psychological factors, mast cells, and PAR-2 signal pathway in irritable bowel syndrome," *Journal of Inflammation Research*, vol. 14, pp. 1427–1436, 2021.

[39] D. Grundmann, E. Loris, S. Maas-Omlor et al., "Enteric glia: S100, GFAP, and beyond," *The Anatomical Record*, vol. 302, no. 8, pp. 1333–1344, 2019.

Hindawi
Evidence-Based Complementary and Alternative Medicine
Volume 2022, Article ID 6548623, 10 pages
https://doi.org/10.1155/2022/6548623

Research Article

Effects of Electroacupuncture at Different Acupoints on Functional Dyspepsia Rats

Yue-Jie Li,[1,2] Na-Na Yang,[1,3] Jin Huang,[1] Lu-Lu Lin,[1,3] Ling-Yu Qi,[1,3] Si-Ming Ma,[1,3] Cheng-Xin Hu,[1] Yu Wang,[1] Jing-Wen Yang,[1,3] and Cun-Zhi Liu[1,3]

[1]*International Acupuncture and Moxibustion Innovation Institute, School of Acupuncture-Moxibustion and Tunia, Beijing University of Chinese Medicine, 11 Beisanhuan East Road, Chaoyang District, Beijing 100029, China*
[2]*School of Acupuncture-Moxibustion and Tunia, Beijing University of Chinese Medicine, Shandong 250300, China*
[3]*School of Acupuncture-Moxibustion and Tunia, Beijing University of Chinese Medicine, 11 Beisanhuan East Road, Chaoyang District, Beijing 100029, China*

Correspondence should be addressed to Jing-Wen Yang; yangjw0626@126.com

Received 2 August 2021; Revised 28 December 2021; Accepted 12 January 2022; Published 1 February 2022

Academic Editor: Ying Li

Although, acupoint specificity is regarded as the core of scientific issues in electroacupuncture (EA), the difference of EA on treating functional dyspepsia (FD) at different acupoints is unclear. Therefore, this study aims to investigate the different therapeutic effects of EA at lower extremity or abdominal acupoints on the mucosal integrity and lower-inflammatory response in FD. The intragastric administration of iodoacetamide (IA) was performed in 48 rats to establish the FD model. These rats were randomly divided into the control group, the model group and the six EA groups receiving stimulation at the lower extremity (ST36, ST37, and ST39) or abdominal acupoints (ST25, CV4, and CV12) separately. The open-field test (OFT) was measured after 8 weeks of IA, and gastric emptying was evaluated after 10 days of the EA treatment. The local inflammation markers of CD45, eosinophil major basic protein (EMBP), and the tight junction proteins ZO1 and Claudin3 were assessed by immunofluorescence in all groups. Western blot analysis showed that the EMBP and Occludin1 levels in the duodenal. EA at lower extremity acupoint ST36 could improve the gastric emptying. EA at lower extremity acupoints reduced the immunoreactivity of EMBP, but the CD45 was reregulated by the ST37 and ST39 acupoints. The lower extremity acupoints also ameliorated FD-tight junction protein in the expression of Claudin3 and ZO1. However, only the ST36 suppressed the expression of EMBP and recovered the expression of Occludin1. Similarly, the effect of EA at abdominal acupoints was not obvious either in facilitating gastric motility or in improving inflammatory and mucosal injury. EA at lower extremity and abdominal acupoints with the same stimulation parameters had different therapeutic effects in gastric emptying, intestinal mucosal integrity, and inflammation response, thus proving the specificity of acupoints.

1. Introduction

Functional dyspepsia (FD), the prevalent gastrointestinal disorder, is the presence of symptoms originating from the gastroduodenal region in the absence of any organic, systemic, or metabolic disease [1]. It affected 8% to 12% of the worldwide population and substantially impaired the quality of life. Furthermore, the duration of FD has a major financial impact, and the annual additional healthcare costs related to FD have been estimated at 18$ billion in the USA [2]. Despite the common occurrence of FD with considerable healthcare expenses and impact on the quality of life, the current treatment options are limited. For example, domperidone has an obvious peripheral blocking effect and could inhibit the occurrence of nausea and vomiting, but it was easy to recur due to discontinuation of the medication. Proton pump inhibitors (PPIs) were often accompanied by gastrointestinal adverse reactions such as abdominal pain and diarrhea [3]. Consequently, effective and convenient treatment with a low risk of adverse effects remains to be developed.

Although structural diseases were an exclusion criterion for FD, recent advance in research show that in a proportion of case of FD, there are tangible but subtle disorders of gut function and immunological disorders, which may be amenable to therapies aimed at the disease rather than at symptom relief [4]. Growing evidence indicated that FD is associated with duodenal disease, including the expansion of activated eosinophils (EOS) in the duodenal, which could cause immune pathology and damage the intestinal mucosal integrity. Therefore, eosinophils in the duodenum are increasingly accepted as key players in the pathogenesis of dyspepsia [5, 6].

Acupuncture may be a potentially effective non-pharmacologic therapy for functional gastric disorders [7, 8]. Our previous randomized controlled trial has shown that acupuncture was an effective and safe method to relieve postprandial distress syndrome, with pretty long-term outcomes [2]. Actually, functional dyspepsia is frequently thought of as an abnormal condition of the stomach, which had been widely recognized. Until recently, changes in the duodenal are receiving increasing attention. In addition to CV4 and CV12, each acupoint belongs to the stomach meridian of the twelve meridians, and is widely used in the clinical treatment of various gastrointestinal diseases. Both the CV4 and CV12 are located on the abdomen, which conforms to the principle of proximal acupoint selection. ST36 is "converging point," ST25 is the "front-mu point" of large intestinal meridian, ST38 and ST39 are the "lower confluent acupoints" of large intestinal meridian and small intestinal meridian, respectively. Rising studies indicated that different acupoints influence the therapeutic effects of acupuncture [2]. Acupoints at the lower extremity and abdominal acupoints are widely applied in functional gastrointestinal disorders, but study argued that electro-acupuncture in the abdomen inhibited gastrointestinal motility [10]. Besides, Ma and his colleagues reported that low-intensity EA at abdominal acupoints cannot generate anti-inflammatory effects after LPS model [11]. Therefore, this study aims to investigate the difference of electro-acupuncture employed at the lower extremities and abdominal acupoints on the symptom of FD rats.

2. Materials and Methods

2.1. Animals. Specific-pathogen-free (SPF) male Sprague-Dawley 10-day-old rats were purchased from the Charles River Laboratory Animal Technology Co. Ltd. (Beijing, China). The rats were housed under the following conditions: the temperature of the feeding environment was $22 \pm 2^{\circ}$C, with a relative humidity of 50%, and 12 light/dark cycle. All procedures had followed the guidelines of the Statute on the Administration of Laboratory Animals. The Institutional Animal Care and Use Committee (IACUC) approved animal activities under the approval number BUCM-2019101801-4019.

2.2. FD Model and Animal Grouping. An established model of FD by LIU [9] was used in this experiment. Briefly, rats were given a gavage of 0.1% iodoacetamide in 2% sucrose daily for six days, and then kept in cages with free water and food until they were eight weeks old. After eight weeks, 60 rats were randomly divided into 8 groups: the control group ($n = 12$), the model group ($n = 12$), and the 6 groups ($n = 6$) receiving EA treatment at bilateral ST25 (Tianshu), ST36 (Zusanli), ST37 (Shangjuxu), ST39 (Xiajuxu), and unilateral CV4 (Guanyuan), CV12 (Zhongwan), respectively.

2.3. EA Intervention. All rats were immobilized in a black controller, with the central part of the abdomen and the four limbs expose without anesthesia, EA intervention was applied for once a day, 30 min lasting for 10 days. After routinely disinfecting the sterile stainless steel acupuncture needles (0.22 mm × 25 mm, Beijing ZhongYan Taihe Medical instrument Co. Ltd., Beijing, China), they were vertical inserted into the skin lasting for 30 min every day. One pair of sterile acupuncture needles was inserted bilaterally to acupoints ST36, ST37, ST38, and ST25, respectively. As for the unilateral acupoints CV4, the needle penetrated into the skin of CV4, a second needle was inserted perpendicularly to a depth of 1 mm at a nonacupoints 1 mm lateral to CV4 to from a pair for EA. The CV4 performed the same operation as CV12 (Table 1 and Figure 1(a)). The needles were connected to an EA apparatus (HANS-200A Nanjing, China) and stimulated at the frequency of 100 Hz via a continuous wave and the intensity of 1 mA. The location of each acupoints is listed in Table 1. The control group and the model group remain immobilized for 30 min.

2.4. Open-Field Test (OFT). The OFT was performed according to Lin. In a dark and quiet room, the rats belonging to the control group and the model group were placed at the center of box (100 cm ∗ 100 cm ∗ 50 cm) one by one and allowed to explore for 3 min, and then the animal dung was wiped and the box dealt with 75% alcohol. We collected the data for analysis, i.e., the total distance (Figure 1(b)).

2.5. Gastric Emptying. In FD rats, gastric emptying of a solid meal was measured as described with modification [10]. In a word, overnight fasting rats were given preweighed 30 g food normal feeding for 3 h with free access to water. Under anesthesia with high concentration isoflurane, animals quickly lost their breathing and heartbeat after 3 h. Open the abdominal cavity and remove fresh duodenal tissue, then the stomachs were removed quickly and weighed thoroughly. The amount of food contained in the stomach was different between the total weight of the stomach before and after stomach emptying. The speed of gastric emptying for the entire 3 h period was calculated as follows: gastric emptying (%) = 100 − (gastric content/food intake) × 100%.

2.6. Immunofluorescence. Under anesthesia with high concentration isoflurane, animals quickly lost their breathing and heartbeat. Open the abdominal cavity and remove fresh duodenal tissue. Part of tissues were rinsed with saline and

Table 1: The location of acupoints in the study.

Acupoints	Location	Operation
ST36 (Zusanli)	Lower lateral knee joint, 3.5 mm below fibula head	Needle perpendicularly with the depth 4-5 mm
ST37 (Shangjuxu)	ST37 was located about 6 mm below ST36 on the hind leg	Needle perpendicularly with the depth 4-5 mm
ST39 (Xiajuxu)	ST39 was located about 12 mm below ST36 on the hind leg	Needle perpendicularly with the depth 4-5 mm
ST25 (Tianshu)	Located lateral to the umbilicus, at the mid-point from the umbilicus to the nipple line	Needle perpendicularly with the depth 5 mm
CV4 (Guanyuan)	Located at the point of 3/5 down the ventral midline connecting the umbilicus to the pubic tubercle	Needle perpendicularly with the depth 5 mm
CV12 (Zhongwan)	Located at the mid-point of the ventral midline connecting the umbilicus to the sternum	Needle perpendicularly with the depth 5 mm

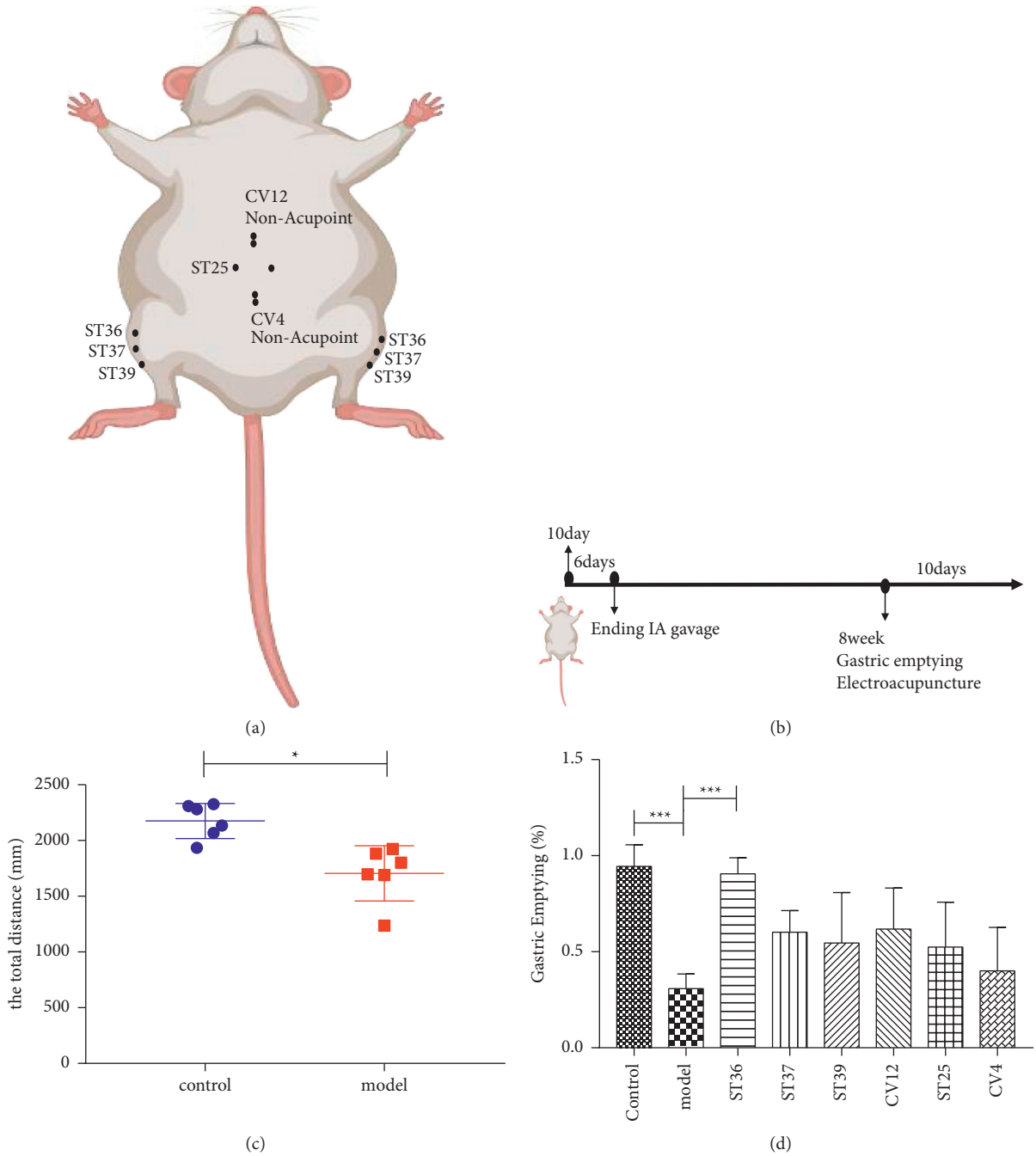

Figure 1: Gastric emptying (%) was differences at EA stimulation abdominal and lower extremity acupoints. The acupoints diagram and important time points ((a, b); the distance of animal explored (c); gastric motility of FD model rats and the EA treatment group was evaluated by gastric emptying (d). all $^{*}p < 0.05$, $^{**}p < 0.01$, compared with the FD model group, $n = 6$.

immersed in 4% paraformaldehyde for 24 hours. Gradient dehydrated in 20% and 30% sucrose in 0.01 PBS at 4°C for 24 hours. Sections of 6 μm were deparaffinized following general procedures, blocking with the bovine serum for 1 h at 37°C, and incubated with rat antimouse primary antibodies ZO-1 (1 : 2000; Abcam), claudin3 (1 : 2000; Proteintech), CD45 (1 : 2000; Proteintech), and EMBP (1 : 2000; Santa Cruz Biotechnology) at 4°C overnight. Subsequently, sections were incubated for 1 h at room temperature in the dark with donkey antirabbit secondary antibody (1 : 2000; Abcam). Cell nuclei were stained with 4′,6-diamidino-2-phenylindole (DAPI; ORIGENE), and the cover glass was enclosed onto the paraffin sections. Photomicrographs were obtained using a microscope (Olympus, Tokyo, Japan). We chose at least 6 representative nonoverlapping high-power field at ×400 magnification in a blinded manner. The number of claudin3 and the number of ZO1, CD45, EMBP-positive cells were quantified using the ImageJ program (National Institutes of Health).

2.7. Western Blot. Duodenal tissues were ground and lysed in RIPA buffer, and 40 μg total protein was separated by 12% SDS-PAGE, and then transferred to the polyvinylidene difluoride membrane. The blots were blocked with 5% skimmed milk powder in PBST and incubated overnight at 4°C with the anti-Occludin1 (1 : 1000, Proteintech Group), anti-EMBP (1 : 500, Santa Cruz Biotechnologies), and anti-β-actin (1 : 5000, Proteintech Group). The membrane was incubated with secondary antibodies in room temperature 1 h. The proteins were imaged by the ChemiDoc imaging system (Biorad, Hercules, CA, USA) after the addition of a chemiluminescent substrate.

2.8. Statistical Analysis. All data were presented as mean ± S.E.M. Paired and unpaired student's *t*-test and one-way and two-way analysis of variance (ANOVA) with post hoc tests for Tukey's multiple comparisons were used to assess the effects of EA on different acupoints. $P < 0.05$ was considered to be statistically significant. Statistical analyses were performed using GraphPad Prism 8.0 (GraphPad Software, San Diego, CA, USA).

3. Results

3.1. The Effects of EA at the Different Acupoints on the Gastric Motility. We assessed the model of FD by open field test (OFT). The distance of locomotion in the model group was significantly lower ($P < 0.05$) than that in the control group, which proved that the model group showed the emotional symptoms (Figure 1(c)).

The gastric motility of rats was measured by gastric emptying, and the motility of gastrointestinal delayed on the model rats. Compared with model group, the gastrointestinal motility of rats was affected through EA treatments. EA at the lower extremities (ST36) significantly increased the motility of gastric emptying (Figure 1(d)) ($P < 0.05$). On the contrary, the effects of EA at abdominal acupoints (ST25, CV4, or CV12) on gastric emptying were not obvious.

3.2. The Effect of EA at the Lower Extremity and Abdominal Acupoints Were Different on the Inflammatory of the Duodenal Mucosa. Low-grade inflammation of duodenal mucosa plays a key role in the pathogenesis of FD. To determine whether electroacupuncture can improve the infiltration of immune cells in the duodenal of FD rats, we used CD45 to detect the number of leukocytes in the duodenal mucosa of rats in each group. A significant increase in the amount of CD45 was observed in the duodenal (Figure 2(a)). EA at ST37 or ST39 significantly reduced the activity of CD45 expression compared with the model group (Figures 2(a) and 2(b)). However, EA at ST36, ST25, CV4, or CV12 acupoints had a mild decrease in CD45 expression, it was no significant (Figure 2(b)) ($P > 0.05$).

Based on the finding of leukocyte infiltration in the duodenum of FD rats, we further explored the effect of EA on the activation of eosinophil (Figure 3). In the duodenal (Figure 3(a)), immunostaining of EMBP was obviously stronger in the model group. However, when intervened with EA, the fluorescence intensity was weakened compared with model rats (Figure 3(b)) ($P < 0.05$). Importantly, we also found that EA at lower extremity could reduce obviously the level of EMBP.

To further prove our observation, we used the Western blot analysis that also revealed remarkable increased expression of the EMBP protein in the FD model group compared with that observed in the control group (Figure 4(a)) ($P < 0.05$). EA treatment at ST36 significantly reduced the level of EMBP compared to other acupoint groups, which showed ST36 was the appropriate acupoint for improving the inflammation of FD (Figure 4(b)).

3.3. The Difference of EA at the Lower Extremity and Abdominal Acupoints on the Duodenal Mucosal Integrity. Persistent low-grade duodenal inflammation can destroy the integrity of its mucosa and damage its function. Therefore, we continued to explore the effect of EA at different acupoints on mucosal integrity. Recent findings have demonstrated that Claudin, Oclaudin, and ZO1 were implicated in the regulation of the mucosa barrier, which were abnormal in FD patients and animal models. We performed immunofluorescence to detect the expression levels of the tight junction proteins Claudin3 and ZO1. As shown in Figure 5(a), the number of Claudin3 was upregulated, and the expression of Claudin3 was apparently stronger in ST36, ST37, or ST39 compared with the model group ($P < 0.05$). Nevertheless, the fluorescence intensity was mildly enhanced after the intervention of CV4, CV12, or ST25, which had no statistical significance (Figure 5(b)) ($P > 0.05$).

Moreover, we observed that there was dropped off ZO1 expression in the model group (Figure 6(a)). On the contrary, the ZO1 positive staining was obviously increased after EA treatment, particularly in the lower extremity acupoints (ST36, ST37, or ST39) groups compared with the model group (Figure 6(b)). The abdominal acupoints seem to have no effect on the expression of ZO1. These findings were consistent with the mucosa reparability determined by immunofluorescence analysis of Claudin3.

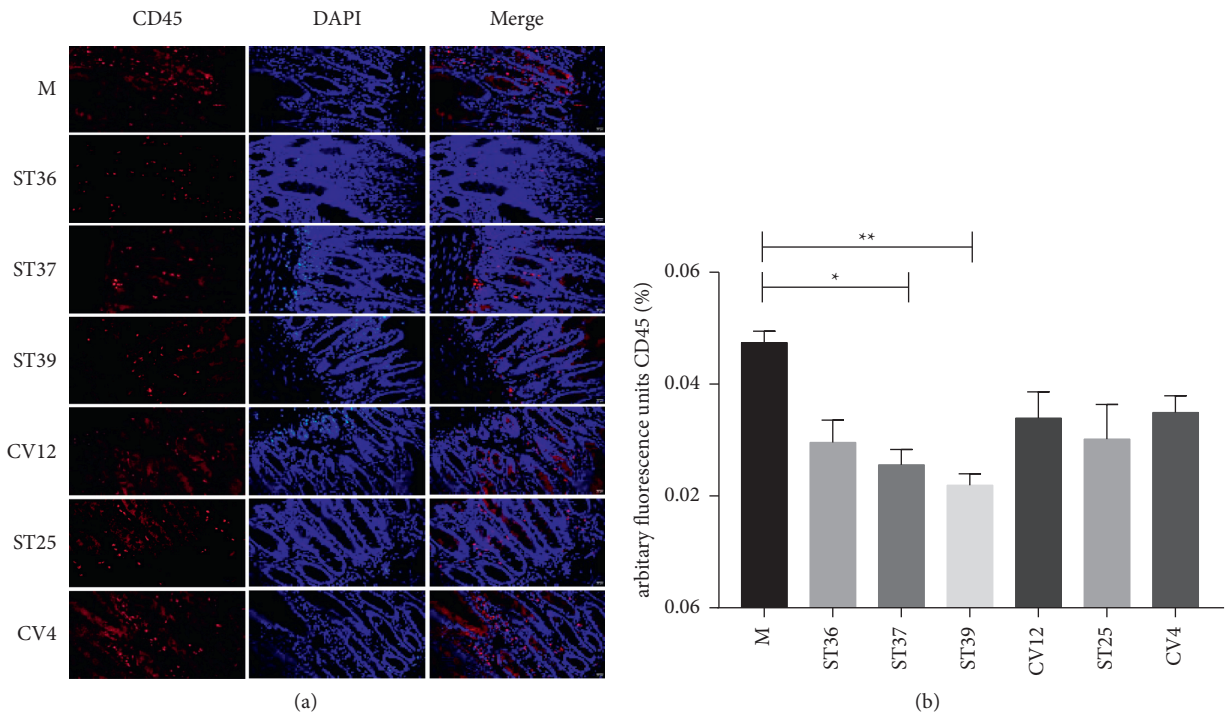

Figure 2: The difference of EA at lower extremity and abdominal acupoints on the inflammatory response of intestinal mucosal. (a) Typical results of immunofluorescence staining to detect the expression of CD45 (red). Blue signals indicate DAPI nuclear staining (scale bar, 20 μm); (b) the percentage of CD45 in duodenal mucosa (% of marked number). The results of quantification are expressed as the mean ± SEM of at 6 photos. $^{*}p < 0.05$, $^{**}p < 0.01$ compared with the FD model group, $n = 6$.

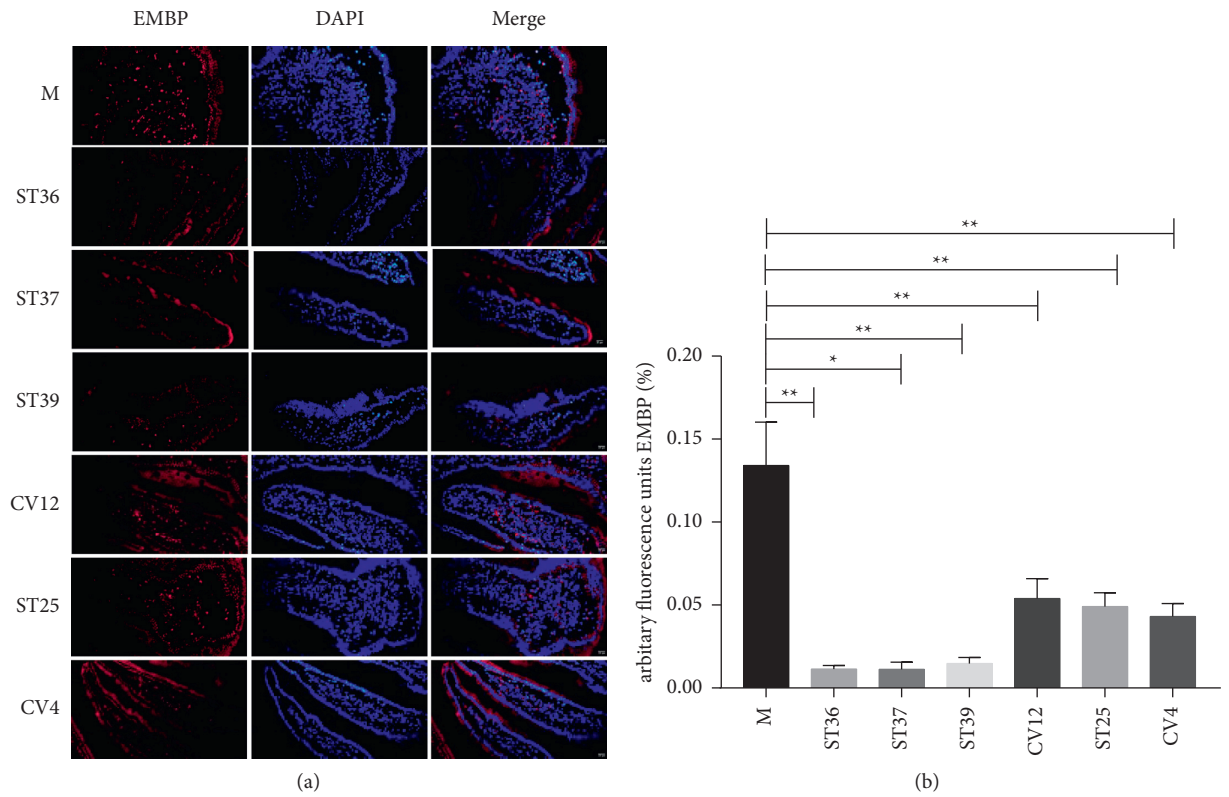

Figure 3: The difference of EA at lower extremity and abdominal acupoints on the content of EMBP. (a) Typical results of immunofluorescence staining to detect the expression of EMBP (red). Blue signals indicate DAPI nuclear staining (scale bar, 20 μm); (b) the percentage of EMBP in duodenal mucosa (% of marked number). The results of quantification are expressed as the mean ± SEM of at 6 photos. $^{*}p < 0.05$, $^{**}p < 0.01$ compared with the FD model group, $n = 6$.

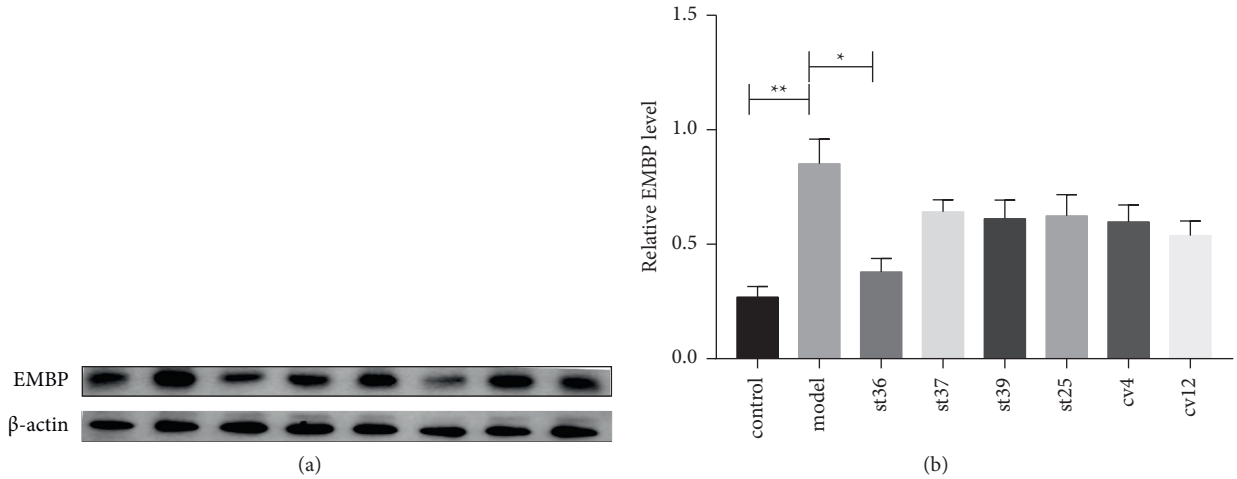

Figure 4: The effect of EA on the expression of EMBP on FD rats. (a) The expression of EMBP; (b) the expression of EMBP. The results of quantification are expressed as the mean ± SEM. $^{*}p < 0.05$, $^{**}p < 0.01$ compared with the FD model group, $n = 6$.

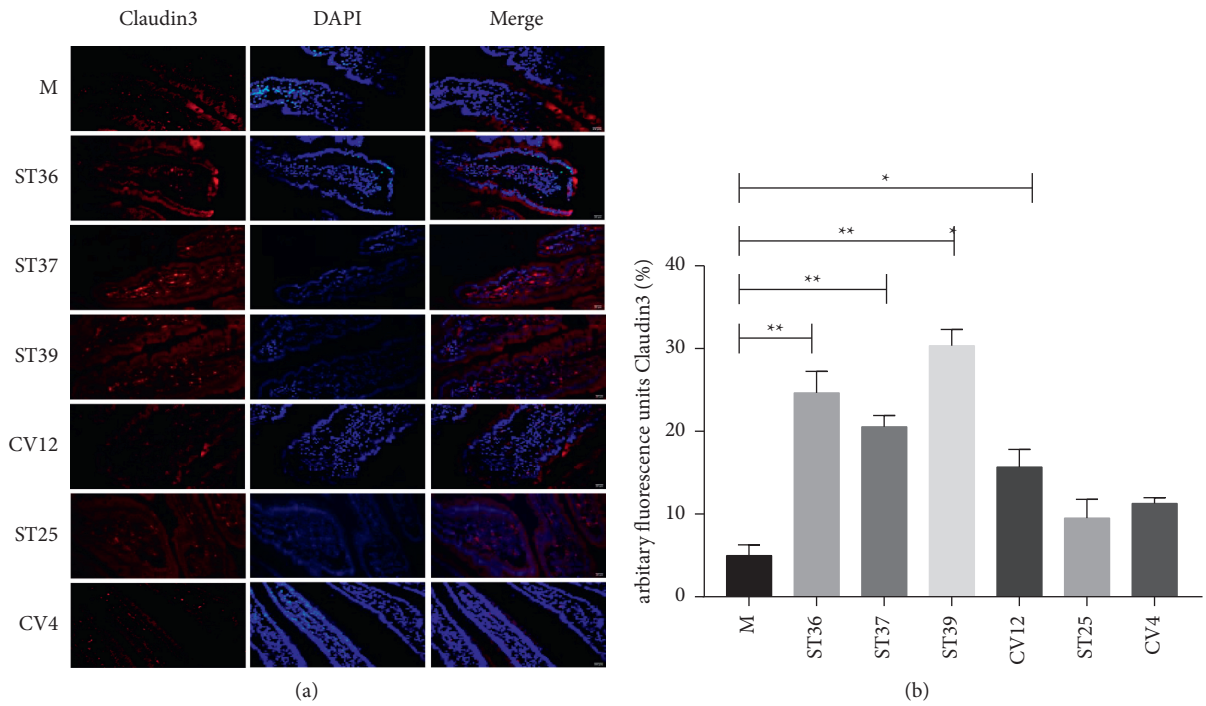

Figure 5: The difference of EA at lower extremity and abdominal acupoints on the content of Claudin3. (a) Typical results of immunofluorescence staining to detect the expression of Claudin3 (red). Blue signals indicate DAPI nuclear staining (scale bar, 20 μm); (b) the percentage of Claudin3 in duodenal mucosa (% of marked area). The results of quantification are expressed as the mean ± SEM of at 6 photos. $^{*}p < 0.05$, $^{**}p < 0.01$ compared with the FD model group, $n = 6$.

To further investigate which acupoints are effective for promoting the recovery of FD mucosal barrier function, western blot analysis was carried out to show the effects of EA at different acupoints in rats. A remarkable difference is found in the expression of Occludin1 between the control group and the FD model group (Figure 7(a)). An improvement was observed in the ST36 group, whereas there was no significant increase in the other acupoints groups (Figure 7(b)) ($P < 0.05$).

This finding was consistent with the trend of tight junction protein determined by immunofluorescence analysis of Claudin1 and ZO-1 staining.

4. Discussion

This study suggested that EA at different acupoints had specific effect on gastric motility, duodenal low-grade inflammation, and duodenal mucosal integrity in functional

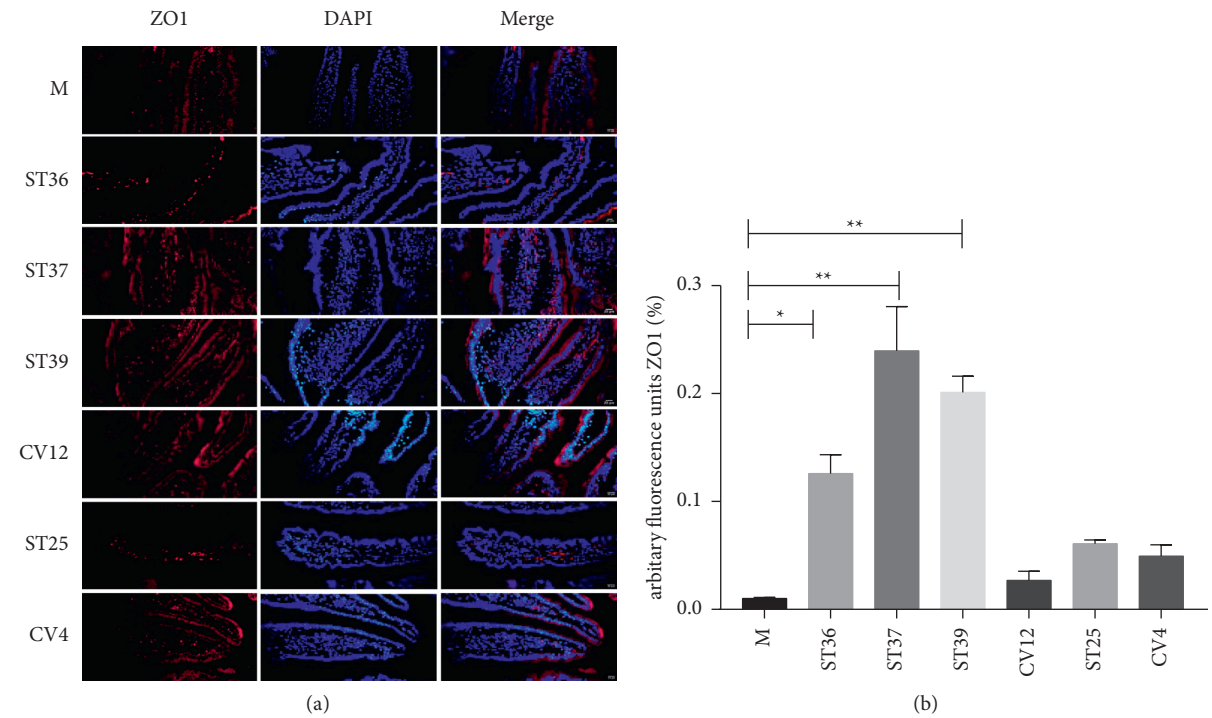

Figure 6: The effect of EA on the expression of ZO1 on FD rats. (a) Typical results of immunofluorescence staining to detect the expression of ZO1 (red). Blue signals indicate DAPI nuclear staining (scale bar, 20 μm); (b) the percentage of ZO1 in duodenal mucosa (% of marked number). The results of quantification are expressed as the mean ± SEM of at 6 photos. $^{*}p < 0.05$, $^{**}p < 0.01$ compared with the FD model group, $n = 6$.

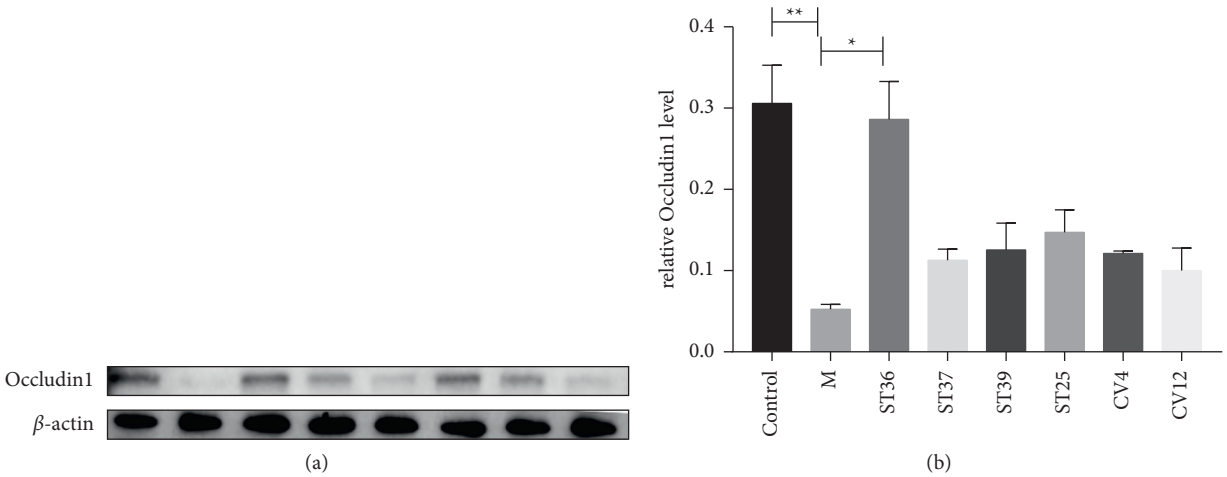

Figure 7: The effect of EA on the expression of Occludin1 on FD rats. (a) The expression of Occludin1; (b) the expression of Occludin1. The results of quantification are expressed as the mean ± SEM. $^{*}p < 0.05$, $^{**}p < 0.01$ compared with the FD model group, $n = 6$.

dyspepsia. Only the lower extremity acupoint ST36 promoted the gastric motility, played mild anti-inflammation, as well as upregulated the expression of tight junction protein in the duodenal mucosal.

The gastrointestinal insufficiency was one of the main symptoms of FD patients. The reduced of gastric motility was proved the FD model was succussed. At the same time, communication between the central nervous and the enteric nervous system had been appreciated, and the fact that brain-gut communications were bidirectional had been realized recently. In this study, we used a previously established rodent model of FD which only were gavage with iodoacetamide whereases not others manipulation. Our results indeed showed that the model reduced the distance of movement, suggesting that there were developed emotional symptoms. The symptoms were highly consistent with the clinical emotional of FD patients, which was laterally verified to be successful of the model. A decrease in gastric motility and tight junction protein expression indicated that duodenal acidification damage the intestinal barrier [14]. At the

same time, intestinal barrier dysfunction was believed to be a key risk factor for intestinal inflammation, and increasing intestinal permeability was a potential pathogenic mechanism that could be involved in the generation of low-grade duodenal inflammation and symptoms in FD [6, 15]. Therefore, we evaluated the presence of low-grade inflammation and measured the expression of adhesion proteins and duodenal mucosal barrier function on FD models after different acupoints EA treatment.

Duodenal inflammation was closely related to the pathogenesis of FD, and the expression of inflammatory cytokines was reduced by EA [16]. The destruction of the duodenal mucosal barrier and the low grade of mucosal inflammation mainly caused by local EOS immune activation might play an important role [17]. The release of EOS after degranulation produced a variety of substances, including EMBP, which acts on the intestinal epithelium and destroys its integrity. Our study indicated that EA could significantly reduce the expression of EMBP in intestinal tissue no matter electroacupuncture at the lower extremity or abdominal acupoints with the high-intensity (2 mA). There were, however, a number of reasons why it is difficult to treat leukocytes, one of which might be considered as CD45 lacked specificity.

As a traditional Chinese therapy, EA had been used to regulate the content of EOS. Carneiro ER [16] showed that acupuncture can reduce the number of EOS in BALF of asthma model, and the regulation of EOS by acupuncture is positively correlated with interleukin-4 (1L-4) and interleukin-10 (1L-10), but negatively correlated with the production of interleukin-1 (1L-1) and interferon-γ (IFN-γ), suggesting that acupuncture may regulate EOS to balance intercellular TH1/TH2 immune response. The regulation of EOS function is probably one of the main mechanisms of acupuncture in the treatment of FD. However, the regulatory effect and mechanism of acupuncture on the differentiation, development, migration, and accumulation of EOS in the inflammatory region of FD need to be further studied. The damage of the intestinal mucosal barrier especially the mechanical barrier may be an important pathogenesis of relapse and delay of FD. The study showed that there was mild inflammation in the duodenum of patients with FD that led to a decrease in the expression of intestinal epithelial tight junction proteins claudin3, ZO1, resulting in abnormal structure and function of intestinal epithelial tight junction proteins, and causing the dysfunction of intestinal mucosal barrier eventually [11, 12].

Studies showed that EA could adjust the structure of tight junction protein and had an obvious therapeutic effect. The experimental study showed that the expression of claudin and ZO1 of tight junction protein in the obese rat model increased. At the same time, it was found that it could effectively improve the intestinal mucosal barrier function by inhibiting colonic inflammation, and then reducing the expression of claudin and ZO1 [13]. The results showed that after treatment, the inflammatory factors IL-6 and TNF-α decreased in FD rats, which could play a therapeutic role in FD by improving the integrity of tight junction protein, reducing intestinal mucosal permeability, and improving low-grade duodenal inflammation [14].

Acupoint specificity regulation was considered as an important characteristic of acupuncture in Chinese medicine. It had been defined as the difference of attending function of different acupoints in the same meridian.

This study indicated that FD impaired duodenal tight junction protein and increased mucosal barrier permeability. EA treatment could repair the damaged mucosal barrier to varying degrees, and the effect of lower extremity acupoints is better. After EA treatment, the expression of tight junction protein increased in different degrees in FD rats, and the lower extremity (ST36 group, ST37 group, ST39 group) upregulated the content of Claudin3 and ZO1significantly. The ST36 increased the expression of Occludin1 that manifested different acupoints played different roles and functions in the treatment of FD. Abdominal acupoints and lower extremities acupoints have different therapeutic effects, strongly demonstrating the specificity of acupoints.

In addition, improving gastric emptying was similar to those in repairing duodenal mucosa in this study. In a previous study, we accessed that EA with different acupoints accelerated gastric motility that had different effects in the postoperative ileus mice [15]. The EA at ST36 improved the rhythm in the rats, patients' stomachs, and regulated gastric emptying [16]. Consistently, this study also proved that EA at ST36 had the function of regulating gastric motility. However, the abdominal acupoints especially the ST25 as a common acupoint for the clinical treatment of gastrointestinal diseases, and we firmly believe its therapeutic effect. The ST25 had the potential therapeutic for gastric motility, which could improve the symptom of FD traditionally. In our study, we only observed the ST25 with 100 Hz, 1 mA had no significantly therapeutic. We could not be sure that changing the parameters would have produced different results. A number of studies proved the parameters of electroacupuncture are crucial, which decided the effect of treatment sometimes. Sato and his colleagues thought that gastric motility was often excited when the acupoints on the limbs were stimulated. Our preliminary research, we found that ST25 with different parameters had different effect. The ST25 with 2/100 Hz could improve the motility of postoperative ileus whereas not 2 Hz, 15 Hz, and 100 Hz.

Interestingly, the specificity of acupoints might have different manifestations in different conditions. The different responses of these regions to different acupoint stimulation might be related to the acupoint's specificity. Recent studies demonstrated that EA at ST37 increased IL-4 and IL-1β in ulcerative colitis model rats, which is beneficial to eliminate inflammatory reactions and repair damaged tissue and has a certain therapeutic effect on ulcerative colitis [17, 18]. Studies have reported that EA at ST39 increased the level of TNF-α in intestinal tissue and the injury of duodenal mucosa [19, 20]. Moreover, the lower extremity acupoints were more effective in repairing duodenal mucosa and improving gastric motility than abdominal acupoints in the FD models. EA at different acupoints had different effects on improving gastric motility, impairing intestinal permeability, and controlling the progression of inflammation. As we all know, ST36, ST37, and ST39 are all located in the stomach

meridian, and from the close physiological function between the stomach, large and small intestinal, there is more mutual influence between batches in the pathological condition. Acupoint locations had different sensitives to EA due to the different stimulation intensities. The high intensity at the abdominal acupoints maybe drive a spinal-sympathetic axis, promoting anti-inflammatory effects that depend on NPYDBH-marked noradrenergic neurons. However, the high intensity at the lower extremities acupoints could also drive a spinal-sympathetic axis and produce vagal efferent independent anti-inflammatory effects. Some studies showed that vagal and sympathetic pathways associated with gastric motility regulate can be evoked from lower extremities and abdominal severally [10, 11]. Therefore, these findings indicated that the surface lower extremity and abdominal acupoints are relatively specific in the treatment of FD. EA at the ST36 could improve the gastric motility, restore mucosal integrity, and reduce the inflammation of FD rats.

5. Conclusion

In conclusion, we confirmed that EA at lower extremities acupoints (ST36, ST37, ST39) and abdominal acupoints (ST25, CV4, CV12) played different roles in the treatment of FD. Mechanistically, EA at ST36 potentially suppressed the low-grade inflammation in the duodenal to increase the integration of duodenal mucosal, in turn, to improve FD symptoms.

Data Availability

The data used to support the findings of this study are included within the article.

Conflicts of Interest

The authors have no competing interests.

Authors' Contributions

Y-JL and N-NY performed the research and wrote the paper. C-ZL and J-WY designed the research, and JH and L-YQ and L-LL and C-XH, and YW and S-MM performed the research and analyzed the data. All authors read and approved the final version of the manuscript.

Acknowledgments

This work was supported by the National Key R&D Program of China (No: 2019YFC1712100) and the National Science Fund for Distinguished Young Scholars (No: 81825024).

References

[1] A. C. Ford, S. Mahadeva, M. F. Carbone, B. E. Lacy, and N. J. Talley, "Functional dyspepsia," *The Lancet*, vol. 396, no. 10263, pp. 1689–1702, 2020.

[2] J.-W. Yang, L.-Q. Wang, X. Zou et al., "Effect of acupuncture for postprandial distress syndrome," *Annals of Internal Medicine*, vol. 172, no. 12, pp. 777–785, 2020.

[3] I. Masuy, L. Van Oudenhove, and J. Tack, "Review article: treatment options for functional dyspepsia," *Alimentary Pharmacology & Therapeutics*, vol. 49, no. 9, pp. 1134–1172, 2019.

[4] P. Enck, F. Azpiroz, G. Boeckxstaens et al., "Functional dyspepsia," *Nature Reviews Disease Primers*, vol. 3, no. 1, Article ID 17081, 2017.

[5] N. J. Talley, M. M. Walker, P. Aro et al., "Non-ulcer dyspepsia and duodenal eosinophilia: an adult endoscopic population-based case-control study," *Clinical Gastroenterology and Hepatology*, vol. 5, no. 10, pp. 1175–1183, 2007.

[6] H. Vanheel, M. Vicario, T. Vanuytsel et al., "Impaired duodenal mucosal integrity and low-grade inflammation in functional dyspepsia," *Gut*, vol. 63, no. 2, pp. 262–271, 2014.

[7] H.-D. Lim, M.-H. Kim, C.-Y. Lee, and U. Namgung, "Anti-inflammatory effects of acupuncture stimulation via the vagus nerve," *PLoS One*, vol. 11, no. 3, Article ID e0151882, 2016.

[8] J. L. Balestrini, D. Tsuchida, H. Fukuda, T. N. Pappas, and T. Takahashi, "Acupuncture accelerates delayed gastrointestinal transit after abdominal surgery in conscious rats," *Scandinavian Journal of Gastroenterology*, vol. 40, no. 6, pp. 734-735, 2005.

[9] L. S. Liu, J. H. Winston, M. M. Shenoy, G. Q. Song, J. D. Z. Chen, and P. J. Pasricha, "A rat model of chronic gastric sensorimotor dysfunction resulting from transient neonatal gastric irritation," *Gastroenterology*, vol. 134, no. 7, pp. 2070–2079, 2008.

[10] F. Dai, Y. Lei, S. Li, G. Song, and J. D. Z. Chen, "Desvenlafaxine succinate ameliorates visceral hypersensitivity but delays solid gastric emptying in rats," *American Journal of Physiology-Gastrointestinal and Liver Physiology*, vol. 305, no. 4, pp. G333–G339, 2013.

[11] M. Taki, T. Oshima, M. Li et al., "Duodenal low-grade inflammation and expression of tight junction proteins in functional dyspepsia," *Neuro-Gastroenterology and Motility*, vol. 31, no. 10, Article ID e13576, 2019.

[12] J. Chen, Y.-h. Xuan, M.-x. Luo et al., "Kaempferol alleviates acute alcoholic liver injury in mice by regulating intestinal tight junction proteins and butyrate receptors and transporters," *Toxicology*, vol. 429, Article ID 152338, 2020.

[13] H. Wu, F. X. Liang, B. G. Chen, and L. Chen, "[Effects of electroacupuncture on inflammatory response and intestinal mucosal barrier in obese rats with insulin resistance]," *Zhongguo Zhen Jiu*, vol. 39, no. 11, pp. 1199–1204, 2019.

[14] X. Chang, L. Zhao, J. Wang, X. Lu, and S. Zhang, "Sini-san improves duodenal tight junction integrity in a rat model of functional dyspepsia," *BMC Complementary and Alternative Medicine*, vol. 17, no. 1, p. 432, 2017.

[15] N. N. Yang, Y. Ye, Z. X. Tian et al., "Effects of electroacupuncture on the intestinal motility and local inflammation are modulated by acupoint selection and stimulation frequency in postoperative ileus mice," *Neuro-Gastroenterology and Motility*, vol. 32, no. 5, Article ID e13808, 2020.

[16] C.-S. Chang, C.-W. Ko, C.-Y. Wu, and G.-H. Chen, "Effect of electrical stimulation on acupuncture points in diabetic patients with gastric dysrhythmia: a pilot study," *Digestion*, vol. 64, no. 3, pp. 184–190, 2001.

[17] Y. Shi, T. Li, J. Zhou et al., "Herbs-partitioned moxibustion combined with acupuncture inhibits TGF-β1-smad-snail-induced intestinal epithelial mesenchymal transition in Crohn's disease model rats," *Evidence-Based Complementary and Alternative Medicine*, vol. 2019, Article ID 8320250, 2019.

[18] Q. H. Yu, L. H. Li, Y. W. Lu et al., "[Moxibustion combined with acupoint catgut embedding promotes recovery of injured

colonic mucosa by suppressing inflammation in ulcerative colitis rats]," *Zhen Ci Yan Jiu*, vol. 45, no. 4, pp. 305–309, 2020.

[19] X. Ling, H. Zhang, X. Q. Yi, and J. F. Wu, "[Effects of electroaupuncture stimulation of "Xiajuxu" (ST 39), etc. on duodenal mucosal injury, serum pro-inflammatory factors levels and duodenal nicotinic acetylcholine receptor alpha 7 expression in duodenal ulcer rats]," *Zhen Ci Yan Jiu*, vol. 41, no. 2, pp. 108–112, 2016.

[20] H. Zhang, Z. Z. Wang, Y. C. Zhang et al., "[Effect of electroacupuncture of "Xiaohai" (SI 8) and "Xiajuxu" (ST 39) on serum TNF-α and duodenal high mobility group protein B 1 levels in duodenal ulcer rats]," *Zhen Ci Yan Jiu*, vol. 40, no. 1, pp. 35–39, 2015.

Hindawi
Evidence-Based Complementary and Alternative Medicine
Volume 2022, Article ID 1614648, 7 pages
https://doi.org/10.1155/2022/1614648

Research Article

The Influence of Psychological Status on Acupuncture for Postprandial Distress Syndrome: A Subgroup Analysis of a Multicenter, Randomized Controlled Trial

Na-Na Yang, Jing-Wen Yang, Chun-Xia Tan, Yue-jie Li, Yu Wang, Ling-Yu Qi, and Cun-Zhi Liu

International Acupuncture and Moxibustion Innovation Institute, School of Acupuncture-Moxibustion and Tunia, Beijing University of Chinese Medicine, Beijing, China

Correspondence should be addressed to Cun-Zhi Liu; lcz_tg@126.com

Received 14 September 2021; Accepted 9 December 2021; Published 31 January 2022

Academic Editor: Haifa Qiao

Background. Postprandial distress syndrome (PDS) is accompanied by a high incidence of mood disorder. Acupuncture is an effective method in relieving dyspepsia symptoms; however, the impact of psychological status on acupuncture for PDS remains mysterious. *Methods*. This secondary analysis of a multicenter, randomized controlled trial aims to evaluate the influence of anxiety and depression on acupuncture for PDS. 138 patients received the same acupuncture treatment and were followed up until week 16. The 2 primary outcomes were the response rate based on overall treatment effect and the elimination rate of all 3 cardinal symptoms after 4 weeks of treatment. *Results*. Of 114 patients, 31 were anxiety patients and 83 were nonanxiety patients or 32 were depressive patients and 82 were nondepressive patients. The response rate and elimination rate at week 4 were 77.4% and 9.7% in anxiety patients versus 84.3% and 27.7% in nonanxiety patients, respectively ($P = 0.388$; $P = 0.041$). No significant difference was noted in the response rate ($P = 0.552$) and elimination rate ($P = 0.254$) at week 4 between nondepressive and depressive patients. There was no significant intergroup difference in the response rate and elimination rate between non-mood-disorder and mood disorder patients ($P > 0.05$) during the 12-week post-treatment follow-up, except for the response rate at week 8 ($P < 0.05$). *Conclusion*. The effect of acupuncture on response rate was similar for both non-mood-disorder and mood disorder patients. However, anxiety but not depression had a negative influence on the elimination rate, especially in postprandial fullness.

1. Introduction

Functional dyspepsia (FD), a chronic functional gastrointestinal disorder (FGID), is characterized by upper abdominal symptoms rooting in the gastroduodenal region, without identified organic causes [1]. Two subgroups were proposed by the Roman III consensus and reiterated in the Roman IV revision: postprandial distress syndrome (PDS) with meal-related symptoms of postprandial fullness and early satiation, and epigastric pain syndrome (EPS) with meal-unrelated epigastric pain and burning [2]. PDS is the most common subtype and was reported to have the greatest negative effect on substantially impaired quality of life [3]. Despite the familiar occurrence of PDS with high prevalence and impressive medical expenses, developing treatments for FD is challenging [4].

Traditional PDS has been conceptualized as brain-gut disorders, with subgroups of patients demonstrating motility abnormalities and psychological distress [5]. Meanwhile, anxiety and depression predicted dyspepsia symptom severity independent of gastric sensorimotor function, indicating the etiological significance of anxiety and depression in FD [6]. Besides, antidepressants are frequently prescribed to treat FD [7]. Therefore, PDS was accompanied by a high incidence of mood disorder and could affect the treatment and prognosis.

Acupuncture has been sufficiently demonstrated as a potentially effective therapy in treating gastrointestinal

symptoms. The efficacy of acupuncture in ameliorating the dyspepsia symptoms, including postprandial fullness and early satiation, was manifested by several randomized clinical trials [8–11]. Meanwhile, our previous trial has also shown that the effects of acupuncture were manifested after 4 weeks of treatment and were maintained during 12-week post-treatment follow-up [12]. However, these studies were focused on the treatment approach used for FD, and hence it was unclear whether psychological status affected the efficacy of acupuncture in patients with PDS. In this subgroup analysis, we sought to evaluate the influence of anxiety and depression on acupuncture for PDS.

2. Methods

2.1. Data Source, Randomization, and Blinding. Detailed descriptions of the protocol of the previous trial were published [12]. Briefly, this trial was a multicenter, randomized, sham-controlled trial conducted between April 2017 and January 2019 at 5 tertiary hospitals in China. The original trial was approved by the institutional review boards (ISRCTN registry number: ISRCTN12511434) and ethics committees of all 5 participating hospitals. Before participation, all patients provided written informed consent. A total of 278 patients were randomly assigned in a ratio of 1 : 1 to undergo acupuncture or sham acupuncture by a central web-based randomization system. Stratified block randomization was used, with a block size of 6. A randomization sequence was generated by a nonparticipating biostatistician in this trial. Patients, outcomes assessors, and statistical analysts were blinded to group assignment until the analysis was completed. Acupuncturists were not blinded to the treatment.

2.2. Interventions. These patients received acupuncture (138 patients) or sham acupuncture (140 patients) stimulation thrice per week with a 20-min duration over 4 weeks and were followed up until week 16 (Figure 1). In this subgroup analysis, only patients in the acupuncture group were included. Acupuncture prescription including 8 obligatory and 1 additional acupoints was manipulation by clinically experienced acupuncturists, who were twirling, rotating, lifting, and thrusting each needle for 30 seconds to achieve the de qi sensation. The obligatory acupoints were Baihui (DU20), Danzhong (RN17), Zhongwan (RN12), Qihai (RN6), and bilateral Tianshu (ST25), Neiguan (PC6), Zusanli (ST36), and Gongsun (SP4). Additional acupoints were chosen individually: Taibai (SP3) for weakness of the qi of the spleen and stomach, Taichong (LR3) for depression of the qi of the liver, and Neiting (ST44) for damp-heat in the stomach. For the current research, a total of 24 (17.4%) patients were excluded in this analysis (21 patients with no primary outcomes and 3 patients with no psychological status evaluation); and 31 anxiety patients and 83 nonanxiety patients or 32 depressive patients and 82 nondepressive patients who received acupuncture treatment were included in this subgroup analysis.

2.3. The Evaluation of the Psychological Status. The psychological status of the patients was evaluated via the Hospital Anxiety and Depression Scale (HADS) at the time of their inclusion into the trial. The HADS is a self-administered scale consisting of 14 items split across anxiety and depression subscales, each with a four-point ordinal response format with values ranging from 0 to 3 [13], which resulted in scale values between 0 and 21 for each scale. It was defined in two ranges for both the scales: 0–7 (nondepressive or nonanxiety patients) and 8–21 (depressive or anxiety patients) [14].

2.4. Outcomes. The 2 primary outcomes for this analysis were similar to the original trial [12]. Briefly, the 2 primary outcomes were the response rate based on overall treatment effect and the elimination rate of all 3 cardinal symptoms: postprandial fullness, upper abdominal bloating, and early satiation after 4 weeks of treatment. The response rate was based on the overall treatment effect questionnaire, which asked, "How were your gastric symptoms during the past week in comparison with the baseline period?" This was scored on a 7-point Likert scale, with options of "extremely improved," "improved," "slightly improved," "not changed," "slightly aggravated," "aggravated," or "extremely aggravated." Patients were considered responders if they answered "extremely improved" or "improved" and were considered nonresponders otherwise. The elimination rate was defined as the proportion of patients whose score on the severity scale for all 3 cardinal symptoms (postprandial fullness, upper abdominal bloating, and early satiation) was 0 at week 4. Acupuncture was considered an effective therapy only if both primary outcomes achieved significance.

Secondary outcomes included the response rate and the elimination rate at weeks 8, 12, and 16.

2.5. Statistical Analysis. We summarized the baseline characteristics with the descriptive statistics for the intention-to-treat population. For baseline data, continuous variables, presented as the mean (SD), were tested by unpaired *t*-tests or nonparametric rank-sum tests. Categorical variables, shown as the number (percent), were assessed with χ^2 tests.

The response rate and elimination rate were evaluated with χ^2 tests at week 4, 8, 12, and 16 for primary and secondary outcomes. The correlations between the psychological assessments and scores of overall treatment effect, postprandial fullness, upper abdominal bloating, and early satiation were assessed with Spearman's correlation test.

All analyses were carried out with SPSS 23.0 software, with a 2-side significance level of less than 0.05.

3. Results

3.1. Patients' Characteristics. A total of 114 patients were eligible for this analysis. Demographic characteristics including age, sex, marital status, occupation, education, body mass index, disease duration, endoscopy findings, and *Helicobacter pylori* status between anxiety and nonanxiety

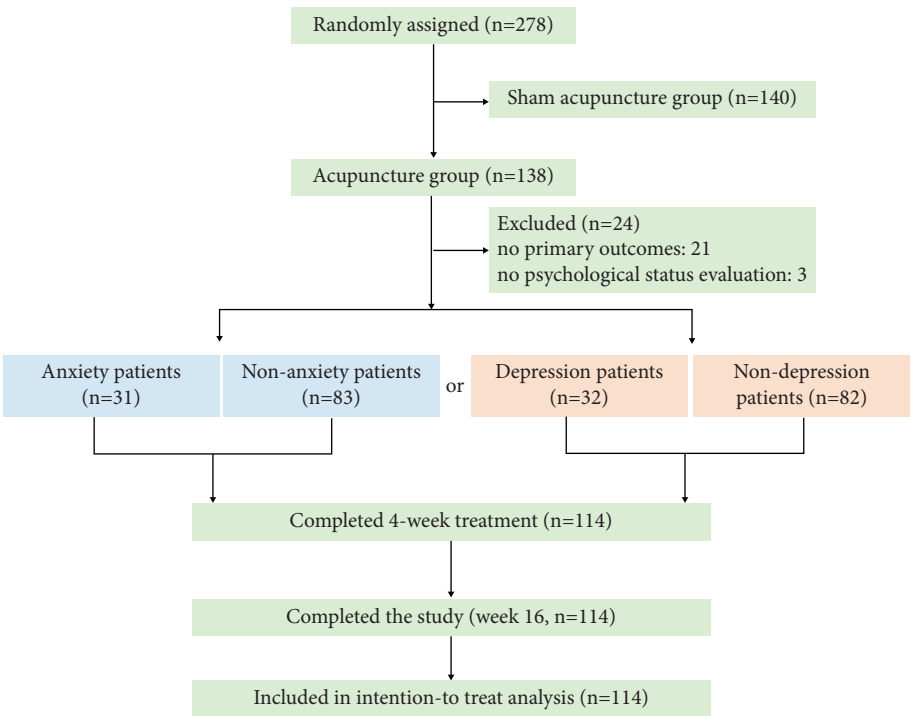

Figure 1: Study flow diagram.

patients or depressive and nondepressive patients were comparable, with no significant difference in parameters (Table 1).

3.2. The Influence of Anxiety on Acupuncture for PDS. There was no significant difference between the two groups in the response rate at week 4 (anxiety group 77.4% vs. nonanxiety group 84.3%, difference: 1.6 percentage points [95% CI, 0.6 to 4.4 percentage points], $P = 0.388$). However, the elimination rate was significantly higher in the non-anxiety patients (27.7%) than anxiety patients (9.7%) after acupuncture treatment (difference: 3.6 percentage points [95% CI, 1.0 to 12.9 percentage points], $P = 0.041$) (Table 2).

The response rate and elimination rate were gradually increased from week 1 in both groups (Figures 2(a) and 2(b)). For the response rate, no significant difference was found until week 8 (anxiety group 74.2% VS nonanxiety group 90.4%, difference: 3.3 percentage points [95% CI, 1.1 to 9.7 percentage points], $P = 0.027$). Compared with anxiety patients, nonanxiety patients have a higher response rate at week 12 and week 16; however, these between-group differences were not statistically significant (week 12: 77.4% vs. 83.1%, difference: 1.4 percentage points [95% CI, 0.5 to 4.0 percentage points], $P = 0.484$; week 16: 71.0% vs. 77.1%, difference: 1.4 percentage points [95% CI, 0.5 to 3.5 percentage points], $P = 0.498$) (Table 3). Similarly, no significant difference was noted in the elimination rate at week 8 (anxiety group 19.4% vs. nonanxiety group 31.3%, difference: 1.9 percentage points [95% CI, 0.7 to 5.2 percentage points], $P = 0.206$), week 12 (anxiety group 22.6% vs. nonanxiety group 28.9%, difference: 1.6 percentage points [95% CI, 0.6 to 4.1 percentage points], $P = 0.360$), and week 16 (anxiety group 29% vs. nonanxiety group 28.9%, difference: 1.0 percentage points [95% CI, 0.4 to 2.5 percentage points], $P = 0.990$) (Table 3).

Furthermore, we also analyzed the relationship between the comorbid anxiety and the score of overall treatment effect or all 3 cardinal symptoms using Spearman's correlation after 4 weeks of treatment. The score of anxiety was positively correlated with the severity score of postprandial fullness ($R = 0.27$, $P = 0.004$). However, the correlation analysis revealed no significant relationship between anxiety and overall treatment effect ($R = 0.18$, $P = 0.058$), upper abdominal bloating ($R = 0.15$, $P = 0.110$), or early satiation ($R = 0.16$, $P = 0.083$) (Figure 2(c)).

3.3. The Influence of Depression on Acupuncture for PDS. With respect to the primary outcomes, the response rate and elimination rate in depressive patients and non-depressive patients were 78.1%, 15.6% and 82.8%, 25.6%, respectively, at week 4. However, these between-group differences were not statistically significant (response rate, difference: 1.4 percentage points [95% CI, 0.5 to 3.8 percentage points], $P = 0.552$; elimination rate, difference: 1.9 percentage points [95% CI, 0.6 to 5.4 percentage points], $P = 0.254$) (Table 4).

At each assessment time point during follow-up, the nondepressive patients had better results than depressive patients in the response rate and elimination rate (Figures 3(a) and 3(b)); however, it was not a significant difference except for the response rate at week 8 (depressive group 75.0% VS nondepressive group 90.2%, difference: 3.1 percentage points [95% CI, 1.0 to 9.1 percentage points], $P = 0.035$) (Table 5).

Table 1: Participant baseline characteristics.

Characteristic	Anxiety ($n = 114$)		Depression ($n = 114$)	
	Anxiety patients, $n = 31$	Nonanxiety patients, $n = 83$	Depressive patients, $n = 32$	Nondepressive patients, $n = 82$
Mean age (SD), *y*	42.3 (2.4)	41.0 (1.4)	41.9 (2.1)	41.1 (1.5)
Sex, *n* (%)				
Female	21 (67.7)	63 (75.9)	23 (71.9)	61 (74.4)
Male	10 (32.3)	20 (24.1)	9 (28.1)	21 (25.6)
Marital status, *n* (%)				
Married	24 (77.4)	60 (72.3)	27 (84.4)	57 (69.5)
Single	7 (22.6)	23 (27.7)	5 (15.6)	25 (30.5)
Occupation, *n* (%)				
Mental work	27 (87.1)	72 (86.7)	31 (96.9)	68 (82.9)
Manual work	4 (12.9)	11 (13.3)	1 (3.1)	14 (17.1)
Education (SD), *y*	14.7 (0.7)	15.1 (0.3)	15.2 (0.6)	14.9 (0.3)
Mean body mass index (SD), kg/m^2	21.5 (0.7)	22.1 (0.4)	22.0 (0.7)	21.9 (0.4)
Mean disease duration (SD), *mo*	66.2 (12.2)	52.2 (5.6)	62.8 (11.0)	53.3 (6.0)
Endoscopy findings, *n* (%)[ƒ]				
Normal	0 (0)	6 (11.8)	4 (19.0)	2 (3.9)
Chronic superficial gastritis	14 (66.7)	32 (62.7)	12 (57.1)	34 (66.7)
Chronic nonatrophic gastritis	7 (33.3)	13 (25.5)	5 (23.8)	15 (29.4)
Helicobacter pylori status, *n* (%)[ʒ]				
Positive	3 (10.3)	20 (26.7)	6 (20.7)	18 (24.0)
Negative	26 (89.7)	55 (73.3)	23 (79.3)	57 (76.0)

*There was significant difference ($P < 0.05$) between the study groups. [ƒ]Data were available for 77 patients. [ʒ]Data were available for 104 patients.

Table 2: Primary outcomes in the anxiety and nonanxiety patients.

Outcome, *n* (%)	Anxiety patients, $n = 31$	Nonanxiety patients, $n = 83$	Difference (95% CI)	*P* value[†]
Response rate	24 (77.4)	70 (84.3)	1.6 (0.6 to 4.4)	0.388
Elimination rate	3 (9.7)	23 (27.7)	3.6 (1.0 to 12.9)	0.041*

[†]Calculated using the χ^2 test. *$P < 0.05$.

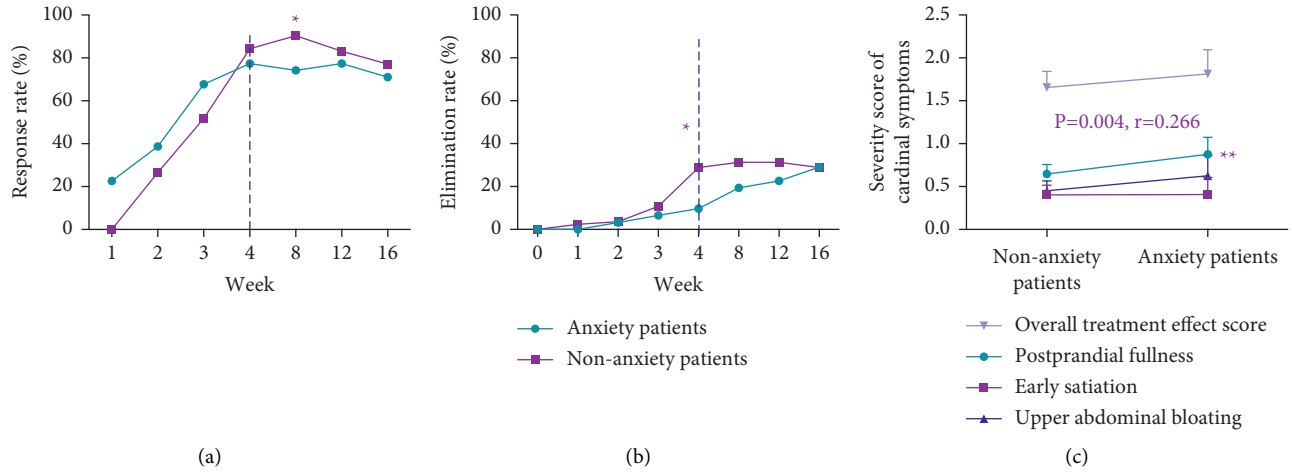

Figure 2: Response rate based on overall treatment effect (a) and elimination rate of all 3 cardinal symptoms (b) at each assessment time point. Spearman's related analysis between the comorbid anxiety and the score of overall treatment effect or all 3 cardinal symptoms at week 4 (c). *$P < 0.05$; **$P < 0.01$.

The correlation analysis revealed no significant relationship between depression and overall treatment effect ($R = 0.17$, $P = 0.077$), the postprandial fullness ($R = 0.18$, $P = 0.053$), early satiation ($R = 0.10$, $P = 0.293$), or upper abdominal bloating ($R = 0.14$, $P = 0.152$) (Figure 3(c)).

Table 3: Secondary outcomes in the anxiety and nonanxiety patients.

Outcome, n (%)	Anxiety patients, $n = 31$	Nonanxiety patients, $n = 83$	Difference (95% CI)	P value[+]
Response rate				
Week 8	23 (74.2)	75 (90.4)	3.3 (1.1 to 9.7)	0.027*
Week 12	24 (77.4)	69 (83.1)	1.4 (0.5 to 4.0)	0.484
Week 16	22 (71.0)	64 (77.1)	1.4 (0.5 to 3.5)	0.498
Elimination rate				
Week 8	6 (19.4)	26 (31.3)	1.9 (0.7 to 5.2)	0.206
Week 12	7 (22.6)	24 (28.9)	1.6 (0.6 to 4.1)	0.360
Week 16	9 (29.0)	24 (28.9)	1.0 (0.4 to 2.5)	0.990

[+]Calculated using the χ^2 test. *$P < 0.05$.

Table 4: Primary outcomes in the depressive and nondepressive patients.

Outcome, n (%)	Depressive patients, $n = 32$	Nondepressive patients, $n = 82$	Difference (95% CI)	P value
Response rate	25 (78.1)	68 (82.8)	1.4 (0.5 to 3.8)	0.552
Elimination rate	5 (15.6)	21 (25.6)	1.9 (0.6 to 5.4)	0.254

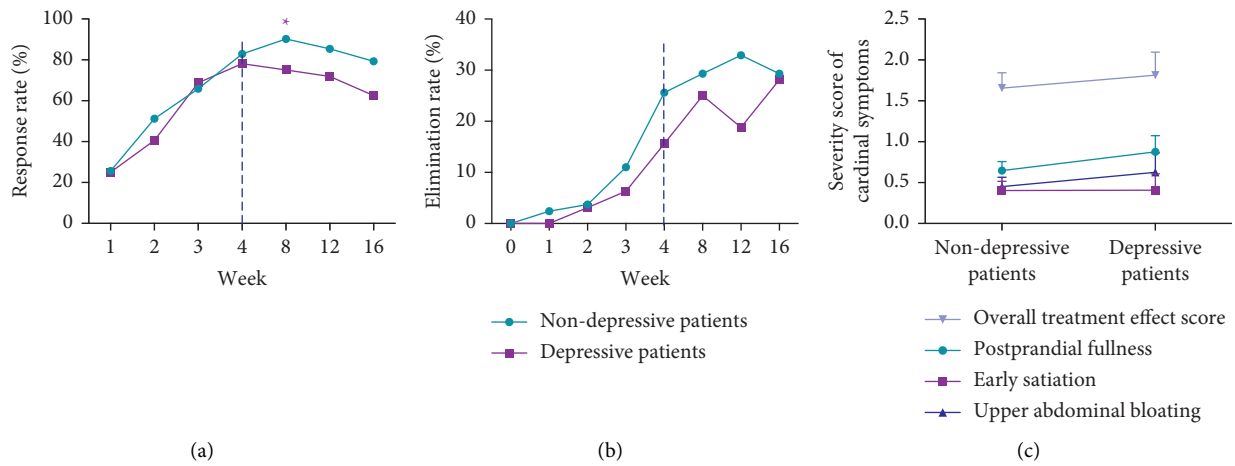

Figure 3: Response rate based on overall treatment effect (a) and elimination rate of all 3 cardinal symptoms (b) at each assessment time point. Spearman's related analysis between the comorbid depression and the score of overall treatment effect or all 3 cardinal symptoms at week 4 (c). *$P < 0.05$.

Table 5: Secondary outcomes in the depressive and nondepressive patients.

Outcome, n (%)	Depressive patients, $n = 32$	Nondepressive patients, $n = 82$	Difference (95% CI)	P value[+]
Response rate				
Week 8	24 (75.0)	74 (90.2)	3.1 (1.0 to 9.1)	0.035*
Week 12	23 (71.9)	70 (85.4)	2.2 (0.9 to 6.1)	0.095
Week 16	20 (62.5)	65 (79.3)	2.3 (0.9 to 5.6)	0.065
Elimination rate				
Week 8	8 (25.0)	24 (29.3)	1.2 (0.4 to 3.1)	0.649
Week 12	6 (18.8)	27 (32.9)	2.1 (0.8 to 5.8)	0.134
Week 16	9 (28.1)	24 (29.3)	1.1 (0.4 to 2.6)	0.904

[+]Calculated using the χ^2 test. *$P < 0.05$.

4. Discussion

To our knowledge, it is the first time to evaluate the impact of psychological status on the outcomes of acupuncture for PDS patients. This trial found that the beneficial effects of acupuncture in the response rate based on overall treatment effect were similar for both non-mood-disorder and mood disorder patients. However, anxiety but not depression had a negative influence on the elimination rate of all 3 cardinal symptoms after acupuncture treatment at week 4.

The putative bio-psycho-social pathophysiological model for FD underscores the importance of psychological distress in the pathogenesis of PDS. A wealth of clinical studies indicated a high degree of comorbidity between PDS and anxiety [15, 16], and anxiety comorbidity correlated with the severity of PDS symptoms [17]. A trial of the Swedish population found that 10 years later the risk of FD developing was a nearly 8-fold increase in those with higher anxiety levels and the risk of FD in those with anxiety was limited to PDS and not EPS [18]. Furthermore, anxiety status might influence the patients' attitude towards disease treatment and the efficacy. In this subgroup analysis, the elimination rate was 18.0 percentage points higher in the nonanxiety patients than anxiety patients after 4 weeks of treatment, which indicated anxiety harmed acupuncture to improve the symptoms of PDS patients. Meanwhile, the elimination rate was 11.9 and 6.3 percentage points higher in the nonanxiety patients than anxiety patients at week 8 and week 12, respectively, but there was no significant intergroup difference. Additionally, even though the results indicated that the positive association between anxiety and the severity of postprandial fullness in acupuncture treatment was possible, the correlation was not sufficiently strong. Therefore, a prospective randomized controlled trial or predesign subgroup analysis based on anxiety may be indispensable to explore the definite causal relationship between anxiety and postprandial fullness in acupuncture treatment. This was consistent with the result of a study in which increasing levels of anxiety were associated with fullness and bloating [19]. These results supported the view that anxiety had a negative influence on the elimination rate, especially in postprandial fullness.

PDS is a symptom-based systemic disease, and the response rate is based on the overall treatment effect, which suggested improvement of the response rate is very meaningful in a clinical study for PDS, although it is a subjective global evaluation. In this secondary analysis, we also noted that nonanxiety patients had 6.9, 16.2, 5.7, and 6.1 percentage point improvement over anxiety patients at week 4, week 8, week 12, and week 16, respectively. Interestingly, the response rate in anxiety subjects was higher than that in nonanxiety subjects from week 1 to week 3. A population-based study found that anxiety but not depression was an independent factor in determining health-care-seeking behavior in Chinese patients with dyspepsia [20]. Therefore, compared with nonanxiety patients, anxiety patients who were willing to receive treatment may get the higher subjective index of response rate during 4-week treatment of acupuncture, but the elimination rate was similar in these two groups.

Depression, the most common mental disorder, leads to a variety of functional diseases and may have the potential to affect the attitude of treatment in patients with diseases, thus reducing the quality of life. Our analysis revealed that the beneficial effect of acupuncture in PDS was similar for both depressive patients and nondepressive patients in the response rate and elimination rate, as assessed over treatment and follow-up. A trial with 703 community subjects provided powerful evidence to support the viewpoint that depression did not affect the risk of FD developing [18]. Besides, the correlation analysis revealed no significant relationship between depression and symptoms of PDS. Similarly, another trial with 193 patients also found that depression was not associated with fullness but had a positive association with abdominal pain, which is the main symptom of EPS. Although antidepressants including tricyclic antidepressants and selective serotonin reuptake inhibitors have been used for irritable bowel syndrome [21], their efficacy in FD management is very uncertain. A multicenter, randomized, placebo-controlled trial with 292 subjects found that antidepressants appeared to benefit some patients with ulcer-like (painful) FD, not dysmotility-like FD, and patients with delayed gastric emptying do not respond to these drugs [7]. These results indicated that the depressive level may have no effect on the improvement of symptoms in patients with PDS by acupuncture treatment.

Notably, the response rate was 16.2 or 15.2 percentage points higher in the nonanxiety or nondepressive patients than anxiety or depressive patients at week 8, with a significant difference. Studies reported an action delay between the initiation of treatment and significant clinical responses in patients with mood disorder because it needed time to reach an effective target concentration [22, 23]. Surveys such as that conducted by Tu Y have shown that acupuncture was efficacious for the severity of depressive disorder after 8-week treatment [24]. In our previous trial, there was a statistical trend for a greater reduction in the HADS score following acupuncture versus sham acupuncture at week 8, though no significant effects were found ($P = 0.051$) [12]. Therefore, it is a plausible assumption that acupuncture has the potential to improve the clinical symptoms of mood disorder patients at week 8, and then these patients were more objectively and calmly evaluating the response rate at this time.

This secondary analysis has limitations. First, this study was conducted as an unplanned, retrospective subgroup analysis, with the number of anxiety or depressive patients being smaller than that in the control group, so it may not be possible to extrapolate the findings. Second, the psychological status of the PDS patients was measured by the HADS in this study, but this scale may not provide good separation between symptoms of anxiety and depression due to presence of a strong general factor [13]. Third, although we found that mood disorder at baseline had influences on the therapeutic effect of acupuncture in PDS patients, the casual relationship between psychological status and symptoms improvement after treatment was still unclear. In our trials, acupuncture improved the symptoms of PDS at week 4 and had a reduction trend of the HADS score at week 8, and these findings indicated that the efficacy of acupuncture for psychological status may be mediated by the improvement of PDS. However, this assumption remains to be further assessed in large and well-designed clinical trials.

5. Conclusion

In conclusion, we present, to the best of our knowledge, the first evidence that the beneficial effect of acupuncture in the response rate was similar for both non-mood-disorder and

mood disorder patients. However, anxiety but not depression had a negative influence on the elimination rate, especially in postprandial fullness, after acupuncture treatment at week 4.

Data Availability

The date used to support the findings of this study are included within this article.

Conflicts of Interest

The authors declare no conflicts of interest, financial or otherwise.

Acknowledgments

This work was supported by the National Science Fund for Distinguished Young Scholars (81825024) and the National Key R&D Program of China (2019YFC1712100).

References

[1] H. Vanheel and R. Farré, "Changes in gastrointestinal tract function and structure in functional dyspepsia," *Nature Reviews Gastroenterology & Hepatology*, vol. 10, no. 3, pp. 142–149, 2013.

[2] L. Wauters, G. Burns, M. Ceulemans et al., "Duodenal inflammation: an emerging target for functional dyspepsia?" *Expert Opinion on Therapeutic Targets*, vol. 24, no. 6, pp. 511–523, 2020.

[3] I. Aziz, O. S. Palsson, H. Törnblom, A. D. Sperber, W. E. Whitehead, and M. Simrén, "Epidemiology, clinical characteristics, and associations for symptom-based Rome IV functional dyspepsia in adults in the USA, Canada, and the UK: a cross-sectional population-based study," *The Lancet Gastroenterology & Hepatology*, vol. 3, no. 4, pp. 252–262, 2018.

[4] L. Wauters, N. J. Talley, M. M. Walker, J. Tack, and T. Vanuytsel, "Novel concepts in the pathophysiology and treatment of functional dyspepsia," *Gut*, vol. 69, no. 3, pp. 591–600, 2020.

[5] N. Powell, M. M. Walker, and N. J. Talley, "The mucosal immune system: master regulator of bidirectional gut-brain communications," *Nature Reviews Gastroenterology & Hepatology*, vol. 14, no. 3, pp. 143–159, 2017.

[6] A. D. P. Mak, G. Northoff, D. K. W. Yeung et al., "Increased glutamate in somatosensory cortex in functional dyspepsia," *Scientific Reports*, vol. 7, no. 1, p. 3926, 2017.

[7] N. J. Talley, G. R. Locke, Y. A. Saito et al., "Effect of amitriptyline and escitalopram on functional dyspepsia: a multicenter, randomized controlled study," *Gastroenterology*, vol. 149, no. 2, pp. 340–349, 2015.

[8] S.-J. Ko, B. Kuo, S.-K. Kim et al., "Individualized acupuncture for symptom relief in functional dyspepsia: a randomized controlled trial," *Journal of Alternative & Complementary Medicine*, vol. 22, no. 12, pp. 997–1006, 2016.

[9] F. A. d. R. Lima, L. E. V. V. d. C. Ferreira, and F. H. D. L. Pace, "Acupuncture effectiveness as a complementary therapy in functional dyspepsia patients," *Arquivos de Gastroenterologia*, vol. 50, no. 3, pp. 202–207, 2013.

[10] Y.-C. Park, W. Kang, S.-M. Choi, and C.-G. Son, "Evaluation of manual acupuncture at classical and nondefined points for treatment of functional dyspepsia: a randomized-controlled trial," *Journal of Alternative & Complementary Medicine*, vol. 15, no. 8, pp. 879–884, 2009.

[11] H. Zheng, J. Xu, X. Sun et al., "Electroacupuncture for patients with refractory functional dyspepsia: a randomized controlled trial," *Neuro-Gastroenterology and Motility: the Official Journal of the European Gastrointestinal Motility Society*, vol. 30, p. e13316, 2018.

[12] J.-W. Yang, L.-Q. Wang, X. Zou et al., "Effect of acupuncture for postprandial distress syndrome," *Annals of Internal Medicine*, vol. 172, no. 12, pp. 777–785, 2020.

[13] S. Norton, T. Cosco, F. Doyle, J. Done, and A. Sacker, "The hospital anxiety and depression scale: a meta confirmatory factor analysis," *Journal of Psychosomatic Research*, vol. 74, no. 1, pp. 74–81, 2013.

[14] R. P. Snaith, "The hospital anxiety and depression scale," *Health and Quality of Life Outcomes*, vol. 1, p. 29, 2003.

[15] B. F. Filipović, T. Randjelovic, T. Ille et al., "Anxiety, personality traits and quality of life in functional dyspepsia-suffering patients," *European Journal of Internal Medicine*, vol. 24, pp. 83–86, 2013.

[16] S. Batebi, A. Masjedi Arani, M. Jafari, A. Sadeghi, M. Saberi Isfeedvajani, and M. H. Davazdah Emami, "A randomized clinical trial of metacognitive therapy and nortriptyline for anxiety, depression, and difficulties in emotion regulation of patients with functional dyspepsia," *Research in Psychotherapy: Psychopathology, Process and Outcome*, vol. 23, no. 2, p. 448, 2020.

[17] J. C. Wu, "Psychological co-morbidity in functional gastrointestinal disorders: epidemiology, mechanisms and management," *Journal of Neurogastroenterology and Motility*, vol. 18, no. 1, pp. 13–18, 2012.

[18] P. Aro, N. J. Talley, S.-E. Johansson, L. Agréus, and J. Ronkainen, "Anxiety is linked to new-onset dyspepsia in the Swedish population: a 10-year follow-up study," *Gastroenterology*, vol. 148, no. 5, pp. 928–937, 2015.

[19] L. Van Oudenhove, H. Törnblom, S. Störsrud, J. Tack, and M. Simrén, "Depression and somatization are associated with increased postprandial symptoms in patients with irritable bowel syndrome," *Gastroenterology*, vol. 150, no. 4, pp. 866–874, 2016.

[20] W. H. C. Hu, W.-M. Wong, C. L. K. Lam et al., "Anxiety but not depression determines health care-seeking behaviour in Chinese patients with dyspepsia and irritable bowel syndrome: a population-based study," *Alimentary Pharmacology & Therapeutics*, vol. 16, no. 12, pp. 2081–2088, 2002.

[21] A. C. Ford, N. J. Talley, P. S. Schoenfeld, E. M. M. Quigley, and P. Moayyedi, "Efficacy of antidepressants and psychological therapies in irritable bowel syndrome: systematic review and meta-analysis," *Gut*, vol. 58, no. 3, pp. 367–378, 2009.

[22] Z. Wang, X. Wang, J. Liu et al., "Acupuncture treatment modulates the corticostriatal reward circuitry in major depressive disorder," *Journal of Psychiatric Research*, vol. 84, pp. 18–26, 2017.

[23] E. J. Daly, J. B. Singh, M. Fedgchin et al., "Efficacy and safety of intranasal esketamine adjunctive to oral antidepressant therapy in treatment-resistant depression," *JAMA Psychiatry*, vol. 75, no. 2, pp. 139–148, 2018.

[24] X. Yang, W. Gong, X. Ma et al., "Factor analysis of electroacupuncture and selective serotonin reuptake inhibitors for major depressive disorder: an 8-week controlled clinical trial," *Acupuncture in Medicine*, vol. 38, no. 1, pp. 45–52, 2020.

Hindawi
Evidence-Based Complementary and Alternative Medicine
Volume 2022, Article ID 3534874, 12 pages
https://doi.org/10.1155/2022/3534874

Research Article

Effects of Herb-Partitioned Moxibustion on Autophagy and Immune Activity in the Colon Tissue of Rats with Crohn's Disease

Jimeng Zhao,[1] **Zhe Ma**,[1] **Handan Zheng**,[1] **Yan Huang**,[1] **Luyi Wu**,[2] **Huangan Wu**,[1] **Yin Shi**,[1] **Huirong Liu**,[1] **and Yanan Liu**[1]

[1]*Key Laboratory of Acupuncture and Immunological Effects, Shanghai Research Institute of Acupuncture and Meridian, Shanghai University of Traditional Chinese Medicine, Shanghai 200030, China*
[2]*Shanghai University of Traditional Chinese Medicine, Shanghai 201203, China*

Correspondence should be addressed to Yin Shi; flysy0636@163.com and Yanan Liu; 5527lyn@163.com

Received 16 September 2021; Accepted 11 January 2022; Published 27 January 2022

Academic Editor: Mi Liu

Objective. To investigate the mechanism of action of herb-partitioned moxibustion on CD from the perspective of autophagy and immunity. *Methods*. The expression of microtubule-associated protein LC3II and SQSTM1/p62 in the colon tissues was detected by immunohistochemistry. Western blot was used to detect the expression of autophagic and immune-related proteins in the colon, such as LC3II, SQSTM1/p62, Beclin1, ATG16L1, NOD2, IRGM, IL-1β, IL-17, and TNF-β. mRNA levels of immune factors, such as IL-1β, IL-17, and TNF-β, and autophagy signaling molecules, such as PI3KC, AKT1, LKB1, and mTOR, were detected by RT-qPCR. *Results*. Herb-partitioned moxibustion reduced the protein levels of ATG16L1, NOD2, IRGM, LC3II, and Beclin1 ($P < 0.01$) and both the protein and mRNA levels of IL-1β, IL-17, and TNF-β in CD rats ($P < 0.01$ or $P < 0.05$), and it also increased the expression of SQSTM1/p62 protein ($P < 0.01$). The modulatory effects of herb-partitioned moxibustion on ATG16L1, NOD2, IRGM, LC3II, TNF-β, and IL-17 protein and IL-1β protein and mRNA were better than those of mesalazine ($P < 0.01$ or $P < 0.05$). Herb-partitioned moxibustion also reduced colon PI3KC, AKT1, and LKB1 mRNA expressions in CD rats ($P < 0.01$ or $P < 0.05$) and increased mTOR protein expression ($P < 0.05$). And the modulatory effect of herb-partitioned moxibustion on AKT1 mRNA was better than that of mesalazine ($P < 0.05$). *Conclusion*. Herb-partitioned moxibustion may inhibit excessively activated autophagy and modulate the expression of immune-related factors by regulating the LKB1-mTOR-PI3KC signal transduction networks, thereby alleviating intestinal inflammation in CD rats.

1. Introduction

Crohn's disease (CD) is a complex, chronic, nonspecific inflammatory bowel disease (IBD). CD often presents as segmental skip lesions, is most common in the terminal ileum and adjacent colon, and can affect any part of the digestive tract from the mouth to the anus. The clinical characteristics of CD are mainly abdominal pain, diarrhea, bloody stool, weight loss, fever, and even parenteral manifestations in the joints, skin, eyes, and liver [1]. Epidemiological investigations have shown that the incidence and prevalence of CD show an increasing trend worldwide [2]. Currently, no treatment can fully cure this disease, and clinical treatment strategies are focused on relieving symptoms to prevent complications and retard disease progression. Although many new biological agents have been used for CD [3], they can cause certain side effects and drug resistance, and patients undergoing biological agent treatment are prone to relapse, which has a great impact on their daily life and work.

The interactions of genetic susceptibility, immunity, and environmental factors are important in the pathogenesis of CD. On a certain genetic background, the excessive inflammatory response induced by the immune imbalance of the intestinal host can damage the intestinal tract and its mucosal barrier, which is a key factor affecting the occurrence and development of CD. In recent years, increasing evidence has shown that autophagy-related genetic

susceptibility is also closely related to the pathogenesis of CD [4, 5]. Autophagy is a process of intracellular catabolism. It is a common mechanism that exists in the development and aging of organisms to eliminate redundant or damaged intracellular organelles. It is essential for a variety of cellular processes and can be used to maintain biological homeostasis under stress [6]. Autophagy can keep the body's immune tolerance at different levels of adaptive immune response. The activation of autophagy helps to relieve the excessive inflammatory response, and its dysfunction can lead to the occurrence of a variety of inflammation, immune, and metabolic disorders [7]. Under normal conditions, the dynamic balance of *T* helper type 1 (Th1) and Th2 activities maintains the immune homeostasis of the body. Breaking this balance will cause inflammation. In the intestinal mucosa of CD patients, autophagy can induce macrophages to present antigens to Th1 cells through major histocompatibility complex class II molecules, after which Th1 cells secrete interferon-γ (IFN-γ) and tumor necrosis factor-β (TNF-β), which in turn promote autophagy in macrophages [8]. Autophagy and inflammatory cytokine actions interact with each other, and abnormal autophagy can break the balance between proinflammatory and anti-inflammatory cytokines, resulting in a severe intestinal inflammatory response and IBD.

Autophagy-related genes such as autophagy-related 16-like 1 (ATG16L1), immunity-related GTP as a family *M* protein (IRGM), and nucleotide-binding oligomerization domain-containing protein 2 (NOD2) have been studied [5]. The genetic variation in these autophagy-related genes is related to the occurrence of CD, and these genes are CD susceptibility genes [9–11]. The key step in the final biological effect of autophagy is the fusion of autophagosomes and lysosomes, leading to the formation of autolysosomes to degrade entrapped cargo materials within autolysosomes, a process collectively called autophagic flux [12]. Heterozygous disruption of the Beclin1 gene in mammals (homolog of yeast Atg6) led to it being the first gene identified in mammals that could induce autophagy [13]. ATG16L1 is a homolog of ATG16 and is mainly involved in the formation of autophagosomes [5]. ATG16L1-mediated autophagy in intestinal epithelial cells plays an important role in the control of intestinal inflammation and TNF-induced apoptosis in colitis [14]. During the process of autophagy, the recognition of ubiquitinated proteins is mediated by the noncovalent interaction between the ubiquitin receptor and ubiquitin through the ubiquitin-binding domain. The ubiquitin-binding protein sequestosome 1 (SQSTM1/p62) is the first reported protein with this adaptor function [15]. SQSTM1/p62 can mediate the autophagic degradation of ubiquitinated proteins and functions as a bridge between microtubule-associated protein 1-light chain 3II (LC3II) and the ubiquitinated substrate to be degraded. SQSTM1/p62 has an important role in the process of autophagic substrate degradation [16].

In addition, a variety of signal transduction pathways are involved in the regulation of autophagy. Many of these signal transduction pathways converge at the target of rapamycin (TOR), which is highly conserved in evolution. This important kinase can regulate the level of autophagy. The mammalian target of the rapamycin (mTOR) signaling pathway plays an important role in the regulation of autophagy. Growth factors regulate mTOR activity mainly through phosphatidylinositol-3-kinase/protein kinase B (PI3K/AKT) signaling pathways, and nutrients and energy inhibit mTOR activity mainly through liver kinase B1/5′-AMP-activated protein kinase (LKB1/AMPK). mTOR is also a key regulator of immune function [17]. Autophagy is involved in the regulation of immune mechanisms in CD via the LKB1-mTOR-PI3KC signal transduction network.

Herb-partitioned moxibustion has definite efficacy in the treatment of CD [18, 19], but its mechanism of action needs to be further elucidated. Using RNA-seq high-throughput sequencing, our preliminary study demonstrated that herb-partitioned moxibustion could regulate autophagy and immune gene expression in CD [20]. Therefore, in this study, we further observed the effect of herb-partitioned moxibustion on the expression of autophagy-related proteins and immune-related factors in CD rat colon tissues. We observed the relationship between herb-partitioned moxibustion and the expression changes of proteins and genes related to the LKB1-mTOR-PI3KC signal transduction network in CD colon tissues to clarify the regulatory effect of herb-partitioned moxibustion on autophagy and immunity in CD. Overall, this study explores the mechanism of the immunological effect of herb-partitioned moxibustion in CD treatment from the perspective of autophagy.

2. Methods

2.1. Experimental Animals. Adult male Sprague-Dawley (SD) rats, weighing 180 ± 20 g, were provided by the Experimental Animal Center of the Shanghai University of Traditional Chinese Medicine and were purchased from Vital River Laboratory Animal Technology Co. Ltd. (Beijing, China). The license for the use of experimental animals was SCXK (Beijing) 2012-0001. All the animals were housed in a clean grade room with controlled temperature (20 ± 2°C), a light/dark (12 h:12 h) cycle, and 50–70% indoor humidity. All experimental protocols were approved by the Animal Research Ethics Committee of the Shanghai University of Traditional Chinese Medicine (NO. PZSHUTCM211115025).

2.2. Preparation of the CD model. The CD models were established by the application of 2,4,6-trinitro-benzenesulfonic acid (TNBS; Sigma, USA) according to Morris' method [21]. Prior to model establishment, the rats were fasted and given water for 24 h. The rats were weighed, and 2% sodium pentobarbital (30 mg/kg) was administered through intraperitoneal injection (ip). The rats were anally injected with a 5% TNBS solution mixed in 50% alcohol at a 1 : 2 ratio (3 ml/kg) using a rubber tube. All groups of rats received the TNBS injection except for the N and NM groups. The rubber tube was put into the anus 6–8 cm deep. Following the injection, the head of the rat was pushed down for about 1 min to prevent loss of the injected solution. The injection was repeated every 7 days for 4 weeks.

2.3. Model Identification. After the experimental CD rat models were established, two rats were respectively selected from normal rats and model rats to ascertain whether the CD model was successfully established by hematoxylin-eosin (HE) staining.

2.4. Grouping and Intervention. 60 rats were randomly divided into normal control (N) group, CD model control (M) group, model control with herb-partitioned moxibustion (MM) group, normal control with herb-partitioned moxibustion (NM), mesalazine (Western Medicine, Med) group, and normal saline (NS) group, with 10 rats in each group.

After the experimental CD rat models were successfully established, the rats were exposed to different treatments. In the MM and NM groups, the Tianshu (bilateral, ST25) and Qihai (CV6) acupoints were selected [22]. The herbal cake is Chinese medicine powder (*Coptis chinensis*, Radix Aconiti Lateralis, Cortex Cinnamomi, Radix Aucklandiae, Flos Carthami, *Salvia miltiorrhiza*, and *Angelica sinensis*) mixed and stirred with yellow wine to form a thick paste, and the herbal cake was prepared with 1 cm in diameter and 0.45 cm in thickness using a mold. The moxa cone was prepared with 0.6 cm in diameter and height using a mold and its weight was 90 mg. When beginning the treatment, the prepared moxa cone was placed on the top of an herbal cake at the ST25 and CV6 acupoints and ignited. Two moxa cones were used at each acupoint for each treatment once daily for 7 days.

The rats in the Med group were fed with mesalazine (Losan Pharma GmbH, Germany), which was prepared at the proportion of adult and rat of 1 : 0.018 [23], once a day for 7 days.

The rats in the NS group were fed with normal saline, 2 ml per time and once a day for 7 days.

The rats in the N and M groups did not receive any treatment but were grabbed and immobilized using the same method applied to other groups.

2.5. Sample Collection. Rats were anesthetized by intraperitoneal injection of 1% pentobarbital sodium (30 mg/kg). After anesthetization, the abdominal cavity was opened and 4–6 cm of distal colon was collected 1 cm from the anus. The colon was divided into three parts: one part was fixed in 10% neutral formalin fixative solution, and the other two parts were placed in cryotubes after cutting into pieces, then frozen in liquid nitrogen for 1 h, and later stored in a −80°C freezer.

2.6. Observation of Histopathology and Scoring of the Colon Tissues. Rat colon tissues were fixed in 10% neutral formalin fixative solution for 24 h, dehydrated, embedded in paraffin, sectioned at a thickness of 4 μm, and subjected to HE staining. Histopathological changes of the colon tissues were observed under an optical microscope (BX33, Olympus).

2.7. Western Blot Analysis of the Expression of Autophagy- and Immune-Related Proteins in Rat Colon Tissues. The colon tissues of each group stored at −80°C were cut into small pieces, and 100 μl of radio-immune precipitation assay lysis buffer was added to every 20 mg of tissue. After full lysing, the supernatant was collected, and the protein concentration was determined using the bicinchoninic acid assay protein concentration assay kit. The protein extracts were taken, and gel electrophoresis was conducted to obtain the gel plates showing the target proteins. The gel plates were then placed in transfer buffer, and protein bands were transferred to membranes in an electroporator (Bio-Rad, USA) in ice water under a 200 mA constant current for 90 min. After the transfer, the polyvinylidene fluoride membrane was removed, blocked in 5% bovine serum albumin (BSA) at room temperature for 2 h, and washed with Tris-buffered saline with Tween 20 (TBST) on a shaker three times for 5 min each. Primary antibodies against LC3II (CST, USA, 1 : 1000), SQSTM1/p62 (Abcam, UK, 1 : 1000), Beclin1 (CST, USA, 1 : 1000), ATG16L1 (CST, USA, 1 : 2000), NOD2 (Abcam, UK, 1 : 2000), IRGM (CST, US, 1 : 2000), IL-1β (CST, US, 1 : 1000), IL-1β (Abcam, UK, 1 : 1000), TNF-β (BOSTER Biological Technology, Wuhan, China, 1 : 400), and GAPDH (Weiao, 1 : 2000) were added onto the membrane, followed by incubation at 4°C overnight in the incubation box. The membrane was washed with TBST three times for 5 min each. Horseradish peroxidase (HRP) (Biotech Well, Shanghai)-labeled goat anti-rabbit secondary antibody (Jackson 1 : 2000) and HRP-labeled goat anti-mouse secondary antibody (Jackson 1 : 2000) were added and incubated with the membrane at room temperature for 2 h. Then, the membrane was washed with TBST five times for 15 min each. The membrane was reacted with the chemiluminescence detection reagent for 2 min. After that, the membrane was exposed to X-ray film in a dark room, and the X-ray film was developed using appropriate developing and fixing solutions. The film was scanned or photographed, and the molecular weight and net optical density of the target bands were analyzed using a gel image processing system (Bio-Rad, USA).

2.8. Detection of mRNAs of Immune Cytokines in Rat Colon Tissue by RT-qPCR. Total RNA was extracted from colon tissue using the Trizol (Invitrogen, USA) method, followed by reverse transcription using a reverse transcription kit (Invitrogen, USA). The reaction system was 0.1% diethyl pyrocarbonate-treated water (8-x) μl, RNase inhibitor (50 U/μl) 0.5 μl, random primers (50pM) 2 μl, and RNA x μl (2 μg). After 65-min water bath treatment, the solution was placed at room temperature for 10 min and centrifuged at high speed for 5 s. The following reagents were added into 1.5 ml centrifuge tubes: RNase inhibitor (50 U/μl) 0.5 μl, 5 × buffer (Invitrogen) 4 μl, dNTPMIX (10 mM/each) 2 μl, dithiothreitol 2 μl, and AMV reverse transcriptase (200 U/μl) 1 μl. The tubes were kept in a water bath at 40°C for 1 h. The solution was treated at 90°C for 5–10 min, then put on ice for 5 min, and centrifuged at high speed for 5s. The prepared cDNA was subjected to PCR amplification. The primer sequences were designed by Primer Express Software v2.0 (ABI, USA), and primers were synthesized by BGI Group. The following were the primer sequences of the targeted

genes—GAPDH: forward 5′-GGCAAGTTCAACGGCA-CAGT-3′, reverse 5′-ATGACATACTCAGCACCGGC-3′; IL-1β: forward 5′-CCCAAGCACCTTCTTTTCCT-3′, reverse 5′-TTCATCTCGAAGCCTGCAGT-3′; IL-17: forward 5′-ATCCAGCAAGAGATCCTGGT-3′, reverse 5′- CAA-TAGAGGAAACGCAGGTG-3'; TNF-β: forward 5′-GAAAGCATGATCCGAGATGT-3′, reverse 5′-CAGGA ATGAGAAGAGGCTGA-3′; PI3KC: forward 5′-ATTGCT TTGCCTAAGCACCG-3′, reverse 5′-TGTGGCTAT-GATTGCCTCCA-3'; AKT1: forward 5′-TTCTACGGT GCGGAGATTGT-3′, reverse 5′-TTATCTTGATGTGCCC GTCC-3'; LKB1: forward 5′-TCAAGGTGGACATCTGG TCA-3′, reverse 5′-CCCGATGTTCTCAAAGAGCT-3'; mTOR: forward 5′-AAAATCCTCATGGTCCGGTC-3′, reverse 5′-TCAAGTTGCCGAGATGGATC-3′. The amplification system was as follows: H2O 5 μl, 2 × SYBR GREEN PCR mix 5 μl, forward primer (10 pM/μl) 1 μl, reverse primer (10 pM/μl) 1 μl, and 1 μl of cDNA. The reaction program was 95°C 2 min, 94°C 10 s, 59°C 10 s, and 72°C 10 s, with a total of 40 cycles. The calculation Ct (target gene) – Ct (internal reference gene) was used to obtain the △Ct value of each gene, the average △Ct value of the model group samples was subtracted from the △Ct value of each experimental group of samples, and this number,△△Ct, was used to calculate $2^{-\triangle\triangle}$Ct to find the final expression change.

2.9. Statistical Methods. SPSS 18.0 software was used for the data analysis. The data were presented as the mean ± standard deviation ($\bar{x} \pm s$), and the comparison of differences among groups was performed using one-way ANOVA if data conformed to the normal distribution. If the variances were homogeneous, the pairwise comparison was performed using the least significant difference (LSD) test. If the variances of all groups were not homogenous, the nonparametric Kruskal–Wallis test was performed for the analysis. Data that did not conform to the normal distribution were presented as the median and quartiles [M (P_{25}, P_{75})], and the rank sum test was performed for the comparison of differences among groups. The significance level of the statistical examination was $\beta = 0.05$. $P < 0.05$ indicated that the difference had statistical significance.

3. Results

3.1. Histopathological Observation of Rat Colon in Each Group. As shown in Figure 1, the colon epithelial tissues of the rats in the normal group and the control moxibustion group were intact, with the glands aligned, and no hyperemia, edema, hyperplasia, or ulcers were observed. In the model group, extensive loss of colonic mucosa and the presence of large ulcerations were observed, reaching deep into the muscularis, and many cells on the surface of the ulcer were exuded and were necrotic. However, no tissue repair was seen. In the herb-partitioned moxibustion group, the mucosal epithelium of the colon was relatively intact, and the glands were partially lost, which manifested as healed, shallow ulcers, and many inflammatory cells and fibroblasts were generated. In the mesalazine group, the ulcer of the colon was covered with hyperplastic mucosal epithelium, forming small healed ulcers, atypical hyperplasia of the glands was observed at the edge of the ulcer, and hyperplasia of many fibroblasts and new capillaries was observed in the submucosa. In the saline group, the mucosa of the colon tissue was largely lost, showing a huge ulcer that reached the muscularis. Atypical hyperplasia of glandular epithelial cells, exudation and necrosis of many cells on the surface of the ulcer, and a large amount of granulation at the bottom of the ulcer were observed.

3.2. Effect of Herb-Partitioned Moxibustion on the Expression of Autophagy-Related Proteins Implicated in CD. The expressions of autophagy-related proteins ATG16L1, NOD2, and IRGM were detected. We also detected the proteins LC3II, SQSTM1/p62, and Beclin1, which play key roles in autophagy. The modulation by herb-partitioned moxibustion of these autophagy-related proteins was evaluated. Immunohistochemistry showed that LC3II expression was higher ($P < 0.01$) and SQSTM1/p62 was lower in the rat colon tissue of the CD model than the normal group ($P < 0.01$). LC3II expression was lower ($P < 0.01$) and SQSTM1/p62 was higher in the rat colon tissue of the herb-partitioned moxibustion group than the model group ($P < 0.01$, Figures 2 and 3).

Western blot analysis showed that ATG16L1, NOD2, IRGM, LC3II, and Beclin1 were significantly higher ($P < 0.01$) and SQSTM1/p62 was significantly lower in the CD model group than the normal group ($P < 0.01$). The levels of these six proteins in the colon of the control moxibustion group were not significantly different from those of the normal group. ATG16L1, NOD2, IRGM, LC3II, and Beclin1 in rat colon tissues of the herb-partitioned moxibustion and mesalazine groups were significantly lower than those in the model group ($P < 0.01$ or $P < 0.05$), and the modulatory effects of herb-partitioned moxibustion on ATG16L1, NOD2, IRGM, and LC3II protein expression were stronger than those of mesalazine ($P < 0.01$ or $P < 0.05$). The expression of SQSTM1/p62 protein was significantly increased only in the moxibustion group ($P < 0.05$), and ATG16L1, NOD2, and IRGM proteins were also significantly lower in the saline group ($P < 0.05$) than the model group (Figure 4).

3.3. Effect of Herb-Partitioned Moxibustion on the Expression of CD-Related Immune Cytokines. Next, we observed the regulatory effect of herb-partitioned moxibustion on the immune-related factors IL-1β, IL-17, and TNF-β in the CD rat colon tissue. RT-qPCR showed that IL-1β, IL-17, and TNF-β mRNAs were significantly higher in the model group than the normal group ($P < 0.01$ or $P < 0.05$), and IL-1β, IL-17, and TNF-β mRNAs in the control moxibustion group were not significantly different from those in the normal group. IL-1β mRNA in the herb-partitioned moxibustion, mesalazine, and saline groups was significantly lower than that in the model group ($P < 0.05$), but IL-17 and TNF-β mRNA expressions were significantly lower only in the herb-partitioned moxibustion group ($P < 0.05$ and $P < 0.01$,

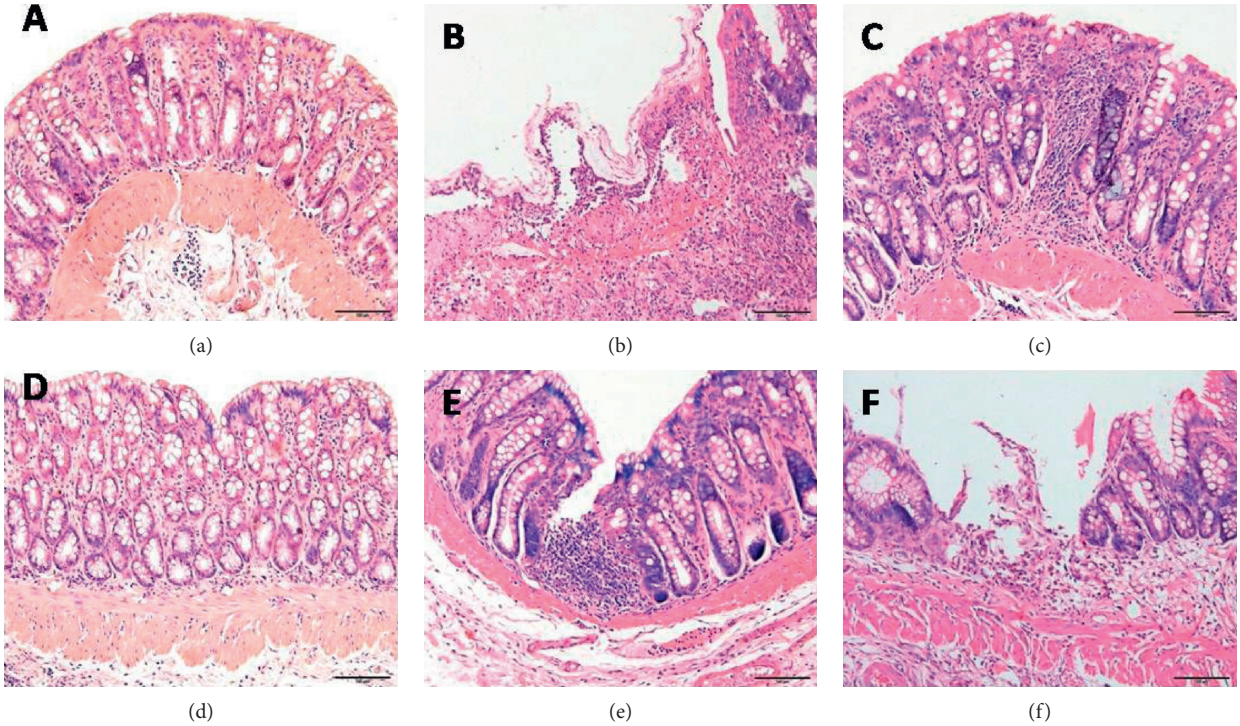

Figure 1: The histological observation of rat colon in each group by HE staining method (200×). (a) normal group; (b) CD model group; (c) CD model with herb-partitioned moxibustion group; (d) normal with herb-partitioned moxibustion group; (e) CD model with mesalazine group; (f) CD model with normal saline group.

respectively). IL-1β mRNA in the mesalazine group was significantly higher than that in the herb-partitioned moxibustion group ($P < 0.05$). Consistent with the RT-qPCR results, Western blot showed that IL-1β, IL-17, and TNF-β proteins were significantly higher in the model group than the normal group ($P < 0.01$) and did not change significantly in the control moxibustion group. IL-1β, IL-17, and TNF-β proteins were significantly lower in the herb-partitioned moxibustion, mesalazine, and saline groups than the model group ($P < 0.01$); however, IL-1β, IL-17, and TNF-β in the mesalazine group were still significantly higher than those in the herb-partitioned moxibustion group ($P < 0.05$ or $P < 0.01$) and significantly lower than those in the saline group ($P < 0.01$, Figure 5).

3.4. Effect of Herb-Partitioned Moxibustion on the Activity of the LKB1-mTOR-PI3KC Signal Transduction Network in CD Rat Colon Tissues. The above experimental results showed that herb-partitioned moxibustion could regulate the expression levels of immune-related cytokines and autophagy-related proteins in the CD rat colon tissues, could significantly inhibit the expression of autophagy-related proteins, and could alleviate local inflammation. However, the effective targets and pathways of this regulatory effect needed to be further studied. Since autophagy can participate in the regulation of the immunologic mechanism of CD through the LKB1-mTOR-PI3KC signal transduction network, we further observed the regulatory effect of herb-partitioned moxibustion on the LKB1-mTOR-PI3KC signal transduction network in CD colon tissues to further explain its mechanism of action.

The results showed that the mRNA levels of PI3KC, AKT1, and LKB1in the rat colon tissues of the model group were significantly greater than those in the normal group ($P < 0.01$). There was no significant difference in PI3KC, AKT1, or LKB1 mRNA expression between the control moxibustion and normal groups. AKT1 mRNA expression was significantly lower in the herb-partitioned moxibustion, mesalazine groups, and normal saline groups than the model group ($P < 0.01$ or $P < 0.05$). Moreover, AKT1 mRNA in the mesalazine group was significantly higher than that in the herb-partitioned moxibustion group ($P < 0.05$). PI3KC and LKB1 mRNAs were significantly lower only in the herb-partitioned moxibustion group ($P < 0.05$). In terms of protein expression, mTOR in rat colon tissues of the model group was significantly lower than that in the normal group ($P < 0.01$), while it was similar between the control moxibustion group and the normal group. Both herb-partitioned moxibustion and mesalazine treatments significantly upregulated mTOR protein in CD rat colon tissues ($P < 0.05$, Figure 6).

4. Discussion

For a long time, CD was considered an autoimmune disease controlled by T cell-dependent immune responses. The discovery of ATG16L1, NOD2, and IRGM, autophagy-related genes implicated in CD, reflects the association between inflammation and innate immune gene

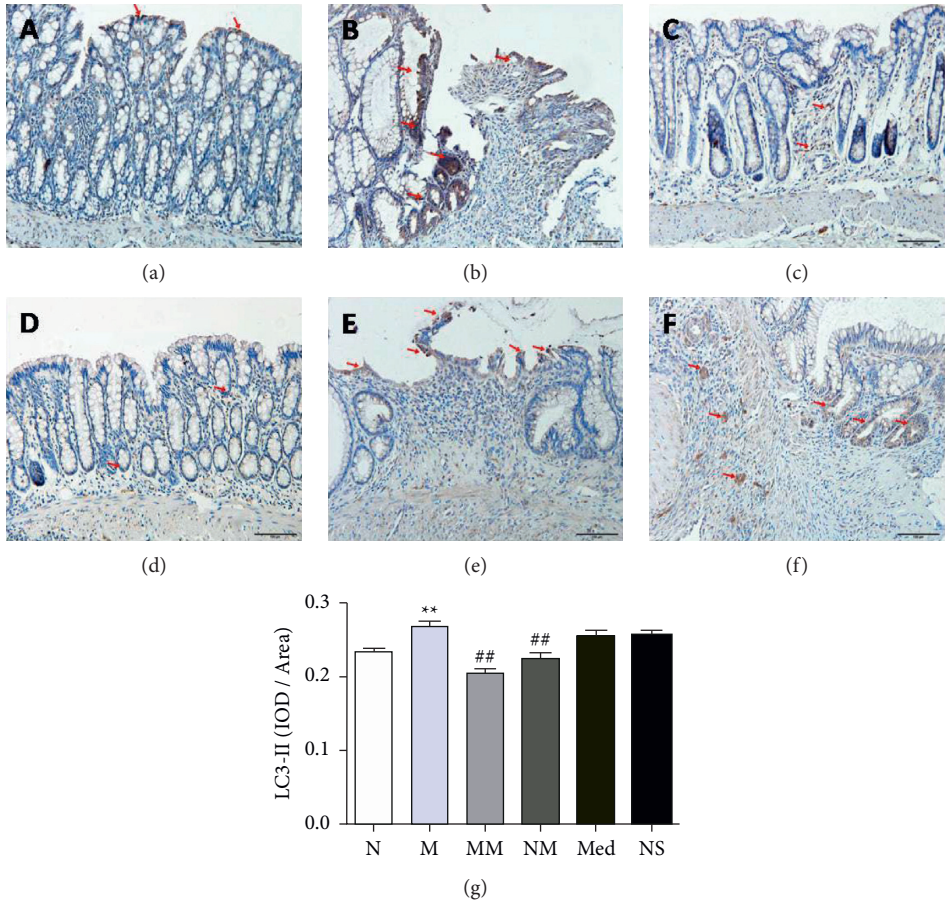

Figure 2: The expression of LC3 protein in colon tissues of rats in each group (200×). (a) normal group; (b) CD model group; (c) CD model with herb-partitioned moxibustion group; (d) normal with herb-partitioned moxibustion group; (e) CD model with mesalazine group; (f) CD model with normal saline group; (g) comparison of LC3 protein expression in colon tissues of rats in each group. $^{**}P < 0.01$ vs. N group; $^{\#\#}P < 0.01$ vs. M group. The data are shown as the mean ± SD.

polymorphism. The ATG16L1 gene is mainly expressed in the colon, small intestine, intestinal epithelial cells, and lymphocytes, and its encoded protein can participate in the metabolism of intracellular autophagosomes and the immune response induced by intracellular pathogens [24]. The single-nucleotide polymorphisms site in the ATG16L1 gene is highly correlated with CD and is an important risk factor for the pathogenesis of CD [25, 26] that can affect intestinal microbes and aggravate the local intestinal inflammatory response in CD [27]. ATG16L1 can also regulate the Nod-dependent cytokine immune response. NOD1 and NOD2, which are closely related to the pathogenesis of CD, can directly enter sites on the bacterial cell membrane with the help of ATG16L1 to initiate autophagy to clear invading pathogens [28, 29]. NOD2 is the earliest discovered gene related to human CD and plays an important role in the intestinal immune system and gut microbiota homeostasis [30]. NOD2 regulates the expression of the proinflammatory cytokines TNF-β, IL-1β, and IL-6 through the Toll-like receptor pathway and by activating nuclear factor kappa B (NF-κB) [31, 32], playing an important role in innate immunity in IBD. Cooney et al. [33] showed that the NOD2 and ATG16L1 genes together induced the autophagy of dendritic cells in CD, and this process was involved in the NOD2-mediated antigen presentation and bacterial treatment. The protein encoded by the IRGM gene plays an important role in the immunity induced by intracellular pathogens and is involved in the induction of autophagy and the maturation of autophagosomes [34]. IRGM is a key player in mediating p62-dependent selective autophagy of NLRP3 [35]. IRGM can mediate SQSTM1/p62-dependent autophagic degradation through direct interaction with the inflammasome to regulate colon inflammation and protect the body against inflammatory diseases [36]. IRGM/Irgm1 negatively regulates IL-1β maturation by suppressing the activation of the NLRP3 inflammasome [35].

Under normal circumstances, autophagy in intestinal epithelial cells can protect tissues against invasion by intestinal pathogens, which is key to the intestinal defense against bacterial invasion [37]. There are abnormalities of autophagy in intestinal cells in CD [38]. The action of TNF-β on human and rat colon epithelial cells results in impaired autophagy and loss of the adhesion ability of intestinal epithelial cells [39]. ATG16L1 is not only widely distributed

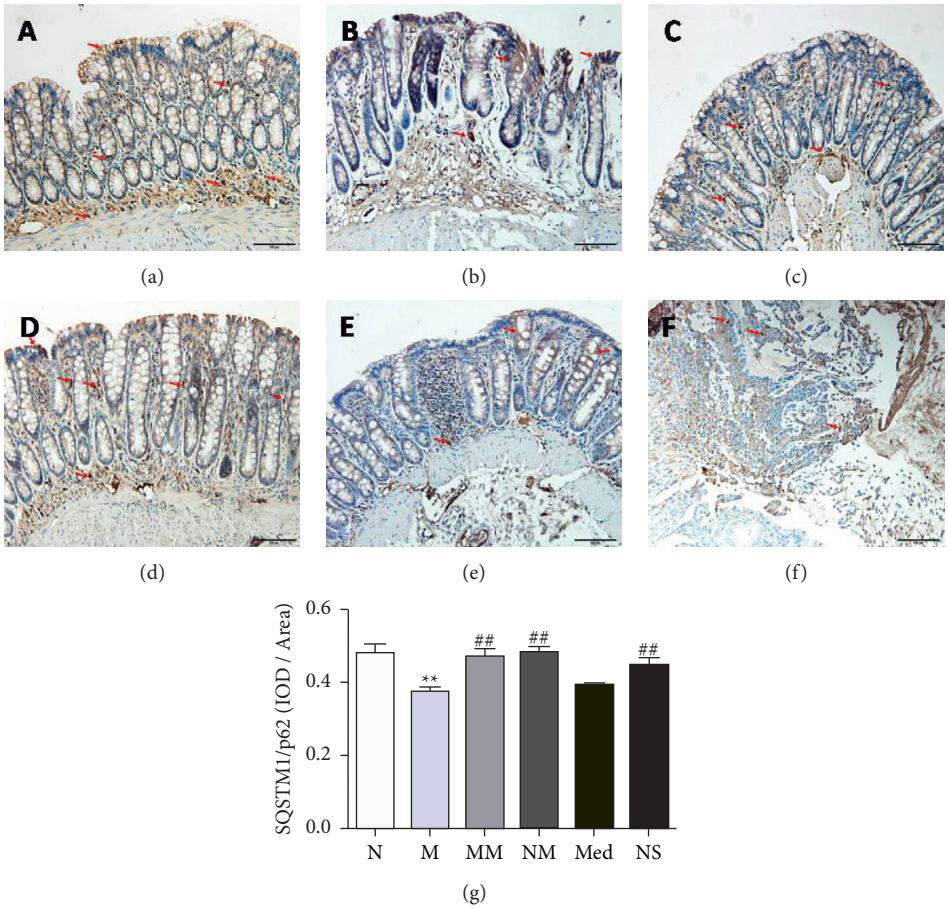

Figure 3: The expression of SQSTM1/p62 protein in colon tissues of rats in each group (200×). (a) normal group; (b) CD model group; (c) CD model with herb-partitioned moxibustion group; (d) normal with herb-partitioned moxibustion group; (e) CD model with Mesalazine group; (f) CD model with normal saline group; (g) comparison of SQSTM1/p62 protein expression in colon tissues of rats in each group. $^{**}P < 0.01$ vs. N group; $^{\#\#}P < 0.01$ vs. M group. The data are shown as the mean ± SD.

in intestinal epithelial cells but also exists in lymphocytes and macrophages. Together with NOD proteins, ATG16L1 plays multiple roles in innate immunity. On the one hand, autophagy dysfunction in colon epithelial cells cannot effectively remove microorganisms, resulting in their long-term survival in the intestine; on the other hand, abnormal expression of ATG16L1 and IRGM can also cause damage to Paneth cell function and increase the secretion of proinflammatory cytokines [40]. A study on protein-protein interaction found that impaired autophagy can degrade key proteins in Paneth cell function, subsequently affecting the homeostasis of Paneth cells [41]. Therefore, abnormal autophagy in intestinal cells may be one of the mechanisms that cause an excessive inflammatory response in CD intestinal mucosa.

Autophagy is an important component of immune homeostasis. Autophagy and biosynthesis work together to maintain the dynamic balance of cellular macromolecules. Beclin1 is an important autophagy-related protein that is also involved in apoptosis. Many autophagy regulatory proteins directly or indirectly bind to different domains or amino acids of Beclin1 to form protein complexes, thereby regulating autophagy levels and inflammatory responses [42–44]. Beclin1 interacts with the phosphatidylinositol-3-kinase (PI3K) complex and plays a role in regulating autophagy in the trans-Golgi apparatus [45]. LC3II is a mammalian homolog of the yeast autophagy-related protein Atg8 [46] and is the most widely studied molecular marker of autophagosomes. SQSTM1/p62 is also a marker protein of autophagy. The reduction in SQSTM1/p62 expression during autophagy can promote the activation of autophagic flux and regulate the secretion of lipopolysaccharide-induced inflammatory factors under the regulation of the autophagy signaling pathway [47].

The autophagy mechanism can regulate a variety of immune inflammatory responses [48, 49], while immune-related factors can also regulate autophagy. Therefore, cytokines can interact with autophagy signaling pathways. When NF-κB signaling is blocked, TNF-β can activate autophagy; the Th1 cytokine IFN-γ stimulates autophagy, while the Th2 cytokines IL-4 and IL-13 inhibit autophagy. IL-4 and IL-13 can induce the AKT-TOR signaling cascade, and their inhibition of autophagy can be transformed into the autophagic regulation of intracellular pathogens [50].

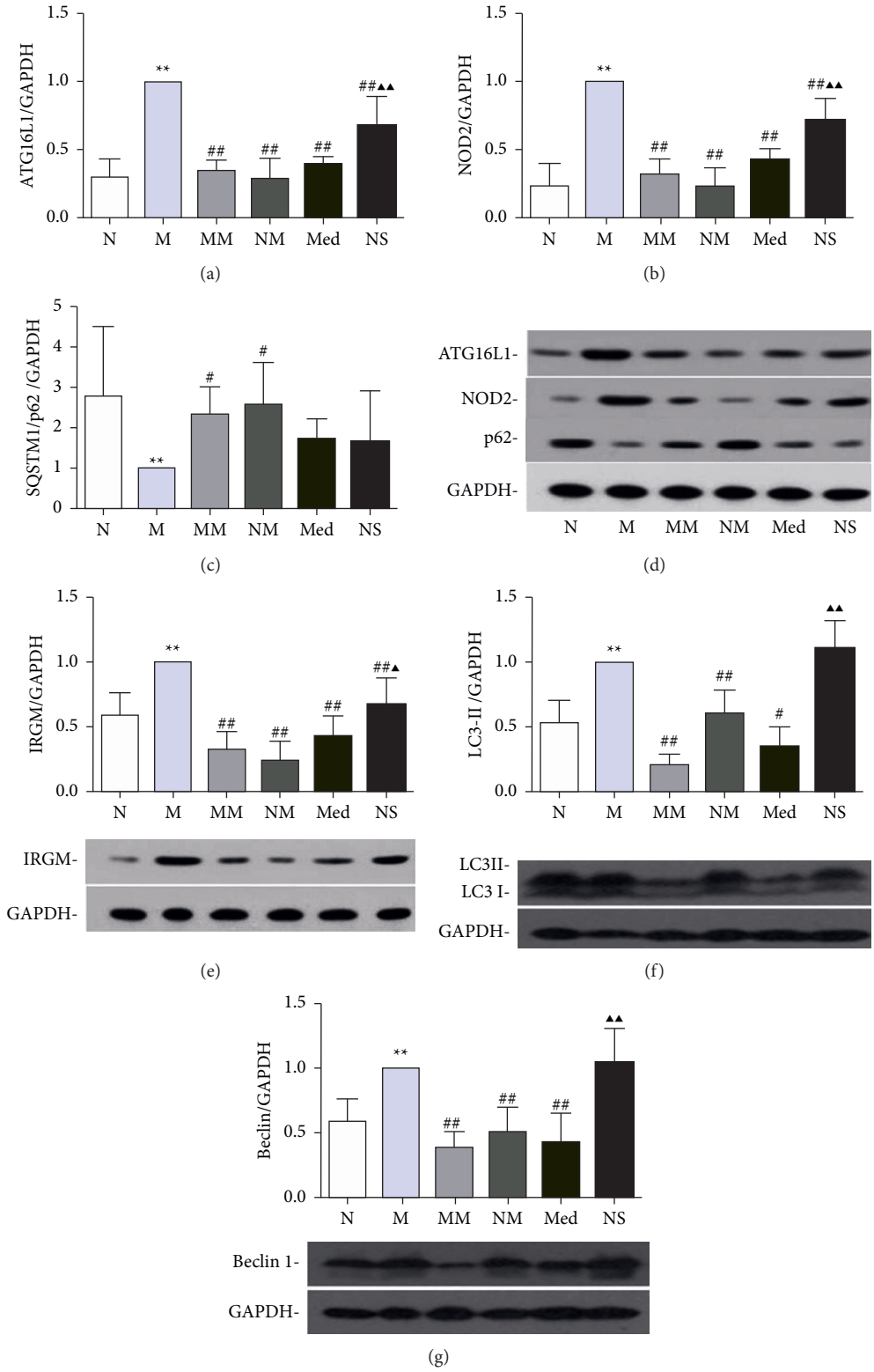

Figure 4: The expression of autophagy-related proteins in colon tissues of rats in each group. (a) expression of ATG16L1 protein in the colon; (b) expression of NOD2 protein in the colon; (c) expression of SQSTM1/p62 protein in the colon; (d) expression of ATG16L1, NOD2, and SQSTM1/p62 proteins in the colon. (e) expression of IRGM protein in the colon; (f) expression of LC3 protein in the colon; and (g) expression of Beclin1 protein in the colon. $^{*}P < 0.05$, $^{**}P < 0.01$ vs. N group; $^{\#}P < 0.05$, $^{\#\#}P < 0.01$ vs. M group; ▲$P < 0.05$, ▲▲$P < 0.01$ vs. Med group. The data are shown as the mean ± SD.

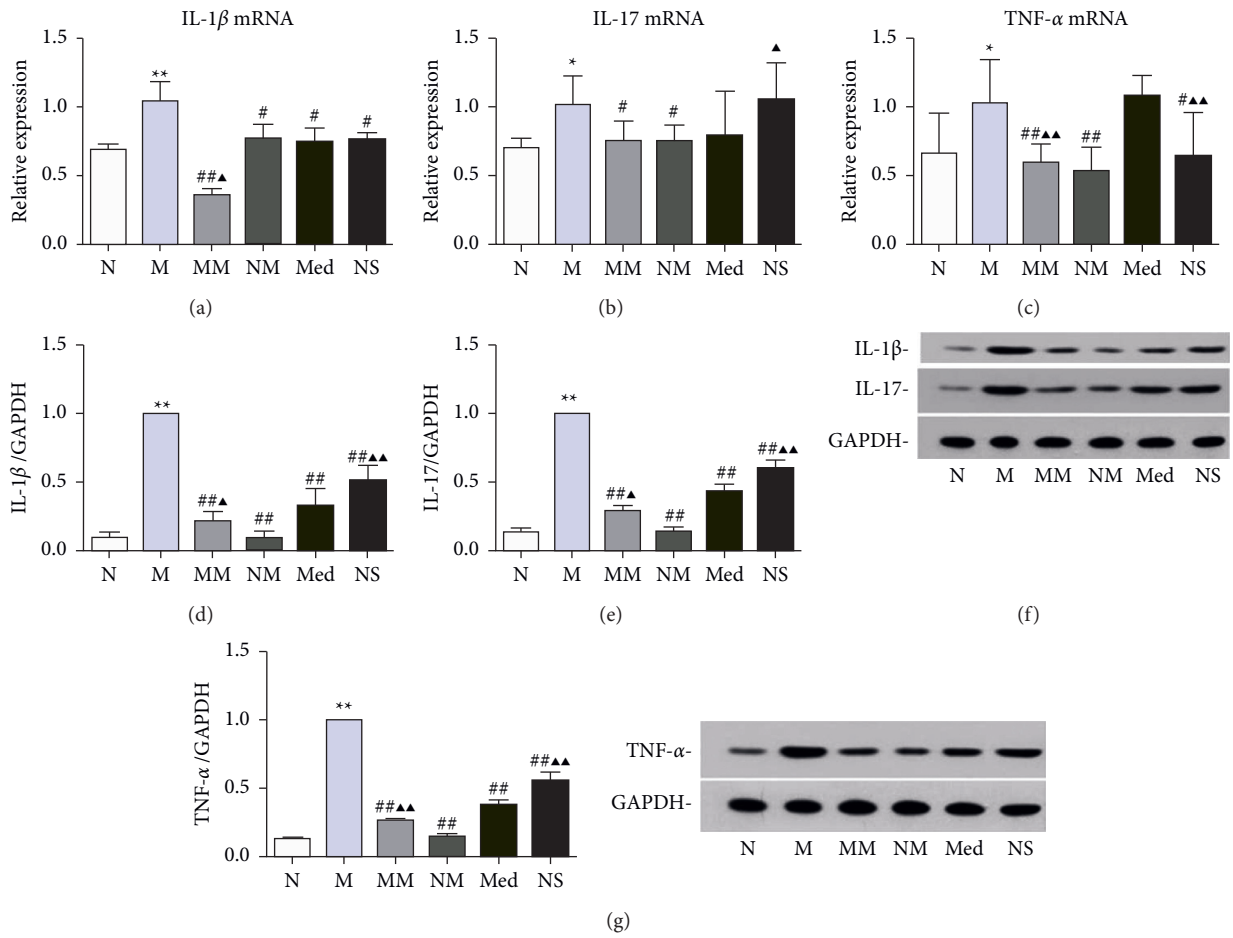

Figure 5: The expression of immune factors in colon tissues of rats in each group. (a–c) mRNA expression of IL-1β, IL-17, and TNF-β in colon tissues; (d–f) protein expression of IL-1β and IL-17 in colon tissues; and (g) protein expression of TNF-β in colon tissues. $^{*}P < 0.05$, $^{**}P < 0.01$ vs. N group; $^{\#}P < 0.05$, $^{\#\#}P < 0.01$ vs. M group; ▲$P < 0.05$, ▲▲$P < 0.01$ vs. Med group. The data are shown as the mean ± SD.

Abnormal immune function is one of the main causes of CD onset. IL-17 is a cytokine secreted by Th17 cells that plays an important role in autoimmune diseases and defense responses. IL-17 can bind to its receptor to induce the secretion of chemokines by effector cytokines, thereby promoting the generation and recruitment of neutrophils and macrophages. IL-1β and TNF-β are important proinflammatory factors. In the onset and progression of CD, they can cause the aggregation and release of inflammatory factors in the intestinal tract; increase the permeability of intestinal epithelial cells; induce inflammation, edema, and the formation of granuloma; and even induce the apoptosis of intestinal epithelial cells [51, 52]. When NF-κB activity is inhibited, IL-1β and TNF-β can induce autophagy, thereby participating in the regulation of inflammation and infectious diseases.

mTOR, as a key protein kinase, not only participates in the regulation of autophagy by the PI3K/AKT signal pathway in CD but also participates in the regulation of inflammation by the PI3K/AKT pathway. It maintains immune homeostasis through various interactions and plays an important role in IBD [53]. PI3K may also negatively regulate CD autophagy by inducing AKT activation [54]. The PI3K/AKT pathway is activated in CD4+ T cells isolated from the peripheral blood of CD patients, inducing the mTOR signaling pathway and causing the activation of the PTEN (a negative feedback regulatory factor) pathway [55]. The PI3K/AKT signal pathway plays an important role in regulating the release of inflammatory mediators and the proliferation of inflammatory cells. The PI3K-AKT-mTOR-TFEB pathway was activated by advanced oxidation protein products (AOPPs) in macrophages. Inhibition of the PI3K pathway effectively alleviated AOPPs-induced autophagy impairment and M1 polarization both in vitro and in vivo, thus reducing intestinal inflammation in AOPPs-challenged mice [56]. The LKB1 gene is an intracellular serine/threonine kinase that is involved in the regulation of cell proliferation, cell cycle arrest, apoptosis, and energy metabolism by the AMPK and mTOR signaling pathways. The LKB1-AMPK pathway is involved in the regulation of CD autophagy. LKB1 can activate AMPK, subsequently inhibits the expression of mTOR, and induces the activation of autophagy [54]. The CD susceptibility allele of ATG16L1 may be related to the immune synapse formation induced by autophagy and negative regulation of T cell activity. LKB1 is recruited to the

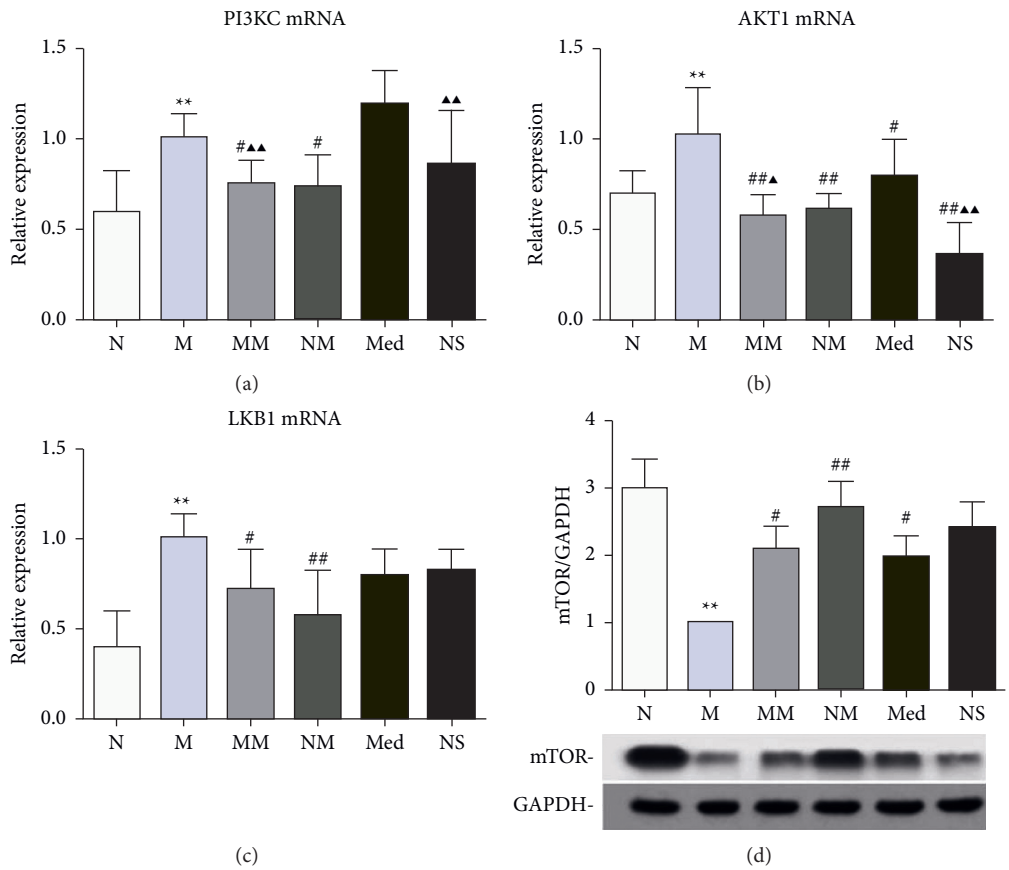

Figure 6: The expression levels of key factors of LKB1-mTOR-PI3KC signal transduction networks in the colon. (a–c) mRNA expression of PI3KC, AKT1, and LKB1 in colon tissues and (d) protein expression of mTOR in colon tissues. $^{*}P < 0.05$, $^{**}P < 0.01$ vs. N group; $^{\#}P < 0.05$, $^{\#\#}P < 0.01$ vs. M group; ▲$P < 0.05$, ▲▲$P < 0.01$ vs. Med group. The data are shown as the mean ± SD.

immune synapse and induces autophagy through LKB1-AMPK [57]. Therefore, the LKB1-mTOR-PI3KC signal transduction network plays an important role in the regulation of CD autophagy.

In this study, the expression levels of Beclin1 and LC3II proteins in CD rat colon tissues were significantly increased, indicating the activation of autophagy in CD rat colon tissues. SQSTM1/p62 is an important indicator that reflects the dynamic activation process of autophagy, mainly mediating the degradation of autophagosomes. The expression of SQSTM1/p62 protein in the colon of CD rats was significantly lower than that of normal rats, indicating the activation of autophagic flux in the colon tissue of CD rats and the degradation of autophagic substrates. However, herb-partitioned moxibustion and mesalazine can both significantly downregulate the expression of Beclin1 and LC3II proteins in the colon of CD rats. Moreover, herb-partitioned moxibustion can upregulate SQSTM1/p62 protein expression and inhibit autophagy activation in the CD rat colon more strongly than mesalazine. The expression levels of the autophagy-related proteins NOD2, ATG16L1, and IRGM in the CD rat colon tissues were significantly higher than normal rats. However, NOD2, ATG16L1, and IRGM proteins were downregulated in both the herb-partitioned moxibustion and mesalazine groups, indicating that autophagy activity in CD rat colon tissues decreased after herb-partitioned moxibustion or mesalazine treatments. Herb-partitioned moxibustion can also downregulate IL-1β, IL-17, and TNF-β mRNAs and proteins in CD rat colon tissues, which reflects the correlation between autophagy and immune cytokines. Further observation of the role of the LKB1-mTOR-PI3KC signal transduction network in CD autophagy and the regulatory effect of herb-partitioned moxibustion showed that PI3K, AKT1, and LKB1 mRNAs in CD rat colon tissues were significantly higher than those in the normal group, and mTOR protein was significantly lower than that in the normal group, indicating that key upstream factors of mTOR, including PI3K, AKT1, and LKB1, in the LKB1-mTOR-PI3KC signal transduction network are all activated in CD colon tissues, which could inhibit the expression of mTOR. As a key protein of the LKB1-mTOR-PI3KC signal transduction network, mTOR had decreased activity, and the autophagy switch was turned on. After treatment with herb-partitioned moxibustion, the mRNA expression levels of PI3K, AKT1, and LKB1 in the CD colon tissue were significantly reduced, indicating that herb-partitioned moxibustion can significantly inhibit PI3K, AKT1, and LKB1 expressions, upstream factors of mTOR in the LKB1-mTOR-PI3KC signal transduction network, and promote mTOR expression.

In summary, herb-partitioned moxibustion can significantly inhibit excessively activated autophagy in CD rat colon tissues, regulate the LKB1-mTOR-PI3KC signal transduction network, and downregulate the immune-related factors IL-1β, IL-17, and TNF-β, thereby alleviating and inhibiting intestinal inflammation in CD rats.

Data Availability

The initial data used to support the findings of this study are included within the article.

Conflicts of Interest

All authors have no conflicts of interest with respect to the manuscript.

Authors' Contributions

Huirong Liu and Huangan Wu designed and obtained the research grants for the current study. Jimeng Zhao, Zhe Ma, and Yanan Liu employed the experiments. Handan Zheng collected and analyzed the data. Jimeng Zhao and Zhe Ma wrote the manuscript. Yan Huang, Luyi Wu, and Yin Shi revised the manuscript. All the authors reviewed the manuscript and agreed for submission. Jimeng Zhao, Zhe Ma, and Handan Zheng contributed equally to this work.

Acknowledgments

This research was supported by the National Natural Sciences Foundation of China (Nos. 81873374 and82074546); Chinese Medicine Inheritance and Innovation "100 Million" Talent Project (Qi Huang Scholar); Shanghai Sailing Program (No. 20YF1445400); and Construction of Shanghai Key Specialties (Acupuncture and Moxibustion) (No. shslczdzk04701).

References

[1] L. Feld, L. R. Glick, and A. S. Cifu, "Diagnosis and management of crohn disease," *JAMA*, vol. 321, no. 18, pp. 1822-1823, 2019.

[2] G. G. Kaplan and S. C. Ng, "Understanding and preventing the global increase of inflammatory bowel disease," *Gastroenterology*, vol. 152, no. 2, pp. 313–321, 2017.

[3] J. Torres, S. Mehandru, J.-F. Colombel, and L. Peyrin-Biroulet, "Crohn's disease," *The Lancet*, vol. 389, no. 10080, pp. 1741–1755, 2017.

[4] T. Iida, Y. Yokoyama, K. Wagatsuma, D. Hirayama, and H. Nakase, "Impact of autophagy of innate immune cells on inflammatory bowel disease," *Cells*, vol. 8, no. 1, p. 7, 2018.

[5] T. Iida, K. Onodera, and H. Nakase, "Role of autophagy in the pathogenesis of inflammatory bowel disease," *World Journal of Gastroenterology*, vol. 23, no. 11, p. 1944, 2017.

[6] S. W. Ryter, S. M. Cloonan, and A. M. K. Choi, "Autophagy: a critical regulator of cellular metabolism and homeostasis," *Molecules and Cells*, vol. 36, no. 1, pp. 7–16, 2013.

[7] R. T. Netea-Maier, T. S. Plantinga, F. L. Van De Veerdonk, J. W. Smit, and M. G. Netea, "Modulation of inflammation by autophagy: consequences for human disease," *Autophagy*, vol. 12, no. 2, pp. 245–260, 2016.

[8] C. Münz, "Enhancing immunity through autophagy," *Annual Review of Immunology*, vol. 27, no. 1, pp. 423–449, 2009.

[9] J. D. Rioux, R. J. Xavier, K. D. Taylor et al., "Genome-wide association study identifies new susceptibility loci for Crohn disease and implicates autophagy in disease pathogenesis," *Nature Genetics*, vol. 39, no. 5, pp. 596–604, 2007.

[10] C. R. Homer, A. L. Richmond, N. A. Rebert, J. P. Achkar, and C. McDonald, "ATG16L1 and NOD2 Interact in an Autophagy-Dependent Antibacterial Pathway Implicated in Crohn's Disease Pathogenesis," *Gastroenterology*, vol. 139, no. 5, pp. 1630–1641, 2010.

[11] S. Rufini, C. Ciccacci, D. Di Fusco et al., "Autophagy and inflammatory bowel disease: Association between variants of the autophagy-related IRGM gene and susceptibility to Crohn's disease," *Digestive and Liver Disease*, vol. 47, no. 9, pp. 744–750, 2015.

[12] A. M. K. Choi, S. W. Ryter, and B. Levine, "Autophagy in human health and disease," *New England Journal of Medicine*, vol. 368, no. 7, pp. 651–662, 2013.

[13] X. H. Liang, S. Jackson, M. Seaman et al., "Induction of autophagy and inhibition of tumorigenesis by beclin 1," *Nature*, vol. 402, no. 6762, pp. 672–676, 1999.

[14] J. Pott, A. M. Kabat, and K. J. Maloy, "Intestinal epithelial cell autophagy is required to protect against TNF-induced apoptosis during chronic colitis in mice," *Cell Host & Microbe*, vol. 23, no. 2, pp. 191–202, 2018.

[15] S. Pankiv, T. H. Clausen, T. Lamark et al., "p62/SQSTM1 binds directly to Atg8/LC3 to facilitate degradation of ubiquitinated protein aggregates by autophagy," *Journal of Biological Chemistry*, vol. 282, no. 33, pp. 24131–24145, 2007.

[16] M. Germain, A. P. Nguyen, J. N. Le Grand et al., "MCL-1 is a stress sensor that regulates autophagy in a developmentally regulated manner," *The EMBO Journal*, vol. 30, no. 2, pp. 395–407, 2011.

[17] R. G. Jones and E. J. Pearce, "MenTORing immunity: mTOR signaling in the development and function of tissue-resident immune cells," *Immunity*, vol. 46, no. 5, pp. 730–742, 2017.

[18] C. H. Bao, L. Y. Wu, and H. G. Wu, "Active Crohn's disease treated with acupuncture and moxibustion:a randomized controlled trial," *Zhongguo Zhen Jiu*, vol. 36, no. 7, pp. 683–688, 2016.

[19] H.-X. Shang, A. Q. Wang, and C. H. Bao, "Moxibustion combined with acupuncture increases tight junction protein expression in Crohn's disease patients," *World Journal of Gastroenterology*, vol. 21, no. 16, pp. 4986–4996, 2015.

[20] J.-M. Zhao, Y.-N. Liu, H.-D. Zheng et al., "Effect of herb-partitioned moxibustion on autophagy and immune-associated gene expression profiles in a rat model of crohn's disease," *Evidence-Based Complementary and Alternative Medicine*, vol. 2019, Article ID 3405146, 13 pages, 2019.

[21] G. P. Morris, P. L. Beck, M. S. Herridge, W. T. Depew, M. R. Szewczuk, and J. L. Wallace, "Hapten-induced model of chronic inflammation and ulceration in the rat colon," *Gastroenterology*, vol. 96, no. 3, pp. 795–803, 1989.

[22] Y. Guo, *Experimental Acupuncture*, China Press of Traditional Chinese Medicine, Beijing, China, 2008.

[23] S. Y. Xu, R. L. Bian, and X. Chen, *Experimental Methodology of Pharmacology*, People's Medical Publishing House, Beijing, China, 3rd edition, 2001.

[24] A. M. Kabat, O. J. Harrison, T. Riffelmacher et al., "The autophagy gene Atg16l1 differentially regulates Treg and TH2 cells to control intestinal inflammation," *Elife*, vol. 5, p. e12444, 2016.

[25] B.-B. Zhang, Y. Liang, B. Yang, and Y.-J. Tan, "Association between ATG16L1 gene polymorphism and the risk of

Crohn's disease," *Journal of International Medical Research*, vol. 45, no. 6, pp. 1636–1650, 2017.

[26] K. G. Lassen and R. J. Xavier, "An alteration in ATG16L1 stability in Crohn disease," *Autophagy*, vol. 10, no. 10, pp. 1858–1860, 2014.

[27] S. Lavoie, K. L. Conway, K. G. Lassen et al., "The Crohn's disease polymorphism, ATG16L1 T300A, alters the gut microbiota and enhances the local Th1/Th17 response," *Elife*, vol. 8, p. e39982, 2019.

[28] M. T. Sorbara, L. K. Ellison, M. Ramjeet et al., "The protein ATG16L1 suppresses inflammatory cytokines induced by the intracellular sensors Nod1 and Nod2 in an autophagy-independent manner," *Immunity*, vol. 39, no. 5, pp. 858–873, 2013.

[29] L. H. Travassos, L. A. M. Carneiro, M. Ramjeet et al., "Nod1 and Nod2 direct autophagy by recruiting ATG16L1 to the plasma membrane at the site of bacterial entry," *Nature Immunology*, vol. 11, no. 1, pp. 55–62, 2010.

[30] J. Van Limbergen, R. K. Russell, E. R. Nimmo et al., "Genetics of the innate immune response in inflammatory bowel disease," *Inflammatory Bowel Diseases*, vol. 13, no. 3, pp. 338–355, 2007.

[31] M. H. Shaw, N. Kamada, N. Warner, Y.-G. Kim, and G. Nuñez, "The ever-expanding function of NOD2: autophagy, viral recognition, and T cell activation," *Trends in Immunology*, vol. 32, no. 2, pp. 73–79, 2011.

[32] Y.-J. Jeong, M.-J. Kang, S.-J. Lee et al., "Nod2 and Rip2 contribute to innate immune responses in mouse neutrophils," *Immunology*, vol. 143, no. 2, pp. 269–276, 2014.

[33] R. Cooney, J. Baker, O. Brain et al., "NOD2 stimulation induces autophagy in dendritic cells influencing bacterial handling and antigen presentation," *Nature Medicine*, vol. 16, no. 1, pp. 90–97, 2010.

[34] P. Nath, K. K. Jena, S. Mehto et al., "IRGM links autoimmunity to autophagy," *Autophagy*, vol. 17, no. 2, pp. 578–580, 2021.

[35] S. Mehto, K. K. Jena, P. Nath et al., "The Crohn's Disease Risk Factor IRGM Limits NLRP3 Inflammasome Activation by Impeding Its Assembly and by Mediating Its Selective Autophagy," *Molecular Cell*, vol. 73, no. 3, pp. 429–445, 2019.

[36] S. Mehto, S. Chauhan, K. K. Jena et al., "IRGM restrains NLRP3 inflammasome activation by mediating its SQSTM1/p62-dependent selective autophagy," *Autophagy*, vol. 15, no. 9, pp. 1645–1647, 2019.

[37] L. Yang, C. Liu, W. Zhao, C. He, J. Ding, and R. Dai, "Impaired autophagy in intestinal epithelial cells alters gut microbiota and host immune responses," *Applied and Environmental Microbiology*, vol. 84, no. 18, pp. e00880–18, 2018.

[38] É. Thachil, J. P. Hugot, B. Arbeille et al., "Abnormal Activation of Autophagy-Induced Crinophagy in Paneth Cells From Patients With Crohn's Disease," *Gastroenterology*, vol. 142, no. 5, pp. 1097–1099, 2012.

[39] M. Saito, T. Katsuno, T. Nakagawa et al., "Intestinal Epithelial Cells with Impaired Autophagy Lose Their Adhesive Capacity in the Presence of TNF-α," *Digestive Diseases and Sciences*, vol. 57, no. 8, pp. 2022–2030, 2012.

[40] M. R. Spalinger, G. Rogler, and M. Scharl, "Crohn's disease: loss of tolerance or a disorder of autophagy?" *Digestive Diseases*, vol. 32, no. 4, pp. 370–377, 2014.

[41] E. J. Jones, Z. J. Matthews, L. Gul et al., "Integrative analysis of Paneth cell proteomic and transcriptomic data from intestinal organoids reveals functional processes dependent on autophagy," *Disease models & mechanisms*, vol. 12, no. 3, p. dmm037069, 2019.

[42] S. Sahni, A. M. Merlot, S. Krishan, P. J. Jansson, and D. R. Richardson, "Gene of the month: becn1," *Journal of Clinical Pathology*, vol. 67, no. 8, pp. 656–660, 2014.

[43] E. Wirawan, S. Lippens, T. Vanden Berghe et al., "Beclin1: a role in membrane dynamics and beyond," *Autophagy*, vol. 8, no. 1, pp. 6–17, 2012.

[44] Y. Lv, L. Fang, P. Ding, and R. Liu, "PI3K/Akt-Beclin1 signaling pathway positively regulates phagocytosis and negatively mediates NF-κB-dependent inflammation in Staphylococcus aureus-infected macrophages," *Biochemical and Biophysical Research Communications*, vol. 510, no. 2, pp. 284–289, 2019.

[45] A. Kihara, Y. Kabeya, Y. Ohsumi, and T. Yoshimori, "Beclin-phosphatidylinositol 3-kinase complex functions at the trans -Golgi network," *EMBO Reports*, vol. 2, no. 4, pp. 330–335, 2001.

[46] T. Shpilka, H. Weidberg, S. Pietrokovski, and Z. Elazar, "Atg8: an autophagy-related ubiquitin-like protein family," *Genome Biology*, vol. 12, no. 7, p. 226, 2011.

[47] F. Han, Q. Q. Xiao, S. Peng et al., "Atorvastatin ameliorates LPS-induced inflammatory response by autophagy via AKT/mTOR signaling pathway," *Journal of Cellular Biochemistry*, vol. 119, no. 2, pp. 1604–1615, 2018.

[48] V. Deretic, T. Saitoh, and S. Akira, "Autophagy in infection, inflammation and immunity," *Nature Reviews Immunology*, vol. 13, no. 10, pp. 722–737, 2013.

[49] V. Deretic and B. Levine, "Autophagy balances inflammation in innate immunity," *Autophagy*, vol. 14, no. 2, pp. 243–251, 2018.

[50] Y. J. Jang, J. H. Kim, and S. Byun, "Modulation of autophagy for controlling immunity," *Cells*, vol. 8, no. 2, p. 138, 2019.

[51] S. Zeissig, C. Bojarski, and N. Buergel, "Downregulation of epithelial apoptosis and barrier repair in active Crohn's disease by tumour necrosis factor antibody treatment," *Gut*, vol. 53, no. 9, pp. 1295–1302, 2004.

[52] M. E. Street, G. de'Angelis, C. Camacho-Hübner et al., "Relationships between Serum IGF-1, IGFBP-2, Interleukin-1Beta and Interleukin-6 in Inflammatory Bowel Disease," *Hormone Research in Paediatrics*, vol. 61, no. 4, pp. 159–164, 2004.

[53] E. C. Steinbach, T. Kobayashi, S. M. Russo et al., "Innate PI3K p110δ Regulates Th1/Th17 Development and Microbiota-Dependent Colitis," *The Journal of Immunology*, vol. 192, no. 8, pp. 3958–3968, 2014.

[54] C. He and D. J. Klionsky, "Regulation mechanisms and signaling pathways of autophagy," *Annual Review of Genetics*, vol. 43, no. 1, pp. 67–93, 2009.

[55] S. H. Long, Y. He, M. H. Chen et al., "Activation of PI3K/Akt/mTOR signaling pathway triggered by PTEN downregulation in the pathogenesis of Crohn's disease," *Journal of Digestive Diseases*, vol. 14, no. 12, pp. 662–669, 2013.

[56] Y. Liao, J. Xu, B. Qin et al., "Advanced oxidation protein products impair autophagic flux in macrophage by inducing lysosomal dysfunction via activation of PI3K-Akt-mTOR pathway in Crohn's disease," *Free Radical Biology and Medicine*, vol. 172, no. 5, pp. 33–47, 2021.

[57] M. E. Wildenberg, A. C. W. Vos, S. C. S. Wolfkamp et al., "Autophagy attenuates the adaptive immune response by destabilizing the immunologic synapse," *Gastroenterology*, vol. 142, no. 7, pp. 1493–1503, 2012.

Hindawi
Evidence-Based Complementary and Alternative Medicine
Volume 2022, Article ID 8528938, 9 pages
https://doi.org/10.1155/2022/8528938

Review Article

A Review on the Immunomodulatory Mechanism of Acupuncture in the Treatment of Inflammatory Bowel Disease

Zhifeng Liu,[1] **Yi Jiao**,[1] **Tianyuan Yu**,[1] **Hourong Wang**,[1] **Yingqi Zhang**,[1] **Di Liu**,[2] **Yajing Xu**,[1] **Qian Guan**,[1] **and Mengqian Lu**[1]

[1]*School of Acupuncture-Moxibustion and Tuina, Beijing University of Chinese Medicine, Beijing 102488, China*
[2]*Acupuncture Department, Oriental Hospital of Beijing University of Chinese Medicine, Beijing 100078, China*

Correspondence should be addressed to Tianyuan Yu; yutianyuan@sina.com and Mengqian Lu; 15201543134@163.com

Received 21 August 2021; Revised 1 November 2021; Accepted 28 December 2021; Published 15 January 2022

Academic Editor: Ying Li

Inflammatory bowel disease (IBD) is a chronic inflammatory disease with a high prevalence and canceration rate. The immune disorder is one of the recognized mechanisms. Acupuncture is widely used to treat patients with IBD. In recent years, an increasing number of studies have proven the effectiveness of acupuncture in the treatment of IBD, and some progress has been made in the mechanism. In this paper, we reviewed the studies related to acupuncture for IBD and focused on the immunomodulatory mechanism. We found that acupuncture could regulate the innate and adaptive immunity of IBD patients in many ways. Acupuncture exerts innate immunomodulatory effects by regulating intestinal epithelial barrier, toll-like receptors, NLRP3 inflammasomes, oxidative stress, and endoplasmic reticulum stress and exerts adaptive immunomodulation by regulating the balance of Th17/Treg and Th1/Th2 cells. In addition, acupuncture can also regulate intestinal flora.

1. Introduction

Inflammatory bowel disease (IBD) is a chronic, inflammatory, and autoimmune intestinal disease, which is characterized by abdominal pain, diarrhea, pus and bloody stool, intestinal obstruction, and intestinal perforation [1, 2]. IBD includes Crohn's disease (CD), a disease involving the whole digestive tract, and ulcerative colitis (UC), a disease only involving the colon [3]. IBD has become a global disease that poses a serious threat to human health worldwide with a high prevalence and canceration rate [4–6]. Epidemiological results show that the prevalence of IBD has been increasing in the past decade. The prevalence rate can be as high as 0.3% to 0.5% in Western countries such as Europe and North America and 0.05% in East Asia [7], with the canceration rate as high as 15% [8]. A cohort study published in 2020 showed that the risk ratios of colorectal cancer occurrence and death between CD patients and the general population were 1.4 and 1.74, respectively [9].

The pathogenesis of IBD is unclear and is generally believed to be the result of the interaction between the host immune system and gut microbiota, as well as genetic susceptibility and environmental susceptibility [10, 11]. The immune disorder is one of the recognized mechanisms, which plays an important role in the occurrence, development, and prognosis of IBD [12, 13]. Under the influence of environmental factors such as diet and smoking and the participation of intestinal flora, genetically susceptible people initiate an intestinal innate and adaptive immune response, resulting in intestinal mucosal barrier damage, ulcer, inflammatory cell infiltration, and other pathological changes.

Acupuncture, one of the most popular non-pharmacological therapies, has been used worldwide to treat patients with IBD due to its remarkable effect [14, 15]. It can not only improve the main symptoms of IBD patients, such as abdominal pain, diarrhea, and bloody purulent stool but also alleviate the accompanying symptoms, such as anxiety, depression, and fatigue [16–18]. A meta-analysis involving 13 RCTs with 1030 participants showed that acupuncture alone and acupuncture combined with medicine were more effective than conventional medicine in the treatment of UC [19]. Another meta-analysis showed that acupuncture and

moxibustion were more effective than oral sulphasalazine in treating patients with IBD [18]. A single-blind randomized trial proved that electroacupuncture can reduce fatigue scores in IBD patients compared with those on the waitlist [17]. In recent years, the mechanism of acupuncture in the treatment of IBD has made certain progress, especially in the regulation of immune disorders. Therefore, this review summarized the previous studies to explain the immunomodulatory mechanism of acupuncture in the treatment of IBD.

2. Immune Disorder is One of the Recognized Mechanisms Leading to IBD

Intestinal immune function is exerted by innate immunity and adaptive immunity. It is believed that the disorder of mucosal barrier function is the main cause of IBD [20]. Antigen stimulates the damage of intestinal mucosa, increases mucosal permeability, stimulates the production of various inflammatory factors, and then makes the body participate in the adaptive immune response network. Therefore, both innate and adaptive immune disorders may lead to IBD.

2.1. Innate Immune System. Innate immunity is the body's first line of defense, which plays a vital role in identifying pathogens and maintaining the balance of the intestinal environment. In the early stage of intestinal inflammation, neutrophils infiltrate intestinal mucosa and epithelium, weaken the function of the epithelial barrier, destroy tissue structure, release proinflammatory factors, and enhance inflammatory response [21]. Immune cells such as macrophages, neutrophils, epithelial cells, and endothelial cells are involved in the intestinal innate immune response.

2.2. Adaptive Immune System. Under normal circumstances, the components of the adaptive immune system cooperate with each other and trigger an effective immune response with the molecules and cells of the innate immune system so as to eliminate invasive pathogens. The imbalanced expression of immune cells is one of the pathogenesis of IBD. $CD4^+$T cells are important immune cells in the human body, and their abnormal activation, as an important mechanism, leads to intestinal mucosal immune response. $CD4^+$T cells are divided into T regulatory (Treg) cells and T helper (Th) cells, among which Th cells are divided into Th1, Th2, Th17, and other subtypes. The imbalance of Th17/Treg and Th1/Th2 is the main cause of IBD.

3. Acupuncture Exerts Immunomodulatory Effects by Regulating the Innate System of the Intestinal Mucosa

3.1. Intestinal Epithelial Barrier. Intestinal epithelial cells and tight junctions between cells constitute the intestinal epithelial barrier. The morphological and functional damage of epithelial cells can lead to intestinal inflammation, and continuous inflammatory stimulation can lead to intestinal fibrosis [22]. Studies have shown that colonic collagen fibers of CD rats proliferate while the expression of collagen fibers decreases after electroacupuncture treatment, and the contents of hyaluronic acid (HA), procollagen III (PC III), and procollagen III (PC III) in serum decrease, indicating that electroacupuncture can improve the pathological state of intestinal fibrosis in CD rats [23]. Tumor necrosis factor-α is the key cytokine causing CD, which can induce intestinal epithelial apoptosis through its receptors (TNFR1 and TNFR2), resulting in intestinal epithelial barrier damage. Acupuncture combined with moxibustion can reduce the contents of TNF-α, TNFR1, and TNFR2 in the intestinal mucosa of CD patients [24, 25], and it can also reduce the apoptosis rate of intestinal epithelial cells [24].

Shi et al. [26] demonstrated that herbs-moxibustion combined with acupuncture at Zusanli (ST36) and Shangjuxu (ST37) could upregulate the expression of E-cadherin, the epithelial cell marker, and downregulate the expression of fibronectin, the mesenchymal cell marker. Also, the overexpression of TGF-β, TβR2, Smad3, and Snail were suppressed. Therefore, herbs-moxibustion combined with acupuncture can prevent intestinal epithelial-mesenchymal transition (EMT) in CD, and its mechanism is related to the TGF-β1-Smad-Snail pathway (Figure 1).

3.2. Toll-Like Receptors. Toll-like receptors (TLRs) are a family of pattern recognition receptors, and the innate immune system disorders mediated by them are the core participants in the pathogenesis of IBD. Toll-like receptor 4 (TLR4) is a receptor on the surface of immune cells, which plays a significant role in body immunity. It can activate the myeloid differentiation factor 88 (MyD88) signal transduction pathway and lead to nuclear translocation of nuclear factors-κB (NF-κB). NF-κB is a key molecule that transduces intestinal inflammation, which regulates each other with inflammatory cytokines and amplifies the inflammatory response [27]. The TLR4/MyD88/NF-κB signaling pathway has been abnormally activated throughout the process of intestinal mucosal damage, which is considered to be one of the targets of UC treatment [28, 29].

Qiao et al. [30] found that the levels of TLR4, MyD88, and NF-κB in the colon of UC rats were significantly higher than those of normal rats, which confirmed the abnormal activation of the TLR4/MyD88/NF-κB signaling pathway. However, after the intervention of electroacupuncture, the levels of TLR4, MyD88, and NF-κB decreased, while the levels of IL-4 and IL-10 increased and IL-17 and PGE_2 decreased, indicating that acupuncture can inhibit the activation of the TLR4/MyD88/NF-κB signaling pathway, decrease the expression of proinflammatory factors, and increase anti-inflammatory factors, thereby reducing the intestinal inflammatory response. Li et al. [31] found electroacupuncture at Tianshu (ST25) could downregulate TLR4, MyD88, and NF-κB p65 in the colon, IL-1β and TNF-α in serum, and upregulate IL-10 in serum, which was more effective than sulphasalazine. The expression of p-IκBα and p-p65 can also be inhibited via manual acupuncture and electroacupuncture, which indicates that acupuncture can inhibit the activation of NF-κB [32] (Figure 1).

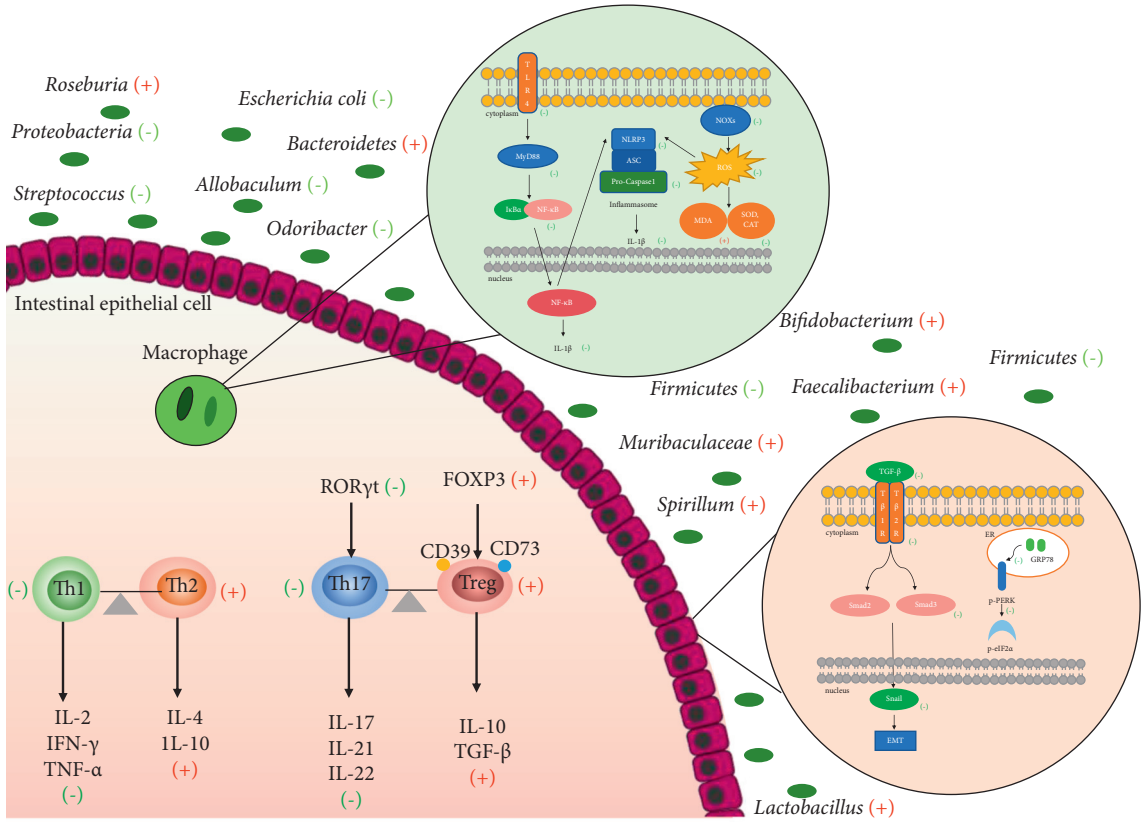

Figure 1: The mechanism underlying immune regulation of acupuncture. (+): upregulate; (−): downregulate.

3.3. NLRP3 Inflammasomes. NOD-like receptor protein 3 (NLRP3) inflammasomes are protein complex in the cytoplasm, which consists of NLRP3, apoptosis-associated spotted protein (ASC), and caspase-1 precursor protein. NLRP3 inflammasomes are crucial for innate immunity and contribute to inflammatory diseases such as IBD [33, 34]. Seo et al. [35] demonstrated in the DSS-induced mice model that the activation of NLRP3 inflammasome was involved in colitis. The activation of NLRP3 can activate macrophages to secrete IL-1β [36]. By inhibiting the activation of NLRP3 in macrophages, the experimental colitis can be improved [37]. Electroacupuncture at ST36 could inhibit the activation of NLRP3 and caspase-1 and reduce the level of IL-1β in macrophages in DSS-induced mice. In the meanwhile, the percentage of M1 macrophages increased and M2 macrophages decreased, which was reversed by electroacupuncture. The results indicated that electroacupuncture may ameliorate colitis by suppressing the NLRP3/IL-1β pathway [38]. Furthermore, the production of reactive oxygen species (ROS) is the main activation mechanism of the NLRP3 inflammasome, which can lead to the activation of the NLRP3 inflammasome and the release of inflammatory factors [39]. NADPH oxidases (NOXs) are rapid reaction enzymes that produce ROS. When activated, it will catalyze the production of ROS, which constitutes the molecular basis of oxidative stress [40]. Zeng et al. [41] found that the expression of NOXs, ROS, NLRP3, and IL-1β increased in TNBS-induced rats compared with those in normal rats but significantly decreased after 14 days of electroacupuncture treatment, which proved that electroacupuncture may treat UC by affecting the NOXs-ROS-NLRP3 signaling pathway (Figure 1).

3.4. Oxidative Stress and Endoplasmic Reticulum Stress. Oxidative stress is involved in the pathogenesis and progression of IBD [42, 43]. It is found that the decreased ability of the body to scavenge oxygen free radicals is one of the factors that cause inflammation and aggravate ulcers [44]. MDA is a marker of oxidative stress. SOD has the physiological function of scavenging oxygen free radicals. In the DSS-induced UC model, MDA activity increases and SOD activity decreases [45]. Endoplasmic reticulum stress (ERS) plays a key role in the occurrence and development of IBD because it relates to the persistence of inflammatory and autoimmunity [46, 47]. Wu et al. [32] demonstrated that both manual acupuncture and electroacupuncture could upregulate SOD and CAT and downregulate MDA in UC rats, which indicated that acupuncture can suppress oxidative stress induced by TNBS. In the meanwhile, the levels of GRP78, p-PERK, and p-eIF2α decreased, indicating that acupuncture can inhibit ERS (Figure 1).

4. Acupuncture Exerts Immunomodulatory Effects by Regulating Adaptive Immune System

4.1. The Balance of Th17/Treg Cells. Th17 cells are involved in the occurrence and development of inflammatory diseases and autoimmune diseases and are the main participants in IBD. Treg cells, the immunomodulatory cells maintaining immune tolerance, can inhibit intestinal inflammation [48]. It was found that Th17 cells in the peripheral blood and intestinal mucosa of IBD patients were significantly higher than those of healthy people, while Treg cells were significantly lower [49]. Th17 cells can secrete cytokines such as IL-17, IL-21, and IL-22. When the body is in a normal state, Th17 cells and their secreted cytokines can resist pathogen infection in vitro, thereby maintaining intestinal immune homeostasis. When the body is stimulated by antigen, the initial $CD4^+$T cells differentiate, leading to the disorder of Th17 cells regulation and inducing an abnormal immune response. Treg cells play an immunosuppressive role by secreting inhibitory cytokines such as IL-10 and TGF-β [50].

4.1.1. The Ratio of Th17 and Treg Cells. Th17 and Treg cells restrict each other to maintain the balance of the immune system [51]. Once the balance is broken, it will cause a variety of autoimmune diseases and intestinal inflammatory responses [52]. The imbalance between the Th17 and Treg cells has been shown to be an important cause of IBD [53]. Adjusting the balance between the two can directly regulate the expression of proinflammatory and anti-inflammatory factors, which can help improve intestinal inflammatory response and rebuild intestinal immune balance [54].

Studies have shown that the number of Treg cells in the mice model was downregulated whereas Th17 cells were upregulated [55]. However, electroacupuncture can upregulate the $CD4^+CD25^+Foxp3^+$Treg cells and downregulate the $CD3^+CD8^+IL\text{-}17^+$Th17 cells in spleen lymphocytes of UC mice [56] so as to improve the ratio of Treg and Th17 cells. The results of Sun et al. also proved this point [57].

4.1.2. Proinflammatory Cytokines. Cytokines are secreted by immune cells [58], such as lymphocytes and macrophages, which can be classified into proinflammatory cytokines and anti-inflammatory cytokines. The balance of two cytokines is essential for maintaining intestinal immune homeostasis. Th17 cells secrete cytokines, such as IL-17, IL-21, and IL-22, which can induce and aggravate inflammatory responses. IL-17 is a hallmark cytokine of Th17 cells, which can induce inflammatory response [59]. IL-17 mRNA and protein levels in the blood of IBD patients are significantly upregulated [49]. IL-22 can maintain the integrity of the epithelial barrier and protect mucin-secreting goblet cells [60]. IL-23 is mainly produced by macrophages, and its overexpression in intestinal mucosa will destroy the defense barrier and affect immune regulation [61]. Existing studies have proven that Th17/IL-23 immune axis is the main immune response pathway in the pathogenesis of CD and plays a key role in intestinal inflammation [62, 63]. IL-6 is the key factor in determining whether the initial $CD4^+$T cells differentiate into Treg cells or Th17 cells. Blocking the IL-6 signaling pathway can inhibit the differentiation of Th17 cells [64].

Liang [65] used warm needle acupuncture to treat patients with UC and found that the levels of IL-17 and IL-23 in serum decreased significantly after two weeks. Chen [66] demonstrated that electroacupuncture at Tianshu (ST25) and Zusanli (ST36) can reduce the contents of IL-6 and IL-17 in the serum of UC rats. In order to observe the effects of moxibustion and acupuncture on the expression of IL-17A and IL-22 in Crohn's disease rats, Liu [67] established the Crohn's disease model with 2,4,6-trinitrobenzene sulfonic acid (TNBS). After 15 minutes of intervention with moxibustion and acupuncture at Tianshu (ST25) and Shangjuxu (ST37), respectively, the results showed that compared with the model group, the expression of IL-17A decreased in the moxibustion group, while there was no change in IL-22. However, there was no difference between IL-17A and IL-22 in the acupuncture group. It is suggested that acupuncture may not inhibit the expression of IL-17A and IL-22 in Crohn's disease model rats.

4.1.3. Anti-Inflammatory Cytokines. Treg cells secrete anti-inflammatory cytokines (IL-10, TGF-β, etc.) that can inhibit intestinal inflammation. IL-10 plays an immunomodulatory role in many ways. For example, it can maintain intestinal immune homeostasis by inhibiting the release of TNF-α [68]. It can also inhibit the proliferation of Th cells and reduce the secretion of harmful cytokines. Studies have shown that IL-10 deficiency can lead to somatic mutation and increase the risk of carcinogenesis in the IBD model [69]. In addition to determining the differentiation of $CD4^+$ cells in collaboration with IL-6, TGF-β also promotes epithelial wound healing and tissue repair [70]. It was found that reduced TGF-β signal transduction in T cells and dendritic cells led to colitis in model mice [71], and TGF-β-deficient colonic epithelial cells and lamina propria showed inflammatory damage. Moreover, TGF-β can be used as an anti-inflammatory cytokine for the treatment of IBD. Zorzi et al. [72] found that TGF-β_1 can improve the fibrosis of IBD.

The study of Chen [66] showed that the level of IL-10 in serum and the positive cells of TGF-β in the colonic mucosa of UC rats decreased significantly. However, the levels of the two increased significantly after electroacupuncture intervention. Electroacupuncture can also elevate the expression of TGF-β, IL-10, and IL-2 in dextran sulfate sodium (DSS)-induced UC mice [57]. Studies also showed that the contents of IL-6 and TGF-β in the serum of DSS mice increased significantly, while electroacupuncture can inhibit the elevation [73].

4.1.4. Transcription Factors. Foxp3 and RORγt determine the direction of T cell differentiation. Foxp3, a member of the fork-head transcription factor family, is a marker transcription factor of Treg cells. It can affect the growth and development of Treg cells [74]. Mutations in Foxp3 lead to

autoimmune diseases, and defects in Foxp3 lead to intestinal mucosal inflammation. RORγt is a key transcription factor for differentiation of Th17 cells. Inhibition of its expression can directly inhibit the differentiation of Th17 cells and reduce the level of Th17 cells, thereby reducing the inflammatory response [75]. When the body is under normal conditions, the two are in dynamic balance. When stimulated, the expression of Foxp3 is downregulated or RORγt is upregulated, which promotes the differentiation of Th17 cells and the release of inflammatory factors. In contrast, Treg cells differentiate and play an anti-inflammatory role [76]. Therefore, the balance between RORγt and Foxp3 is the key in determing the balance of Th17/Treg cells and regulating the immune state of the body. Sun et al. [57] found that the expression of RORγt increased and Foxp3 decreased in the colon of DSS-induced UC mice. After the intervention of electroacupuncture and moxibustion, the expression of RORγt was downregulated and Foxp3 was upregulated. Chen [66] demonstrated that electroacupuncture at Tianshu (ST25) and Zusanli (ST36) can increase the contents of Foxp3 and DAF in the intestinal tissue. Decay-accelerating factor (DAF) is a cell regulatory factor that regulates T cell response [77]. Signal transducers and activators of transcription 3 (STAT3), a key target for alleviating inflammatory response, can regulate the expression of IL-17 and promote Th17 differentiation [78, 79]. Hypoxia-inducible factor 1α (HIF-1α) can inhibit Treg cell differentiation by promoting Foxp3 degradation [80]. Both STAT3 and HIF-1α act on RORγt and Foxp3. Acupuncture can effectively reduce the expression of STAT3 and HIF1-α protein in the colon of UC mice induced by DSS [81, 82].

4.1.5. CD39 and CD73. CD39 and CD73 are special markers on the surface of Treg cells. In UC mice, CD39-deficient Treg cells failed to exert immunosuppressive effects, and CD73-deficient Treg cells failed to produce extracellular adenosine [83, 84]. The CD39/CD73/A2a adenosine metabolic pathway plays an important role in the immune tolerance function of Treg cells. Studies have shown that patients with UC have lower adenosine levels, and the use of adenosine receptor A2a agonist can effectively reduce colitis and inhibit the production of proinflammatory factors [85, 86]. Zhuang et al. [87] found that the fluorescence intensity, the number of positive cells, and protein expression of CD39, DC73, and A2a in the colon of DSS mice increased after acupuncture. In the meanwhile, the ratio of CD39- and CD73-positive Treg cells in the peripheral blood, inguinal drainage lymph nodes, and spleen increased, indicating that the effect of electroacupuncture on UC mice may be related to the regulation of the CD39/CD73/A2a adenosine metabolic pathway and the influence of the anti-inflammatory effect of Treg cells.

4.2. The Balance of Th1/Th2 Cells. Th1 cells mediate cellular immunity and promote inflammation, mainly secreting IL-2, IFN-γ, and TNF-α. Th2 cells mediate humoral immunity and suppress inflammation, mainly secreting IL-4 and IL-10 [88].

To explore the effect of acupuncture and moxibustion on Th1/Th2 immune balance in UC rats, Chen [89] found that after the 14th intervention of electroacupuncture at Tianshu (ST 25) and Qihai(CV6), the ratio of $CD4^+IFN\text{-}\gamma^+/CD4^+IL\text{-}4^+$ cells in the model group was higher than that in the control group, and the ratio in the electroacupuncture group was lower than that in the model group; the levels of IFN-γ and IL-12 in the electroacupuncture group were lower than those in the model group, and IL-4 and IL-10 were higher, which proved that acupuncture and moxibustion can regulate the balance of Th1/Th2 cells.

5. Acupuncture Exerts an Immunomodulatory Effects by Regulating Intestinal Flora

Intestinal flora plays a crucial role in the maintenance of physical health and the pathogenesis of gastrointestinal diseases [90]. Some studies have shown that the composition and number of the intestinal flora of IBD patients are lower than those of healthy people [91–93]. Intestinal flora can regulate immune cells in a certain way and then induce immune-inflammatory response. The imbalance of intestinal flora can affect the balance of Th17/Treg differentiation in certain ways, resulting in abnormal secretion of related inflammatory factors and intestinal inflammation, which is vital in the pathogenesis of IBD [94, 95]. In order to explore whether acupuncture and moxibustion can improve UC symptoms by regulating the intestinal flora and whether the diversity of intestinal flora is related to Treg and Th17 cells, Wei et al. [96] detected the genome of intestinal flora through Illumina-MiSeq sequencing. The results showed that electroacupuncture and moxibustion can improve the alpha diversity indices and beta diversity of the intestinal flora and inhibit *Streptococcus*, *Odoribacter*, and *Allobaculum* but facilitate *Lactobacillus*. Also, the correlation analysis showed that the increase in the abundance and diversity of the intestinal flora was positively correlated with Treg cells and negatively correlated with Th17 cells. It can also increase the content of *Lactobacillus* and *Spirillum* and reduce the content of *Clostridium* bicarbonate in UC model rats [97].

Gut microbiota is also closely related to the intestinal barrier [98]. Wang et al. [99] found that electroacupuncture can upregulate Bacteroidetes, Muribaculaceae, *Faecalibacterium*, *Roseburia*, and Bifidobacterium, while downregulating Firmicutes, Proteobacteria, *Escherichia-Shigella*, and *Erysipelatoclostridium*. To further confirm the influence of gut microbiota on the barrier protective effect of electroacupuncture, a fecal microbiota transplantation (FMT) experiment was used. Compared with DSS mice, mice that received microbiota from electroacupuncture have less colonic inflammation and better barrier integrity, which indicates that electroacupuncture maintains the integrity of the intestinal barrier by modulating the gut microbiota. Electroacupuncture can modulate the overall structure and structural segregation of the gut microbiota, specifically in the downregulation of Turicibacteraceae, Clostridiaceae, and Erysipelotrichaceae and upregulation of Lactobacillaceae [100].

6. Conclusion

By reviewing the existing literature, we found that the immunomodulatory mechanism of acupuncture in the treatment of IBD has the following characteristics: First of all, from the perspective of intervention methods, the studies of manual acupuncture and electroacupuncture have been the most studied, especially electroacupuncture. Although warm needle acupuncture and fire acupuncture are effective, their mechanisms are rarely studied. Then, from the perspective of research direction, the current research on immune regulation mainly focuses on adaptive immunity, especially on the balance of Th17/Treg axis, which may be due to the current recognition and clarity of the mechanism. The mechanism of innate immunity is insufficiently studied, such as oxidative stress and endoplasmic reticulum stress. In terms of the research results, the mechanism underlying the immune regulation of acupuncture involves innate immunity (intestinal epithelial barrier, toll-like receptors, NLRP3 inflammasomes, oxidative stress, and endoplasmic reticulum stress) and adaptive immunity (the balance of Th17/Treg and Th1/Th2 cells) as well as the intestinal flora. Although the current research has made certain progress, the explanation of the immune regulation of acupuncture is far from enough, and further research is needed.

Conflicts of Interest

The authors have no conflicts of interest to declare.

Authors' Contributions

Zhifeng Liu and Yi Jiao contributed equally to this study.

Acknowledgments

The authors have received funding for research, writing, and publication of this paper from the National Natural Science Foundation of China (No. 81704193).

References

[1] Y. S. Kim, H. Zhang, S. Lee et al., "CU06-1004 alleviates experimental colitis by modulating colonic vessel dysfunction," *Frontiers in Pharmacology*, vol. 11, Article ID 571266, 2020.

[2] A. Z. Agista, T. B. Rusbana, J. Islam et al., "Fermented rice bran supplementation prevents the development of intestinal fibrosis due to DSS-induced inflammation in mice," *Nutrients*, vol. 13, 2021.

[3] T. Sakurai, H. Nishiyama, T. Nagai, S. Goto, H. Ogata, and M. Kudo, "Deficiency of Gankyrin in the small intestine is associated with augmented colitis accompanied by altered bacterial composition of intestinal microbiota," *BMC Gastroenterology*, vol. 20, p. 12, 2020.

[4] M. Yalchin, A. M. Baker, T. A. Graham, and A. Hart, "Predicting colorectal cancer occurrence in IBD," *Cancers*, vol. 13, 2021.

[5] E. A. Linson and S. B. Hanauer, "Epidemiology of colorectal cancer in inflammatory bowel disease - the evolving landscape," *Current Gastroenterology Reports*, vol. 23, p. 16, 2021.

[6] G. G. Kaplan and J. W. Windsor, "The four epidemiological stages in the global evolution of inflammatory bowel disease," *Nature Reviews Gastroenterology and Hepatology*, vol. 18, pp. 56–66, 2021.

[7] S. C. Ng, H. Y. Shi, N. Hamidi et al., "Worldwide incidence and prevalence of inflammatory bowel disease in the 21st century: a systematic review of population-based studies," *Lancet*, vol. 390, pp. 2769–2778, 2017.

[8] S. R. Knowles, L. Keefer, H. Wilding, C. Hewitt, L. A. Graff, and A. Mikocka-Walus, "Quality of life in inflammatory bowel disease: a systematic review and meta-analyses-Part II," *Inflammatory Bowel Diseases*, vol. 24, pp. 966–976, 2018.

[9] O. Olén, R. Erichsen, M. C. Sachs et al., "Colorectal cancer in Crohn's disease: a Scandinavian population-based cohort study," *Lancet Gastroenterol and Hepatology*, vol. 5, pp. 475–484, 2020.

[10] G. P. Ramos and K. A. Papadakis, "Mechanisms of disease: inflammatory bowel diseases," *Mayo Clinic Proceedings*, vol. 94, pp. 155–165, 2019.

[11] J. X. Q. Pang, H. Kheirkhahrahimabadi, S. Bindra et al., "Differential effect of genetic burden on disease phenotypes in Crohn's disease and ulcerative colitis in a Canadian cohort," *Journal of the Canadian Association of Gastroenterology*, vol. 4, pp. 65–72, 2021.

[12] F. A. Silva, B. L. Rodrigues, M. L. Ayrizono, and R. F. Leal, "The immunological basis of inflammatory bowel disease," *Gastroenterology Research and Practice*, vol. 2016, Article ID 2097274, 2016.

[13] M. C. Choy, K. Visvanathan, and P. De Cruz, "An overview of the innate and adaptive immune system in inflammatory bowel disease," *Inflammatory Bowel Diseases*, vol. 23, pp. 2–13, 2017.

[14] J. Ji, Y. Huang, X. F. Wang et al., "Review of clinical studies of the treatment of ulcerative colitis using acupuncture and moxibustion," *Gastroenterology Research and Practice*, vol. 2016, Article ID 9248589, 2016.

[15] S. Rabitti, C. M. Giovanardi, and D. Colussi, "Acupuncture and related therapies for the treatment of gastrointestinal diseases," *Journal of Clinical Gastroenterology*, vol. 55, pp. 207–217, 2021.

[16] C.-h. Bao, J.-z. Zhang, L.-y. Wu, J. Li, X.-q. Zeng, and H.-r. Liu, "Effect of electroacupuncture and herbal cake-partitioned moxibustion on anxiety and depression in patients with Crohn's disease in remission," *Journal of Acupuncture and Tuina Science*, vol. 14, pp. 87–92, 2016.

[17] D. Horta, A. Lira, M. Sanchez-Lloansi et al., "A prospective pilot randomized study: electroacupuncture vs. Sham procedure for the treatment of fatigue in patients with quiescent inflammatory bowel disease," *Inflammatory Bowel Diseases*, vol. 26, pp. 484–492, 2020.

[18] J. Ji, Y. Lu, H. Liu et al., "Acupuncture and moxibustion for inflammatory bowel diseases: a systematic review and meta-analysis of randomized controlled trials," *Evidence-Based Complementary and Alternative Medicine*, vol. 2013, Article ID 158352, 2013.

[19] X. Wang, N. Q. Zhao, Y. X. Sun et al., "Acupuncture for ulcerative colitis: a systematic review and meta-analysis of randomized clinical trials," *BMC Complementary Medicine and Therapies*, vol. 20, p. 309, 2020.

[20] H. Vargas-Robles, K. F. Castro-Ochoa, A. F. Citalán-Madrid, and M. Schnoor, "Beneficial effects of nutritional supplements on intestinal epithelial barrier functions in experimental colitis models in vivo," *World Journal of Gastroenterology*, vol. 25, pp. 4181–4198, 2019.

[21] M. Quiros and A. Nusrat, "Saving problematic mucosae: SPMs in intestinal mucosal inflammation and repair," *Trends in Molecular Medicine*, vol. 25, pp. 124–135, 2019.

[22] C. Lee, S. N. Hong, E. R. Kim, D. K. Chang, and Y. H. Kim, "Epithelial regeneration ability of Crohn's disease assessed using patient-derived intestinal organoids," *International Journal of Molecular Sciences*, p. 22, 2021.

[23] Y. Ren, C. Zhang, C. An et al., "Effects of herb-partitioned moxibustion and electroacupuncture on serum indexes of intestinal fibrosis in rats with Crohn's disease," *Journal of Acupuncture and Tuina Science*, vol. 9, pp. 13–16, 2011.

[24] Y. Shi, C. H. Bao, H. G. Wu, and W. F. Chen, "Effects of herbs-partitioned moxibustion on the expression of intestinal mucosa TNF-α, TNFR1, TNFR2 and apoptosis of intestinal epithelial cells in Crohn's disease patients," *Traditional Chinese Medicine*, vol. 45, pp. 46–50, 2011.

[25] J. Zhou, "Study on the regulatory mechanism of acupuncture and moxibustion on intestinal epithrlial mesenchymal transformation in Crohn's disease based on TNF-α/NF-κB/Snail1 and TGF-β1/Smad3/Snail1pathways," *Thesis, Shanghai University of Traditional Chinese Medicine*, 2019.

[26] Y. Shi, T. Li, J. Zhou et al., "Herbs-Partitioned moxibustion combined with acupuncture inhibits TGF-beta1-smad-snail-induced intestinal epithelial mesenchymal transition in Crohn's disease model rats," *Evidence-Based Complementary and Alternative Medicine*, vol. 2019, Article ID 8320250, 2019.

[27] N. Shen, Z. Wang, C. Wang, J. Zhang, and C. Liu, "Methane alleviates inflammation and apoptosis of dextran sulfate sodium-induced inflammatory bowel diseases by inhibiting toll-like receptor 4 (TLR4)/Myeloid differentiation factor 88 (MyD88)/Nuclear translocation of nuclear factor-κb (NF-κB) and endoplasmic reticulum stress pathways in mice," *Medical Science Monitor*, vol. 26, Article ID e922248, 2020.

[28] X. Ke, F. Zhou, Y. Gao et al., "Qing Hua Chang Yin exerts therapeutic effects against ulcerative colitis through the inhibition of the TLR4/NF-κB pathway," *International Journal of Molecular Medicine*, vol. 32, pp. 926–930, 2013.

[29] C. X. Qiao, S. Xu, D. D. Wang et al., "MicroRNA-19b alleviates lipopolysaccharide-induced inflammatory injury in human intestinal cells by up-regulation of Runx3," *European Review for Medical and Pharmacological Sciences*, vol. 22, pp. 5284–5294, 2018.

[30] C. X. Qiao, G. Zhao, L. Z. Zhang et al., "Intervention mechanism of electroacupuncture in rats with ulcerative colitis: an analysis based on the Toll-like receptor 4/myeloid differentiation factor 88/nuclear factor-kappa B signaling pathway," *Zhen Ci Yan Jiu*, vol. 45, pp. 180–187, 2020.

[31] H. Y. Li and H. Liang, "Therapy of electroacupuncture on tianshu(ST25) has effect on TLR4/NF-κB signaling pathway in rats with ulcerative colitis," *Journal of New Chinese Medicine*, vol. 50, pp. 20–24, 2018.

[32] Y. Y. Wu, M. J. Liu, S. J. YIn, and A. Y. Wang, "Acupuncture reduce colonic inflammation by suppresing oxidative stres and endoplasmic reticu- lum stres in rats with ulcerative colitis," *Acupuncture Research*, vol. 45, pp. 8–14, 2020.

[33] C. S. Yang, D. M. Shin, and E. K. Jo, "The role of NLR-related protein 3 inflammasome in host defense and inflammatory diseases," *International Neurourology Journal*, vol. 16, pp. 2–12, 2012.

[34] C. Bauer, P. Duewell, H. A. Lehr, S. Endres, and M. Schnurr, "Protective and aggravating effects of Nlrp3 inflammasome activation in IBD models: influence of genetic and environmental factors," *Digestive Diseases*, vol. 30, no. 1, pp. 82–90, 2012.

[35] S. U. Seo, N. Kamada, R. Muñoz-Planillo et al., "Distinct commensals induce interleukin-1β via NLRP3 inflammasome in inflammatory monocytes to promote intestinal inflammation in response to injury," *Immunity*, vol. 42, pp. 744–755, 2015.

[36] C. Bauer, P. Duewell, C. Mayer et al., "Colitis induced in mice with dextran sulfate sodium (DSS) is mediated by the NLRP3 inflammasome," *Gut*, vol. 59, pp. 1192–1199, 2010.

[37] B. Bang and L. M. Lichtenberger, "Methods of inducing inflammatory bowel disease in mice," *Current Protocols in Pharmacology*, vol. 72, pp. 51–55, 2016.

[38] S. Song, J. An, Y. Li, and S. Liu, "Electroacupuncture at ST-36 ameliorates DSS-induced acute colitis via regulating macrophage polarization induced by suppressing NLRP3/IL-1beta and promoting Nrf2/HO-1," *Molecular Immunology*, vol. 106, pp. 143–152, 2019.

[39] J. Tschopp and K. Schroder, "NLRP3 inflammasome activation: the convergence of multiple signalling pathways on ROS production?" *Nature Reviews Immunology*, vol. 10, pp. 210–215, 2010.

[40] H. Zhu and Y. R. Li, "Oxidative stress and redox signaling mechanisms of inflammatory bowel disease: updated experimental and clinical evidence," *Experimental Biology and Medicine*, vol. 237, pp. 474–480, 2012.

[41] Y. H. Zeng, F. Yang, and Y. H. He, "Experimental study on acupuncture and moxibustion through NOx - ROS - NLRP3 signaling pathway in the treatment of ulcerative colitis in rats," *Lishizhen Medicine and Materia Medica Research*, vol. 29, pp. 1002–1004, 2018.

[42] T. Tian, Z. Wang, and J. Zhang, "Pathomechanisms of oxidative stress in inflammatory bowel disease and potential antioxidant therapies," *Oxidative Medicine and Cellular Longevity*, vol. 2017, Article ID 4535194, 2017.

[43] E. Alemany-Cosme, E. Sáez-González, I. Moret et al., "Oxidative stress in the pathogenesis of Crohn's disease and the interconnection with immunological response," *Microbiota, External Environmental Factors, and Epigenetics. Antioxidants*, vol. 10, 2021.

[44] A. Piechota-Polanczyk and J. Fichna, "Review article: the role of oxidative stress in pathogenesis and treatment of inflammatory bowel diseases," *Naunyn-Schmiedeberg's Archives of Pharmacology*, vol. 387, pp. 605–620, 2014.

[45] X. Yang, Y. Yan, J. Li et al., "Protective effects of ethanol extract from Portulaca oleracea L on dextran sulphate sodium-induced mice ulcerative colitis involving anti-inflammatory and antioxidant," *American Journal of Translational Research*, vol. 8, pp. 2138–2148, 2016.

[46] A. Kaser, E. Martínez-Naves, and R. S. Blumberg, "Endoplasmic reticulum stress: implications for inflammatory bowel disease pathogenesis," *Current Opinion in Gastroenterology*, vol. 26, pp. 318–326, 2010.

[47] A. Coope, L. B. Pascoal, J. D. Botezelli et al., "ER stress activation in the intestinal mucosa but not in mesenteric adipose tissue is associated with inflammation in Crohn's disease patients," *PLoS One*, vol. 14, Article ID e0223105, 2019.

[48] J. D. Lord, "Promises and paradoxes of regulatory T cells in inflammatory bowel disease," *World Journal of Gastroenterology*, vol. 21, pp. 11236–11245, 2015.

[49] X. Geng and J. Xue, "Expression of Treg/Th17 cells as well as related cytokines in patients with inflammatory bowel

disease," *Pakistan Journal of Medical Sciences*, vol. 32, pp. 1164–1168, 2016.

[50] L. A. Zenewicz, A. Antov, and R. A. Flavell, "CD4 T-cell differentiation and inflammatory bowel disease," *Trends in Molecular Medicine*, vol. 15, pp. 199–207, 2009.

[51] G. Yao, J. Qi, J. Liang et al., "Mesenchymal stem cell transplantation alleviates experimental Sjögren's syndrome through IFN-β/IL-27 signaling axis," *Theranostics*, vol. 9, pp. 8253–8265, 2019.

[52] F. Ma, H. Hao, X. Gao et al., "Melatonin ameliorates necrotizing enterocolitis by preventing Th17/Treg imbalance through activation of the AMPK/SIRT1 pathway," *Theranostics*, vol. 10, pp. 7730–7746, 2020.

[53] Y. J. Liu, B. Tang, F. C. Wang et al., "Parthenolide ameliorates colon inflammation through regulating Treg/Th17 balance in a gut microbiota-dependent manner," *Theranostics*, vol. 10, pp. 5225–5241, 2020.

[54] A. Luo, S. T. Leach, R. Barres, L. B. Hesson, M. C. Grimm, and D. Simar, "The microbiota and epigenetic regulation of T helper 17/regulatory T cells: in search of a balanced immune system," *Frontiers in Immunology*, vol. 8, p. 417, 2017.

[55] Z. Xu, C. Wei, R. U. Zhang, J. Yao, D. Zhang, and L. Wang, "Epigallocatechin-3-gallate-induced inhibition of interleukin-6 release and adjustment of the regulatory T/T helper 17 cell balance in the treatment of colitis in mice," *Experimental and Therapeutic Medicine*, vol. 10, pp. 2231–2238, 2015.

[56] C. Y. L. Wang, L. L. Zeng, Y. Geng, and X. Wang, "Efect of electroacupuncture stimulation of "Guanyuan" (CV 4) and "Zusanli" (ST 36) on Splen lymphocytes Treg/Th 17Immune balance in ulcerative colitis mice," *Acupuncture Research*, vol. 41, pp. 55–59, 2016.

[57] J. Sun, H. Zhang, C. Wang et al., "Regulating the balance of Th17/treg via electroacupuncture and moxibustion: an ulcerative colitis mice model based study," *Evidence-Based Complementary and Alternative Medicine*, vol. 2017, Article ID 7296353, 2017.

[58] Q. Guan and J. Zhang, "Recent advances: the imbalance of cytokines in the pathogenesis of inflammatory bowel disease," *Mediators of Inflammation*, vol. 2017, Article ID 4810258, 2017.

[59] P. Patel, D. K. Malipatlolla, S. Devarakonda et al., "Dietary oat bran reduces systemic inflammation in mice subjected to pelvic irradiation," *Nutrients*, vol. 12, 2020.

[60] K. Sugimoto, A. Ogawa, E. Mizoguchi et al., "IL-22 ameliorates intestinal inflammation in a mouse model of ulcerative colitis," *Journal of Clinical Investigation*, vol. 118, pp. 534–544, 2008.

[61] X. R. Xu, C. Q. Liu, B. S. Feng, and Z. J. Liu, "Dysregulation of mucosal immune response in pathogenesis of inflammatory bowel disease," *World Journal of Gastroenterology*, vol. 20, pp. 3255–3264, 2014.

[62] İ Karaboga, S. Demirtas, and T. Karaca, "Investigation of the relationship between the Th17/IL-23 pathway and innate-adaptive immune system in TNBS-induced colitis in rats," *Iranian Journal of Basic Medical Sciences*, vol. 20, pp. 870–879, 2017.

[63] E. Bettelli, Y. Carrier, W. Gao et al., "Reciprocal developmental pathways for the generation of pathogenic effector TH17 and regulatory T cells," *Nature*, vol. 441, pp. 235–238, 2006.

[64] R. Basu, R. D. Hatton, and C. T. Weaver, "The Th17 family: flexibility follows function," *Immunological Reviews*, vol. 252, pp. 89–103, 2013.

[65] S. J. Liang, "Effect of needle warming moxibustion on the expression of IL-17 and IL-23 in the serum of ulcerative colitis," *Thesis, Fujian University of Traditional Chinese Medicine*, 2016.

[66] M. S. Chen, "Mechanism of electroacupuncture at "Tianshu" and "Zusanli" mediated FOXP3/DAF pathway regulating Treg/Th17 balance in UC rats," *Thesis, Liaoning University of Traditional Chinese Medicine*, 2020.

[67] X. Y. Liu, "Effects of moxibustion and acupuncture on intestinal related immune factors IL-17A, IL-22 and IFN-γ in rats with Crohn's disease," *Thesis, Hunan University of Chinese Medicine*, 2020.

[68] A. P. Hutchins, D. Diez, and D. Miranda-Saavedra, "The IL-10/STAT3-mediated anti-inflammatory response: recent developments and future challenges," *Briefings in Functional Genomics*, vol. 12, pp. 489–498, 2013.

[69] Y. Sato, S. Takahashi, Y. Kinouchi et al., "IL-10 deficiency leads to somatic mutations in a model of IBD," *Carcinogenesis*, vol. 27, pp. 1068–1073, 2006.

[70] S. Rosini, N. Pugh, A. M. Bonna, D. J. S. Hulmes, R. W. Farndale, and J. C. Adams, "Thrombospondin-1 promotes matrix homeostasis by interacting with collagen and lysyl oxidase precursors and collagen cross-linking sites," *Science Signaling*, vol. 11, 2018.

[71] S. Ihara, Y. Hirata, and K. Koike, "TGF-β in inflammatory bowel disease: a key regulator of immune cells, epithelium, and the intestinal microbiota," *Journal of Gastroenterology*, vol. 52, pp. 777–787, 2017.

[72] F. Zorzi, E. Calabrese, and G. Monteleone, "Pathogenic aspects and therapeutic avenues of intestinal fibrosis in Crohn's disease," *Clinical Science*, vol. 129, pp. 1107–1113, 2015.

[73] Y. Geng, J. G. Sun, C. Y. L. Wang, and J. L. Zhao, "IL-6, TGF-BETA effect of the DSS induced ulcerative colitis mice serum with electroacupuncture," *Journal of Chengdu University of TCM*, vol. 38, pp. 9–12, 2015.

[74] A. Wang, M. Yang, R. Liang et al., "Mouse double minute 2 homolog-mediated ubiquitination facilitates forkhead box P3 stability and positively modulates human regulatory T cell function," *Frontiers in Immunology*, vol. 11, p. 1087, 2020.

[75] Z. Etesam, M. Nemati, M. A. Ebrahimizadeh et al., "Altered expression of specific transcription factors of Th17 (RORγt, RORα) and Treg lymphocytes (FOXP3) by peripheral blood mononuclear cells from patients with multiple sclerosis," *Journal of Molecular Neuroscience*, vol. 60, pp. 94–101, 2016.

[76] S. Chellappa, H. Hugenschmidt, M. Hagness et al., "Regulatory T cells that co-express RORγt and FOXP3 are pro-inflammatory and immunosuppressive and expand in human pancreatic cancer," *OncoImmunology*, vol. 5, Article ID e1102828, 2016.

[77] A. Esposito, B. Suedekum, J. Liu et al., "Decay accelerating factor is essential for successful corneal engraftment," *American Journal of Transplantation*, vol. 10, pp. 527–534, 2010.

[78] D. Lu, L. Liu, X. Ji et al., "The phosphatase DUSP2 controls the activity of the transcription activator STAT3 and regulates TH17 differentiation," *Nature Immunology*, vol. 16, pp. 1263–1273, 2015.

[79] S. Zundler and M. F. Neurath, "Integrating immunologic signaling networks: the JAK/STAT pathway in colitis and colitis-associated cancer," *Vaccines*, vol. 4, 2016.

[80] E. V. Dang, J. Barbi, H. Y. Yang, D. Jinasena, H. Yu, and Y. Zheng, "Control of T(H)17/T(reg) balance by hypoxia-inducible factor 1," *Cell*, vol. 146, pp. 772–784, 2011.

[81] S. R. Lin, H. J. Zhang, and Q. F. Wu, "Effect of acupuncture and moxibustion on expression of signal transducers and activators of transcription 3 and hypoxia-inducible factor 1alpha in colon mucosa in ulcerative colitis mice," *Zhen Ci Yan Jiu*, vol. 45, pp. 696–701, 2020.

[82] H. J. Z. Zhang, "Effect of acupuncture and moxibustion on STAT3 and HIF-1 alpha protein in colonic tissues of mice with ulcerative colitis," *Chengdu University of Traditional Chinese Medicine*, 2017.

[83] D. J. Gibson, L. Elliott, E. McDermott et al., "Heightened expression of CD39 by regulatory T lymphocytes is associated with therapeutic remission in inflammatory bowel disease," *Inflammatory Bowel Diseases*, vol. 21, pp. 2806–2814, 2015.

[84] M. S. Bynoe, A. T. Waickman, D. A. Mahamed, C. Mueller, J. H. Mills, and A. Czopik, "CD73 is critical for the resolution of murine colonic inflammation," *Journal of Biomedicine and Biotechnology*, vol. 2012, Article ID 260983, 2012.

[85] M. Onodera, K. Endo, Y. Kakuta et al., "ATP-binding cassette subfamily B member 1 1236C/T polymorphism significantly affects the therapeutic outcome of tacrolimus in patients with refractory ulcerative colitis," *Journal of Gastroenterology and Hepatology*, vol. 32, pp. 1562–1569, 2017.

[86] A. Bahreyni, S. S. Samani, M. Khazaei, M. Ryzhikov, A. Avan, and S. M. Hassanian, "Therapeutic potentials of adenosine receptors agonists and antagonists in colitis; Current status and perspectives," *Journal of Cellular Physiology*, vol. 233, pp. 2733–2740, 2018.

[87] Z. Q. Zhuang, "Regulation effect of acupuncture and moxibustion of Treg cells in mice with ulcerative colitis based on CD39/CD73/A2a adenosine metabolic pathway," *Chengdu University of Traditional Chinese Medicine*, 2018.

[88] A. Salmani, M. Mohammadi, R. Farid Hosseini et al., "A significant increase in expression of FOXP3 and IL-17 genes in patients with allergic rhinitis underwent accelerated rush immunotherapy," *Iranian Journal of Basic Medical Sciences*, vol. 22, pp. 989–996, 2019.

[89] Y. P. Chen, "Effect of moxibustion and electroacupuncture on Th1/Th2 immune balance in rats with experimental colitis," *Acupuncture Research*, vol. 41, pp. 210–214, 2016.

[90] S. R. Fehily, C. Basnayake, E. K. Wright, and M. A. Kamm, "The gut microbiota and gut disease," *Internal Medicine Journal*, vol. 51, pp. 1594–1604, 2021.

[91] J. Qin, R. Li, J. Raes, M. Arumugam, K. S. Burgdorf, and C. Manichanh, "A human gut microbial gene catalogue established by metagenomic sequencing," *Nature*, vol. 464, pp. 59–65, 2010.

[92] R. Hansen, R. K. Russell, C. Reiff et al., "Microbiota of de-novo pediatric IBD: increased Faecalibacterium prausnitzii and reduced bacterial diversity in Crohn's but not in ulcerative colitis," *American Journal of Gastroenterology*, vol. 107, pp. 1913–1922, 2012.

[93] Z. F. Dai, X. Y. Ma, R. L. Yang et al., "Intestinal flora alterations in patients with ulcerative colitis and their association with inflammation," *Experimental and Therapeutic Medicine*, vol. 22, p. 1322, 2021.

[94] C. B. Larmonier, K. W. Shehab, F. K. Ghishan, and P. R. Kiela, "T lymphocyte dynamics in inflammatory bowel diseases: role of the microbiome," *BioMed Research International*, vol. 2015, Article ID 504638, 2015.

[95] S. Omenetti and T. T. Pizarro, "The Treg/Th17 Axis: a dynamic balance regulated by the gut microbiome," *Frontiers in Immunology*, vol. 6, p. 639, 2015.

[96] D. Wei, L. Xie, Z. Zhuang et al., "Gut microbiota: a new strategy to study the mechanism of electroacupuncture and moxibustion in treating ulcerative colitis," *Evidence-Based Complementary and Alternative Medicine*, vol. 2019, Article ID 9730176, 2019.

[97] T. S. Hou, X. X. Han, Y. Yang, and J. L. Zhao, "Efect of electroacupuncture intervention on enteric microecology in ulcerative colitis rats," *Acupuncture Research*, vol. 39, pp. 27–34, 2014.

[98] S. Fernández-Tomé, L. Ortega Moreno, M. Chaparro, and J. P. Gisbert, "Gut microbiota and dietary factors as modulators of the mucus layer in inflammatory bowel disease," *International Journal of Molecular Sciences*, p. 22, 2021.

[99] L. Wang, J. An, S. Song et al., "Electroacupuncture preserves intestinal barrier integrity through modulating the gut microbiota in DSS-induced chronic colitis," *Life Sciences*, vol. 261, Article ID 118473, 2020.

[100] G. H. Liu, H. M. Liu, Y. S. Chen, and T. Y. Lee, "Effect of electroacupuncture in mice with dextran sulfate sodium-induced colitis and the influence of gut microbiota," *Evidence-Based Complementary and Alternative Medicine*, vol. 2020, Article ID 2087903, 2020.

Hindawi
Evidence-Based Complementary and Alternative Medicine
Volume 2021, Article ID 8329366, 16 pages
https://doi.org/10.1155/2021/8329366

Review Article

Electroacupuncture for Gastrointestinal Function Recovery after Gynecological Surgery: A Systematic Review and Meta-Analysis

Xiang Gao,[1] Yuzhuo Zhang,[2] Yizhe Zhang,[1] YuTzu Ku,[2] and Yi Guo [2]

[1]*Shanxi Province Hospital of Traditional Chinese Medicine, Shanxi Provincial Institute of Traditional Chinese Medicine, Taiyuan 030012, China*
[2]*Guangzhou University of Chinese Medicine, Guangzhou 510120, China*

Correspondence should be addressed to Yi Guo; doctorguo1010@163.com

Received 13 July 2021; Revised 3 September 2021; Accepted 6 November 2021; Published 21 December 2021

Academic Editor: Ying Li

Background. Evidence for the efficacy and safety of electroacupuncture (EA) on gastrointestinal function recovery after gynecological surgery is unclear. *Objective*. This meta-analysis aimed to evaluate the effects of EA on recovery of postoperative gastrointestinal function for patients receiving gynecological surgery. Data sources: PubMed, Cochrane Central Register of Controlled Trials (CINAHL), Embase, China National Knowledge Infrastructure (CNKI), Weipu (CQVIP), and Wanfang databases were systematically searched from the inception dates to May 30, 2020, for relevant randomized controlled trials (RCTs). Study selection: RCTs that evaluated EA for postoperative gastrointestinal function directly related to gynecological surgery in adults aged 18 years or over. Data extraction and synthesis: paired reviewer independently extracted the data and assessed study quality. Standardized mean differences (SMD) were calculated as the effect measure from a random effects model. Main outcomes and measures: time to first flatus (TFF), time to bowel sounds recovery (TBS), and time to first defecation (TFD) were recorded as primary outcomes; postoperative nausea and vomiting (PONV), motilin (MTL), gastrin (GAS), pH value of gastric mucosa (pHi), gastric mucosal partial pressure of carbon dioxide (PgCO2), vasoactive intestinal peptide (VIP), and adverse event were reported as secondary outcomes. *Results*. We included eighteen RCTs (1117 participants). Our findings suggested that compared to the control group (CG), electroacupuncture group (EG) showed significant effects on TFF (SMD = −0.98, 95% CI: [−1.28, −0.68], $P < 0.00001$, $I^2 = 69\%$), TBS (SMD = −0.98, 95% CI: [−1.84, −0.12], $P = 0.03$, $I^2 = 92\%$), and TFD (SMD = −1.23, 95% CI: [−1.59, −0.88], $P < 0.0001$, $I^2 = 0\%$). Moreover, the incidence of PONV at postoperative 6 h (OR = 0.42, 95% CI: [0.27, 0.64], $P < 0.0001$, $I^2 = 0\%$) and 24 h (OR = 0.46, 95% CI: [0.32, 0.68], $P < 0.0001$, $I^2 = 0\%$) was lower in the EG than that in the CG, whereas no significant difference in ratio of PONV at postoperative 48 h (OR = 0.55, 95% CI: [0.20, 1.51], $P = 0.25$, $I^2 = 0\%$) was detected between the two groups. Meanwhile, there was a significant effect in favor of EA on the level of MTL at postoperative 6 h (SMD = −0.93, 95% CI: [−1.36, −0.61], $P < 0.0001$, $I^2 = 21\%$), while no significant effect was observed at postoperative 24 h (SMD = −0.43, 95% CI: [−0.89, 0.02], $P = 0.06$, $I^2 = 69\%$) in the EG when compared to the CG. Additionally, a large significant effect on decreasing $PgCO_2$ was found in the EG in comparison to the CG, but no significant effect in favor of EA on GAS, VIP, or pHi was observed. It was reported that there was one participant with pain at the needling sites and bruising, and three participants withdrew because they were not intolerant to EA. *Conclusions*. EA could be a promising strategy for the prevention and treatment of gastrointestinal dysfunction after gynecological surgery, including shortening TFF and TFD, TBS, regulating MTL, and decreasing the ratio of PONV within postoperative 24h. The effects on MTL and PONV varied with different intervention points, and EA used at 30 min prior to surgery might be recommended. However, the evidence quality ranged from low to very low, and large-scale and high-quality RCTs were warranted.

1. Introduction

Postoperative recovery of gastrointestinal function was considered as one of the most important parts for the rehabilitation after surgery, which was a condition that mainly related to surgical stress, anesthesia regimen, surgical treatment, and postoperative analgesia method [1]. The short-term gastrointestinal dysfunction after surgery was referred to as postoperative ileus (POI), which could cause undesirable consequences, including abdominal distension,

lack of flatus and defecation, and nausea and vomiting. As was reported, POI would influence postoperative experience, increase the length of hospital stay, and even raise the risk of morbidity and mortality, which not only strongly prevented rehabilitation after surgery, but also posed a substantial economic burden on family and society [2].

POI was frequently observed after gastroenterological surgery, and it was followed by gynecological surgery [3]. It was reported that the prevalence of POI ranged from 5% to 25% among patients undergoing gynecological surgery [4], and even the incidence was up to 50% in patients receiving surgical therapy for gynecological cancers [5]. In recent years, minimally invasive surgery, such as laparoscopy surgery, has become more commonly used for gynecologic indications [6]. However, the incidence of gastrointestinal dysfunction following surgery is not decreased [7]. Even though increasing studies focusing on improving recovery of postoperative gastrointestinal function have been conducted, strategies with satisfactory efficacy are still rarely reported, especially for gynecological population. Thus, apart from improving anesthesia regimen and surgical technique, so far it is still urgent and essential to develop an effective and safety method of promoting the return of gastrointestinal function for patients receiving gynecological surgery.

Acupuncture, as one of the conventional Chinese medical therapies, has been applied to promote gastrointestinal function for thousands of years [8]. Electroacupuncture (EA) is a modified technique involving traditional acupuncture and electrical stimulation to achieve a greater response, which has been proved to be a promising approach to reduce complications and accelerate rehabilitation after surgery in the field of orthopedic, abdominal, and gynecological diseases. Moreover, there are an increasing number of studies focusing on EA for treatment and prevention of POI. But the results concerning the efficacy of EA on POI are inconsistent [9, 10]. It was reported in the previous meta-analyses [11–14] that supported the benefits of EA/acupuncture to POI, but the efficacy of EA on POI for gynecological patients still lacked evidence basis. Gynecological surgery was unlike gastroenterological surgery or other surgery in terms of pathology and surgical methods, which might lead to difference outcomes of gastrointestinal function recovery after surgery. Consequently, the purpose of this study was to evaluate the safety and efficacy of EA on postoperative recovery of gastrointestinal function for the patients receiving gynecological surgery, which could provide new evidence for promoting rehabilitation after gynecological surgery.

2. Methods

This study was conducted according to the Preferred Reporting Items for Systematic Reviews and Meta-Analyses (PRISMA) guidelines [15]. Moreover, the protocol of this study was registered in PROSPERO, and the registration number is CRD42021260096. In the process of retrieval, we found that most of the literatures were published in Chinese, so we retrieved with increased numbers of Chinese database. However, due to the delay of preliminary preparation time, the deadline for literature retrieval was extended to May 30, 2021. We had submitted the amendments in the registration system.

2.1. Search Strategy. In order to identify relevant studies, we systematically search the electronic databases including PubMed, Cochrane Central Register of Controlled Trials (CINAHL), Embase, China National Knowledge Infrastructure (CNKI), Weipu (CQVIP), and Wanfang from inception to May 30, 2021. The search terms, such as "postoperative ileus," "postoperative gastrointestinal motility disorder," "postoperative gastrointestinal function recovery," "postoperative gastrointestinal dysfunction," "postoperative gastrointestinal function," "postoperative nausea and vomiting," and "electroacupuncture," were used to search in each database without language or disease restrictions. The search strategy was described in Supplementary Figure 1.

2.2. Inclusion Criteria. We formulated inclusion and exclusion criteria based on PICOS (patients, intervention, comparator, outcomes, and study design) approach [16].

2.2.1. Patients

(i) Subjects aged 18 or over
(ii) Subjects with gynecological disease receiving surgical treatment

2.2.2. Interventions. EA should be used in the experimental group in the included study.

2.2.3. Comparators. EA versus (vs) other therapy, EA+ other therapy vs. other therapy, EA vs. nonintervention.

2.2.4. Outcomes. The literature reporting more than or equal to one index for assessing gastrointestinal function after surgery would be included in this study. The outcomes were listed as follows:

Primary Outcomes

(i) Time to first flatus (TFF)
(ii) Time to bowel sounds recovery (TBS)
(iii) Time to first defecation (TFD)

Secondary Outcomes

(i) Postoperative nausea and vomiting (PONV)
(ii) Motilin (MTL)
(iii) Gastrin (GAS)
(iv) pH value of gastric mucosa (pHi)
(v) Gastric mucosal partial pressure of carbon dioxide ($PgCO_2$)
(vi) Vasoactive intestinal peptide (VIP)
(vii) Adverse event

2.2.5. Study Design

(i) Clinical randomized controlled trials (RCTs)

(ii) Published in a peer-reviewed journal

(iii) Language: Chinese or English

2.3. Exclusion Criteria. (1) Pregnancy, or participants receiving obstetric surgery; (2) manual acupuncture, acupoint massage, transcutaneous electrical nerve stimulation, transcutaneous electrical acupoints stimulation, and neuromuscular electrical stimulation; (3) repeated publications, conference abstracts, comments, protocol, meta-analysis, or reviews, or full-text unavailable articles.

2.4. Literature Screening. Paired investigators (X. Gao and Yu Z. Zhang) independently screened the retrieved studies. Firstly, all the studies were imported to EndNote X8 (Bld 10063) to remove duplicates. Secondly, the remaining studies were preliminarily selected by reading the titles and abstracts. Thirdly, the included studies were identified based on the inclusion and exclusion criteria by full-text reading.

2.5. Data Extraction. The relevant data were independently extracted from the included studies by the two reviewers, including study characteristics (e.g., author names, publication year, study design, and sample size), participant characteristics (e.g., age, year), intervention type, intervention characteristics (e.g., acupoints, model, and intensity), and outcomes. During the process of screening and data extraction, any discrepancies would be resolved by discussion, or consultation with a third reviewer (Y. Guo) until a consensus was reached.

2.6. Quality Assessment. In accordance with the Cochrane Collaboration's Risk of Bias tool V 2.0, the two reviewers assessed the quality of the included literatures from seven dimensions: bias arising from the randomisation process, bias from deviations from the intended interventions, bias from missing outcome data, bias due to measurement of the outcome, bias from the selection of the reported results, and overall risk of bias [16]. The risk of each item is divided into three levels: high, unclear, and low. Meanwhile, the two researchers evaluated the methodological quality of included studies according to the Physiotherapy Evidence Database (PEDro) scale [17], which includes 10 items for assessment of trial quality from various aspects, including randomisation procedure, concealed allocation, similar baseline, patients blinding, therapists blinding, assessors blinding, adequate follow-up (dropout rate <15%), intention to treat analysis, between-group statistical analysis, and point and variability measures; the total score ranged from 0 to 10. According to the total score, quality of study was categorized into three degrees, including high ($10 \geq$ PEDro score ≥ 6), fair ($6 >$ PEDro score ≥ 4), and low ($0 \leq$ PEDro score ≤ 3) [18].

2.7. Statistical Analysis. We conducted the data analysis by using review manager (version 5.3, the Nordic Cochrane Centre, Copenhagen, Denmark) and Stata (version 13.0, the StataCorp LP, TX, USA). For continuous variables, standardized mean differences (SMDs) and 95% confidence intervals (95% CI) were calculated as the effect measure by using a random effects model, and standard mean effect sizes were divided to different categories, including no change (0), small effect (0.2), moderate effect (0.5), and large effect (0.8) [18]. Enumeration data was analyzed by using a random effects method and expressed as the odds ratios (OR) and 95% CI. All the corresponding meta-analysis results were illustrated by the forest map intuitively. Cochran's Q-test and I^2 index were employed to estimate heterogeneity [19], and I^2 statistic greater than 50% was considered as substantially heterogeneous. When a substantially heterogeneous was observed, subgroups analysis or sensitivity analyses were used to determine the risk factor resulted in the high heterogeneity. Grading of recommendations, assessment, development, and evaluation (GRADE) approach was utilized to evaluate the quality of evidence [20]. In addition, publication bias was assessed by Begg's and Egger's tests [19], and the visual inspection of funnel plots would be applied if the index was reported in more than 10 included studies. The significant difference level was set at $P < 0.05$.

3. Results

3.1. Study Selection. A total of 2889 potentially relevant strings were retrieved from the Chinese and English databases. After removing duplicates and screening titles and reading summary, 2857 trials were eliminated. Consequently, the remaining 32 studies were screened by reading full text. Finally, eighteen RCTs [21–38] fulfilled the inclusion criteria, and 1117 subjects including 557 subjects in the electroacupuncture group (EG) and 560 subjects in the control group (CG) were involved. Flowchart of the structured review is illustrated in Figure 1.

3.2. Study Characteristics. The included studies involved 1117 subjects who received gynecological surgery. Seven studies [22, 23, 25–27, 32, 33] reported the effects of EA on postoperative gastrointestinal function recovery for patients undergoing total abdominal hysterectomy, and eleven studies [21, 24, 28–31, 34–38] involved laparoscopic surgery. Anesthesia type included general anesthesia and epidural anesthesia [25, 33]. In addition, EA was performed at 24 h prior to surgery in three studies [16, 21, 30], at 30 min prior to surgery or before the start of surgery in ten studies [22, 24, 28, 29, 31, 34–38], and after surgery in five studies [23, 25, 27, 32, 33]. Among all the acupoints involved in the included studies, Zusanli (ST36) (14/18) and Neiguan (PC6) (11/15) were most frequently selected, while less frequently selected acupoints included Hegu (LI4) (4/18), Shangjuxu (ST37) (3/18), Zhongwan (RN12) (3/18), Tianshu (ST25) (3/18), Liangqiu (ST34) (2/18), Sanjinjiao (SP6) (2/18), Liangmen (ST21) (2/18), Xuehai (SP10) (1/18), and Taichong (LR3) (1/18). Tables 1 and 2 presented the characteristics of each included study.

3.3. Risk of Bias in Included Studies. The detailed results are depicted in Figure 2. All the included studies were reported as random generation, and four of the RCTs [21, 22, 29, 38] were

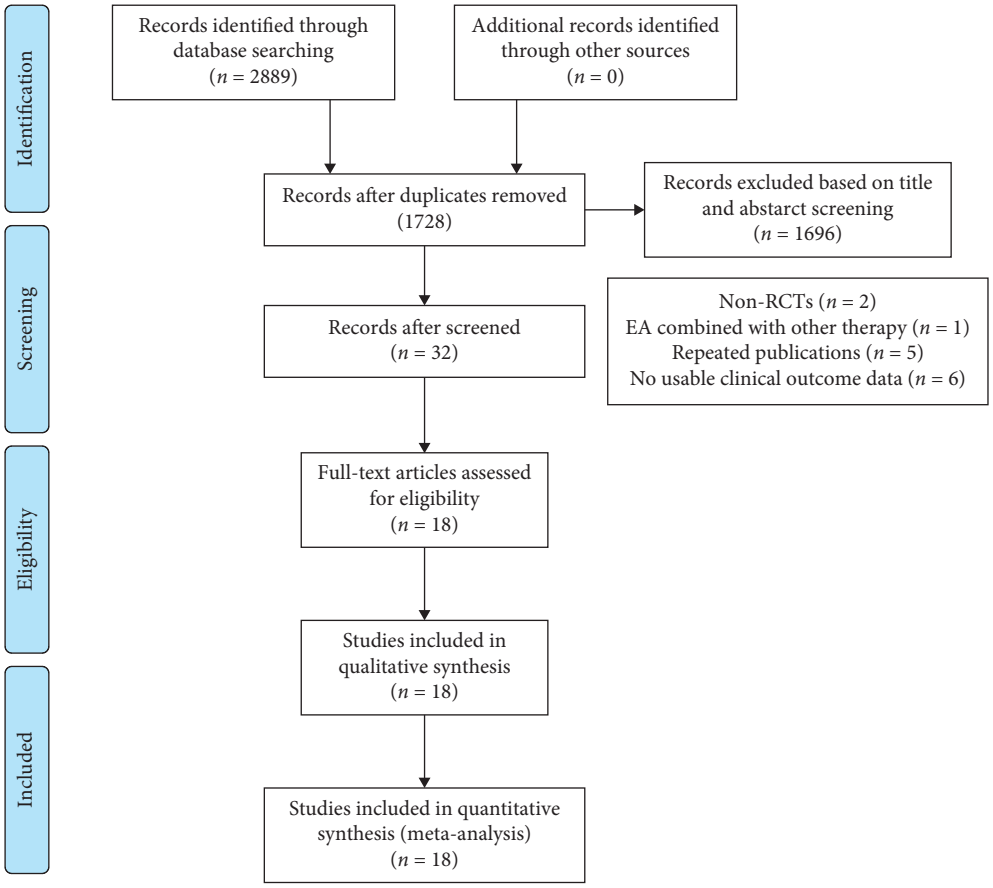

Figure 1: Flowchart of study selection.

conducted with concealed allocation. Participants were blinded to the group allocation in four studies [21, 22, 29, 38], and assessment blinding was reported in seven RCTs [21, 22, 24, 27, 29, 36, 38]. Meanwhile, based on the evaluation of PEDro, all the scores of the included studies ranged from 5 to 9 (mean score + standard deviation = 6.61 ± 1.42; Supplementary Table 1), which indicated that the methodological quality of included studies was fair to high. All the included studies were described as random generation, while blinding was recorded only in four trials [21, 22, 29, 38]. Additionally, none of the studies reported a follow-up rate of more than 15%, and intention-to-treat analysis was not found in any of the included studies.

3.4. Meta-Analysis

3.4.1. Primary Outcomes

(1) Time to First Flatus. Ten of the included studies reported TFF [21, 23, 25, 26, 28–30, 32–34], and result from meta-analysis suggested that, overall, EG showed a significantly effect on TFF compared to the CG (SMD = −0.98, 95% CI: [−1.28, −0.68], $P < 0.00001$, $I^2 = 69\%$). Moreover, TFF was significantly shorter in the EG than that in the CG, either for laparoscopic surgery (SMD = −0.97, 95% CI: [−1.23, −0.72], $P < 0.00001$, $I^2 = 0\%$) or total abdominal hysterectomy (SMD = −1.01, 95% CI: [−1.57, −0.44], $P = 0.0005$, $I^2 = 84\%$) (Figure 3). Furthermore, we conducted the subgroup analysis by anesthesia types, intervention points, and comparators. All the results supported that EA shortened TFF, no matter for general anesthesia (SMD = −1.01, 95% CI: [−1.37, −0.65], $P < 0.00001$, $I^2 = 70\%$) or epidural anesthesia (SMD = −0.88, 95% CI: [−1.61, −0.16], $P = 0.02$, $I^2 = 81\%$) (Supplementary Figure 2), EA applied at 24 h prior to surgery (SMD = −1.23, 95% CI: [−1.73, −0.73], $P < 0.00001$, $I^2 = 51\%$), 30 min prior to surgery (SMD = −0.97, 95% CI: [−1.37, −0.57], $P < 0.00001$, $I^2 = 36\%$), or after surgery (SMD = −0.84, 95% CI: [−1.41, −0.26], $P = 0.004$, $I^2 = 83\%$) (Supplementary Figure 3). And a shorter TFF was observed in the EG than that in the CG by comparators as EA VS control (SMD = −1.27, 95% CI: [−1.52, −1.03], $P < 0.00001$, $I^2 = 0\%$), EA + other therapy vs. other therapy (SMD = −1.40, 95% CI: [−2.03, −0.77], $P < 0.0001$, $I^2 = 84\%$), and EA vs. ginger partitioned moxibustion on umbilicus (SMD = −0.35, 95% CI: [−0.67, −0.03], $P = 0.03$, $I^2 = 1\%$) (shown in Supplementary Figure 4). However, there was no significant difference in the ratio of subjects with TFF >72 h (OR = 0.16, 95% CI: [0.02, 1.35], $P = 0.09$, $I^2 = 0\%$) (Figure 4).

(2) Time to Bowel Sounds Recovery. Meta-analysis of four studies showed a significantly shorter TBS for the EG compared to the CG (SMD = −0.98, 95% CI: [−1.84, −0.12], $P = 0.03$, $I^2 = 92\%$). Nevertheless, subgroup analysis showed that EG presented a shorter TBS when EA performed at

Table 1: Characteristics of the included studies.

First author (year)	Age (years)		Sample size	Type of surgery	Type of anesthesia	Duration of anesthesia/surgery	
	EG	CG	EG/CG			EG	CG
Li et al. (2017) [21]	35.2 ± 6.1	34.4 ± 9.1	20/20	Laparoscopic surgery	General anesthesia (I/II)	89.3 ± 38.9	95.5 ± 32.8
Praveena et al. (2016) [22]	47.5 ± 7.94	48.72 ± 6.72	32/32	Total abdominal hysterectomy	General anesthesia (I/II)	149.06 ± 42.64	151.97 ± 50.71
Bai et al. (2012) [23]	42~60		30/30	Total abdominal hysterectomy	General anesthesia (I/II)	—	—
Chen et al. (2014) [24]	18~65		27/27	Laparoscopic surgery	General anesthesia (I/II)	95.2 ± 39.4	77.8 ± 23.8
Jin and Jing (2015) [25]	35~66 (48.3 ± 6.3)		45/45	Total abdominal hysterectomy	Epidural anesthesia	—	—
Li et al. (2019) [26]	37.26 ± 8.83	36.96 ± 9.05	30/30	Total abdominal hysterectomy	General anesthesia (I/II)	—	—
Lu et al. (2010) [27]	40~60		29/30	Total abdominal hysterectomy	General anesthesia (I/II)	—	—
Toronui (2019) [28]	40.54 ± 5.82	40.62 ± 5.84	29/29	Laparoscopic surgery	General anesthesia	84.31 ± 35.21	84.58 ± 35.56
Wang et al. (2018) [29]	35.76 ± 7.15	34.88 ± 7.28	27/28	Laparoscopic surgery	General anesthesia (I/II)	68.69 ± 29.34	67.62 ± 34.42
Wang et al. (2018) [30]	34.9 ± 5.1	34.8 ± 6.2	27/28	Laparoscopic surgery	General anesthesia (I/II)	80.2 ± 36.9	85.3 ± 31.8
Wang et al. (2011) [31]	41.2 ± 6.1	39.3 ± 8.5	30/30	Laparoscopic surgery	General anesthesia (I/II)	67.2 ± 16.0	70.0 ± 10.2
Wang and Xi (2017) [32]	31.3 ± 4.5	31.5 ± 4.3	40/40	Total abdominal hysterectomy	—	138 ± 24	132 ± 30
Xi and Wang (2015) [33]	33 ± 3	33 ± 3	37/38	Total abdominal hysterectomy	Epidural anesthesia	103.2 ± 30.6	102.6 ± 31.8
Yang et al. (2012) [34]	32 ± 9	30 ± 10	30/30	Laparoscopic surgery	General anesthesia (I/II)	78 ± 23	80 ± 25
Huang et al. (2021) [35]	31~56		30/30	Laparoscopic surgery	General anesthesia (I/II)	—	—
Ye and Huang (2019) [36]	33 ± 9	35 ± 10	40/40	Laparoscopic surgery	General anesthesia (I/II)	97 ± 9	95 ± 10
Yu and Ning (2016) [37]	31 ± 4.4	30 ± 5.4	27/26	Laparoscopic surgery	General anesthesia (I/II)	78.1 ± 16.2	75.0 ± 13.7
Zhang et al. (2013) [38]	34.74 ± 5.64	36.81 ± 9.26	27/27	Laparoscopic surgery	General anesthesia (I/II)	—	—

30 min prior to surgery (SMD = −2.14, 95% CI: [−2.79, −1.48], $P < 0.00001$, I^2 = not applicable), whereas subjects receiving EA therapy after surgery in the EG showed no difference to the CG with respect to TBS (SMD = −0.62, 95% CI: [−1.41, 0.17], $P = 0.12$, $I^2 = 89\%$) (Figure 5). In addition, there was no significant difference in TBS between patients receiving EA and ginger partitioned moxibustion on umbilicus (SMD = −0.22, 95% CI: [−0.53, −0.10], $P = 0.18$, $I^2 = 0\%$) (Supplementary Figure 5).

(3) Time to First Defecation. In this study, two trials recorded TFD. Meta-analysis result revealed that, compared to the CG, TFD was significantly shorter in the EG (SMD = −1.23, 95% CI: [−1.59, −0.88], $P < 0.0001$, $I^2 = 0\%$) (Figure 6).

3.4.2. Secondary Outcomes

(1) Postoperative Nausea and Vomiting (PONV). The incidence of PONV at postoperative 6 h, 24 h, and 48 h was reported in eight [21–23, 27, 29–31, 35], ten [21–23, 27, 29–31, 35–37], and four studies [23, 27, 29, 31], respectively. Meta-analysis results suggested a lower incidence of PONV at postoperative 6 h (OR = 0.42, 95% CI: [0.27, 0.64], $P < 0.0001$, $I^2 = 0\%$), 24 h (OR = 0.46, 95% CI: [0.32, 0.68], $P < 0.0001$, $I^2 = 0\%$) in the EG than that in the CG, whereas no significant difference in ratio of PONV at postoperative 48 h (OR = 0.55, 95% CI: [0.20, 1.51], $P = 0.25$, $I^2 = 0\%$) was detected between the two groups (Figure 7). Subgroup analysis revealed that no difference in the ratio of PONV at postoperative 6 h was observed between the two groups when EA performed at 24 h prior to surgery (OR = 0.53, 95% CI: [0.22, 1.27], $P = 0.15$, $I^2 = 0\%$) or after surgery (OR = 0.48, 95% CI: [0.22, 1.06], $P = 0.07$, $I^2 = 0\%$), but its ratio was lower in the EG when EA was performed at 30 min prior to surgery in comparison to the CG (OR = 0.34, 95% CI: [0.19, 0.63], $P = 0.0006$, $I^2 = 0\%$). Regarding the ratio of PONV at postoperative 24 h, it was lower in the EG than that in the CG whenever EA was conducted at 24 h (OR = 0.25, 95% CI: [0.09, 0.67], $P = 0.006$, $I^2 = 0\%$) or

Table 2: Interventions, outcomes, and study design on the included studies.

First author (year)	Intervention	Intervention parameters	Intervention dose	Main outcome	Study design
Li et al. (2017) [21]	EG : EA + routine treatment; CG: routine treatment.	Acupoints: bilateral Neiguan (PC6) and Zusanli (ST36), mode: dense-disperse wave; frequency: 20/100 Hz; intensity (mA) : strong but comfortable.	24 hours prior to the surgery, once for 30 min.	TFF, PONV	RCT
Praveena et al. (2016) [22]	EG : EA + routine treatment, CG: routine treatment.	7548 acupoints: bilateral Hegu (LI4) and Neiguan (PC6), mode: continuous wave, frequency: 2 Hz; intensity (mA): Level 1.	Before the start of surgery until the end of surgery.	PONV	RCT
Bai et al. (2012) [23]	EG : EA + Tropisetron (5 mg, intravenous injection after anesthesia induction) + routine treatment; CG : Tropisetron (5 mg, intravenous injection after anesthesia induction) + routine treatment.	Acupoints: bilateral Neiguan (PC6) and Zusanli (ST36), Shangjuxu (ST37), Zhongwan (RN12), Tianshu (ST25), mode: unreported; frequency: 2 Hz; intensity (mA): unclear.	At hour 5, 23, and 27 after surgery, 30 min/once.	PONV, TFF, MTL, GAS	RCT
Chen et al. (2014) [24]	EG : EA + routine treatment; CG: routine treatment	Acupoints: bilateral Liangqiu (ST34) and Zusanli (ST36), mode: continuous wave; frequency: 2 Hz; intensity (mA): maximum tolerable.	30 minutes prior to the surgery until the end of surgery.	PHi, $PgCO_2$	RCT
Jin and Jing (2015) [25]	EG : EA + routine treatment; CG: routine treatment	Acupoints: bilateral Zusanli (ST36); mode: unreported; frequency and intensity (mA): unclear.	At hour 5 after surgery, twice a day, until time to first flatus.	TBS, TFF, TFD	RCT
Li et al. (2019) [26]	EG : EA + routine treatment; CG: routine treatment.	Acupoints: bilateral Neiguan (PC6), Xuehai (SP10), Hegu (LI4) and Zusanli (ST36), mode: dense-disperse wave; frequency: 2/10/50/100 Hz; intensity (mA): unclear.	24 hours prior to the surgery, once for 30 min.	TFF, PONV,	RCT
Lu et al. (2010) [27]	EG : EA + Tropisetron (5 mg, intravenous injection prior to the end of surgery) + routine treatment; CG : Tropisetron (5 mg, intravenous injection prior to the end of surgery) + routine treatment.	Acupoints: bilateral Neiguan (PC6) and Zusanli (ST36), Hegu (LI4), Sanyinjiao (SP6), Taichong (LR3), mode: dense-disperse wave; frequency: 2/10 Hz; intensity (mA): maximum tolerable.	At hours 1, 5, and 23 after surgery, 30 min/once.	PONV, number of TFF more than 72 h	RCT
Toronui (2020) [28]	EG : EA + routine treatment; CG: routine treatment.	Acupoints: bilateral Zusanli (ST36), frequency: 2/10 Hz.	Prior to the surgery, once for 15 min.	TBS, TFF, TFD, PONV	RCT
Wang et al. (2018) [29]	EG : EA + Tropisetron (5 mg, intravenous injection prior to the end of surgery) +routine treatment; CG : Tropisetron (5 mg, intravenous injection prior to the end of surgery) + routine treatment.	Acupoints: bilateral Neiguan (PC6) and Zusanli (ST36), mode: dense-disperse wave; frequency: 2 Hz; intensity (mA): maximum tolerable.	30 minutes prior to the surgery, once for 30 min.	PONV, TFF	RCT
Wang et al. (2018) [30]	EG : EA + Tropisetron (5 mg, intravenous injection prior to the end of surgery) + routine treatment; CG : Tropisetron (6 mg, intravenous injection prior to the end of surgery) + routine treatment.	Acupoints: bilateral Neiguan (PC6) and Zusanli (ST36), mode: dense-disperse wave; frequency: 2 Hz; intensity (mA): maximum tolerable.	24 hours prior to the surgery, once for 30 min.	TFF, PONV	RCT
Wang et al. (2011) [31]	EG : EA + routine treatment; CG: routine treatment.	Acupoints: bilateral Zusanli (ST36), Neiguan (PC6), mode: continuous wave; frequency: 2 Hz; intensity (mA): maximum tolerable.	Prior to the surgery, once for 15 min.	PONV, MTL, VIP, number of TFF more than 72 h	RCT

Table 2: Continued.

First author (year)	Intervention	Intervention parameters	Intervention dose	Main outcome	Study design
Wang and Xi (2017) [32]	EG : EA + routine treatment; CG : Ginger partitioned moxibustion on umbilicus + routine treatment.	Acupoints: bilateral Liangmen (ST21) and Zusanli (ST36), Shangjuxu (ST37), Zhongwan (RN12), Tianshu (ST25), mode: continuous wave.	After surgery, once for 30 min, once a day, for 3 d.	TBS, TFF	RCT
Xi and Wang (2015) [33]	EG : EA + routine treatment; CG1 : Ginger partitioned moxibustion on umbilicus + routine treatment	Acupoints: bilateral Liangmen (ST21) and Zusanli (ST36), Shangjuxu (ST37), Zhongwan (RN12), Tianshu (ST25), mode: continuous wave; intensity (mA): maximum tolerable.	After surgery, once for 30 min, once a day, for 3 d.	TBS, TFF, MTL, GAS,	
VIP	RCT				
Yang et al. (2012) [34]	EG : EA + routine treatment; CG: routine treatment.	Acupoints: bilateral Sanyinjiao (SP6) and Zusanli (ST36), mode: dense-disperse wave; frequency: 2/100 Hz; intensity (mA): maximum tolerable.	30 minutes prior to the surgery until the end of surgery.	TFF	RCT
Huang et al. (2021) [35]	EG : EA + routine treatment; CG: routine treatment.	Acupoints: bilateral Neiguan (PC6), mode: dense-disperse wave; frequency: 3/20 Hz; intensity (mA): unclear.	Prior to the surgery, once for 20 min.	PONV, MTL, GAS	RCT
Ye and Huang (2019) [36]	EG : EA + routine treatment; CG: routine treatment.	Acupoints: bilateral Neiguan (PC6), mode: unreported, frequency: 3/21 Hz; intensity (mA): comfortable.	Prior to the surgery, once for 20 min.	PONV	RCT
Yu and Ning (2016) [37]	EG : EA + Tropisetron (2 mg, intravenous injection prior to the end of surgery) + routine treatment; CG1 : Tropisetron (2 mg, intravenous injection prior to the end of surgery) + routine treatment.	Acupoints: bilateral Neiguan (PC6), and Hegu (LI4), mode: dense-disperse wave; frequency: 20/100 Hz; intensity (mA): 10 mA.	Prior to the surgery, once for 30 min.	PONV	RCT
Zhang et al. (2013) [38]	EG : EA + routine treatment; CG: routine treatment.	Acupoints: bilateral Liangqiu (ST34) and Zusanli (ST36), mode: continuous wave; frequency: 2 Hz; intensity (mA): maximum tolerable.	30 minutes prior to the surgery until the end of surgery.	pHi, $PgCO_2$	RCT

EG: electroacupuncture group; CG: control group; EA: electroacupuncture; TFF: time to first flatus; TFD: time first to defecation; TFBS: time to first bowel sound; PONV: postoperative nausea and vomiting; MTL: motilin; GAS: gastrin; pHi : PH value of gastric mucosa; $PgCO_2$: gastric mucosal partial pressure of carbon dioxide; VIP: vasoactive intestinal peptide; and RCT: randomized controlled trials.

30 min prior to surgery (OR = 0.46, 95% CI: [0.28, 0.76], $P = 0.03$, $I^2 = 0\%$), or after surgery (OR = 0.03, 95% CI: [0.13, 0.67], $P = 0.003$, $I^2 = 0\%$). However, there was no significant difference in the ratio of PONV at postoperative 48 h between the EG and CG regardless of the preoperative (OR = 0.64, 95% CI: [0.10, 4.15], $P = 0.64$, I^2 = not applicable) or postoperative electroacupuncture treatment (OR = 0.52, 95% CI: [0.16, 1.71], $P = 0.28$, $I^2 = 0\%$).

(2) Motilin (MTL). Two studies [23, 35] investigated the effects of EA on MTL at postoperative 6 h, and four studies [23, 31, 33, 35] evaluated the effect at postoperative 24 h. Meta-analysis results suggested that a significant effect in favor of EA on level of MTL at postoperative 6 h (SMD = −0.93, 95% CI: [−1.36, −0.61], $P < 0.0001$, $I^2 = 21\%$), while no significant effect was observed at postoperative 24 h (SMD = −0.43, 95% CI: [−0.89, 0.02], $P = 0.06$, $I^2 = 69\%$) in the EG when compared to the CG (Figure 8).

(3) Gastrin (GAS). Two studies [23, 35] compared patients receiving EA to those in the control condition in terms of GAS at postoperative 6 h, and three studies [23, 33, 35] estimated the effect of EA on GAS at postoperative 24 h. Meta-analysis results revealed that no significant effect on GAS was observed at neither postoperative 6 h (SMD = 0.20, 95% CI: [−1.62, 2.01], $P = 0.83$, $I^2 = 96\%$) nor 24 h (SMD = 0.63, 95% CI: [−0.57, 1.84], $P = 0.30$, $I^2 = 94\%$) (Figure 9).

(4) Vasoactive Intestinal Peptide (VIP). Meta-analysis of two studies [31, 33] demonstrated a small, but non-significant, overall effect concerning VIP (SMD = 0.12, 95% CI: [−0.26, 0.50], $P = 0.53$, $I^2 = 20\%$) (Figure 10).

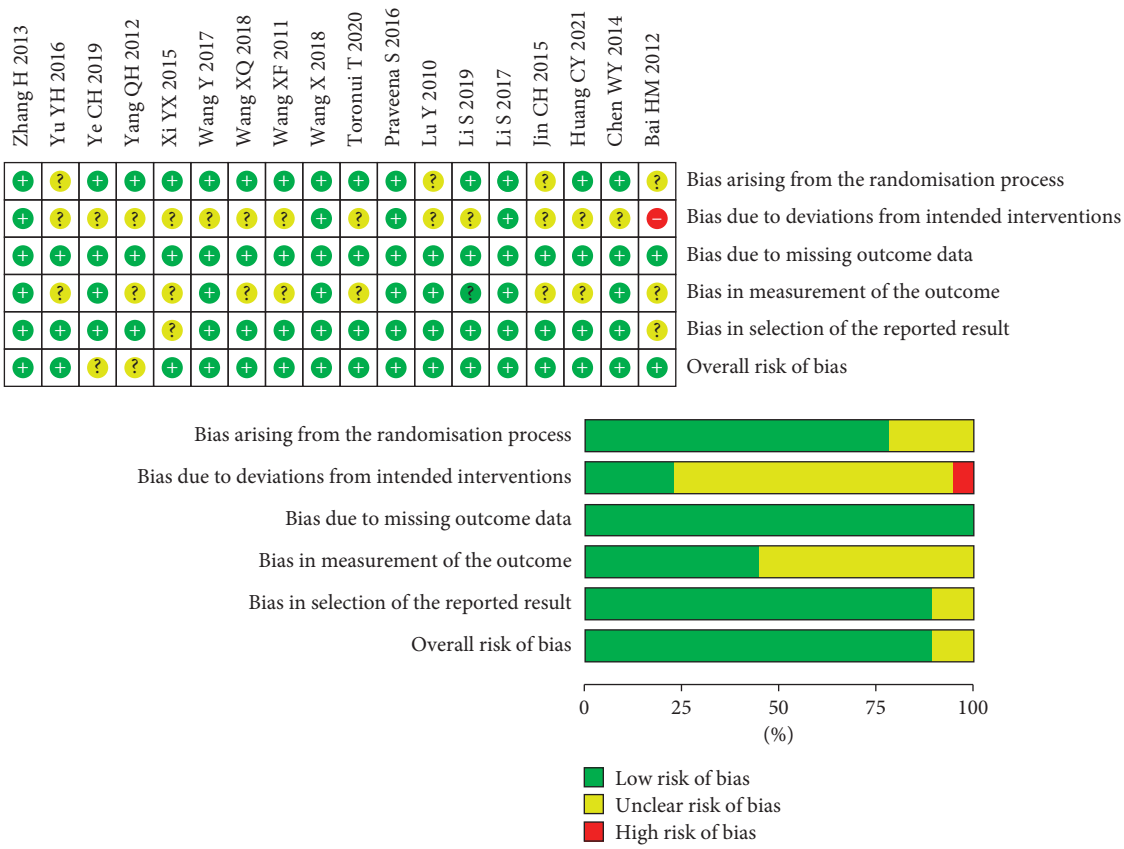

Figure 2: Risk of bias graph.

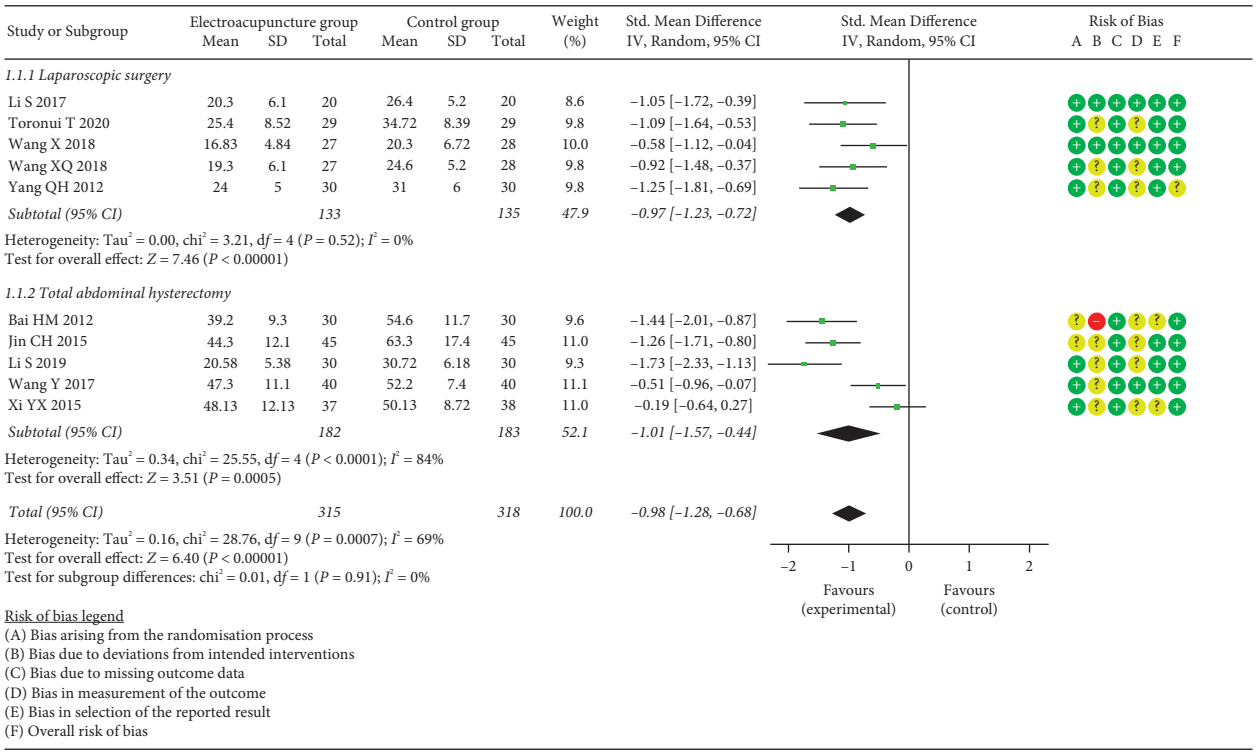

Figure 3: Meta-analysis and forest plot for time to first flatus.

Study or Subgroup	Electroacupuncture group Events	Total	Control group Events	Total	Weight (%)	Odds Ratio M-H, Random, 95% CI
Lu Y 2010	0	29	2	30	48.8	0.19 [0.01, 4.20]
Wang XF 2011	0	30	3	30	51.2	0.13 [0.01, 2.61]
Total (95% CI)		*59*		*60*	*100.0*	*0.16 [0.02, 1.35]*
Total events	0		5			

Heterogeneity: Tau^2 = 0.00, chi^2 = 0.03, df = 1 (P = 0.85); I^2 = 0%
Test for overall effect: Z = 1.69 (P = 0.09)

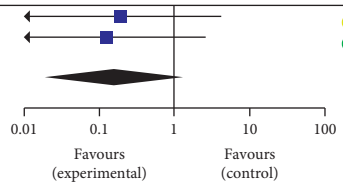

Risk of bias legend
(A) Bias arising from the randomisation process
(B) Bias due to deviations from intended interventions
(C) Bias due to missing outcome data
(D) Bias in measurement of the outcome
(E) Bias in selection of the reported result
(F) Overall risk of bias

Figure 4: Meta-analysis and forest plot for ratio of time to first flatus >72 h.

Study or Subgroup	Electroacupuncture group Mean	SD	Total	Control group Mean	SD	Total	Weight (%)	Std. Mean Difference IV, Random, 95% CI
1.4.1 30 min prior to surgery								
Toronui T 2020	10.01	3.24	29	18.34	4.37	29	23.6	−2.14 [−2.79, −1.48]
Subtotal (95% CI)	*0*		*29*			*29*	*23.6*	*−2.14 [−2.79, −1.48]*
Heterogeneity: Not applicable								
Test for overall effect: Z = 6.41 (P < 0.00001)								
1.4.2 after surgery								
Jin CH 2015	36.5	10.3	45	55.5	15.3	45	25.3	−1.44 [−1.91, −0.98]
Wang Y 2017	28.7	3.5	40	29.6	4.2	40	25.6	−0.23 [−0.67, 0.21]
Xi YX 2015	29.15	4.32	37	30.13	5.38	38	25.4	−0.20 [−0.65, 0.26]
Subtotal (95% CI)			*122*			*123*	*76.4*	*−0.62 [−1.41, 0.17]*
Heterogeneity: Tau^2 = 0.44, chi^2 = 18.32, df = 2 (P = 0.0001); I^2 = 89%								
Test for overall effect: Z = 1.54 (P = 0.12)								
Total (95% CI)			*151*			*152*	*100.0*	*−0.98 [−1.84, −0.12]*
Heterogeneity: Tau^2 = 0.70, chi^2 = 36.58, df = 3 (P < 0.00001); I^2 = 92%								
Test for overall effect: Z = 2.24 (P = 0.03)								
Test for subgroup differences: chi^2 = 8.36, df = 1 (P = 0.004); I^2 = 88.0%								

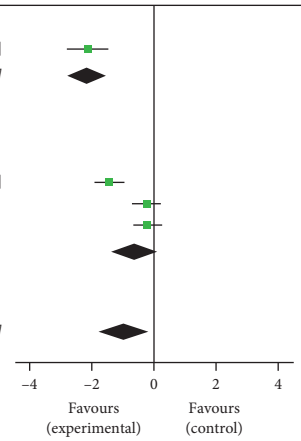

Risk of bias legend
(A) Bias arising from the randomisation process
(B) Bias due to deviations from intended interventions
(C) Bias due to missing outcome data
(D) Bias in measurement of the outcome
(E) Bias in selection of the reported result
(F) Overall risk of bias

Figure 5: Meta-analysis and forest plot for time to bowel sounds recovery.

Study or Subgroup	Electroacupuncture group Mean	SD	Total	Control group Mean	SD	Total	Weight (%)	Std. Mean Difference IV, Random, 95% CI
Jin CH 2015	50.4	11.8	45	67.3	14.4	45	60.3	−1.27 [−1.73, −0.82]
Toronui T 2020	35.98	6.88	29	44.38	7.21	29	39.7	−1.18 [−1.74, −0.62]
Total (95% CI)			*74*			*74*	*100.0*	*−1.23 [−1.59, −0.88]*

Heterogeneity: Tau^2 = 0.00, chi^2 = 0.07, df = 1 (P = 0.79); I^2 = 0%
Test for overall effect: Z = 6.85 (P < 0.00001)

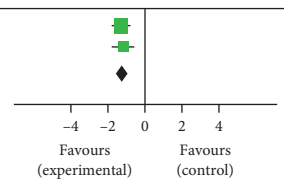

Risk of bias legend
(A) Bias arising from the randomisation process
(B) Bias due to deviations from intended interventions
(C) Bias due to missing outcome data
(D) Bias in measurement of the outcome
(E) Bias in selection of the reported result
(F) Overall risk of bias

Figure 6: Meta-analysis and forest plot for time to first defecation.

(5) pH Value of Gastric Mucosa (pHi). Meta-analysis of two studies [24, 38] indicated that no significant difference in pHi was determined between the two groups neither at pneumoperitoneum for 30 min (SMD = 0.70, 95% CI: [−0.47, 1.88], P = 0.24, I^2 = 88%) nor at 30 min after the end of pneumoperitoneum (SMD = 1.15, 95% CI: [−0.95, 3.24], P = 0.28, I^2 = 96%) (Figure 11).

(6) Gastric Mucosal Partial Pressure of Carbon Dioxide ($PgCO_2$). Two studies examined the effect of EA on $PgCO_2$.

Study or Subgroup	Electroacupuncture group Events	Total	Control group Events	Total	Weight (%)	Odds Ratio M-H, Random, 95% CI
1.5.1 Postoperative 6 h						
Bai HM 2012	13	30	18	30	16.9	0.51 [0.18, 1.42]
Huang CY 2021	4	30	11	30	10.7	0.27 [0.07, 0.96]
Li S 2017	4	20	8	20	8.9	0.38 [0.09, 1.54]
Lu Y 2010	20	29	25	30	11.5	0.44 [0.13, 1.54]
Praveena S 2016	5	32	15	32	12.8	0.21 [0.06, 0.68]
Wang X 2018	4	27	5	28	8.6	0.80 [0.19, 3.36]
Wang XF 2011	12	30	19	30	16.4	0.39 [0.14, 1.09]
Wang XQ 2018	8	27	11	28	14.2	0.65 [0.21, 2.00]
Subtotal (95% CI)		*225*		*228*	*100.0*	*0.42 [0.27, 0.64]*
Total events	70		112			
Heterogeneity: Tau^2 = 0.00, chi^2 = 3.37, df = 7 (P = 0.85); I^2 = 0%						
Test for overall effect: Z = 4.05 (P < 0.0001)						
1.5.2 Postoperative 24 h						
Bai HM 2012	5	30	13	30	10.3	0.26 [0.08, 0.87]
Huang CY 2021	5	30	6	30	8.6	0.80 [0.22, 2.97]
Li S 2019	10	30	21	30	12.5	0.21 [0.07, 0.64]
Lu Y 2010	8	29	16	30	12.6	0.33 [0.11, 0.99]
Praveena S 2016	4	32	6	32	7.9	0.62 [0.16, 2.44]
Wang X 2018	3	27	4	28	5.8	0.75 [0.15, 3.72]
Wang XF 2011	6	30	10	30	10.8	0.50 [0.15, 1.62]
Wang XQ 2018	1	27	2	28	2.4	0.50 [0.04, 5.86]
Ye CH 2019	10	40	19	40	16.5	0.37 [0.14, 0.95]
Yu YH 2016	14	27	12	26	12.7	1.26 [0.43, 3.70]
Subtotal (95% CI)		*302*		*304*	*100.0*	*0.46 [0.32, 0.68]*
Total events	66		109			
Heterogeneity: Tau^2 = 0.00, chi^2 = 7.86, df = 9 (P = 0.55); I^2 = 0%						
Test for overall effect: Z = 3.92 (P < 0.0001)						
1.5.3 Postoperative 48 h						
Bai HM 2012	3	30	7	30	46.9	0.37 [0.08, 1.58]
Lu Y 2010	2	29	2	30	24.3	1.04 [0.14, 7.90]
Wang X 2018	0	27	0	28		Not estimable
Wang XF 2011	2	30	3	30	28.8	0.64 [0.10, 4.15]
Subtotal (95% CI)		*116*		*118*	*100.0*	*0.55 [0.20, 1.51]*
Total events	7		12			
Heterogeneity: Tau^2 = 0.00, chi^2 = 0.70, df = 2 (P = 0.70); I^2 = 0%						
Test for overall effect: Z = 1.16 (P = 0.25)						
Test for subgroup differences: chi^2 = 0.31, df = 2 (P = 0.86); I^2 = 0%						

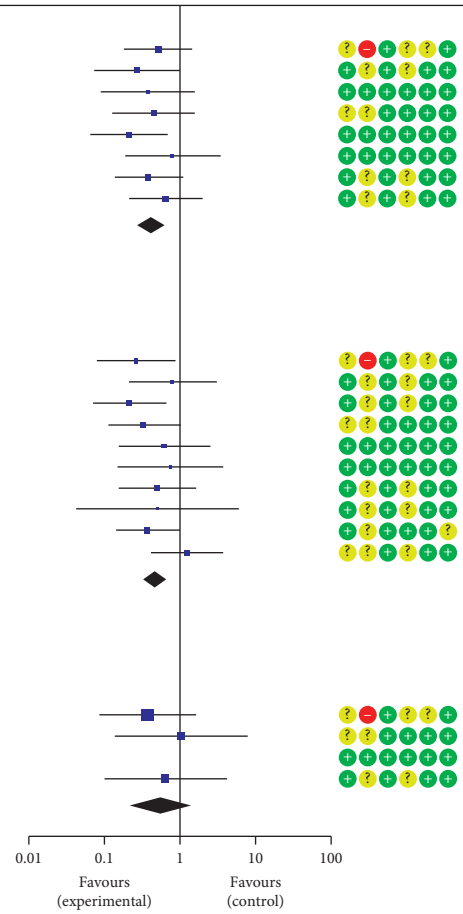

Risk of bias legend
(A) Bias arising from the randomisation process
(B) Bias due to deviations from intended interventions
(C) Bias due to missing outcome data
(D) Bias in measurement of the outcome
(E) Bias in selection of the reported result
(F) Overall risk of bias

Figure 7: Meta-analysis and forest plot for ratio of PONV.

Study or subgroup	Electroacupuncture group Mean	SD	Total	Control group Mean	SD	Total	Weight (%)	Std. Mean Difference IV, Random, 95% CI
1.6.1 Postoperative 6 h								
Bai HM 2012	339.99	19.18	30	373.71	35.69	30	48.1	−1.16 [−1.71, −0.61]
Huang CY 2021	303	32	30	330	41	30	51.9	−0.72 [−1.25, −0.20]
Subtotal (95% CI)			*60*			*60*	*100.0*	*−0.93 [−1.36, −0.51]*
Heterogeneity: Tau^2 = 0.02, chi^2 = 1.27, df = 1 (P = 0.26); I^2 = 21%								
Test for overall effect: Z = 4.28 (P < 0.0001)								
1.6.2 Postoperative 24 h								
Bai HM 2012	308.64	20.37	30	341.73	36.32	30	23.8	−1.11 [−1.66, −0.56]
Huang CY 2021	269	13	30	272	15	30	24.9	−0.21 [−0.72, 0.30]
Wang XF 2011	157	34	30	175	44	30	24.7	−0.45 [−0.96, 0.06]
Xi YX 2015	183.5	35.2	37	184.1	39.5	38	26.6	−0.02 [−0.47, 0.44]
Subtotal (95% CI)			*127*			*128*	*100.0*	*−0.43 [−0.89, 0.02]*
Heterogeneity: Tau^2 = 0.15, chi^2 = 9.82, df = 3 (P = 0.02); I^2 = 69%								
Test for overall effect: Z = 1.86 (P = 0.06)								
Test for subgroup differences: chi^2 = 2.49, df = 1 (P = 0.11); I^2 = 59.8%								

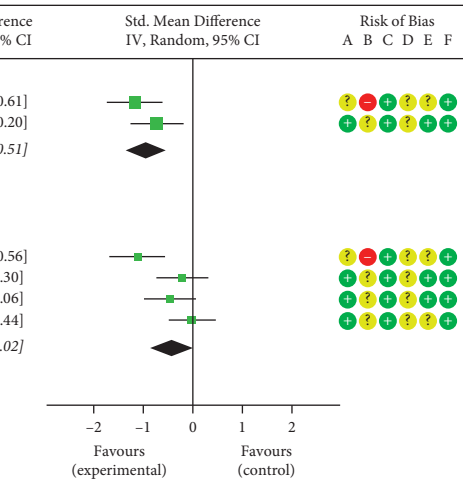

Risk of bias legend
(A) Bias arising from the randomisation process
(B) Bias due to deviations from intended interventions
(C) Bias due to missing outcome data
(D) Bias in measurement of the outcome
(E) Bias in selection of the reported result
(F) Overall risk of bias

Figure 8: Meta-analysis and forest plot for motilin.

Study or subgroup	Electroacupuncture group Mean	SD	Total	Control group Mean	SD	Total	Weight (%)	Std. Mean Difference IV, Random, 95% CI
1.7.1 Postoperative 6 h								
Bai HM 2012	174.97	25.01	30	148.4	21.46	30	49.9	1.13 [0.58, 1.67]
Huang CY 2021	89	13	30	99	14	30	50.1	−0.73 [−1.25, −0.21]
Subtotal (95% CI)			*60*			*60*	*100.0*	*0.20 [−1.62, 2.01]*
Heterogeneity: Tau^2 = 1.65, chi^2 = 23.06, df = 1 (P < 0.00001); I^2 = 96%								
Test for overall effect: Z = 0.21 (P = 0.83)								
1.7.2 Postoperative 24 h								
Bai HM 2012	205.21	15.57	30	167.07	21.34	30	32.5	2.02 [1.39, 2.64]
Huang CY 2021	46.3	12.7	37	47.1	11.6	38	33.9	−0.07 [−0.52, 0.39]
Xi YX 2015	76	6	30	76	6	30	33.5	0.00 [−0.51, 0.51]
Subtotal (95% CI)			*97*			*98*	*100.0*	*0.63 [−0.57, 1.84]*
Heterogeneity: Tau^2 = 1.06, chi^2 = 31.79, df = 2 (P < 0.00001); I^2 = 94%								
Test for overall effect: Z = 1.03 (P = 0.30)								
Test for subgroup differences: chi^2 = 0.15, df = 1 (P = 0.69); I^2 = 0%								

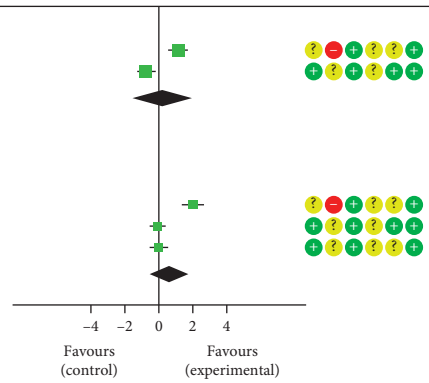

Risk of bias legend
(A) Bias arising from the randomisation process
(B) Bias due to deviations from intended interventions
(C) Bias due to missing outcome data
(D) Bias in measurement of the outcome
(E) Bias in selection of the reported result
(F) Overall risk of bias

Figure 9: Meta-analysis and forest plot for gastrin.

Study or subgroup	Electroacupuncture group Mean	SD	Total	Control group Mean	SD	Total	Weight (%)	Std. Mean Difference IV, Random, 95% CI
Wang XF 2011	1.68	0.4	30	1.54	0.43	30	45.3	0.33 [−0.18, 0.84]
Xi YX 2015	28.5	10.1	37	29.1	11.3	38	54.7	−0.06 [−0.51, 0.40]
Total (95% CI)			*67*			*68*	*100.0*	*0.12 [−0.26, 0.50]*
Heterogeneity: Tau^2 = 0.01, chi^2 = 1.24, df = 1 (P = 0.26); I^2 = 20%								
Test for overall effect: Z = 0.62 (P = 0.53)								

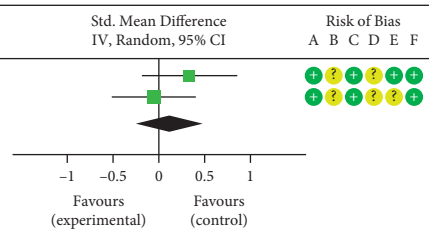

Risk of bias legend
(A) Bias arising from the randomisation process
(B) Bias due to deviations from intended interventions
(C) Bias due to missing outcome data
(D) Bias in measurement of the outcome
(E) Bias in selection of the reported result
(F) Overall risk of bias

Figure 10: Meta-analysis and forest plot for VIP.

Study or subgroup	Electroacupuncture group Mean	SD	Total	Control group Mean	SD	Total	Weight (%)	Std. Mean Difference IV, Random, 95% CI
1.9.1 pneumoperitoneum for 30 min								
Chen WY 2014	7.33	0.07	27	7.23	0.08	27	49.4	1.31 [0.72, 1.90]
Zhang H 2013	7.26	0.11	27	7.2	0.74	27	50.6	0.11 [−0.42, 0.65]
Subtotal (95% CI)			*54*			*54*	*100.0*	*0.70 [−0.47, 1.88]*
Heterogeneity: Tau^2 = 0.64, chi^2 = 8.69, df = 1 (P = 0.003); I^2 = 88%								
Test for overall effect: Z = 1.17 (P = 0.24)								
1.9.2 30 min after the end of pneumoperitoneum								
Chen WY 2014	7.37	0.07	27	7.2	0.08	27	49.5	2.23 [1.54, 2.92]
Zhang H 2013	7.32	0.87	27	7.24	0.87	27	50.5	0.09 [−0.44, 0.62]
Subtotal (95% CI)			*54*			*54*	*100.0*	*1.15 [−0.95, 3.24]*
Heterogeneity: Tau^2 = 2.19, chi^2 = 23.11, df = 1 (P < 0.00001); I^2 = 96%								
Test for overall effect: Z = 1.07 (P = 0.28)								
Test for subgroup differences: chi^2 = 0.13, df = 1 (P = 0.72); I^2 = 0%								

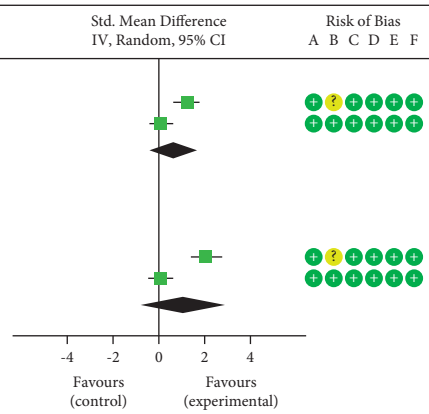

Risk of bias legend
(A) Bias arising from the randomisation process
(B) Bias due to deviations from intended interventions
(C) Bias due to missing outcome data
(D) Bias in measurement of the outcome
(E) Bias in selection of the reported result
(F) Overall risk of bias

Figure 11: Meta-analysis and forest plot for pHi.

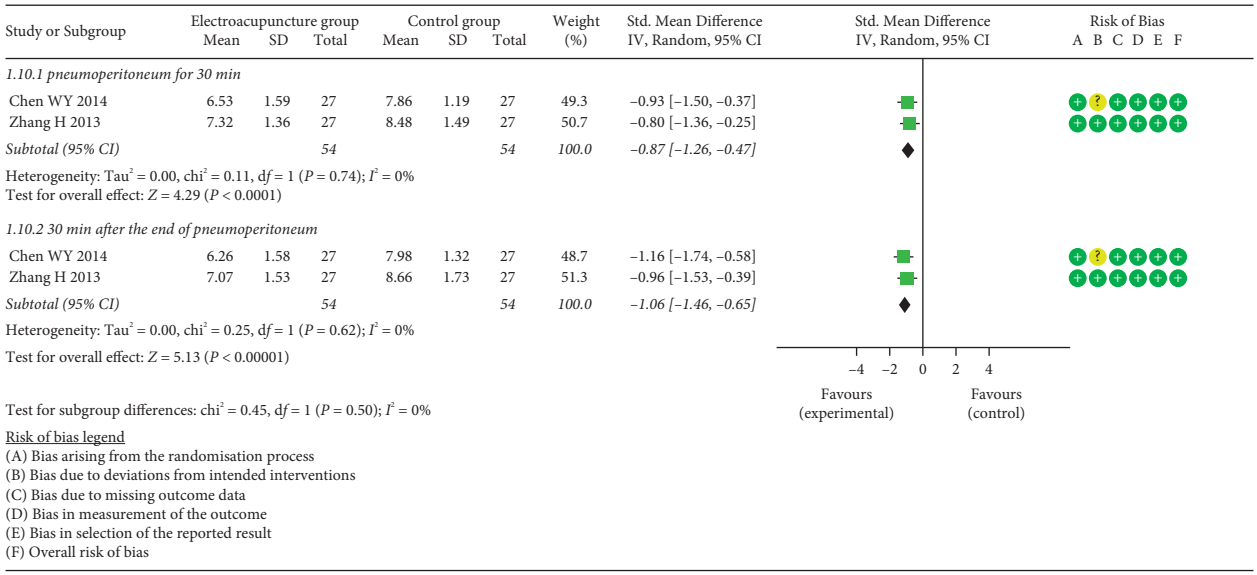

Figure 12: Meta-analysis and forest plot for $PgCO_2$.

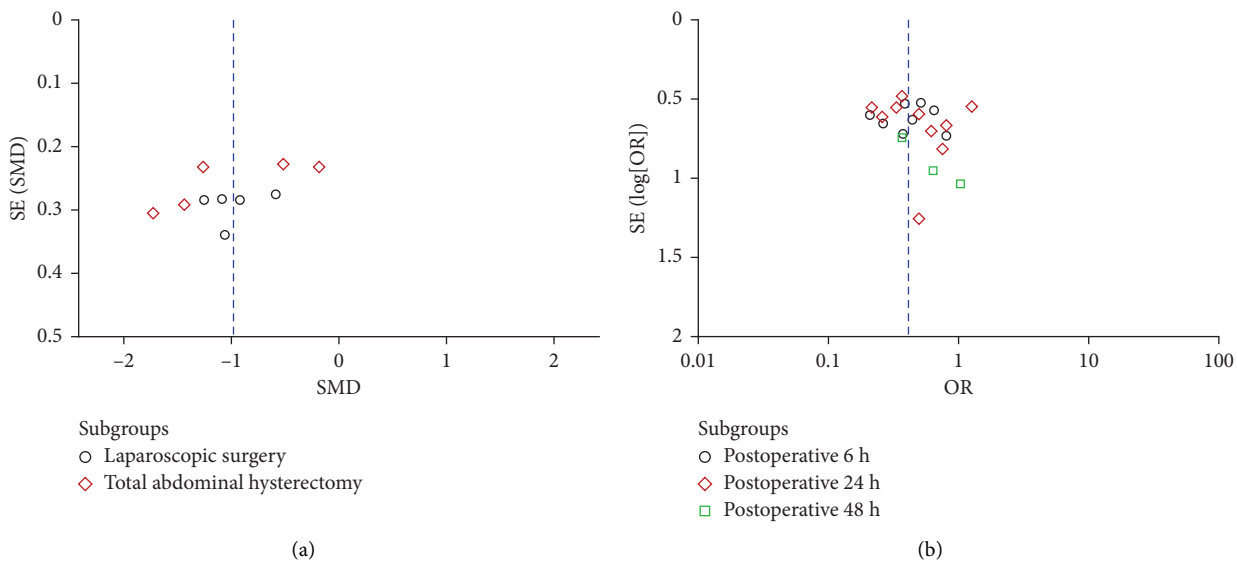

Figure 13: Publication bias assessed by funnel plots for TFF (a) and PONV (b).

Meta-analysis results revealed that a large significant effect on decreasing $PgCO_2$ was found in the EG VS CG, both at pneumoperitoneum for 30 min (SMD = −0.87, 95% CI: [−1.26, −0.47], $P < 0.0001$, $I^2 = 0\%$) and 30 min after the end of pneumoperitoneum (SMD = −1.06, 95% CI: [−1.46, −0.65], $P < 0.00001$, $I^2 = 0\%$) (Figure 12).

(7) Hospital Stay. In the study, hospital stay was recorded in only one study [30], which reported that electroacupuncture applied at 24 h prior to surgery showed no significant effect on the duration of hospital stay (EG vs. CG: (3.6 ± 0.4) *d* vs. (3.9 ± 0.2) *d*, $P = 0.492$).

(8) Adverse Event. One participant in one study [21] reported pain at the needling sites and bruising, while the side effects were alleviated spontaneously without any medical assistance. In addition, it was reported in two studies [30, 38] that three participants withdrew because they were not intolerant to EA.

3.5. Sensitivity Analysis. In this study, we conducted the sensitivity analysis to evaluate the robustness of primary outcome indicators with high heterogeneity by removing studies from the analysis individually. After sensitivity analysis for TFF, no substantial change about overall heterogeneities and results was detected (Supplementary Table 2). Meanwhile, we performed sensitivity analysis for TBS, and the results were listed in Supplementary Table 3. The overall effect indicated no statistically significant difference

when the study reported by Jin and Jing [25] (SMD = −0.83, 95% CI: [−1.09, 0.24], $P = 0.13$, $I^2 = 93\%$) or Toronui [28] (SMD = −0.62, 95% CI: [−1.41, 0.17], $P = 0.12$, $I^2 = 89\%$) was eliminated. However, the results of subgroup analysis by intervention time points for the remaining studies [28, 32, 33] showed no substantial change. It was found that TBS was significantly shorter in the EG than that in the CG when EA was received prior to surgery than that in the CG (SMD = −2.14, 95% CI: [−2.79, −1.48], $P < 0.00001$, I^2 = not applicable), whereas no significant difference was detected with no heterogeneity when EA was applied after surgery (SMD = −0.22, 95% CI: [−0.53, 0.10], $P = 0.18$, $I^2 = 0\%$).

3.6. Publication Bias. In the present study, Begg's test and Egger's test were employed to examine publication bias for the indices recorded more than 2 included trails. It was suggested that there should be no publication bias except for MTL at postoperative 24 h ($P = 0.042$) (Supplementary Table 4). Moreover, visual inspection of funnel plots seemed to be relatively symmetrical for TFF and PONV (Figure 13), indicating no evidence for publication bias.

3.7. Evidence Quality Assessment According to GRADE. Based on GRADE guidelines, we evaluated the quality of evidence from five aspects, including risk of bias, inconsistency, indirectness, imprecision, and publication bias. During the treatment period, EA therapists directly contacted to participants, which led to the high risk of performance bias, and consequently lowered the evidence quality. In this study, there was low evidence in TFF, TFD and PONV, and very low evidence in the remaining. Details were recorded in Supplementary Table 5.

4. Discussion

In spite of continuous improvement for surgical approach and technique, postoperative gastrointestinal dysfunction still commonly occurred after gynecological surgery. To resolve this clinical concern, EA has been proposed to promote gastrointestinal function recovery, while relevant evidence is sparse. To the best of our knowledge, this is first systematical review and meta-analysis regarding the efficacy and safety of EA on recovery of gastrointestinal function for patients receiving gynecological surgery.

We found that EA was able to shorten the time to first flatus, first defecation after gynecological surgery. These findings were in accordance with those reported by the previous meta-analyses [11–14] for other patient populations, but there were some new findings after subgroup analysis in the current study. Our findings suggested that EA was beneficial to reduce the time to first of bowel sounds recovery when EA was used at 30 min prior to surgery. However, no significant effect on TBS was observed when patients undergoing gynecological surgery received EA treatment after surgery. Additionally, the evidence in favor of EA for decreasing the ratio of PONV was observed only at postoperative 6 h and 24 h, which echo the results reported by Lee et al. [39], while the benefits were unobvious at postoperative 48 h. Similarly, the effect of EA on MTL was detected only within postoperative 6 h. Thus, our findings showed that the benefits of EA for PONV and MTL concentrate within 24 h after surgery, and even earlier. MTL stimulated gastrointestinal motility and accelerated gastric emptying, which could induce or aggravate nausea and vomiting [40, 41]. Thus, it could be the reason that EA decreased MTL level and consequently resulted in lowering the ratio of PONV at with postoperative 24 h. After subgroup analysis for PONV by intervention points, we found that EA presented a largest effect in lowering the ratio of PONV when it was applied at 30 min prior to surgery, whereas no or very small effect was found when patients were treated with EA after gynecological surgery. It might be the reason that factors contributing to postoperative gastrointestinal dysfunction mainly generated during intraoperative period; it should be more proper to applied EA before the start of surgery until the end of surgery, while the effectiveness of EA would be weakened when used too early, and postoperative application seems to be late.

$PgCO_2$ is a sensitive indicator reflecting the changes of blood oxygen in gastric mucosa [42]. It was proved that pHi was closely related with intestinal oxygen consumption, and decreased gastric pHi level prognosticated morbidity and mortality [43]. The results of this meta-analysis revealed that EA deceased the $PgCO_2$ both at 30 min after the start of pneumoperitoneum and 30 min after the end of pneumoperitoneum, whereas it was ineffective for mediation of pHi after surgery. Additionally, GAS was the hormone primarily responsible for gastric acid secretion [44], and VIP was a gut peptide hormone regulating gut motility [45]; hence, they were associated with postoperative gastrointestinal function [46]. However, EA showed no significant effect on GAS and VIP after gynecological surgery. Therefore, EA accelerated the recovery of postoperative gastrointestinal function through other pathways, not depending on the mediation of GAS or VIP.

Several potential limitations should be considered in the present review had. Firstly, the EA parameters including acupoints, and times and frequency of electroacupuncture were selected without a consolidated standard in the included studies, which could be a potential source of clinical heterogeneity; secondly, blind methods of the included studies were rarely provided in detail; thirdly, as was reported in the previous basic experimental studies, EA mediated of the autonomic nervous system, improved dysmotility and local inflammation, and consequently ameliorated POI to restore gastrointestinal function [47], and the therapeutic effects was different when using lower limb and abdomen acupoints [48]. However, few clinical trials focus on examining the different effect of EA by using different acupoints.

Given the limitations of this work, large-scale RCTs with more rigorous and robust methods are still needed in future studies. Most importantly, the majority of the studies were not blind to participants and acupuncturists; sham-controlled studies should be performed to avoid performance bias. Hence, more studies should be conducted strictly following standard reporting guidelines such as CONSORT

[49]. Furthermore, more RCTs in the future should investigate the therapeutic effects of EA using different acupoints in order to identify the definitely effective acupoints.

5. Conclusion

In this analysis, we systematically reviewed and quantified the effect of EA on gastrointestinal function after gynecological surgery. Overall, EA was an effective and safe treatment for promoting recovery of postoperative gastrointestinal function, such as shortening TFF and TFD, TBS, regulating MTL, and decreasing the ratio of PONV within postoperative 24h, for patients receiving gynecological surgery through abdominal and laparoscopic approaches, while the effects on MTL and PONV varied with different intervention points, and EA used at 30 min prior to surgery might be recommended. Moreover, EA could regulate $PgCO_2$ during anesthesia process, which was associated with the recovery of postoperative gastrointestinal function. However, EA exerted no significant impact on mediating GAS, VIP, and pHi. Thus, EA could be a promising strategy for the prevention and treatment of gastrointestinal dysfunction after gynecological surgery. Notably, evidence quality ranged from low to very low; large-scale and high-quality RCTs were needed.

Data Availability

The original data analyzed in this study are presented in the article; further inquiries should be directed to the corresponding authors.

Conflicts of Interest

The authors declare that they have no conflicts of interest regarding the publication of this paper.

Authors' Contributions

Y-G and X-G designed the study. X-G and YuZ-Z performed the literature searches and designed the data-extraction form. X-G and YuZ-Z selected the studies. X-G and YuZ-Z extracted the data. X-G and YT-K completed the statistical analyses. Y-G, YiZ-Z, and YT-K revised the manuscript.

Supplementary Materials

Supplementary file 1: Supplementary Figure 1. The search strategy in this review. *Supplementary Figure 2.* Forest plot of time to first flatus by subgroup analysis for anesthesia type. *Supplementary Figure 3.* Forest plot of time to first flatus by subgroup analysis for intervention points. *Supplementary Figure 4.* Forest plot of time to first flatus by subgroup analysis for comparators. *Supplementary Figure 5.* Forest plot of time to bowel sounds recovery by subgroup analysis for comparators. *Supplementary Table 1.* Sensitivity analysis for time to first flatus. *Supplementary Table 1.* PEDro scores of the included studies. *Supplementary Table 2.* Sensitivity analysis for time to first flatus. *Supplementary Table 3.* Evidence quality assessment according to GRADE. *Supplementary file 2.* PRISMA checklist. (*Supplementary Materials*)

References

[1] Q. Zhou, L. Cao, D. Wen, and Z. Chen, "The assessment on influencing factors for postoperative recovery of gastrointestinal function based on the gynecological abdominal surgery," in *Proceedings of the 2012 IEEE International Conference on Bioinformatics and Biomedicine Workshops*, pp. 472–476, Philadelphia, PA, USA, October 2012.

[2] Z. L. Li, B. C. Zhao, W. T. Deng et al., "Incidence and risk factors of postoperative ileus after hysterectomy for benign indications," *International Journal of Colorectal Disease*, vol. 35, no. 11, pp. 2105–2112, 2020.

[3] F. Oyama, M. Futagami, T. Shigeto et al., "Preventive effect of daikenchuto, a traditional Japanese herbal medicine, on onset of ileus after gynecological surgery for malignant tumors," *Asia-Pacific Journal of Clinical Oncology*, vol. 16, no. 4, pp. 254–258, 2020.

[4] J. Fanning and R. Hojat, "Safety and efficacy of immediate postoperative feeding and bowel stimulation to prevent ileus after major gynecologic surgical procedures," *Journal of the American Osteopathic Association*, vol. 111, no. 8, pp. 469–472, 2011.

[5] A. Nanthiphatthanachai and P. Insin, "Effect of chewing gum on gastrointestinal function recovery after surgery of gynecological cancer patients at rajavithi hospital: a randomized controlled trial," *Asian Pacific Journal of Cancer Prevention*, vol. 21, no. 3, pp. 761–770, 2020.

[6] D. Ruan, J. Li, J. Liu et al., "Acupoint massage can effectively promote the recovery of gastrointestinal function after gynecologic laparoscopy," *Journal of Investigative Surgery*, vol. 34, no. 1, pp. 91–95, 2021.

[7] D. Ruan, J. Li, J. Liu et al., "Acupoint massage can effectively promote the recovery of gastrointestinal function after gynecologic laparoscopy," *Journal of Investigative Surgery*, vol. 34, no. 1, pp. 91–95, 2021.

[8] H. Li, T. He, Q. Xu et al., "Acupuncture and regulation of gastrointestinal function," *World Journal of Gastroenterology*, vol. 21, no. 27, pp. 8304–8313, 2015.

[9] S. S. Ng, W. W. Leung, S. S. Hon, J. C. Li, C. Y. Wong, and J. F. Lee, "Electroacupuncture for ileus after laparoscopic colorectal surgery: a randomised sham-controlled study," *Hong Kong Medical Journal*, vol. 19, no. S9, pp. 33–35, 2013.

[10] Z. Q. Meng, M. K. Garcia, J. S. Chiang et al., "Electro-acupuncture to prevent prolonged postoperative ileus: a randomized clinical trial," *World Journal of Gastroenterology*, vol. 16, no. 1, pp. 104–111, 2010.

[11] K. B. Cheong, J. Zhang, and Y. Huang, "Effectiveness of acupuncture in postoperative ileus: a systematic review and Meta-analysis," *Journal of Traditional Chinese Medicine*, vol. 36, no. 3, pp. 271–282, 2016.

[12] Y. H. Liu, G. T. Dong, Y. Ye et al., "Effectiveness of acupuncture for early recovery of bowel function in cancer: a systematic review and meta-analysis," *Evidence-Based Complementary and Alternative Medicine*, vol. 2017, Article ID 2504021, 15 pages, 2017.

[13] Y. Liu, B. H. May, A. L. Zhang et al., "Acupuncture and related therapies for treatment of postoperative ileus in colorectal cancer: a systematic review and meta-analysis of randomized controlled trials," *Evidence-Based Complementary and Alternative Medicine*, vol. 2018, Article ID 3178472, 18 pages, 2018.

[14] K. B. Chen, Y. Huang, X. L. Jin et al., "Electroacupuncture or transcutaneous electroacupuncture for postoperative ileus after abdominal surgery: a systematic review and meta-

analysis," *International Journal of Surgery*, vol. 70, pp. 93–101, 2019.

[15] M. J. Page, J. E. McKenzie, P. M. Bossuyt et al., "The PRISMA 2020 statement: an updated guideline for reporting systematic reviews," *BMJ*, vol. 372, p. n71, 2021.

[16] J. A. C. Sterne, J. Savović, M. J. Page et al., "RoB 2: a revised tool for assessing risk of bias in randomised trials," *BMJ*, vol. 366, p. l4898, 2019.

[17] Y. Wang, Z. Chen, Z. Wu, X. Ye, and X. Xu, "Pilates for overweight or obesity: a meta-analysis," *Frontiers in Physiology*, vol. 12, p. 643455, 2021.

[18] T. Van Criekinge, S. Truijen, J. Schröder et al., "The effectiveness of trunk training on trunk control, sitting and standing balance and mobility post-stroke: a systematic review and meta-analysis," *Clinical Rehabilitation*, vol. 33, no. 6, pp. 992–1002, 2019.

[19] Z. Chen, X. Ye, Y. Xia et al., "Effect of pilates on glucose and lipids: a systematic review and meta-analysis of randomized controlled trials," *Frontiers in Physiology*, vol. 12, Article ID 641968, 2021.

[20] G. H. Guyatt, A. D. Oxman, G. E. Vist et al., "GRADE: an emerging consensus on rating quality of evidence and strength of recommendations," *BMJ*, vol. 336, no. 7650, pp. 924–926, 2008.

[21] S. Li, M. Zheng, W. Wu, J. Guo, F. Ji, and Z. Zheng, "Effects of electroacupuncture administered 24hours prior to surgery on postoperative nausea and vomiting and pain in patients undergoing gynecologic laparoscopic surgery: a feasibility study," *Explore*, vol. 13, no. 5, pp. 313–318, 2017.

[22] S. Praveena Seevaunnamtum, K. Bhojwani, and N. Abdullah, "Intraoperative electroacupuncture reduces postoperative pain, analgesic requirement and prevents postoperative nausea and vomiting in gynaecological surgery: a randomised controlled trial," *Anesthesiology and Pain Medicine*, vol. 6, no. 6, Article ID e40106, 2016.

[23] H. Bai, J. Sun, and J. Zhang, "Effect of electroacupuncture combined with tropisetron in treating postoperative nausea and vomiting in patients undergoing total hysterectomy," *Journal of Clinical Anesthesiology*, vol. 28, no. 12, pp. 1158–1160, 2012.

[24] W. Chen, G. Fu, L. Wang, L. Yuan, W. Shen, and M. Zhang, "The effect of electroacupuncture at tsusanli on gastric mucosal blood gas in gynecological laparoscopic surgery," *Journal of Clinical Anesthesiology*, vol. 30, no. 08, pp. 781–784, 2014.

[25] C. Jin and X. Jing, "Effect of electroacupuncture at Zusanli on recovery of gastrointestinal function and electrolyte level after total hysterectomy," *Journal of new Chinese medicine*, vol. 47, no. 05, pp. 248-249, 2015.

[26] S. Li, G. Yang, X. Wang, M. Zheng, and S. Ji, "Effect of preoperative electroacupuncture at different times on the quality of early postoperative recovery in patients undergoing total abdominal hysterectomy," *Jiangsu Journal of Traditional Chinese Medicine*, vol. 51, no. 12, pp. 65–67, 2019.

[27] Y. Lu, W. Tian, G. Xu et al., "Effect of electroacupuncture on morphine analgesia inducing digestive function disorder in patients undergoing hysterectomy," *Practical Pharmacy and Clinical Remedies*, vol. 13, no. 6, pp. 405-406, 2010.

[28] Toronui·Turson, "Effect of electroacupuncture zusanli on laparoscopic surgery in gynecological Patients," *China Health Standard Management*, vol. 10, no. 23, pp. 94–97, 2019.

[29] X. Wang, W. Wu, M. Zheng, and S. Li, "Randomized controlled pilot trial of electroacupuncture for prevention and treatment of gastrointestinal dysfunction after operation," *Journal of Liaoning university of TCM*, vol. 20, no. 06, pp. 179–182, 2018.

[30] X. Wang, W. Wu, M. Zheng, and S. Li, "Preoperative electroacupuncture on gastrointestinal function in patients with gynecologic laparoscopy," *Journal of Clinical Acupuncture and Moxibustion*, vol. 34, no. 02, pp. 35–38, 2018.

[31] X. Wang, Linqin, X. Yang et al., "The effect of Electroacupuncture on gastrointestinal complications after laparoscopic surgery," *Fujian journal of TCM*, vol. 42, no. 6, pp. 9-10, 2011.

[32] Y. Wang and Y. Xi, "Treatment of 40 cases of gastrointestinal dysfunction after gynecological abdominal operation by electroacupuncture combined with umbilical moxibustion," *Henan traditional Chinese medicine*, vol. 37, no. 03, pp. 538–540, 2017.

[33] Y. Xi and Y. Wang, "Therapeutic observation of electroacupuncture plus umbilical moxibustion for gastrointestinal dysfunction after gynecological abdominal operation," *Shanghai Journal of Acupuncture and Moxibustion*, vol. 34, no. 11, pp. 1076–1079, 2015.

[34] Q. Yang, W. Ma, and Y. Li, "Comparison of the effects of acupuncture-assisted anesthesia with different acupoints combination in gynecological laparoscopic operation," *Chinese Acupuncture and Moxibustion*, vol. 32, no. 1, pp. 59–64, 2012.

[35] C. Huang, Z. Dai, X. Jin, and Y. Chen, "Effect of preoperative acupuncture at bilateral neiguan points on postoperative nausea and vomiting andplasma gastrointestinal hormone levels after gynecological laparoscopy," *Journal of Shenyang Medical College*, vol. 23, no. 02, pp. 129–131+166, 2021.

[36] C. Ye and F. Huang, "Effect of electroacupuncture at Neiguan on nausea and vomiting after gynecological laparoscopic surgery," *World Latest Medicine Information*, vol. 19, no. 93, pp. 223-224, 2019.

[37] Y. Yu and C. Ning, "Effects of electroacupuncture on preventing postoperative nausea and vomiting after gynecological laparoscopic surgery," *Chinese Journal of Woman and Child Health Research*, vol. 27, no. 08, pp. 1015–1017, 2016.

[38] He Zhang, Wanglan, M. Zhang et al., "Electroacupuncture for improving the CO2 pneumoperitoneum stress injury during surgery," *Journal of Clinical Acupuncture and Moxibustion*, no. 8, pp. 30–35, 2013.

[39] A. Lee, S. K. Chan, and L. T. Fan, "Stimulation of the wrist acupuncture point PC6 for preventing postoperative nausea and vomiting," *Cochrane Database of Systematic Reviews*, vol. 2015, no. 11, Article ID CD003281, 2015.

[40] C. Y. Chen and C. Y. Tsai, "Ghrelin and motilin in the gastrointestinal system," *Current Pharmaceutical Design*, vol. 18, no. 31, pp. 4755–4765, 2012.

[41] Y. Liu, L. Yang, and S. J. Tao, "Effects of hydromorphone and morphine intravenous analgesia on plasma motilin and postoperative nausea and vomiting in patients undergoing total hysterectomy," *European Review for Medical and Pharmacological Sciences*, vol. 22, no. 17, pp. 5697–5703, 2018.

[42] J. Pascual-Ramírez, L. G. Collar Viñuelas, J. Martín, G. Bernal, A. Bosque Castro, and N. García-Serrano, "Mucosal tonometry as early warning of gastrojejunal leak in laparoscopic Roux-en-y gastric bypass," *Obesity Surgery*, vol. 22, no. 5, pp. 843–846, 2012.

[43] N. Arya, M. A. Sharif, L. L. Lau et al., "Retroperitoneal approach to abdominal aortic aneurysm repair preserves splanchnic perfusion as measured by gastric tonometry," *Annals of Vascular Surgery*, vol. 24, no. 3, pp. 321–327, 2010.

[44] Y. Hayakawa, W. Chang, G. Jin, and T. C. Wang, "Gastrin and upper GI cancers," *Current Opinion in Pharmacology*, vol. 31, pp. 31–37, 2016.

[45] M. Iwasaki, Y. Akiba, and J. D. Kaunitz, "Recent advances in vasoactive intestinal peptide physiology and pathophysiology: focus on the gastrointestinal system," 2019.

[46] J. J. Cullen, J. C. Eagon, and K. A. Kelly, "Gastrointestinal peptide hormones during postoperative ileus. Effect of octreotide," *Digestive Diseases and Sciences*, vol. 39, no. 6, pp. 1179–1184, 1994.

[47] M. Okada, K. Itoh, H. Kitakoji, and K. Imai, "Mechanism of electroacupuncture on postoperative ileus induced by surgical stress in rats," *Medical Acupuncture*, vol. 31, no. 2, pp. 109–115, 2019.

[48] N. N. Yang, Y. Ye, Z. X. Tian et al., "Effects of electroacupuncture on the intestinal motility and local inflammation are modulated by acupoint selection and stimulation frequency in postoperative ileus mice," *Neuro-Gastroenterology and Motility*, vol. 32, no. 5, Article ID e13808, 2020.

[49] K. F. Schulz, D. G. Altman, D. Moher et al., "CONSORT 2010 statement: updated guidelines for reporting parallel group randomised trials," *Trials*, vol. 11, no. 1, p. 32, 2010.

Hindawi
Evidence-Based Complementary and Alternative Medicine
Volume 2021, Article ID 1975228, 10 pages
https://doi.org/10.1155/2021/1975228

Research Article

Electroacupuncture Regulates TRPV1 through PAR2/PKC Pathway to Alleviate Visceral Hypersensitivity in FD Rats

Yong-li Han,[1] **Xing-ming Peng**,[2] **Hong-xing Zhang**,[3] **Song Chen**,[1,4] **and Liang-yu Zhang**[5]

[1]*College of Acupuncture and Orthopedics, Hubei University of Chinese Medicine, Wuhan, Hubei 430061, China*
[2]*Institute of Internal Medicine, Huangjiahu Hospital of Hubei University of Chinese Medicine, Wuhan, Hubei 430065, China*
[3]*Department of Acumoxa, Wuhan Intergrated TCM & Western Medicine Hospital, Wuhan, Hubei 430022, China*
[4]*Second People's Hospital of Jingzhou, Jingzhou, Hubei 434099, China*
[5]*Digestive Endoscopy Treatment Center, Second Affiliated Hospital, Nanjing University of Chinese Medicine, Nanjing, Jiangsu 210017, China*

Correspondence should be addressed to Song Chen; chensong19860221@hbtcm.edu.cn and Liang-yu Zhang; zlyuya618@163.com

Received 18 June 2021; Revised 17 August 2021; Accepted 28 October 2021; Published 29 November 2021

Academic Editor: Mi Liu

Visceral hypersensitivity (VH) is the predominant pathogenesis of functional dyspepsia (FD). Duodenal hypersensitivity along with nausea further reduces the comfort level in gastric balloon dilatation and inhibits gastric receptive relaxation. The potential mechanism behind electroacupuncture- (EA-) mediated alleviation of VH has not been elucidated. In an FD rat model with tail clamping stress, iodine acetamide (IA) induced VH. The rats were treated with EA with or without PAR2 antagonist FSLLRY-NH2, and the body weight, gastric sensitivity, compliance, and gastrointestinal motility were determined. Mast cells and activated degranulation were stained with toluidine blue (TB) staining and visualized under a transmission electron microscope (TEM). Immunofluorescence was used to detect the expression of PAR2, PKC, and TRPV1 in the duodenum and dorsal root ganglion (DRG) and that of CGRP, SP in DRG, and c-fos in the spinal cord. EA alone and EA + antagonist enhanced the gastrointestinal motility but diminished the expression of TRPV1, CGRP, SP, and c-fos-downstream of PAR2/PKC pathway and alleviated VH in FD rats. However, there was no obvious superposition effect between the antagonists and EA + antagonists. The effect of EA alone was better than that of antagonists and EA + antagonists 2 alone. EA-induced amelioration of VH in FD rats was mediated by TRPV1 regulation through PAR2/PKC pathway. This protective mechanism involved several pathways and included several targets.

1. Introduction

Functional dyspepsia (FD), a common chronic gastrointestinal disease, is characterized by upper abdominal pain or burning sensation, postprandial fullness, early satiety, belching, and other symptoms [1]. According to the diagnostic criteria of Rome IV functional gastrointestinal diseases, FD was classified into two subgroups: epigastric pain syndrome (EPS) and postprandial distress syndrome (PDS) [2]. The global prevalence rate of FD is 21.8%, though there is a significant variation of this rate from country to country [3]. Although the pathophysiological mechanism of FD remains unknown to date, its association with brain–intestinal interaction, gastrointestinal motility, visceral hypersensitivity (VH), gastrointestinal microbiota, mucosal barrier, and immune activation, and abnormality of the central nervous system, resulting from the comprehensive action of multiple factors, has been investigated [4].

Along with EPS symptoms, VH is also associated with nonpainful sensations (such as postprandial fullness, abdominal distension, and hiccups) [5]. Moreover, an increase in gastrointestinal sensitivity gradually intensifies the severity of gastrointestinal symptoms in patients suffering from FD. Research in Malaysia confirmed the onset of FD resulting from a high intake of chili peppers [6]. Selectively activated by capsaicin, transient receptor potential vanilloid-

1 (TRPV1) induces the release of neuropeptides, including calcitonin gene-related peptide (CGRP) and P substance (SP). These neuropeptides increase VH and induce FD symptoms (including abdominal pain and nausea) [7]. Various stimuli result in the activation and degranulation of mast cells, releasing a large amount of trypsin and tryptase (TRY), which, in turn, activate protease-activated receptor 2 (PAR2) on nociceptive neurons, causing neuronal excitement and releasing nociceptive neurotransmitters CGRP and SP, ultimately increasing VH in patients with FD [8]. PAR2 and TRPV1 are colocalized in the primary afferent nerve and coexpressed in more than 60% of L4–6 DRG cells, whereas both CGRP and SP are evident in 20% of the 35% PAR2-expressing neurons [9]. A synergistic effect of PAR2 with TRPV1 on VH regulation is documented. Excessive activation of the PAR2-PKC pathway mediates TRPV1 phosphorylation and decreases the TRPV1 opening threshold and abnormal visceral pain perception, eventually leading to VH [10, 11].

Acupuncture has been explored as a potentially effective nondrug therapy for functional gastrointestinal diseases. Efficacy of the electroacupuncture (EA) therapy in improving the dyspeptic symptoms of refractory FD patients was confirmed in a Chinese randomized controlled trial (RCT) involving 200 refractory FD patients, and its effect was found to be better than that of the sham acupuncture group [12]. High-quality RCT also validated significant amendment with acupuncture thrice a week in the PDS symptoms of FD patients with improved quality of life. After termination of the treatment, the curative effect was maintained for 12 weeks, and the adverse reactions were minimal during the treatment period [13]. Our previous studies also reported that EA at the acupoints ("Zusanli" and "Taichong") improved gastrointestinal motility and reduced low-grade duodenal inflammation in FD model rats [14, 15], substantiating the effectiveness of these two acupoints. The present study employed iodine acetamide (IA) combined with tail clamping stress to induce the FD rat model and explored the effect of EA on intestinal hypersensitivity in FD rats to determine whether EA alleviated intestinal hypersensitivity through the PAR2/TRPV1 signal pathway.

2. Materials and Methods

2.1. Animal. The Experimental Animal Center of the Three Gorges University (license number is SCXK (E) 2017–0012) provided 42 SPF male 10-day-old SD (Sprague-Dawley) young rats. The animals were maintained in the Experimental Center of traditional Chinese Medicine of Hubei University of Traditional Chinese Medicine. The animal feeding environment was as follows: room temperature $(20 \pm 2)^{\circ}$C, humidity (50 ± 10)%, normal light replacement, 24 h supply of aseptic feed, and drinking water. All animals were fed adaptively for three days before the initiation of the experiment.

2.2. Construction and Evaluation of FD Model. Studies have shown that iodoacetamide intragastric administration can simulate better the pathological states of human visceral hypersensitivity and reduce gastric compliance [16, 17]. In contrast, the traditional tail pinch stress method simulates the symptoms of reduced food intake, delayed gastric emptying, and increased visceral sensitivity, which also stimulates rats to produce emotional changes such as anxiety and irritability, and simulates some causes of FD to a certain extent [18]. In order to completely simulate the symptoms and pathological states of FD patients, such as high visceral sensitivity, reduced gastric compliance, and delayed gastric emptying, the FD rat model was induced by IA along with tail clamping stress. The 42 10-day-old SD rats were randomly divided into control group ($n = 8$) and model group ($n = 34$). Each rat in the control group was administered 2% sucrose solution 0.2 mL/d for six days, and each rat in the model group was given a mixture of 0.1% IA and 2% sucrose 0.2 mL/d for six days. Following intragastric administration, the rats in each group were fed normally to the age of seven weeks. From the age of seven weeks, the rats in the model group were induced by Guo's tail stimulation method for one week; however, the control group did not receive any intervention until the rats were eight weeks old. The body weight of rats was recorded during intragastric administration (from 13 days to 20 days old). At the age of eight weeks, the gastric sensitivity of rats was estimated (the rate of EMG root mean square change of cervical trapezius muscle during gastric dilatation stimulation reflected the evaluation index), and compliance was evaluated (the volume/pressure of intragastric balloon during gastric dilatation stimulation represented the evaluation index). According to the evaluation of the model, 32 rats in the model group were successfully established.

2.3. Animal Grouping and Intervention. Thirty-two rats were randomly classified into four groups, with eight rats in each group (two cages/group; four rats/cage). Overall, there were five groups: control group, model group, EA group, antagonist group, and EA + antagonist group. The control group and model group did not receive any intervention for 14 consecutive days. EA group had acupuncture on both sides of "Zusanli" (located at about 5 mm under the fibula head under the knee joint of rats) and "Taichong" (located at the depressions between the first and second metatarsals of the dorsal foot of the left hindlimb) with one-off acupuncture of 0.30 mm × 25 mm specification, direct needling 1 mm, and Han's acupoint nerve stimulator with the continuous wave, frequency 2 Hz, current intensity 1 mA. The degree implied no obvious discomfort and rejection in the limbs of the rats. The needle was retained for 30 min, once daily for 14 days. The antagonist group [19] received no intervention in the first 11 days, until the intrathecal injection of 10 μL PAR2 antagonist FSLLRY-NH2 (10 mg/L) was continuously given three days before sampling once daily three times. The EA + antagonist group had the previously mentioned EA intervention for 14 days, and intrathecal injection of FSLLRY-NH2 was given three days before sampling.

2.4. Organizational Preparation. After completing all interventions, the rats were fasted for 24 h and weighed and

were fed 2 mL/100 g nutritious semisolid paste (5 g carboxymethylcellulose, 8 g milk powder, 4 g white sugar, and 4 g starch dissolved in 125 mL distilled water to prepare 150 g nutritious semisolid paste) and 1 mL/100 g ink according to their body weight. Following intragastric administration for 1 h, the rats were killed by cervical dislocation. The stomach and small intestine were collected, and the stomach's total weight and net weight were recorded. The difference between the two was calculated as the gastric residual weight, and then, the gastric residual rate was calculated as follows: (total gastric weight-Wei net weight)/given paste weight × 100%. The total length of the small intestine and the propulsive length of the ink (that is, the length from the pylorus to the front of the ink) were measured. Furthermore, the tissues of the gastric antrum, duodenum, T8–10 spinal cord, and dorsal root ganglion were frozen in liquid nitrogen and preserved in 4% paraformaldehyde and 2.5% glutaraldehyde fixation solution, respectively.

2.5. Hematoxylin-Eosin (HE) Staining. After dewaxing the paraffin sections of the stomach and duodenum to water, these sections were stained with hematoxylin staining solution, dehydrated, then placed in eosin dye solution for 5 min, then again dehydrated and sealed, and examined by the microscope, and the images were collected for analysis. The nucleus was stained blue and the cytoplasm red.

2.6. Toluidine Blue (TB) Staining. The paraffin sections of duodenal tissue were dewaxed to water, stained with TB dye for 2 min, and differentiated with 0.5% glacial acetic acid until the nuclei and particles were visible. After drying for more than 4 h, the sections were placed in xylene to make them transparent and sealed with neutral gum. The cytoplasm of mast cells was purplish-red, and mast cells were counted under the microscope.

2.7. Transmission Electron Microscope (TEM). After rinsing, the duodenal tissue was fixed by 1% osmic acid 0.1 m phosphate buffer (pH 7.4) at room temperature (20°C) for 2 h, dehydrated by a series of alcohol gradients, and then permeated with acetone: epoxy resin (2 : 1), acetone: epoxy resin (1 : 1), epoxy resin, each time for 8–12 h. The infiltrated duodenal tissue was embedded in epoxy resin and then sliced and stained with uranium and lead. Finally, the ultrastructural characteristics of fragmentary or allergic degranulation of duodenal mast cells were visualized under the electron microscope.

2.8. Immunohistochemistry. Paraffin sections of duodenal tissue were dewaxed to water and placed in a repair box filled with EDTA antigen repair buffer (pH 9.0) for antigen repair. The slices were shaken dry. A circle around the tissue was drawn with a histochemical pen, and then, the slices were incubated with BSA dripping in the circle for 30 min. After dripping an anti-(TRY), washing the slide on the slice, and drying it, the covering tissue of the second antibody (HRP labeled goat anti-rabbit) was added to the circle and incubated for 50 min at room temperature. After washing the slide again and shaking it dry, DAB chromogenic agent was added to the circle, dehydrated with anhydrous ethanol, and sealed with xylene transparent neutral gum. In mast cells, TRY was mainly expressed in the granules in the cytoplasm, which was stained brown and yellow. Each slice in each group was randomly screened with at least three 200-fold visual fields to be photographed. While taking photos, the whole field of vision of the organization should be filled to ensure consistency in the background light of each photo. The same brown and yellow color was selected as the unified standard for judging the positivity of all photos by using Image-Pro Plus 6.0. The integrated optical density (IOD) of each positive photo was obtained by analyzing each photo.

2.9. Immunofluorescence. Paraffin sections of duodenal tissue were dewaxed to water sections and placed in a repair box filled with EDTA antigen repair buffer (pH 9.0) for antigen repair. The slices were shaken dry, incubated for 30 min with BSA dripping in the circle after drawing a circle around the tissue with a histochemical pen. The first antibody (including PAR2, PKC, and TRPV1) was added to the slice. After washing and drying the slide, the second antibody (including CY3-labeled goat anti-mouse and CY3-labeled goat anti-rabbit) covering tissue of the corresponding species was introduced in the circle and incubated for 50 min at room temperature. After washing the slide again and shaking it dry, DAB chromogenic agent was added to the circle, dehydrated with anhydrous ethanol, and sealed with xylene transparent neutral gum. The images were observed and collected under the fluorescence microscope. The nucleus stained by DAPI was blue under UV excitation, whereas the positive expression was red or green light labeled with the corresponding fluorescein. The same method was adopted to detect the expression of PAR2, PKC, TRPV1, CGRP, SP in DRG, and c-fos in the spinal cord. Each slice in each group was randomly selected with at least three 200-fold visual fields to be photographed. The red fluorescent monochromatic photos were converted into black-and-white pictures with the help of the Image-Pro Plus 6.0 software. The same black was then selected as the unified standard to judge the positive of all photos. Each photo was analyzed to retrieve the individual IOD value.

2.10. Western Blot. Add tissue protein extraction reagent 10 times the volume of the kidney tissue, collect the total protein solution, centrifuge, and then spot samples to denature the total protein solution. Prepare 10% separation gel and 5% concentrated gel, fill the gel immediately after adding TEMED, then start electrophoresis, transfer, and block, and incubate the primary and secondary antibodies at 4bC overnight. Drop the freshly prepared ECL mixed solution onto the protein side of the membrane for luminescence detection. The film is scanned and archived, and the AlphaEaseFC software processing system analyzes the optical density value of the target zone.

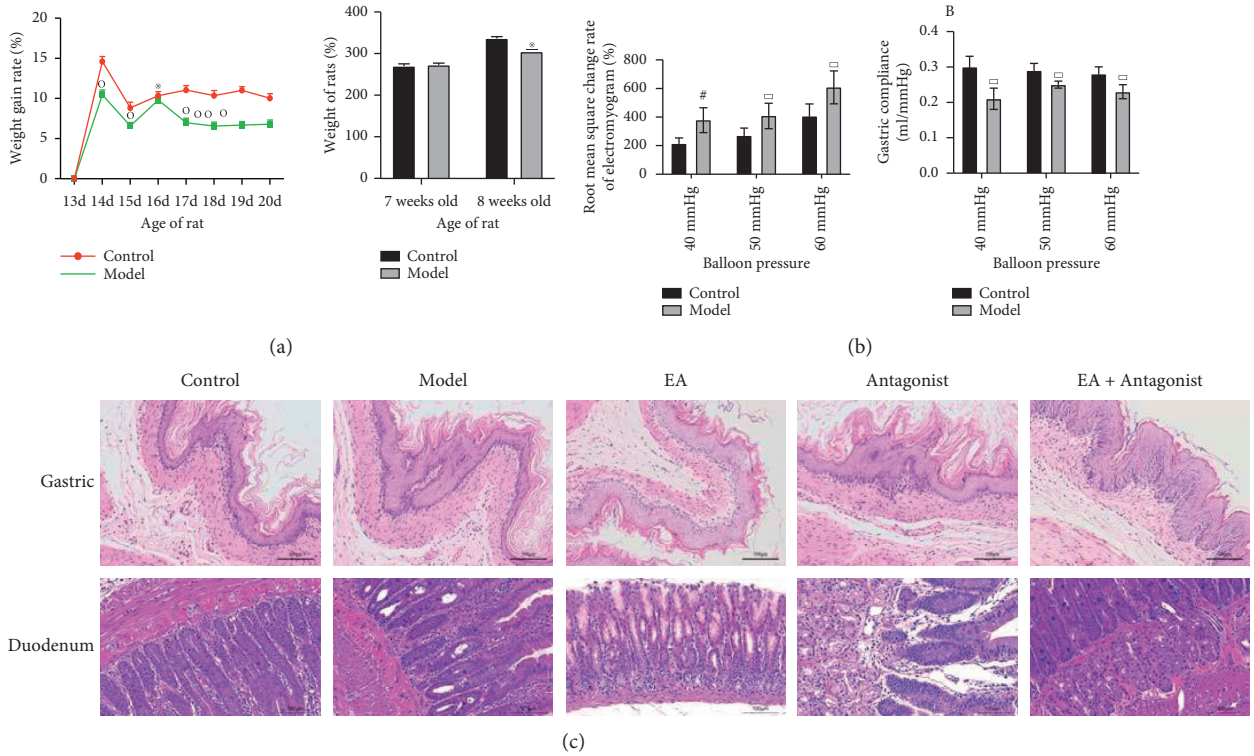

Figure 1: Decrease in the growth rate of body weight and increase in the sensitivity in the model group. (a) The body weight in two groups at different times. (b) Stomach sensitivity and compliance. (c) HE staining of gastrointestinal tissue (× 200 magnification). No pathological alterations, including ulcer and bleeding, were observed in the intestinal mucosa of the stomach and duodenum in all groups. Scale bar: 100 um. Compared with the control group, $^{※}P < 0.05$, $^{□}P < 0.0$, $^{\#}P < 0.001$, and $^{△}P < 0.0001$.

2.11. Statistical Analysis. The experimental data were analyzed by IBM-SPSS 22.0 software. The measurement data were described in terms of mean ± SD ($x \pm s$). Each group was compared with analysis of variance (ANOVA), followed by independent t-test and Bonferroni posttest. Kruskal-Wallis analysis of variance was employed to determine the statistical differences of macro and micro scores among groups. $P < 0.05$ was considered to be statistically significant.

3. Result

3.1. Successfully Constructing an FD Rat Model with High Visceral Sensitivity. The period of intragastric administration of IA (13–20 days old) was marked by a significantly lower growth rate of body weight in the model group than that in the control group. At the age of seven weeks, no significant difference in body weight was documented among the other three groups. However, as illustrated in Figure 1(a), the body weight of rats in the model group was significantly lower than that in the control group at the age of seven weeks, one week after tail clamping stimulation (8 weeks old). The gastric sensitivity and compliance test results of eight-week-old rats witnessed no significant difference in electromyogram (EMG) RMS change rate and compliance of cervical trapezius muscle induced by gastric dilatation stimulation at 10–30 mmHg pressure between the control group and model group. Figure 1(b) shows significantly higher root mean square change rate of the cervical trapezius muscle, whereas there was a significantly decreased gastric compliance in the model group compared with the control group, when the intragastric balloon pressure was 40–60 mmHg. No pathological alterations such as ulcers and bleeding were evident in the intestinal mucosa of the stomach and duodenum in all groups. As observed under the optical microscope, the intestinal mucosa of the stomach and duodenum in the model, EA, antagonist, and EA + antagonist groups were disordered, the intrinsic glands were relaxed, and a small amount of eosinophil infiltration was noted (which might be related to intestinal mucosal damage during visceral sensitivity measurement). The gastric and duodenal mucosal layers of rats in the control group were neatly arranged. There was no abnormality in the intrinsic glands. The structure of the submucosa and muscle layer was prominent with no obvious eosinophil infiltration (Figure 1(c)).

3.2. EA Mediates the Beneficial Effects of Visceral Hypersensitive FD. EA significantly enhances gastrointestinal motility. Compared with the control group, the gastric residual rate was increased, and the intestinal propulsion rate was significantly decreased in the other four groups. The previously mentioned results confirmed the successful establishment of the FD rat model in this experiment. Compared with the EA group, the gastric residual rate increased in the antagonist and EA + antagonist groups. Furthermore, a

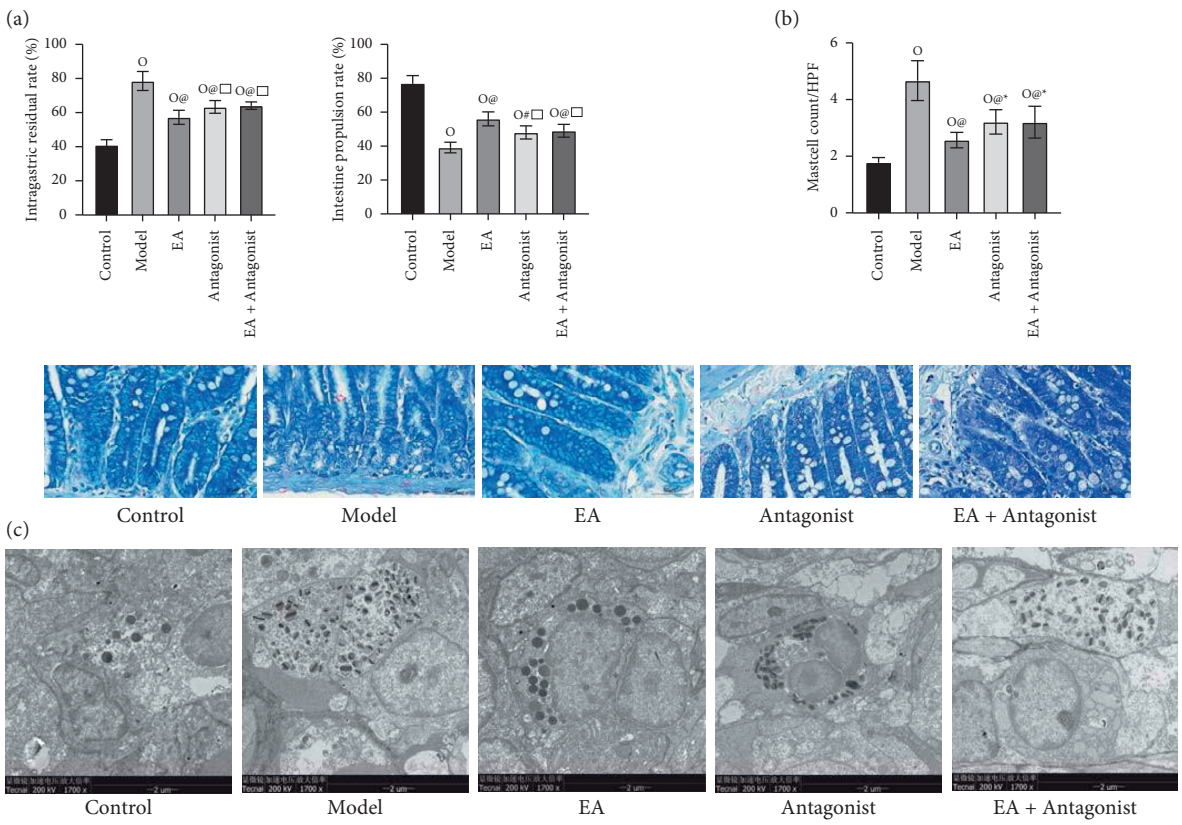

Figure 2: Electroacupuncture mediates the beneficial effects of visceral hypersensitive FD. (a) EA-mediated reduction in the residual rate in the stomach and increase in the propulsive rate of the small intestine in rats. (b) EA reduced the number and activation of mast cells in the duodenum. (c) The ultrastructural characteristics of fragmented or allergic degranulation of duodenal mast cells were observed under TEM (×1700 magnification). Compared with the control group, $^{\triangle}P < 0.0001$, $^{\square}P < 0.01$; compared with the model group, $^{\#}P < 0.001$, $^{\star}P < 0.0001$; compared with the EA group, $^{※}P < 0.05$, $^{\square}P < 0.01$. Scale bar: 50 um.

decrease in the intestinal propulsion rate was documented in the antagonist group and the EA + antagonist group compared with that of the EA group (Figure 2(a)).

EA reduces the number of mast cells in the duodenum and inhibits the activation and degranulation of mast cells. TB staining substantiated an increased number of mast cells in the other four groups compared with the control group. Nonetheless, the number of mast cells in the EA group, antagonist group, and EA + antagonist group decreased compared with the model group. Moreover, the number of mast cells in the EA group was lower than that in the antagonist group and EA + antagonist group. As seen in TEM, the morphology of mast cells in the control group was regular and quasi-round, and the cell membrane was intact and without degranulation. Compared with the control group, an irregularity was evident in the shape of mast cells in the model group, and there were many flocs around the cells, which were in the state of degranulation. However, with respect to the model group, the mast cells in the EA group were regular and oval, with few pieces of flocs around them, and the degree of degranulation was not obvious. Moreover, the morphology of mast cells in the antagonist group and EA + antagonist group was regular and oval, and there were few flocs around them. The degree of degranulation was not obvious (Figures 2 (b) and 2(c)). The results validated EA-induced significant activation and degranulation of mast cells in duodenal mucosa of VH in FD rats. Findings also confirmed that EA inhibited the number and activated degranulation of mast cells in duodenal mucosa.

3.3. EA Downregulates the Positive Expression of TRY, PAR2, PKC, and TRPV1 in Duodenal Mast Cells. The results from the experiments (Figure 3(a)) reflected an increased IOD value of TRY in the other four groups compared with the control group. However, the IOD value of TRY in the EA group, antagonist group, and EA + antagonist group decreased with regards to the model group. Furthermore, the IOD value of TRY in the EA group was lower than that in the antagonist group and EA + antagonist group. These findings revealed a significant increase in the release of TRY in the model group, whereas EA inhibited the release of TRY in duodenal mast cells.

EA reduces the expression of PAR2, PKC, and TRPV1 in the duodenum. As evident from Figure 3(b), enhanced IOD values of PAR2, PKC, and TRPV1 in the other four groups were manifested compared with the control group. On the other hand, the IOD values of PAR2, PKC, and TRPV1 in the EA group, antagonist group, and EA + antagonist group decreased compared with the model group. The IOD values of PAR2, PKC, and TRPV1 in the EA group were lower than

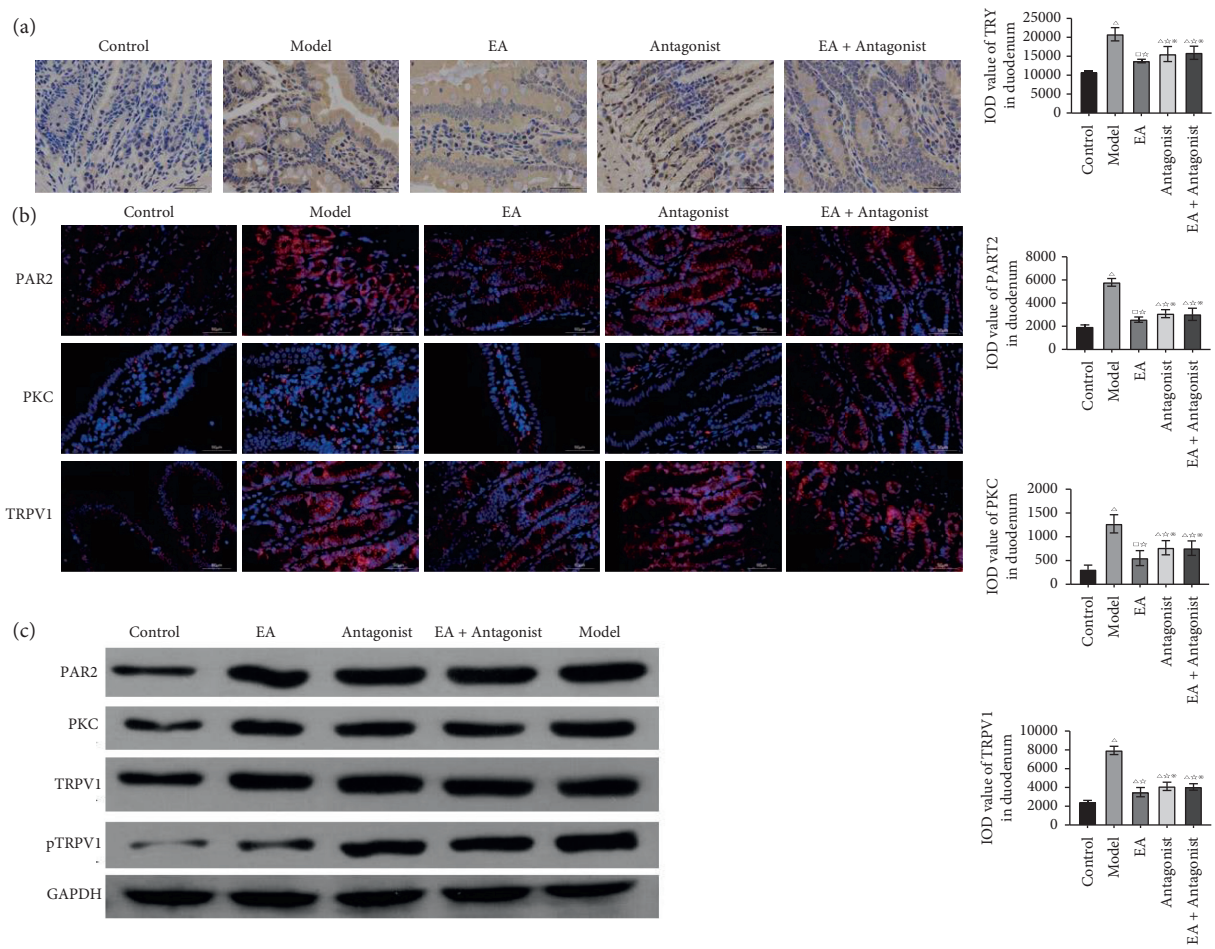

Figure 3: EA downregulates the positive expression of TRY, PAR2, PKC, and TRPV1 in duodenal mast cells. (a) The positive expression of TRY in the duodenum was detected by immunohistochemistry (× 400 magnification). (b) The positive expressions of PAR2, PKC, and TRPV1 in the duodenum were identified by immunofluorescence (× 400 magnifications). (c) The protein expression levels of PAR2, PKC, TRPV1, and pTRPV1 in the duodenum were detected by western blot. Compared with the control group, $^{\triangle}P < 0.0001$, $^{\square}P < 0.01$; compared with the model group, $^{\star}P < 0.0001$; compared with EA group, $^{※}P < 0.05$. Scale bar: 50 um.

those in the antagonist and EA + antagonist groups. Figure 3(c) confirms the previously mentioned results. Thus, the results confirmed significantly increased expression of PAR2, PKC, and TRPV1 in the model group and EA-mediated inhibition of the expression of PAR2, PKC, and TRPV1 in duodenal mast cells.

3.4. EA Diminished the Levels of PAR2, PKC, TRPV1, CGRP, and SP in DRG and c-fos in the Spinal Cord. Compared with the control group, increased IOD values for PAR2, PKC, and TRPV1 in the other four groups were obtained. Decreased IOD values of PAR2, PKC, and TRPV1 in the EA group, antagonist group, and EA + antagonist group compared with the model group. The IOD values of PAR2, PKC, and TRPV1 in the EA group were lower than those in the antagonist and EA + antagonist groups (Figure 4(a)). Overall, it was found that the expression of PAR2, PKC, and TRPV1 increased significantly in the model group, whereas EA inhibited the expression of PAR2, PKC, and TRPV1 in DRG.

EA reduces the expression of CGRP and SP in DRG. Increased IOD values of CGRP and SP in the other four groups were observed compared with the control group. A similar decrease in the IOD values of CGRP and SP in the EA group, antagonist group, and EA + antagonist group were observed concerning the model group. The IOD values of CGRP and SP in the EA group were lower than those in the antagonist group and EA + antagonist group. Figure 4(a) illustrates these findings. The results substantiated a significant increase in the expression of CGRP and SP in the model group, whereas EA impeded the expression of CGRP and SP in DRG. Figure 4(b) also confirms that EA reduced the protein expression levels of PAR2, PKC, TRPV1, pTRPV1, CGRP, and SP in DRG.

EA reduces the expression of c-fos in the spinal cord. Compared with the control group, the IOD value of c-fos in the model group increased, while the IOD value of c-fos in the EA group, antagonist group, and EA + antagonist group was lower than that of the model group. Decreased IOD value of c-fos in the EA group was also witnessed than that in the antagonist group and EA + antagonist group

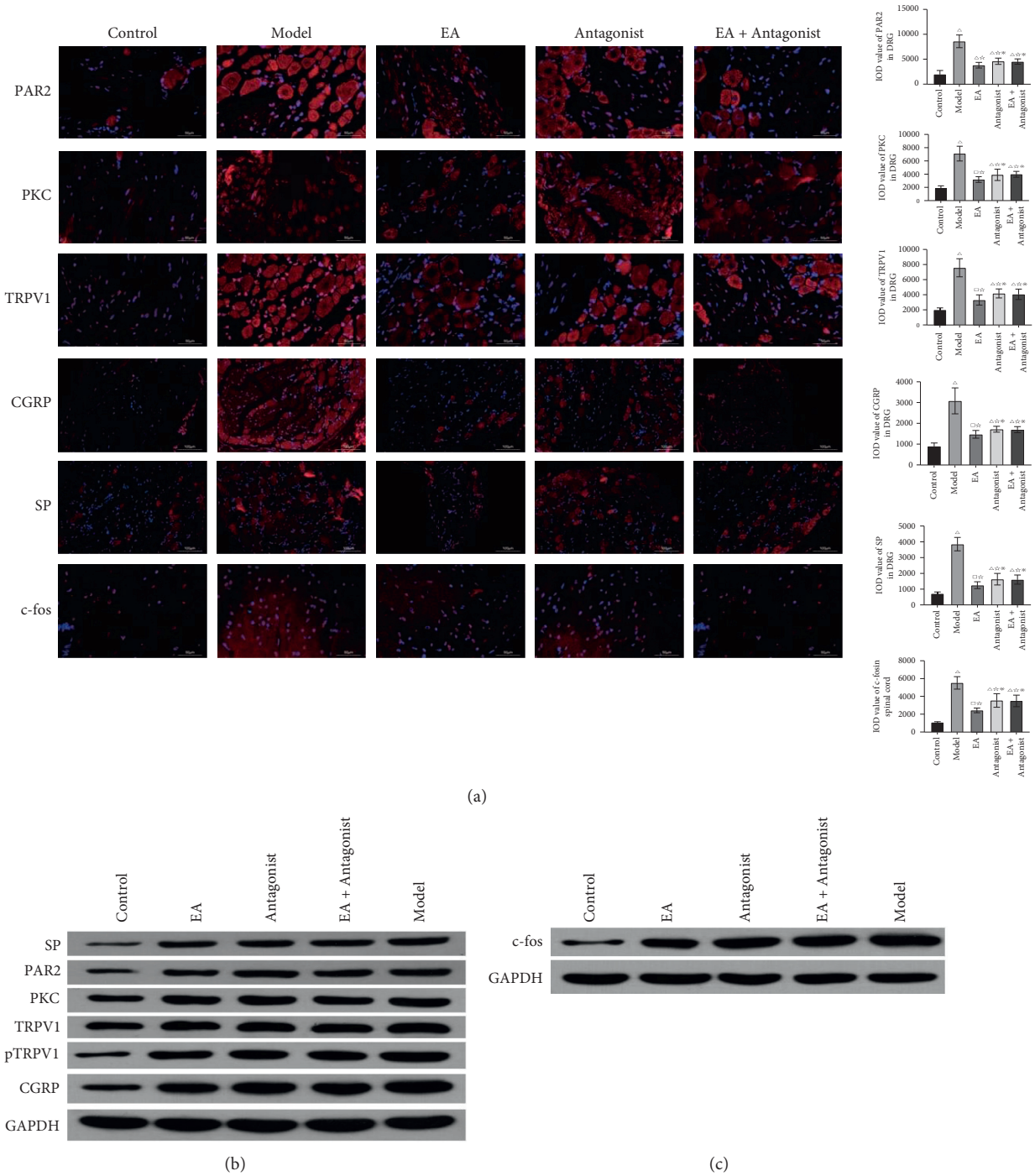

Figure 4: EA reduced the positive expression of PAR2, PKC, TRPV1, CGRP, and SP in DRG and c-fos in the spinal cord. (a) The positive expressions of PAR2, PKC, and TRPV1 in DRG were detected by immunofluorescence (× 400 magnification). (b) The protein expressions of PAR2, PKC, TRPV1, ptrpv1, CGRP, and SP in DRG were detected by western blot. (c) The protein expression of c-fos in spinal cord were detected by western blot. Compared with the control group, $^{*}P < 0.05$, $^{\square}P < 0.01$; compared with model group, $^{\#}P < 0.05$, $^{☆}P < 0.0001$; compared with EA group, $^{※}P < 0.05$.

(Figure 4(a)). Figure 4(c) confirms that EA reduces the protein expression of c-fos in the spinal cord. These findings confirmed that EA repressed the expression of c-fos in the spinal cord.

Compared with the antagonist and EA + antagonist group, $^{\triangle}P < 0.05$. Scale bar: 50 um.

4. Discussion

Early inflammatory stimulation is a predisposing factor for the formation of VH. The pathological mechanism of VH was better induced by the intragastric administration of IA as an early inflammatory response [20]. Anxiety and

depression also repressed the visceral sensory threshold, enhancing the VH of patients [21]. In summary, our results well replicated the three pathological mechanisms of VH in FD, visceral hypersensitivity, decreased gastric compliance, and delayed gastric emptying. At present, the duodenum is believed to be the key site of functional gastroenteropathy symptoms [22, 23]. FD patients manifest a correlation between duodenal mast cells and neuronal signal changes. However, the potential disease mechanism of central sensitization has not been explored systematically [24]. Medium and small neurons in DRG are major targets for visceral pain signal transduction and regulation [25].

Studies have revealed that mast cell activation induces alteration in duodenal permeability and sensitivity in patients suffering from FD [26–28]. A positive correlation was noted between the symptoms of FD patients with the percentage of degranulated mast cells. FD patients demonstrated increased density and activity of mast cells in duodenal mucosa. Moreover, the expression of specific receptor TRPV1 targeting primary afferent nerve endings in duodenal mucosa increased significantly [29]. PAR2 receptor antagonists block visceral nociceptive sensory information, significantly improve acute and chronic colitis, reduce the activation and degranulation of mast cells, diminish the release of TRY, and alleviate VH [30]. In this study, the active site of mast cells in FD was expanded from the stomach to the duodenum. EA significantly decreased the number of mast cells in the duodenum, inhibited the activation and degranulation of mast cells, and downregulated the positive expression of TRY in duodenal mast cells.

PAR2 is one of the upstream molecules of PKC. Inhibition of PAR2 also impedes the activation of PKC [31, 32]. The role of the PAR2-PKC pathway in the generation and maintenance of pain has been well established [33]. The vital role of PKC, on the peripheral sensory nerve, especially PKC ε, is also observed in hyperalgesia caused by inflammation. The mechanism involves TRPV1 phosphorylation-mediated reduction of the open threshold of ion channels [34]. PKC ε activator aggravated the response of TRPV1 to capsaicin and temperature, while TRPV1 knockout mice failed to develop hyperalgesia when treated with PKC ε activator [35]. Meanwhile, PKC blocker induced alleviation of VH caused by TRY [36]. Our study found that the positive IOD values of PAR2, PKC, and TRPV1 in duodenum and DRG decreased following EA and with or without inhibitor treatment. The present study also revealed that the IOD values of PAR2, PKC, and TRPV1 in the EA group were lower than those in the antagonist group and EA + antagonist group. It is presumed that the expression of PAR2, PKC, and TRPV1 in the peripheral and central nervous systems was downregulated by EA.

Activation of TRPV1 on sensory neurons results in depolarization of neuronal cell membrane, directly or indirectly triggering afferent nerve endings to release sensory neuropeptides such as SP and CGRP and inducing VH [37, 38]. Alteration of visceral sensitivity is attributed to both central and peripheral CGRP release [39–41]. In the process of pain conduction in the spinal cord, neuropeptides, such as CGRP and SP, released at the central end of the primary afferent nerve fibers, contribute to the depolarization of neurons in the superficial layer of the posterior foot of the spinal cord [42]. The increased expression of c-fos during pain reflects the partial adaptive response of the spinal cord to continuous and subsequent nociceptive inputs [43, 44]. Our study highlighted EA-mediated significant reduction of the positive IOD values of neuropeptides CGRP and SP in DRG and c-fos in the spinal cord. EA also inhibited the expression of c-fos in the spinal cord induced by pain injury and effectively alleviated VH in FD rats.

There is growing evidence regarding the application of EA in relieving FD with VH. EA ameliorated gastric hypersensitivity in IA rats, which may be related to improving the balance of the sympathetic nerve and reducing the level of stress hormone [45]. Stress-induced gastric hypersensitivity in FD rats was blocked by adrenoceptor antagonists [46]. EA prevented or inhibited stress-induced gastric hypersensitivity by restoring sympathetic balance. To summarize, our results illustrated that EA and antagonists and EA + antagonists increased gastrointestinal motility and decreased the expression of PAR2, PKC, TRPV1, CGRP, SP, and c-fos downstream of PAR2/PKC pathway in FD rats, thus alleviating VH, though no significant superposition effect between antagonists and EA + antagonists was documented. Overall, our results strongly corroborated that EA regulates TRPV1 through PAR2/PKC pathway to improve VH in FD rats, and its protective mechanism is the comprehensive effect of multipathway and multitarget.

Data Availability

The data used to support the findings of this study are available from the corresponding author upon request.

Conflicts of Interest

The authors declare that they have no conflicts of interest.

Acknowledgments

The study was granted and supported by the National Natural Science Foundation of China (no. 81473790).

References

[1] V. Stanghellini, F. K. L. Chan, W. L. Hasler et al., "Gastroduodenal disorders," *Gastroenterology*, vol. 150, no. 6, pp. 1380–1392, 2016.

[2] Z. C. Wei, Q. Yang, and Q. Yang, "Rome III, Rome IV, and potential asia symptom criteria for functional dyspepsia do not reliably distinguish functional from organic disease," *Clinical and Translational Gastroenterology*, vol. 11, Article ID e00278, 2020.

[3] A. C. Ford, A. Marwaha, R. Sood, and P. Moayyedi, "Global prevalence of, and risk factors for, uninvestigated dyspepsia: a meta-analysis," *Gut*, vol. 64, no. 7, pp. 1049–1057, 2015.

[4] L. Wauters, N. J. Talley, M. M. Walker, J. Tack, and T. Vanuytsel, "Novel concepts in the pathophysiology and treatment of functional dyspepsia," *Gut*, vol. 69, no. 3, pp. 591–600, 2020.

[5] J. Vandenberghe, R. Vos, P. Persoons, K. Demyttenaere, J. Janssens, and J. Tack, "Dyspeptic patients with visceral hypersensitivity: sensitisation of pain specific or multimodal pathways?" *Gut*, vol. 54, no. 7, pp. 914–919, 2005.

[6] S. Mahadeva, H. Yadav, S. Rampal, S. M. Everett, and K. L. Goh, "Ethnic variation, epidemiological factors and quality of life impairment associated with dyspepsia in urban Malaysia," *Alimentary Pharmacology and Therapeutics*, vol. 31, pp. 1141–1151, 2010.

[7] J. Hammer and H. Vogelsang, "Characterization of sensations induced by capsaicin in the upper gastrointestinal tract," *Neuro-Gastroenterology and Motility*, vol. 19, no. 4, pp. 279–287, 2007.

[8] M. M. Wouters, M. Vicario, and J. Santos, "The role of mast cells in functional GI disorders," *Gut*, vol. 65, no. 1, pp. 155–168, 2016.

[9] S. Li and L. P. Duan, "Research progress in the relationship between TRPV1 and visceral hypersensitivity in functional gastrointestinal diseases," *Journal of Peking University*, vol. 43, pp. 311–314, 2011.

[10] B. Huang, S. Huang, T. Zhang, and Y. N. Chen, "PAR2-PKC pathway regulated TRPV1 mediates visceral hyperalgesia to participate in the irritable bowel syndrome," *Chinese Journal of Gastroenterology and Hepatology*, vol. 24, pp. 488–490, 2015.

[11] N. Vergnolle, "Protease-activated receptors as drug targets in inflammation and pain," *Pharmacology & Therapeutics*, vol. 123, no. 3, pp. 292–309, 2009.

[12] H. Zheng, J. Xu, X. Sun et al., "Electroacupuncture for patients with refractory functional dyspepsia: a randomized controlled trial," *Neuro-Gastroenterology and Motility*, vol. 30, Article ID e13316, 2018.

[13] J.-W. Yang, L.-Q. Wang, X. Zou et al., "Effect of acupuncture for postprandial distress syndrome," *Annals of Internal Medicine*, vol. 172, no. 12, pp. 777–785, 2020.

[14] Y. Yang, P. D. Xu, Y. Xin, Z. X. Kang, H. X. Zhang, and L. Zhou, "Involvement of neurotensin-mediated brain-gut axis in electroacupuncture intervention induced improvement of functional dyspepsia in rats," *Acupuncture Research*, vol. 41, no. 01, pp. 35–39+50, 2016.

[15] D. Wang, H. X. Zhang, and P. J. Rong, "Effects of TLR4 and NF-κB P65 on duodenum with the intervention of electroacupuncture in functional dyspepsia model rats with liver stagnation and spleen deficiency," *Journal of Basic Chinese Medicine*, vol. 26, pp. 1337–1340, 2020.

[16] L. S. Liu, J. H. Winston, M. M. Shenoy, G. Q. Song, J. D. Z. Chen, and P. J. Pasricha, "A rat model of chronic gastric sensorimotor dysfunction resulting from transient neonatal gastric irritation," *Gastroenterology*, vol. 134, no. 7, pp. 2070–2079, 2008.

[17] M. Römer, E. Painsipp, and I. Schwetz, "Facilitation of gastric compliance and cardiovascular reaction by repeated isobaric distension of the rat stomach," *Neuro-Gastroenterology and Motility*, vol. 17, no. 3, pp. 399–409, 2010.

[18] W. Wei, X. Li, and J. Hao, "Proteomic analysis of functional dyspepsia in stressed rats treated with traditional Chinese medicine "Wei Kangning"," *Journal of Gastroenterology and Hepatology*, vol. 26, no. 9, pp. 1425–1433, 2011.

[19] Y. J. Li, *The Mechanisms of Probiotic VSL#3 in a Rat Model of Visceral Hypersensitivity Involves the Mast Cell-PAR2-TRPV1 Pathway*, China Medical University, Taichung, Taiwan, 2019.

[20] J. H. Winston, J. E. Aguirre, X.-Z. Shi, and S. K. Sarna, "Impaired interoception in a preclinical model of functional dyspepsia," *Digestive Diseases and Sciences*, vol. 62, no. 9, pp. 2327–2337, 2017.

[21] E. Salameh, M. Meleine, G. Gourcerol et al., "Chronic colitis-induced visceral pain is associated with increased anxiety during quiescent phase," *American Journal of Physiology-Gastrointestinal and Liver Physiology*, vol. 316, no. 6, pp. G692–G700, 2019.

[22] M. Pesce, M. Cargiolli, S. Cassarano et al., "Diet and functional dyspepsia: clinical correlates and therapeutic perspectives," *World Journal of Gastroenterology*, vol. 26, no. 5, pp. 456–465, 2020.

[23] A. C. Ford, S. Mahadeva, M. F. Carbone, B. E. Lacy, and N. J. Talley, "Functional dyspepsia," *The Lancet*, vol. 396, no. 10263, pp. 1689–1702, 2020.

[24] C. Cirillo, T. Bessissow, A.-S. Desmet, H. Vanheel, J. Tack, and P. Vanden Berghe, "Evidence for neuronal and structural changes in submucous ganglia of patients with functional dyspepsia," *American Journal of Gastroenterology*, vol. 110, no. 8, pp. 1205–1215, 2015.

[25] T. T. Lv, *P2X7 and P2Y1 Receptors in the DRG Mediated Analgesia Effect of Electroacupuncture on Rats with IBS Visceral Pain*, Shanghai university of traditional Chinese medicine, Shanghai, China, 2019.

[26] H. P. Yuan, *The Study on Duodenal Immune Activation and Alteration the Changes of Neurotransmitters in Patients with Functional Dyspepsia*, Shandong University, Jinan, China, 2012.

[27] J. Sousa-Valente, L. Calvo, V. Vacca, R. Simeoli, J. C. Arévalo, and M. Malcangio, "Role of TrkA signalling and mast cells in the initiation of osteoarthritis pain in the monoiodoacetate model," *Osteoarthritis and Cartilage*, vol. 26, no. 1, pp. 84–94, 2018.

[28] H. Vanheel and R. Farré, "Changes in gastrointestinal tract function and structure in functional dyspepsia," *Nature Reviews Gastroenterology & Hepatology*, vol. 10, no. 3, pp. 142–149, 2013.

[29] G. Sarnelli, M. Pesce, L. Seguella et al., "Impaired duodenal palmitoylethanolamide release underlies acid-induced mast cell activation in functional dyspepsia," *Cellular and Molecular Gastroenterology and Hepatology*, vol. 11, no. 3, pp. 841–855, 2021.

[30] W. L. Xu, *Explore the Mechanism of Electroacupuncture on Visceral Hypersensitivity in PI-IBS Rats Based on the Cycle of MC Degranulation-PAR2-CGRP*, Nanjing University of Traditional Chinese Medicine, Nanjing, China, 2019.

[31] P. Mrozkova, J. Palecek, and D. Spicarova, "The role of protease-activated receptor type 2 in nociceptive signaling and pain," *Physiological Research*, vol. 65, pp. 357–367, 2016.

[32] Y. Chen, C. Yang, and Z. J. Wang, "Proteinase-activated receptor 2 sensitizes transient receptor potential vanilloid 1, transient receptor potential vanilloid 4, and transient receptor potential ankyrin 1 in paclitaxel-induced neuropathic pain," *Neuroscience*, vol. 193, pp. 440–451, 2011.

[33] Z.-J. Huang, H.-C. Li, A. A. Cowan, S. Liu, Y.-K. Zhang, and X.-J. Song, "Chronic compression or acute dissociation of dorsal root ganglion induces cAMP-dependent neuronal hyperexcitability through activation of PAR2," *Pain*, vol. 153, no. 7, pp. 1426–1437, 2012.

[34] H. k. Hong, Y. Ma, and H. Xie, "TRPV1 and spinal astrocyte activation contribute to remifentanil-induced hyperalgesia in rats," *NeuroReport*, vol. 30, no. 16, pp. 1095–1101, 2019.

[35] X. Zhao, B. Xia, J. Cheng, M. X. Zhu, and Y. Li, "PKCε SUMOylation is required for mediating the nociceptive

signaling of inflammatory pain," *Cell Reports*, vol. 33, Article ID 108191, 2020.

[36] A. Kayssi, S. Amadesi, F. Bautista, N. W. Bunnett, and S. Vanner, "Mechanisms of protease-activated receptor 2-evoked hyperexcitability of nociceptive neurons innervating the mouse colon," *The Journal of Physiology*, vol. 580, no. 3, pp. 977–991, 2007.

[37] E. Jochmann, M. K. Boettger, P. Anand, and H.-G. Schaible, "Antigen-induced arthritis in rats is associated with increased growth-associated protein 43-positive intraepidermal nerve fibres remote from the joint," *Arthritis Research and Therapy*, vol. 17, no. 1, p. 299, 2015.

[38] M. M. Wouters, D. Balemans, S. Van Wanrooy et al., "Histamine receptor H1-mediated sensitization of TRPV1 mediates visceral hypersensitivity and symptoms in patients with irritable bowel syndrome," *Gastroenterology*, vol. 150, no. 4, pp. 875–887, 2016.

[39] F. F. Zhang and J. Z. Mo, "Effect of calcitonin gene related peptide on sensitivity alteration of visceral nervous system," *Chinese Journal of Gastroenterology and Hepatology*, vol. 14, pp. 200–202, 2005.

[40] T. Ono, M. Nagao, H. Imoto et al., "Effects of calcitonin gene-related peptide on colonic motility and defecation in conscious dogs," *Journal of Gastrointestinal Surgery*, vol. 22, no. 12, pp. 2097–2103, 2018.

[41] L. F. Wang, S. J. Zhang, J. Q. Si, H. Y. Hu, and Y. Z. Wang, "The role of substance P in the non central nervous system," *Journal of Shihezi University*, vol. 7, pp. 336–340, 2003.

[42] M. N. Islam, N. Maeda, E. Miyasato et al., "Expression of huntingtin-associated protein 1 in adult mouse dorsal root ganglia and its neurochemical characterization in reference to sensory neuron subpopulations," *IBRO Reports*, vol. 9, pp. 258–269, 2020.

[43] R. E. Coggeshall, "Fos, nociception and the dorsal horn," *Progress in Neurobiology*, vol. 77, pp. 299–352, 2005.

[44] N. Kalynovska, P. Adamek, and J. Palecek, "TRPV1 receptors contribute to paclitaxel-induced c-Fos expression in spinal cord dorsal horn neurons," *Physiological Research*, vol. 66, pp. 549–552, 2017.

[45] X. Ouyang, S. Li, J. Zhou, and J. D. Chen, "Electroacupuncture ameliorates gastric hypersensitivity via adrenergic pathway in a rat model of functional dyspepsia," *Neuromodulation: Technology at the Neural Interface*, vol. 23, no. 8, pp. 1137–1143, 2020.

[46] J. Zhou, S. Li, Y. Wang et al., "Inhibitory effects and mechanisms of electroacupuncture via chronically implanted electrodes on stress-induced gastric hypersensitivity in rats with neonatal treatment of iodoacetamide," *Neuromodulation: Technology at the Neural Interface*, vol. 20, no. 8, pp. 767–773, 2017.

Hindawi
Evidence-Based Complementary and Alternative Medicine
Volume 2021, Article ID 4296216, 11 pages
https://doi.org/10.1155/2021/4296216

Research Article

A Comparison Study of the Effect on IBS-D Rats among Ginger-Partitioned Moxibustion, Mild Moxibustion, and Laser Moxibustion

Chao Sun,[1] Xiaofeng Yang,[2] Sirui Xie,[3] Ziqin Zhou,[1] Guoliang Yu,[1] Shangsheng Feng,[4] Jingyu Zhao,[5] Jiangtao Wu,[1] and Changchun Ji[3]

[1]*Key Laboratory of Thermo-Fluid Science and Engineering of MOE, Xi'an Jiaotong University, Xi'an 710049, China*
[2]*Department of Pathogenic Microbiology and Immunology, School of Basic Medical Sciences, Xi'an Jiaotong University, Xi'an 710061, China*
[3]*Department of Acupuncture and Moxibustion, Shaanxi Traditional Chinese Medicine Hospital, Xi'an 710003, China*
[4]*School of Life Science and Technology, Xi'an Jiaotong University, Xi'an 710049, China*
[5]*Department of Acupuncture and Moxibustion, Xi'an Traditional Chinese Medicine Hospital, Xi'an 710021, China*

Correspondence should be addressed to Jiangtao Wu; jtwu@mail.xjtu.edu.cn and Changchun Ji; jichangchun1984@163.com

Received 12 September 2021; Revised 8 October 2021; Accepted 11 October 2021; Published 17 November 2021

Academic Editor: Mi Liu

Background. Diarrhea-predominant irritable bowel syndrome (IBS-D) is a functional gastrointestinal disorder that severely affects patients' life. Moxibustion is believed to be an effective way to treat IBS-D. However, the therapeutic effects and the underlying mechanisms in symptom management of IBS-D by different moxibustion therapies remain unclear. *Methods*. IBS-D model rats were divided into groups and treated with ginger-partitioned moxibustion (GPM), mild moxibustion (MM), and laser moxibustion (LM) at a temperature of 43°C, respectively. The temperature curves of acupoints were recorded during interventions. The therapeutic effects were evaluated on the basis of general condition, stool, and hematoxylin-eosin staining of the colon tissue. Moreover, the expression of transient receptor potential vanilloid 1 (TRPV1) receptors in both acupoint tissue and colon tissue was analyzed by immunohistochemistry. *Results*. After moxibustion treatment, the symptoms were improved. The expression of TRPV1 was increased in acupoint tissue and decreased in colon tissue. GPM and MM showed a more significant influence on IBS-D rats compared with LM. The temperature profile of GPM and MM was wave-like, while LM had an almost stable temperature curve. *Conclusion*. GPM, MM, and LM could improve the symptoms in IBS-D rats. Moxibustion might activate TRPV1 channels in the acupoint tissue and induce acupoint functions, which in turn inhibit the pathological activation state of the colon's TRPV1, followed by improvements in abdominal pain and diarrheal symptoms. LM with stable temperature might lead to the desensitization of TRPV1 receptors and the tolerance of acupoint. GPM and MM provided dynamic and repetitive thermal stimulations that perhaps induced acupoint sensitization to increase efficacy. Therefore, dynamic and repetitive thermal stimulation is recommended in the application of moxibustion.

1. Introduction

Irritable bowel syndrome (IBS) is a chronic functional gastrointestinal disorder characterized by altered bowel habits, abdominal pain, and bloating, with a global incidence as high as 23% [1, 2]. Diarrhea-predominant (IBS-D) is reported as the most common subtype of IBS (28%–46%), with recurrent abdominal pain and diarrhea as the main manifestations [3, 4]. IBS-D is characterized by prolonged treatment and easy relapse and is often accompanied by mental and psychological disorders such as anxiety and depression that will severely affect the quality of patients' lives and consume medical resources. According to the theory of Traditional Chinese Medicine, IBS-D patients have multiple spleen and stomach problems, loss of health and vitality, diarrhea, spleen and kidney issues, and loss of

kidney yang. Moxibustion, as one treatment of Traditional Chinese Medicine, is carried out by applying thermal stimulation on specific acupoints, which is believed to prevent and treat IBS-D [5].

With the continuous promotion and innovation of moxibustion therapies, there are more types of moxibustion therapy for clinical treatment of IBS-D. Numerous studies have shown the positive effects of moxibustion therapies for the treatment of IBS-D [6, 7]. Ma et al. [8] observed that herb-partitioned moxibustion greatly alleviated the symptoms of patients with IBS-D, and this appears to be a promising and efficacious treatment for IBS-D. Tong et al. performed mild moxibustion intervention on IBS-D models rats for one week and found that mild moxibustion improved the symptoms of diarrhea significantly [9]. Shi et al. [10] found that both electroacupuncture and moxibustion were effective in treatment of IBS patients. However, the intervention effect of different moxibustion therapies on IBS-D is still unclear, and there has been no consistent standard so far for the choice of moxibustion therapy for the treatment of IBS-D, which hampers the clinical application and promotion of moxibustion intervention in IBS-D.

The intensity of thermal stimulation is the premise for the desired therapeutic effect of moxibustion [11]. As *Lingshu Cijiezhenxie* says, "the fire is energized, the blood is right." Different intensities of thermal stimulation are related to different therapeutic effects in the treatment of IBS-D [12]. Temperature is a good quantitative form of the intensity of thermal stimulation [13–16]. Local moxibustion temperatures were closely related to the reaction of local receptors, which induced the thermal function of moxibustion [17]. Transient receptor potential vanilloid 1 (TRPV1), which can be activated by noxious thermal stimulation (>43°C) [18], is believed to be a key target in producing the therapeutic effect of moxibustion [19]. However, little attention has been paid to the temperature and its relationship with TRPV1 for the treatment of IBS-D in existing research. In addition, we must pay attention to not only the temperature value reached during moxibustion, but also the process of temperature variation, that is, the temperature characteristics of moxibustion.

In this study, we selected commonly used ginger-partitioned moxibustion, mild moxibustion, and laser moxibustion as thermal stimulation methods and IBS-D as the disease model. We applied moxibustion treatment in IBS-D rats and controlled the temperature of rat skin at approximately 43°C during moxibustion intervention. From the perspective of thermophysics, we investigated the therapeutic effect and molecular biological mechanisms of the three moxibustion therapies in IBS-D rats and explored the relationship of temperature characteristics and therapeutic effects.

2. Materials and Methods

2.1. Experimental Animals. Forty male Sprague Dawley rats weighing 150 g ± 20 g were supplied by the Laboratory Animal Center of Xi'an Jiaotong University. Each rat was housed in an individual cage. The room temperature and relative humidity were maintained at 20°C~25°C and 50%~70%, respectively. All experimental procedures were performed on the basis of the guidelines provided by the National Institute of Health for the Care and Use of Laboratory Animals, and the experimental protocol was approved by the Animal Ethics Committee of Shaanxi Traditional Chinese Medicine Hospital.

2.2. IBS-D Modeling and Identification. After three days of adaptive feeding, all rats without adverse reactions were randomly divided into normal group ($n = 8$) and IBS-D modeling group ($n = 32$). IBS-D was induced by intracolonic instillation of 1 mL glacial acetic acid (40 mL/L) at 8 cm proximal to the anus for 30 s. Then, 1 ml phosphate buffered saline (PBS, 0.01 mol/L) was injected to flush the colon [20]. In addition, the restraint stress stimulus was performed by restraining the rat's front shoulders, upper limbs, and chest using wide transparent tape to restrict it from scratching its head and face, lasting 2 h/day for one week [21].

To verify the modified IBS-D model and mental state, fur appearance and activity of rats were monitored. The 24 h food and water intakes were recorded. Weight increases of rats before and after modeling were calculated. Moreover, stools of rats were analyzed by the diarrhea index and Bristol stool scale.

Each rat in the normal group and the modeling group was put into a cage with a sparse grid at the bottom, and a tray was placed under the cage. A piece of filter paper the same size as the tray was put into it. Six hours later, all rats were put back into the feeding cage. The stools contaminated with filter paper were considered as loose stools, otherwise they were dry stools, and the loose stool rate was defined as the percentage of the number of loose stools to the total number of stools. Loose stools were graded by the measured contamination diameters according to Table 1, and then all loose stool grades were summed and divided by the total number of loose stools to obtain the final loose stool grade. Diarrhea index was obtained from the final loose stool grade multiplied with the loose stool rate.

As shown in Table 2, fecal scores of rats were recorded according to the Bristol stool scale to evaluate the fecal morphology [22]. According to the IBS-D classification criteria [23], loose stools (paste-like stools) or watery stools accounted for more than 25% of the total stool numbers, and hard or lumpy stools accounted for less 25% of the total stool numbers. The loose (paste-like) or watery stools and hard or lumpy stools corresponded to grades 1-2 and grades 6-7 of the Bristol classification, respectively.

2.3. Animal Grouping and Treatment. In our study, the rats were divided into a normal group for controls and a modeling group for further analysis. After successful establishment of the IBS-D model, rats in modeling group were randomly divided into four groups. As a result, we had five groups as follows:

Group 1. Normal (NC group, $n = 8$). Rats took food and water freely.

Table 1: Grades corresponding to the pollution diameter of loose stool.

Pollution diameter	Grade
<1.0 cm	1
≥1.0 cm and <2.0 cm	2
≥2.0 cm and <3.0 cm	3
≥3.0 cm	4

Table 2: Bristol stool scale classification of rat stool samples.

Performance	Characteristics	Score
Constipation	Separated hard lumps	1
	Sausage-like lumps	2
Normal	Strip-shaped excrement with fractures	3
	Soft and slick snake-like strip	4
Diarrhea	Soft crumbs with clear boundary	5
	Fluffy paste with ragged borders	6
	Watery stool without solid lumps	7

Group 2. IBS-D (MC group, n = 8). Rats took food and water freely.

Group 3. IBS-D + Ginger-Partitioned Moxibustion (GPM Group, n = 8). Ginger slice (18 mm in diameter and 3 mm in thickness) was placed on the Tianshu acupoint (ST25), and a moxa cone (7 mm in diameter and 9 mm in height, weight 50 mg) was placed on the ginger slice and ignited. When a moxa cone burned out, it was replaced by a new one. The moxibustion intervention lasted for one week for 30 min/day. ST25 is located on a horizontal line 5 "cun" above the symphysis pubis and 2 "cun" lateral to the midline [24].

Group 4. IBS-D + Mild Moxibustion (MM Group, n = 8). The ignited moxa stick (0.5 cm in diameter) was suspended approximately 1 cm above the Tianshu acupoint of rats for one week for 30 min/day. Ash deposited under the burning moxa stick was removed.

Group 5. IBS-D + Laser Moxibustion (LM Group, n = 8). A laser system (STL808T1-4.0 W, Beijing Stone Laser Technology Co., Ltd.) with an output power of 125 mW, and a laser beam radius of 2.5 mm was applied on ST25 of rats for one week for 30 min/day.

Surface temperatures of all rats at the ST25 acupoint during moxibustion treatment were recorded. For the GPM group, temperature was recorded by T-type thermocouples (Omega Engineering Inc., Stamford, CT, USA), while, for the MM group and LM group, temperatures were recorded by infrared camera (FLIR™ T420). The details of temperature recording and analysis can be found in our previous report [16]. In addition, mental state, fur appearance, activity, and weight changes of rats were monitored during moxibustion intervention. Stools of rats were also analyzed as modeling process did.

2.4. Preparation of Acupoint and Colon Tissue Samples. After seven-day treatment, tissue samples from ST25 acupoint area (2 cm in length by 2 cm in width) and colon (3 cm in length) at 8 cm proximal to the anus were collected. Acupoint tissue samples were used to observe the expression of TRPV1 in the acupoint area. Each colon sample was divided into two pieces for separate histological and immunohistochemistry analysis. All tissue samples were fixed with 4% paraformaldehyde solution.

2.5. Histological Analysis. To detect the epithelial structure and infiltration of inflammatory cells, colon samples were stained with hematoxylin-eosin (H&E). The samples fixed in 4% paraformaldehyde solution were dehydrated, paraffin-embedded, and sectioned at a 4 μm thickness. The colon tissue sections were soaked in hematoxylin staining solution for 5 min, followed by rinsing in running water several times, and placed into 1% hydrochloric acid alcohol for 2 s. Then, the sections were extracted and rinsed quickly with tap water. After that, the sections were placed into dilute lithium carbonate aqueous solution for about 30 s, followed by rinsing with tap water and dehydration with 80% ethanol, and finally, the sections were immersed in eosin staining solution for 20 s. The stained sections were placed into 95% ethanol (2 lanes, 10 s each), anhydrous ethanol (2 lanes, 2 min each), and xylene (2 lanes, 2 min each) in turn, and coverslips were mounted on the glass slides using neutral gum. All stained sections were observed with a light microscope.

2.6. Immunohistochemistry to Detect TRPV1 Expression. The expression of TRPV1 in the acupoint tissue and colonic tissue of all rats was detected by immunohistochemistry (IHC) staining. The paraffin sections of colon and acupoint tissue were deparaffinized in xylene I and II solutions for 10 min each and rehydrated in 100%, 95%, 85%, and 75% ethanol for 5 min. After washing with PBS for 30 min, tissue sections were immersed in 0.01 M citrate buffer (pH 6.0) and heated in a microwave at 98°C for 2.5 min, 1.5 min, and 1 min, with 15 min intervals for antigen retrieval. After cooling to room temperature, tissue sections were placed in 1% H_2O_2 for 10 min and washed in PBS. The tissue sections were incubated with endogenous peroxidase enzyme-blocking buffer for 10 min at room temperature, followed by washing in PBS. After 10 min of incubation with normal goat serum for blocking and washing in PBS, the sections were incubated with rabbit anti-TRPV1 antibody (bs-23927R, Bioss) overnight at 4°C. The sections were then rinsed with PBS and incubated with goat anti-rabbit/mouse IgG for 10 min at room temperature. After rinsing with PBS, the sections were incubated with streptavidin-HRP for 10 min at room temperature. Finally, DAB color development working solution was added on the tissue sections. The color development time was controlled by observation under the microscope, and when the best color development effect was achieved, the color development was discontinued by rinsing with tap water. After color development, the sections were restained with hematoxylin, dehydrated, and mounted with neutral gum. All stained sections were observed with a light microscope.

The positive expression fraction of TRPV1 was observed under the optical microscope as light yellow, brownish-yellow, or tan. Professional image analysis software Image-Pro Plus 6.0 was used for semiquantitative analysis of immunohistochemical-positive expression, and the mean optical density (MOD) was calculated. The tissue measurement area with staining tone on the image was selected randomly. Then, the integral optical density (IOD) and the size (or known as area of interest, AOI) of the selected area were calculated. The ratio of the integrated optical density to the positive area is the MOD; MOD = IOD/AOI. The MOD reflects the average depth of the positive signal, and a large MOD value is associated with strong protein expression, while a small MOD value is associated with weak protein expression.

2.7. Statistical Analysis. The results are presented as mean values ± standard error. Statistical analysis was performed using SPSS 21.0. One-way ANOVA was performed for experimental data among groups, and post-hoc tests were used for further analysis with significant effects. Significant differences were considered by a P-value of less than 0.05.

3. Results

3.1. Identification of IBS-D Model Rats. By comparing the appearance between the normal group and the modeling group, we found that rats in the normal group were active and alert. Their fur was white and shiny, and auricles were pale pink. The anus and tail were clean with no fecal staining. Rats in the modeling group appeared mentally fatigued with a thin body, were less active but aggressive, and liked to curl up in the corners. Their fur was withered and yellowish, and auricles were pale in color. Loose stools were stuck around their anus and tail.

Table 3 shows the statistics on food and water intake, weight change percent, and diarrhea index and Bristol stool scale of rats in the normal and modeling groups. After the modeling process, rats in the modeling group took less food and water compared with the normal group ($P < 0.05$). The weight change percent of rats in the modeling group was also much lower than that of the normal group ($P < 0.05$), and the weight change percent of IBS-D rats was negative, indicating that the weight of the rats was decreasing during the modeling process. After modeling, both the diarrhea index and Bristol stool scale of rats in modeling group were higher compared with the normal group ($P < 0.05$), and the Bristol stool scale classification for rats in the modeling group was in the range of diarrhea, as shown in Table 2. In all, our IBS-D model was successful.

3.2. Improvements in IBS-D Rats after Moxibustion Treatment. After one week of moxibustion treatment, rats in the three intervention groups showed improvement in their mental state. They increased self-motivated activities and their fur became shiny. No fecal material was found around the anus. Rats in the modeling group were thin and inactive. Fecal staining could be found around the anus and tail. The weight increases of rats in three intervention groups were higher than that in the modeling group, but no statistical differences in water and food intake were found among the groups.

Figure 1 shows the comparison of rat stool among groups. We can see that moxibustion treatment improved diarrheal symptoms in IBS-D rats. Loose stool rate and Bristol stool scale of rats in three moxibustion treatment groups were lower than in the modeling group ($P < 0.05$). In addition, the loose stool rate and Bristol stool scale of rats in the GPM and MM groups were lower than in the LM group, but there were no statistical differences in the Bristol stool scale.

3.3. Histological Observation. Figure 2 shows the results of hematoxylin-eosin (H&E) staining of rat colon tissue under a light microscope x100. There were no obvious pathological changes in the H&E staining of rat colon tissue in each group, suggesting that IBS-D is a nonorganic gastrointestinal disease. The colon tissue and mucosal structure of rats in the normal group and each intervention group were intact without hyperplasia of fibrous connective tissue. The colonic mucosa of rats in the IBS-D model group showed low-grade inflammation, cellulose exudation, and submucosal vasodilation but no obvious erosion and ulcer formation.

3.4. TRPV1 Expression in the ST25 Acupoint Area. Figure 3 shows the IHC staining of the TRPV1 receptor in acupoint tissues of rats (×200). The positive expression of TRPV1 receptor appears brownish-yellow or tan. Figure 4 shows the comparison of the MOD values of TRPV1 receptor expression in acupoint tissues of rats after moxibustion intervention (IHC staining, × 200). The MOD values of TRPV1 in the acupoint tissues of rats in the model group were higher than those in the normal group, and the difference was statistically significant ($P < 0.05$), indicating that TRPV1 receptor expression in the acupoint tissues of IBS-D rats was increased under pathological conditions. The expression of TRPV1 in the acupoint tissues of rats in the three moxibustion intervention groups was higher than that in the model group ($P < 0.05$), indicating that TRPV1 receptor expression was further increased after moxibustion intervention.

The expression of TRPV1 receptors in the acupoint tissues of GPM and MM were higher than that of LM ($P < 0.05$), indicating that GPM and MM were more effective than LM in increasing TRPV1 expression in the acupoint tissues. The effect on TRPV1 expression between GPM and MM showed nearly no difference.

3.5. TRPV1 Expression in the Colon Tissue. Figure 5 shows the IHC staining of the TRPV1 receptor in colon tissues of rats (×400). The positive expression of the TRPV1 receptor appears brownish-yellow or tan. Figure 6 shows the comparison of the MOD values of TRPV1 receptor expression in colon tissues of rats after moxibustion intervention (IHC staining, ×400). The mean optical density values of TRPV1 in the colon tissues of rats in the model group were higher

Table 3: Comparison of food and water intake, weight change rate, and stool of rats between normal and modeling groups after modeling.

Groups	n	Food intake	Water intake	Weight change percent	Diarrhea index	Bristol stool scale
Normal	8	24.4 ± 2.2	39.2 ± 4.2	26.9 ± 2.8	0	3.2 ± 0.4
Modeling	32	4.4 ± 0.5*	25.0 ± 3.5*	−17.4 ± 8.4*	0.7 ± 0.2*	5.7 ± 0.8*

*Compared with the normal group, $P < 0.05$.

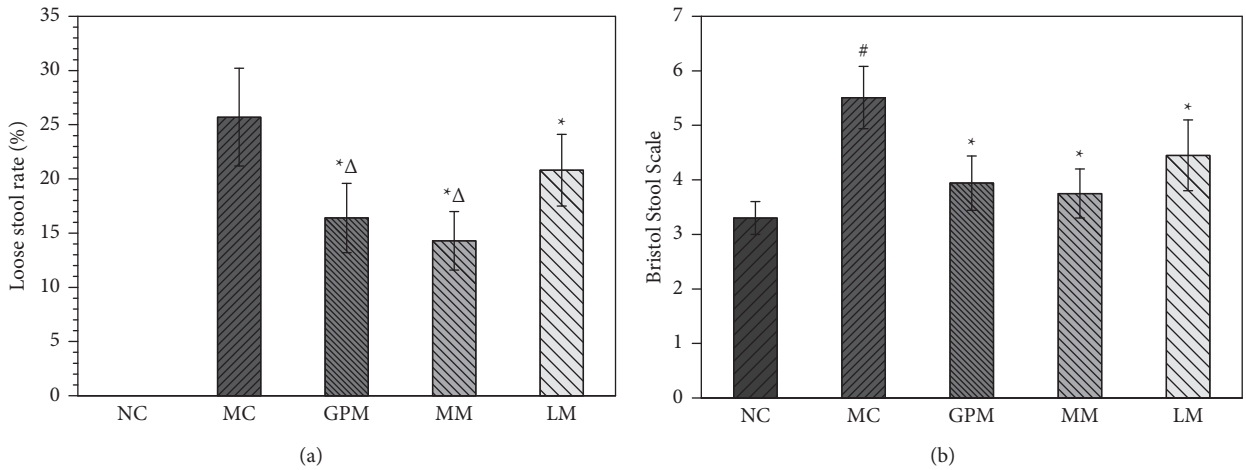

Figure 1: Comparison of rat stool among groups after treatment. NC: normal group; MC: IBS-D model group; GPM: IBS-D + ginger-partitioned moxibustion group; MM: IBS-D + mild moxibustion group; LM: IBS-D + laser moxibustion group. *Compared with MC, $P < 0.05$; $^{\Delta}$compared with LM, $P < 0.05$; $^{\#}$compared with NC, $P < 0.05$.

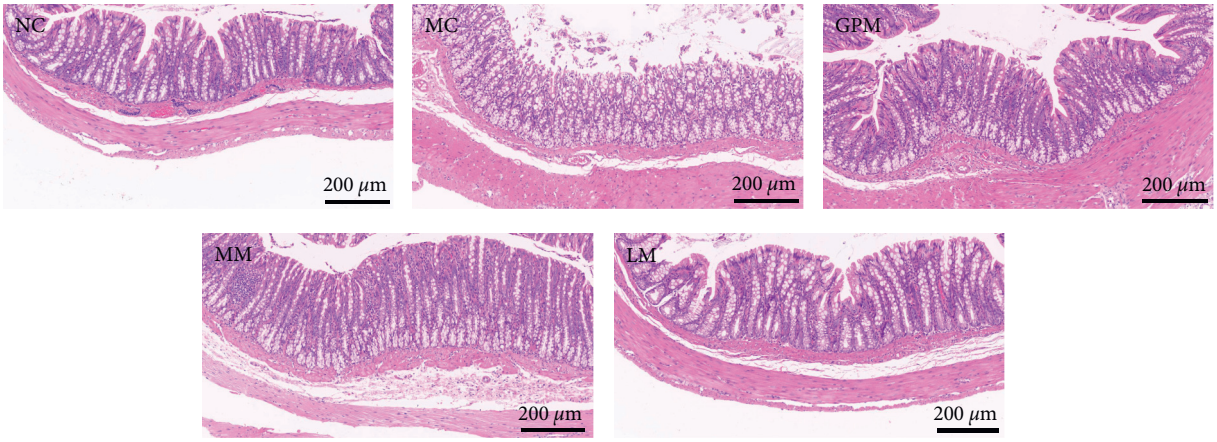

Figure 2: Pathological changes of colon tissue in rats (H&E staining, ×100). NC: normal group, MC: IBS-D model group; GPM: IBS-D + ginger-partitioned moxibustion group; MM: IBS-D + mild moxibustion group; LM: IBS-D + laser moxibustion group.

than those in the normal group, and the difference was statistically significant ($P < 0.05$), indicating that the modeling process in IBS-D rats could induce the expression of the.

The expression of TRPV1 in the colon tissues of rats in the three moxibustion intervention groups was lower than that in the model group ($P < 0.05$), indicating that moxibustion interventions effectively decreased the expression of TRPV1 receptor. By comparing the expression of TRPV1 receptors among three moxibustion treatment groups, it was the lowest in GPM, followed by MM, and highest in LM, but no significant statistical differences were observed between GPM and MM.

3.6. Temperature Profiles of the Acupoint during Moxibustion Intervention. Figure 7 shows temperature profiles of rat ST25 acupoints during moxibustion intervention. Ginger-partitioned moxibustion group (GPM), mild moxibustion group (MM), and laser moxibustion group (LM) are represented by a red line, black line, and green line, respectively. The temperature curve of GPM presents a wave-like change

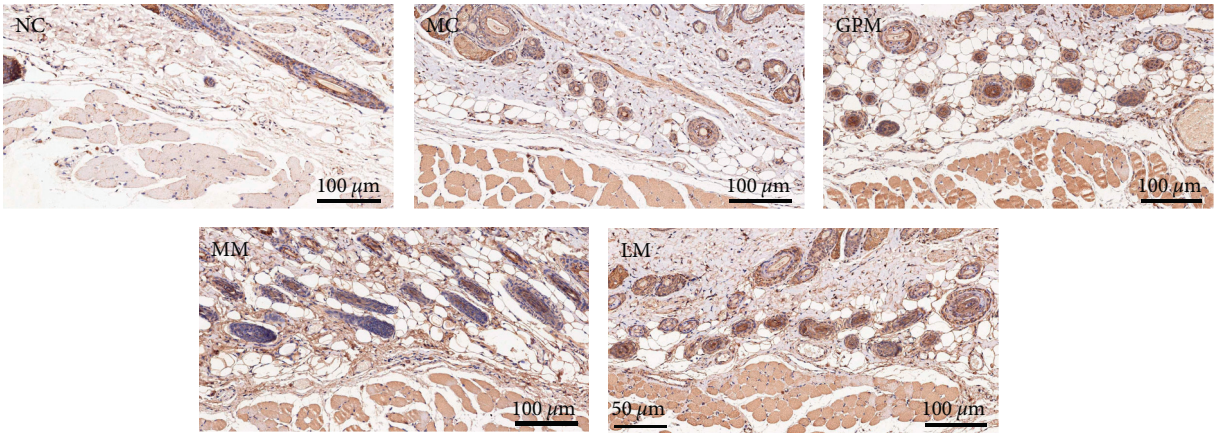

Figure 3: TRPV1 expression of acupoint tissue in rats (IHC staining, ×200). NC: normal group; MC: model group; GPM: IBS-D + ginger-partitioned moxibustion group; MM: IBS-D + mild moxibustion group; LM: IBS-D + laser moxibustion group.

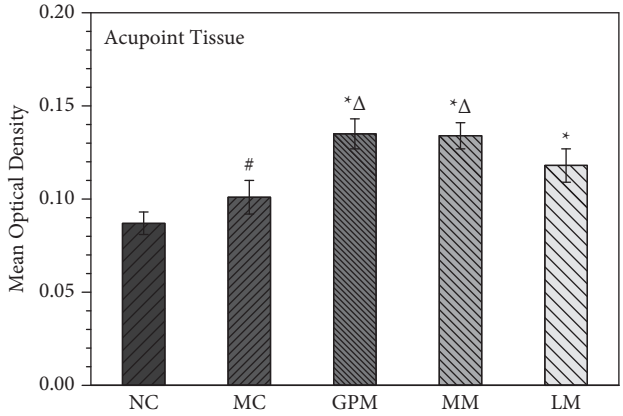

Figure 4: TRPV1 expression of acupoint tissue in rats. NC: normal group; MC: model group; GPM: IBS-D + ginger-partitioned moxibustion group; MM: IBS-D + mild moxibustion group; LM: IBS-D + laser moxibustion group. #Compared with NC, $P < 0.05$; *compared with MC, $P < 0.05$; Δcompared with LM, $P < 0.05$.

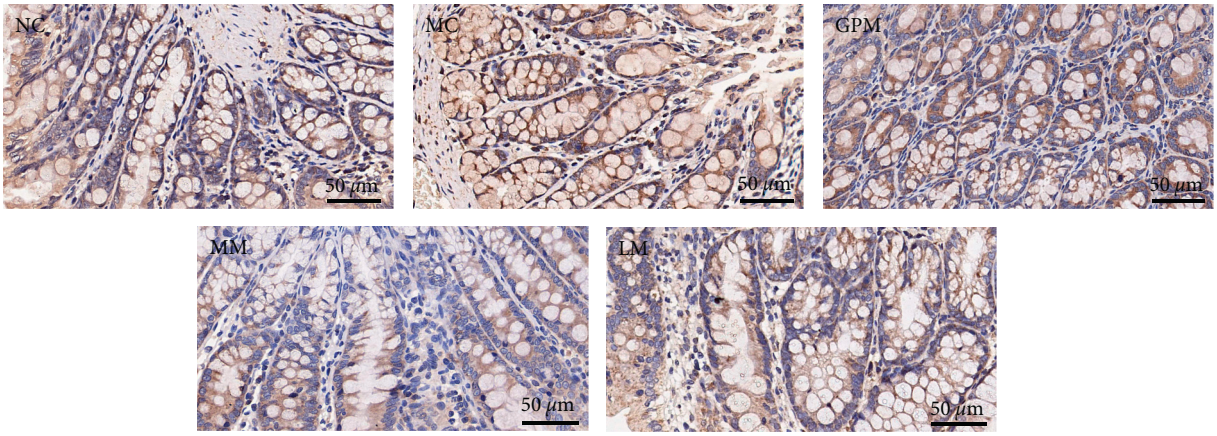

Figure 5: TRPV1 expression of colon tissue in rats (IHC staining, ×400). NC: normal group; MC: model group; GPM: IBS-D + ginger-partitioned moxibustion group; MM: IBS-D + mild moxibustion group; LM: IBS-D + laser moxibustion group.

that first rises and then falls, with a total of seven wave crests. The values of its first two crests were around 40.5°C and 42°C, respectively. After the third crest, the highest temperature during GPM reached approximately 43°C. The temperature curve of MM also showed a wave-like change but with a faster frequency compared with GPM. The value

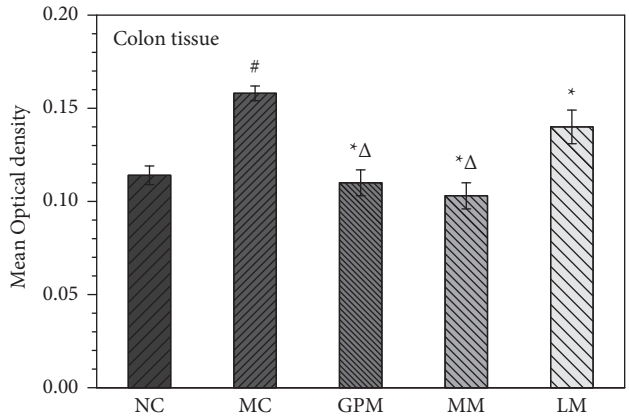

Figure 6: TRPV1 expression in rat colon tissue. NC: normal group; MC: model group; GPM: IBS-D + ginger-partitioned moxibustion group; MM: IBS-D+ mild moxibustion group; LM: IBS-D + laser moxibustion group. #Compared with NC, $P < 0.05$; *compared with MC, $P < 0.05$; Δcompared with LM, $P < 0.05$.

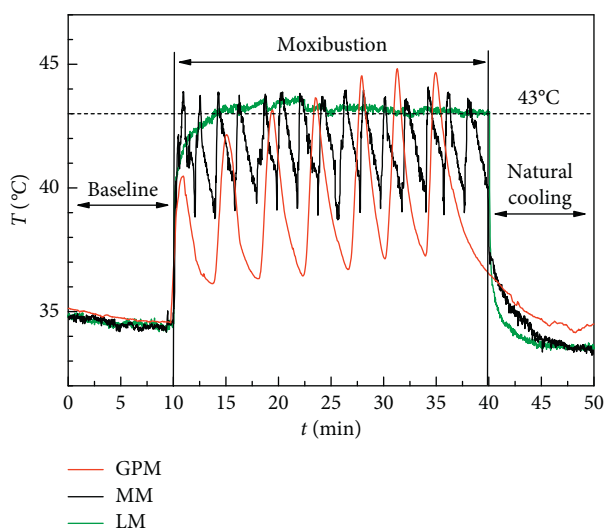

Figure 7: Temperature of rats in ST25 acupoints during moxibustion. GPM: ginger-partitioned moxibustion; MM: mild moxibustion; LM: laser moxibustion.

of the crest during MM also reached approximately 43°C. For LM, rat temperature increased quickly to around 40 upon the initiation of the laser system and reached approximately 43°C within next 3 min. Then, the temperature remained fairly stable at 43°C until the end of laser treatment.

4. Discussion

4.1. The Therapeutic Effect of Moxibustion Therapies on IBS-D Rats. According to the clinical manifestations of IBS-D, Chinese medicine classifies it as diarrhea and abdominal pain. The *JingYue QuanShu Xiexie* says "the origin of diarrhea is always due to the spleen and stomach," pointing to internal injury to the spleen and stomach as the root cause of diarrhea. According to the concept of seeking the root cause of the disease in Chinese medicine, spleen deficiency is the root of the pathogenesis of IBS-D, and its pathogenesis is related to the dysfunction of the spleen, liver, kidney, and other internal organs. Although the etiology of diarrhea is complex, the basic pathological changes are spleen deficiency and dampness obstruction. Meanwhile, the liver and spleen are physiologically coordinated with each other, while pathologically they affect each other, with the liver being responsible for drainage and the spleen being responsible for transportation and transformation. If the qi in liver is stagnant and crosses to the spleen, it leads to spleen dysfunction, spleen deficiency, and liver exuberance. Then, abdominal pain and diarrhea occur as a result.

The *Yixuerumen Zhenjiu* says "the deficient patients get moxibustion, so that the fire is helpful for their yuan yang; the sufficient patients get moxibustion, so that their sufficient pathogenic factors disperse with the fire; the cold patients get moxibustion, so that their qi will be rewarmed." Moxibustion plays the role of "warm dredging" and "warm nourishing" via thermally stimulating the body. The "moxibustion can make a supplement for the spleen and stomach" is described in the *Weishengbaojian*, which also means that moxibustion can warm the yang of the spleen and stop diarrhea. In Traditional Chinese Medicine, ST25 is a "mu" point of the large intestine, which regulates the function of the large intestine, spleen, and stomach [25]. According to our previous investigation on the selection rules of acupoint on treating IBS-D, ST25 is the most used acupoint during acupuncture and moxibustion intervention [26]. The results in this study indicated that all three moxibustion interventions on ST25 can improve the symptoms in IBS-D rats, showing a good therapeutic effect. This was shown by a significant improvement in the general condition of the rats and decreases in loose stools, the diarrhea index, and Bristol stool scale and increase of normal stools after treatment. In addition, GPM and MM showed a better therapeutic effect compared with LM, but no significant difference was observed between GPM and MM.

4.2. The Role of TRPV1 in IBS-D Management by Moxibustion Therapies. TRPV1 is one of the ligand-gated, nonselective positive ion channels that is activated when it binds to the corresponding ligand, and the channel opens to allow inward flow of Ca^{2+}, inducing biological effects [27]. Activation of TRPV1 induces the release of neuropeptides, such as substance P and calcitonin-related peptides, from neurons and their fibers [28]. TRPV1 acts as an injury receptor that responds to heat and a variety of chemicals, such as capsaicin, noxious thermal stimuli (>43°C), voltage, and acidic pH [18], so it plays an important role in pain physiology and pharmacology. Some studies have confirmed that moxibustion thermal stimulation can effectively regulate the expression of TRPV1, and TRPV1 is a key target in producing the therapeutic effects of moxibustion [19]. Comparison of the effects of moxibustion-like warm stimulation at different temperatures on gastric motility in TRPV1 knockout (TRPV1-/-) mice and C57BL/6 wild-type mice showed that moxibustion-like stimulation above 42°C

modulated gastric motility significantly, while TRPV1 knockout significantly reduced the related effects [29].

TRPV1 is widely expressed within sensory neurons innervating the gastrointestinal tract and its fibers and can be involved in various functions, such as protection of the gastrointestinal mucosa, gastrointestinal motility, sensation, and endocrine activity, and has important significance in the pathogenesis of visceral hypersensitivity and gastrointestinal motility disorders in functional gastrointestinal diseases [30–32]. The hypersensitivity of the intestine to pain sensation is one of the main pathological features of IBS, and the main mechanism of its formation is closely related to the increased sensitivity of intestinal receptors and abnormal excitation of sensory afferent nerves. It has been found that activation of TRPV1 in the gastrointestinal tract opens Ca^{2+} channels and causes the release of neurotransmitters such as vasoactive intestinal peptide and SP from neurons and their fibers, thereby regulating visceral sensation and gastrointestinal dynamics and triggering or facilitating the pain process [33]. Clinical trials found that the expression level of TRPV1 in the colonic mucosa of IBS patients was 3.5 times higher than that in healthy control subjects and was positively correlated with the degree of abdominal pain [34–36]. The sensitivity of rats with TRPV1 knockout was significantly reduced when their gastrointestinal tract was mechanically stimulated [37]. Thus, TRPV1 plays an important role in the pathogenesis of IBS-D and in the generation of visceral hypersensitivity [38, 39].

In this study, we found that the expression of TRPV1 receptors in both acupoint tissues and colonic tissues of IBS-D model rats was higher than that in normal healthy rats, indicating that the acupoint area may become activated from a dormant state, and the colonic tissues showed a pathologically activated state. The intervention of three moxibustion treatments further increased the expression of the TRPV1 receptor in acupoint tissue while decreasing the expression of the TRPV1 receptor in colon tissue. Moxibustion might play a role in the treatment of IBS-D by thermal stimulation to activate TRPV1 channels in the acupoint tissue and induce acupoint functions, which in turn inhibit the pathological activation state of TRPV1 ion channels in the colon, followed by a reduction of intestinal hypersensitivity and regulation of colon motility, as well as improvements in abdominal pain and diarrheal symptoms.

The investigation on the signaling pathway between acupoint function and the reaction of viscera is a significant and crucial topic for acupoint intervention on intestinal diseases. Some innovative efforts have been made to reveal the possible signaling pathway of acupoint intervention on IBS-D. For example, Chen et al. [40] and Li [41] proposed that acupoint intervention might modulate Pirt-TRPV1 signaling pathway and PLC-TRPV1 signaling pathway, respectively, and inhibit the abnormal expression of TRPV1 in colonic tissues, followed by the alleviation of visceral pain. However, the exact pathogenesis of IBS remains unclear, as it has become apparent that multiple pathways are activated in the condition, including inflammation, immunology, neurology, and psychology [42]. More biomedical experiments are needed in the future to explore how acupoint inhibits the pathological activation of TRPV1 ion channel in colon in the treatment of IBS-D by acupoint intervention.

4.3. Dynamic and Repeated Thermal Stimulation Induce Sensitization of Receptors and Acupoints. The activation of TRPV1 receptors is closely related to the temperature of the thermal stimulus. It was shown that a rapid temperature rise enables relatively fast activation of TRPV1 receptors, with channel currents reaching a plateau in less than 500 ms [43]. In addition, the temperature threshold at which TRPV1 is activated is not fixed but regulated by chemical ligands and channel phosphorylation status. For example, when the TRPV1 receptor is phosphorylated by protein kinase C, its channel can be opened at the normal body temperature [44]. Studies have shown that, after the initial burning sensation following local skin application of capsaicin, sensory nerves become desensitized to heat, capsaicin, and other types of stimuli, and removal of extracellular calcium ions can greatly diminish or even eliminate the desensitization phenomenon [45]. When high concentrations of capsaicin are applied to sensory nerve cells over a long period of time, TRPV1 channel currents show an initial spike followed by a low flat "plateau" in a biphasic manner [46]. Sustained thermal stimulation can also lead to desensitization of TRPV1 receptors in a noncalcium-dependent manner [47]. When TRPV1 receptor desensitization occurs, the probability of receptor activation or the value of channel currents in response to noxious thermal stimulation will decrease.

Research from multiple disciplines supports the notion that the temporal characteristics of repetitive drug, electrophysiological, or psychological stimuli influence the direction of cellular and behavioral adaptation. Chronic continuous stimulation is usually associated with the development of tolerance, whereas intermittent stimulation may have the opposite effect and be associated with sensitization or reverse tolerance [48]. Studies have shown that repetitive stimulation can cause sensitization of the nervous system, or an enhancement of the response, generally arising from injury to the receptors [49]. For example, Bessou and Perl [50] found that repetitive noxious thermal stimulation (>45°C) can induce the sensitization of cutaneous C receptor. In recent years, the tolerance and sensitization of acupoints have gradually become a focus of traditional Chinese medicine research [51–53]. The study of acupoint analgesia by electroacupuncture found that the analgesic effect of electroacupuncture with a frequency of once a day was not cumulative but weakened, with the increase in the intensity of electroacupuncture resulting from the emergence of acupoint tolerance [54]. Heat-sensitive moxibustion usually showed a greater therapeutic effect compared with traditional moxibustion [55, 56]. Moreover, sensitized acupoint stimulation could improve gastrointestinal function in irritable bowel syndrome rats, either through electroacupuncture or moxibustion [57, 58].

Based on the previously mentioned analysis, different moxibustion therapies could induce different temperature curves on the skin of rat acupoints. The fluctuating temperature profiles of GPM and MM could provide dynamic

and repetitive thermal stimulation on the acupoint area and perhaps induce acupoint sensitization for better efficacies. The temperature profile of LM basically remained stable after a rapid increase, which might lead to the desensitization of TRPV1 receptors and tolerance in the acupoint, reducing the therapeutic effect as a result. Therefore, for the clinical application of moxibustion therapies, it is recommended to perform dynamic and repetitive thermal stimulation on the acupoints to induce acupoint sensitization and thus improve the therapeutic effect of moxibustion.

5. Conclusion

In summary, we compared the therapeutic effects of pretreatment of the Tianshu (ST25) acupoint on IBS-D model rats under three moxibustion therapies. Some conclusions are as follows: GPM, MM, and LM with temperature of 43°C could effectively improve the symptoms of IBS-D rats. Moxibustion might play a role in the treatment of IBS-D by activating TRPV1 channels in the acupoint tissue and induce acupoint functions, which in turn inhibit the pathological activation state of TRPV1 ion channels in the colon, followed by improvements in abdominal pain and diarrheal symptoms. LM with stable temperature might lead to the desensitization of TRPV1 receptors and tolerance in the acupoint. The fluctuating temperature profiles of GPM and MM could provide dynamic and repetitive thermal stimulation for the acupoint area and perhaps induce acupoint sensitization for better efficacy. Therefore, dynamic and repetitive thermal stimulation is recommended in the application of moxibustion.

Data Availability

The data used to support the findings of this study are available from the corresponding author upon request.

Disclosure

Chao Sun and Xiaofeng Yang are the co-first authors.

Conflicts of Interest

The authors declare that they have no conflicts of interest.

Acknowledgments

The authors thank Baojun Zhang for his assistance during the animal experiments. This work was supported by the National Natural Science Foundation of China (82074560, 51706177, and 51676156) and Innovation Capability Support Program of Shaanxi (2020KJXX-075).

References

[1] D. Keszthelyi, F. J. Troost, and A. A. Masclee, "Irritable bowel syndrome: methods, mechanisms, and pathophysiology. Methods to assess visceral hypersensitivity in irritable bowel syndrome," *American Journal of Physiology - Gastrointestinal and Liver Physiology*, vol. 303, no. 2, pp. G141–G154, 2012.

[2] L. Saha, "Irritable bowel syndrome: pathogenesis, diagnosis, treatment, and evidence-based medicine," *World Journal of Gastroenterology*, vol. 20, no. 22, pp. 6759–6773, 2014.

[3] G. F. Longstreth, W. G. Thompson, W. D. Chey, L. A. Houghton, F. Mearin, and R. C. Spiller, "Functional bowel disorders," *Gastroenterology*, vol. 130, no. 5, pp. 1480–1491, 2006.

[4] D. J. Gracie and A. C. Ford, "Irritable bowel syndrome-type symptoms are associated with psychological comorbidity, reduced quality of life, and health care use in patients with inflammatory bowel disease," *Gastroenterology*, vol. 153, no. 1, pp. 324-325, 2017.

[5] H. Y. Li, W. M. Liu, and K. Jie, "Advances in the treatment of diarrheal irritable bowel syndrome with Chinese medicine," *Modern Journal of Integrated Traditional Chinese and Western Medicine*, vol. 30, no. 2, pp. 221–225, 2021.

[6] G. Chen, G. U. O. Song, and X. Su, "Research progress of moxibustion in treatment of irritable bowel syndrome," *World Journal of Acupuncture-Moxibustion*, vol. 31, no. 2, pp. 136–140, 2020.

[7] X. Lin, X. Liu, J. Xu et al., "Metabolomics analysis of herb-partitioned moxibustion treatment on rats with diarrhea-predominant irritable bowel syndrome," *Chinese Medicine*, vol. 14, no. 1, p. 18, 2019.

[8] Y. X. Ma, X. Liu, C. Z. Liu et al., "Randomized clinical trial: the clinical effects of herb-partitioned moxibustion in patients with diarrhoea-predominant irritable bowel syndrome," *Evidence-based Complementary and Alternative Medicine: eCAM*, vol. 2013, Article ID 605460, 2013.

[9] L. Tong, L. B. Wu, and N. Li, "Moxibustion relieves abdominal hypersensitivity and diarrhea by regulating colonic 5-hydroxytryptamine signaling pathway in rats with diarrhea type irritable bowel syndrome," *Acupuncture Research*, vol. 45, no. 7, pp. 535–540, 2020.

[10] Y. Shi, Y. H. Chen, and X. J. Yin, "Electroacupuncture versus moxibustion for irritable bowel syndrome: a randomized, parallel-controlled trial," *Evidence-Based Complementary and Alternative Medicine*, vol. 2015, Article ID 361786, 2015.

[11] L. Li, J. S. Yang, and P. J. Rong, "Effect of moxibustion-like thermal stimulation with different temperature and covering different areas of "zhongwan" (CV12) on discharges of neurons in medullary subnucleus reticularis dorsalis of rats," *Acupuncture Research*, vol. 36, no. 5, pp. 313–320, 2011.

[12] J.-M. Zhao, L. Y. Wu, and H. R. Liu, "Factorial study of moxibustion in treatment of diarrhea-predominant irritable bowel syndrome," *World Journal of Gastroenterology*, vol. 20, no. 37, pp. 13563–13572, 2014.

[13] C. Sun, C. Ji, and Y. Li, "A comparison study of photothermal effect between moxibustion therapy and laser irradiation on biological tissue," *International Journal of Thermal Sciences*, vol. 164, Article ID 106924, 2021.

[14] Y. Li, C. Sun, and J. Kuang, "The effect of moxibustion stimulation on local and distal skin temperature in healthy subjects," *Evidence-Based Complementary and Alternative Medicine*, vol. 2019, Article ID 3185987, 2019.

[15] C. Sun, Y. Li, J. Kuang, X. Liang, J. Wu, and C. Ji, "The thermal performance of biological tissue under moxibustion therapy," *Journal of Thermal Biology*, vol. 83, pp. 103–111, 2019.

[16] Y. Li, C. Sun, and J. Kuang, "An in vitro and numerical study of moxibustion therapy on biological tissue," *IEEE Transactions on Biomedical Engineering*, vol. 65, no. 4, pp. 779–788, 2017.

[17] H. Deng and X. Shen, "The mechanism of moxibustion: ancient theory and modern research," *Evidence-based*

Complementary and Alternative Medicine: eCAM, vol. 2013, Article ID 379291, 2013.

[18] M. J. Caterina, M. A. Schumacher, M. Tominaga, T. A. Rosen, J. D. Levine, and D. Julius, "The capsaicin receptor: a heat-activated ion channel in the pain pathway," *Nature*, vol. 389, no. 6653, pp. 816–824, 1997.

[19] J. Jinfeng, W. Xinjun, W. Xiaojing, and Y. Zhi, "Analysis of factors influencing moxibustion efficacy by affecting heat-activated transient receptor potential vanilloid channels," *Journal of Traditional Chinese Medicine*, vol. 36, no. 2, pp. 255–260, 2016.

[20] J.-H. La, T. W. Kim, and T. S. Sung, "Visceral hypersensitivity and altered colonic motility after subsidence of inflammation in a rat model of colitis," *World Journal of Gastroenterology*, vol. 9, no. 12, pp. 2791–2795, 2003.

[21] C. L. Williams, R. G. Villar, J. M. Peterson, and T. F. Burks, "Stress-induced changes in intestinal transit in the rat: a model for irritable bowel syndrome," *Gastroenterology*, vol. 94, no. 3, pp. 611–621, 1988.

[22] M. R. Blake, J. M. Raker, and K. Whelan, "Validity and reliability of the Bristol Stool Form Scale in healthy adults and patients with diarrhoea-predominant irritable bowel syndrome," *Alimentary Pharmacology & Therapeutics*, vol. 44, no. 7, pp. 693–703, 2016.

[23] X. Yao, Y.-S. Yang, K.-B. Zhao, G. Sun, Y.-S. Liu, and W.-F. Wang, "Clinical features and subtypes of irritable bowel syndrome based on Rome III diagnostic criteria," *World Chinese Journal of Digestology*, vol. 16, no. 5, pp. 563–566, 2008.

[24] H.-R. Liu, X.-M. Wang, E.-H. Zhou et al., "Acupuncture at both ST25 and ST37 improves the pain threshold of chronic visceral hypersensitivity rats," *Neurochemical Research*, vol. 34, no. 11, pp. 1914–1918, 2009.

[25] E.-H. Zhou, H.-R. Liu, H.-G. Wu et al., "Herb-partition moxibustion relieves chronic visceral hyperalgesia and 5-HT concentration in colon mucosa of rats," *Neurological Research*, vol. 31, no. 7, pp. 734–737, 2009.

[26] P. Wang, Y. F. Bi, and C. C. Ji, "Research on the selection rules of acupoint selection on treating diarrhea-predominant irritable bowel syndrome with acupuncture and moxibustion," *International Journal of Translation & Community Medicine*, vol. 43, no. 3, pp. 285–289, 2021.

[27] O. Gouin, K. L'Herondelle, N. Lebonvallet et al., "TRPV1 and TRPA1 in cutaneous neurogenic and chronic inflammation: pro-inflammatory response induced by their activation and their sensitization," *Protein & Cell*, vol. 8, no. 9, pp. 644–661, 2017.

[28] E. Cao, M. Liao, Y. Cheng, and D. Julius, "TRPV1 structures in distinct conformations reveal activation mechanisms," *Nature*, vol. 504, no. 7478, pp. 113–118, 2013.

[29] Y. S. Su, J. J. Xin, Z. K. Yang et al., "Effects of different local moxibustion-like stimuli at zusanli (ST36) and zhongwan (CV12) on gastric motility and its underlying receptor mechanism," *Evidence-based Complementary and Alternative Medicine: eCAM*, vol. 2015, Article ID 486963, 2015.

[30] X.-J. Luo, J. Peng, and Y.-J. Li, "Recent advances in the study on capsaicinoids and capsinoids," *European Journal of Pharmacology*, vol. 650, no. 1, pp. 1–7, 2011.

[31] K. Alawi and J. Keeble, "The paradoxical role of the transient receptor potential vanilloid 1 receptor in inflammation," *Pharmacology & Therapeutics*, vol. 125, no. 2, pp. 181–195, 2010.

[32] J. Peng and Y. J. Li, "The vanilloid receptor TRPV1: role in cardiovascular and gastrointestinal protection," *European Journal of Pharmacology*, vol. 627, no. 1-3, pp. 1–7, 2010.

[33] P. Holzer, E. Painsipp, and R. Schuligoi, "Differential effects of intragastric acid and capsaicin on gastric emptying and afferent input to the rat spinal cord and brainstem," *BMC Neuroscience*, vol. 6, no. 1, pp. 60–69, 2005.

[34] G. Barbara, C. Cremon, R. De Giorgio et al., "Mechanisms underlying visceral hypersensitivity in irritable bowel syndrome," *Current Gastroenterology Reports*, vol. 13, no. 4, pp. 308–315, 2011.

[35] W. Boesmans, G. Owsianik, J. Tack, T. Voets, and P. Vanden Berghe, "TRP channels in neurogastroenterology: opportunities for therapeutic intervention," *British Journal of Pharmacology*, vol. 162, no. 1, pp. 18–37, 2011.

[36] A. B. Beckers, Z. Z. R. M. Weerts, Z. Helyes, A. A. M. Masclee, and D. Keszthelyi, "Review article: transient receptor potential channels as possible therapeutic targets in irritable bowel syndrome," *Alimentary Pharmacology & Therapeutics*, vol. 46, no. 10, pp. 938–952, 2017.

[37] S. M. Brierley, "Visualising vagal afferent neurons and their terminals whilst silencing TRPV1," *The Journal of physiology*, vol. 588, no. 21, pp. 4069-4070, 2010.

[38] M. H. Farzaei, R. Bahramsoltani, M. Abdollahi, and R. Rahimi, "The role of visceral hypersensitivity in irritable bowel syndrome: pharmacological targets and novel treatments," *Journal of Neurogastroenterology and Motility*, vol. 22, no. 4, pp. 558–574, 2016.

[39] A. Akbar, Y. Yiangou, P. Facer, J. R. F. Walters, P. Anand, and S. Ghosh, "Increased capsaicin receptor TRPV1-expressing sensory fibres in irritable bowel syndrome and their correlation with abdominal pain," *Gut*, vol. 57, no. 7, pp. 923–929, 2008.

[40] Y. Chen, Y. Zhao, and L. Wang, "Involvement of Pirt/TRPV1 signaling in acupuncture-induced reduction of visceral hypersensitivity in diarrhea-predominant irritable bowel syndrome rats," *Acupuncture Research*, vol. 46, no. 4, pp. 278–283, 2021.

[41] T. Li, *Study on the Mechanism of Moxibustion Intervention in Visceral Pain of IBS Based on PLC-TRPV1 Pathway*, Shanghai University of Traditional Chinese Medicine, Shanghai, China, 2019.

[42] K. Yaklai, S. Pattanakuhar, N. Chattipakorn, and S. C. Chattipakorn, "The role of acupuncture on the gut-brain-microbiota axis in irritable bowel syndrome," *American Journal of Chinese Medicine*, vol. 49, no. 02, pp. 285–314, 2021.

[43] P. Hayes, H. J. Meadows, M. J. Gunthorpe et al., "Cloning and functional expression of a human orthologue of rat vanilloid receptor-1," *Pain*, vol. 88, no. 2, pp. 205–215, 2000.

[44] V. Vellani, S. Mapplebeck, A. Moriondo, J. B. Davis, and P. A. McNaughton, "Protein kinase C activation potentiates gating of the vanilloid receptor VR1 by capsaicin, protons, heat and anandamide," *The Journal of physiology*, vol. 534, no. 3, pp. 813–825, 2001.

[45] A. Szallasi and P. M. Blumberg, "Vanilloid (Capsaicin) receptors and mechanisms," *Pharmacological Reviews*, vol. 51, no. 2, pp. 159–212, 1999.

[46] V. Lukacs, Y. Yudin, G. R. Hammond, E. Sharma, K. Fukami, and T. Rohacs, "Distinctive changes in plasma membrane phosphoinositides underlie differential regulation of TRPV1 in nociceptive neurons," *Journal of Neuroscience*, vol. 33, no. 28, pp. 11451–11463, 2013.

[47] M. Tominaga, M. J. Caterina, A. B. Malmberg et al., "The cloned capsaicin receptor integrates multiple pain-producing stimuli," *Neuron*, vol. 21, no. 3, pp. 531–543, 1998.

[48] R. M. Post, "Intermittent versus continuous stimulation: effect of time interval on the development of sensitization or tolerance," *Life Sciences*, vol. 26, no. 16, pp. 1275–1282, 1980.

[49] S. A. Prescott, "Interactions between depression and facilitation within neural networks: updating the dual-process theory of plasticity," *Learning & Memory (Cold Spring Harbor, N.Y.)*, vol. 5, no. 6, pp. 446–466, 1998.

[50] P. Bessou and E. R. Perl, "Response of cutaneous sensory units with unmyelinated fibers to noxious stimuli," *Journal of Neurophysiology*, vol. 32, no. 6, pp. 1025–1043, 1969.

[51] H. Tan, S. Tumilty, C. Chapple et al., "Understanding acupoint sensitization: a narrative review on phenomena, potential mechanism, and clinical application," *Evidence-based Complementary and Alternative Medicine: eCAM*, vol. 2019, Article ID 6064358, 2019.

[52] Y.-N. Luo, Y.-M. Zhou, X. Zhong et al., "Observation of pain-sensitive points in patients with knee osteoarthritis: a pilot study," *European Journal of Integrative Medicine*, vol. 21, pp. 77–81, 2018.

[53] B. Zhu, "The sensitization phenomenon of acupoint and biological significances," *Chinese Acupuncture & Moxibustion*, vol. 39, no. 2, pp. 115–121, 2019.

[54] H. C. Wang, Y. Wang, and L. Yao, "Comparison of the therapeutic effect of electroacpuncture with different interval for treatment of chronic neuropathic pain in rats," *Acupuncture Research*, vol. 2, pp. 112–118, 2002.

[55] A. J. Xiao, L. He, X. Ouyang, J. M Liu, and M. R Chen, "Comparison of the anti-apoptotic effects of 15- and 35-minute suspended moxibustion after focal cerebral ischemia/reperfusion injury," *Neural Regeneration Research*, vol. 13, no. 2, pp. 257–264, 2018.

[56] H. Huang, F. Feng, J. Wang et al., "Effect of moxibustion at sensitized-acupoints on quality of life in patients with chronic superficial gastritis," *Journal of Acupuncture and Tuina Science*, vol. 18, no. 6, pp. 425–430, 2020.

[57] C. C. Lei, L. Li, and H. Zhang, "Effect of electroacupuncture stimulation of sensitized acupoints on bowel dysfunction in rats with diarrhea-predominant irritable bowel syndrome," *Acupuncture Research*, vol. 42, no. 5, pp. 413–417, 2017.

[58] H. Zhang, F. Xie, and H. Gong, "Effects of heat-sensitive moxibustion on HPA axis in rats with irritable bowel syndrome," *Chinese Acupuncture & Moxibustion*, vol. 37, no. 12, pp. 1315–1321, 2017.

Hindawi
Evidence-Based Complementary and Alternative Medicine
Volume 2021, Article ID 9945121, 12 pages
https://doi.org/10.1155/2021/9945121

Research Article

Genome-Wide Regulation of Acupuncture and Moxibustion on Ulcerative Colitis Rats

Zhaoqin Wang,[1,2] **Yan Huang**,[2,3] **Di Wang**,[2,3] **Rumeng Wang**,[4] **Kunshan Li**,[2,3] **Qin Qi**,[3] **Zhe Ma**,[2,3] **Muen Gu**,[3] **Handan Zheng**,[2,3] **Yuan Lu**,[2,3] **and Luyi Wu**[5]

[1]*Department of Aeronautics and Astronautics, Shanghai Key Laboratory of Acupuncture Mechanism and Acupoint Function, Fudan University, Shanghai 200433, China*
[2]*Shanghai Research Institute of Acupuncture and Meridian, Shanghai 200030, China*
[3]*Yueyang Hospital of Integrated Traditional Chinese and Western Medicine, Shanghai University of Traditional Chinese Medicine, Shanghai 200437, China*
[4]*Shanghai TCM-integrated Hospital, Shanghai University of Traditional Chinese Medicine, Shanghai 200082, China*
[5]*Shanghai University of Traditional Chinese Medicine, Shanghai 201203, China*

Correspondence should be addressed to Yuan Lu; luyuan_sh@163.com and Luyi Wu; luyitcm@163.com

Received 20 June 2021; Revised 4 September 2021; Accepted 6 September 2021; Published 8 October 2021

Academic Editor: Mi Liu

Acupuncture and moxibustion have definite clinical effects on treating ulcerative colitis (UC), but their mechanism is still unclear. To investigate the molecular mechanisms, we applied herb-partitioned moxibustion or electroacupuncture at the Tianshu (ST25) points on UC rats and used RNA sequencing to identify molecular consequences. Male Sprague Dawley (SD) rats were divided into 6 groups randomly: the normal control (NC) group, the control + herb-partitioned moxibustion (NCHM) group, the control + electroacupuncture (NCEA) group, the model (UC) group, the model + herb-partitioned moxibustion (UCHM) group, and the model + electroacupuncture (UCEA) group. Compared to the UC group, HE staining in the UCHM group and UCEA group indicated that colitis was relieved, the histopathological score and MPO were both significantly reduced, and the serum hs-CRP concentration was decreased significantly. The results of RNA-seq suggested that, compared to the NC group, 206 upregulated genes and 167 downregulated genes were identified in colon tissues from the UC group; compared to the UC group, the expression levels of some genes were both affected in the UCHM group and the UCEA group (684 differentially expressed genes were identified in the UCHM group, and 1182 differentially expressed genes were identified in the UCEA group). KEGG signal pathway analysis indicated that the differentially expressed genes in the UCHM group were associated with the JAK-STAT signaling pathway and cell adhesion molecule (CAM); the differentially expressed genes in the UCEA group were associated with the NF-κB signaling pathway, the toll-like receptor signaling pathways, the PI3K-Akt signaling pathway, the MAPK signaling pathway, and the Wnt signaling pathway. This is the first study to reveal the gene expression characteristics of the anti-inflammatory effect of UC rats from the perspective of acupuncture and moxibustion control, which provide a clue for further investigation into the molecular mechanisms of UC treatment by acupuncture and moxibustion.

1. Introduction

Ulcerative colitis (UC) is characterized by chronic nonspecific inflammation involving the colonic and rectal mucosa. UC is considered an intractable disease in clinical practice, and the etiology and pathogenesis have been incompletely elucidated. The clinical manifestations mainly include abdominal pain, diarrhea, and bloody purulent stool. Most patients experience lifelong recurrence, which causes immense pain and severely influences their quality of life. In recent decades, statistical analyses have shown that the incidence of UC in Europe and North America shows an increasing trend year by year [1]. In China, the incidence of UC is rising sharply in recent years as people's lifestyles have changed and diagnostic levels have improved [2]. The pathogenesis of UC is not yet

completely clear, and modern medicine considers that its onset may be associated with many factors, mainly including genetics, environment, diet, gut microbiota, and immunity [3]. The current treatment methods for UC in clinical practice mainly include drug control and surgery; however, both methods have certain limitations. Drugs used to treat UC can only improve symptoms and delay disease progression but cannot effectively control or cure UC, and the long-term therapeutic efficacy is not ideal. In addition, adverse reactions to drugs have caused many problems for patients that further influence the therapeutic efficacy.

Acupuncture and moxibustion have better therapeutic effects on UC, and their simple, practical, inexpensive, and convenient features are accepted by some patients. We have carried out many clinical trials and animal experiments, and the results indicate that acupuncture and moxibustion have excellent therapeutic effects on UC [4–7]. Joos et al. performed randomized controlled studies to observe the therapeutic effects of acupuncture and moxibustion on UC patients and confirmed that the acupuncture and moxibustion procedures of traditional Chinese medicine (TCM) had certain efficacy in the treatment of UC [8]. Acupuncture and moxibustion have advantages for controlling disease activity in UC patients, improving patients' quality of life, maintaining clinical remission, and preventing and treating complications [9–12]. However, the effect of acupuncture and moxibustion on the regulation of colon tissue transcriptome remains unknown. There is an urgent need to reveal the commonalities and differences between acupuncture and moxibustion in the molecular mechanism of anti-inflammation in UC. Therefore, we applied acupuncture and moxibustion in UC rats to evaluate the anti-inflammatory effects of acupuncture and moxibustion and explored the mechanism of acupuncture and moxibustion at the molecular level of the transcriptome by RNA sequencing. Our data suggest the difference in gene expression and signaling pathways between each group, which contribute to our knowledge of the effect of acupuncture and moxibustion on UC rats at the molecular level.

2. Materials and Methods

2.1. Experimental Animals. We carried out all experimental procedures in strict accordance with the regulations of "Instructive Notions with Respect to Caring for Laboratory Animals" released by the Ministry of Science and Technology, China. The animal certificate number is 2015000516185. Any rats that died during surgery were excluded from the study. Healthy adult male Sprague Dawley (SD) rats with a bodyweight of 180 ± 200g were purchased from Shanghai SLAC Laboratory Animal Co., Ltd, and the license number was SCXK (Beijing) 2012–0001. All animals were maintained in cages under a 12/12-h light/dark cycle at 20 ± 2°C and a controlled relative humidity of 50%–70%, and they were allowed free access to food and water for one week.

2.2. Model Establishment. A total of 66 normal rats were used in this study, 33 of which were randomly selected for model establishment. After 1 w of adaptive feeding, the SD rats received 4% dextran sulfate sodium (DSS, MP biomedicals, No. 0216011080) in water for 7 d, followed by 1% DSS in water for another 7 d [13]. The bodyweight and overall conditions of the rats were recorded daily. After that, the model of UC rats was identified. The colonic mucosa of UC rats showed large ulcer formation, abnormal morphology of glands, or even heterogeneous hyperplasia, and disorderly arrangement, a large number of inflammatory cells infiltrating the mucosa and submucosa, congestion, and edema were seen, which confirmed the successful establishment of the UC rat model [14].

2.3. Grouping and Treatment. Rats that met the study requirements were randomly selected for model establishment. UC model establishment was evaluated by comparing three model rats with three normal rats. In the experiment, 30 rats were randomized to the normal control (NC) group, the control + herb-partitioned moxibustion (NCHM) group, and the control + electroacupuncture (NCEA) group, 10 rats in each group. A total of 30 rats were studied, which were randomly divided into the model (UC) group, the model + herb-partitioned moxibustion (UCHM) group, and the model + electroacupuncture (UCEA) group, 10 rats in each group. In the NC and UC groups, the rats did not receive any treatment but underwent the same manipulation and immobilization as in the treatment groups. In the NCHM group and UCHM group, the rats received herb-partitioned moxibustion at the ST25 acupoints (bilateral). Based on an anatomic method referenced in the "Map of Animal Acupoints" from Shi Yan Zhen Jiu Xue written by Lin WZ, ST25 is located on the abdomen of the rat, level with the umbilicus and 5 mm next to it (Figure 1). In the NCEA group and UCEA group, the rats received electroacupuncture at the ST25 acupoints (bilateral).

2.4. Herb-Partitioned Moxibustion and Electroacupuncture Interventions

2.4.1. Herb-Partitioned Moxibustion. The rats were immobilized with custom-made rat fixators. The weight of the moxa cone was approximately 90 mg. The medicinal cake contained aconite and cinnamon and was mixed and stirred with yellow wine to form a thick paste. The medicinal cakes were prepared using a mold with a thickness of approximately 0.5 cm and a diameter of 1 cm. The medicinal cakes were placed at the bilateral ST25 acupoints. Each acupoint received two moxa cones each time (about 10 mins in total). Moxibustion was performed once daily for a total of seven treatments.

2.4.2. Electroacupuncture. The rats were immobilized with custom-made rat fixators. Acupuncture needles were vertically inserted (2 mm) into the bilateral ST25 acupoints. The needle handle was connected to Han's acupoint nerve

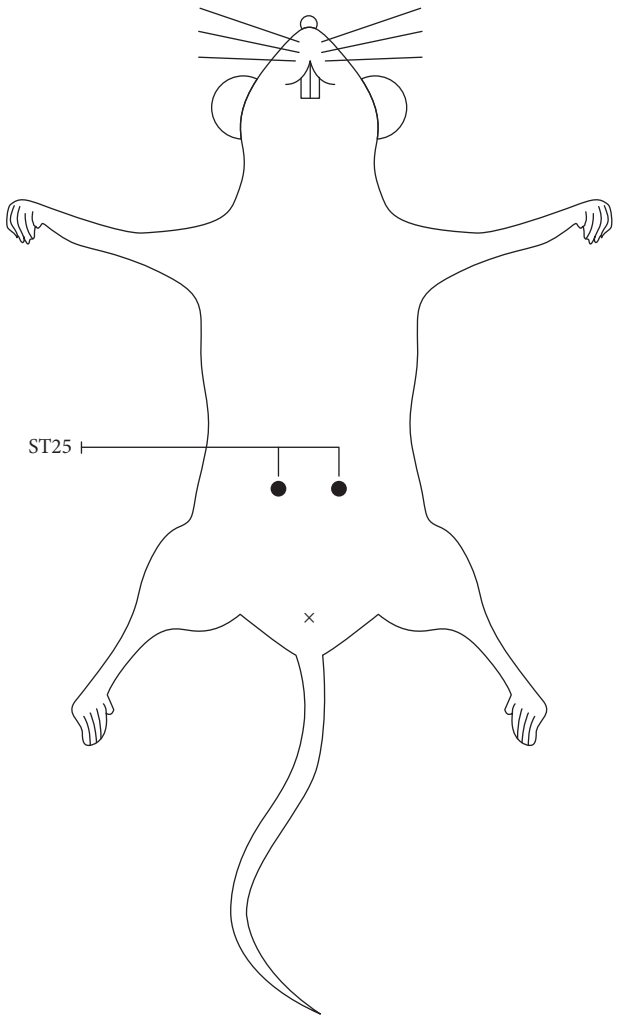

Figure 1: Location of ST25 of a rat.

stimulator (Hans-200). An electroacupuncture needle with a frequency of 2/100 Hz and a current of 1 mA was used. Electroacupuncture was performed once daily at the same time for 10 min for a total of seven treatments.

In the control group and the model group, all rats were immobilized with custom-made rat fixators for 10 min once daily.

2.5. Specimen Collection and Processing. One week after the end of the intervention, the rats were anesthetized by an intraperitoneal injection of 2% pentobarbital sodium (40–50 mg/kg). After anesthesia induction, the abdominal cavity of each rat was opened, and a 4 cm segment of the colon 2 cm above the anus was collected. The colon was cut open longitudinally along the mesentery to observe the gross condition of the colon and perform macroscopic injury scoring. Finally, a 3 cm segment of the colon from the bottom to the top was collected and divided into three pieces. One piece was fixed in a 10% neutral formalin solution and stored for future use, and the other two pieces were minced, mixed, and divided into two copies, which were both placed in cryotubes and temporarily stored in liquid nitrogen. After the material collection was complete, the copies were transferred to a -80 °C freezer for storage and future use.

2.6. Pathological Observations of Rat Colon Tissues. The rat colon samples fixed in 10% neutral formalin solution were trimmed to an appropriate size, dehydrated, embedded, and prepared into 4 μm thick sections. After the sections were stained with hematoxylin-eosin (HE), colonic mucosal epithelia and colonic crypts were observed under a light microscope to identify inflammatory cell infiltration or proliferation of granulation tissue. Histopathological colon injury scoring was performed with reference to the method of Butzner et al. [15].

2.7. ELISA Detection. The concentration of high-sensitivity C-reactive protein (hs-CRP) in serum and the enzyme activity of myeloperoxidase (MPO) in colon tissue were detected using ELISA. Six rat samples from each group were randomly selected for detection. The specific manipulation procedure is described below. A 96-well microplate was used, and two replicate wells were set up. Standards were sequentially added to standard wells at 50 μl/well. Except for blank wells, the samples to be measured were sequentially added to the sample wells at 10 μl/well, and then a diluted sample solution was added at 40 μl/well and evenly mixed. Horseradish peroxidase-labeled antibody was added to the standard wells and sample wells at 100 μl/well but not the blank wells. The plate was incubated in a 37°C incubator for 60 min. The plate was washed five times and completely dried on a filter paper. Substrates A and B were sequentially added to each well at 50 μl/well, followed by incubation in a 37°C incubator in the dark for 15 min. The stop solution was added at 50 μl/well, and the optical density (OD) value (450 nm wavelength) of each well was measured within 15 min using a microplate reader.

2.8. RNA High-Throughput Sequencing. In the NC group, UC group, UCHM group, and UCEA group, colon tissues from 3 rats in each group were randomly collected, and total RNA was extracted using the Trizol-based method. Quality control of the extracted total RNA was performed using the Agilent 2200. Libraries were constructed, and library quality was examined using the Agilent 2200. Finally, high-throughput sequencing of the extracted samples was performed using the HiSeq 4000 sequencing platform. The data obtained from sequencing were filtered, subjected to strict quality control, and analyzed using bioinformatics.

2.9. RT-qPCR. 32 RNA samples from HC, UC, UCHM, and UCEA (8 samples each group) were examined with RT-qPCR. 1 μg total RNA from each sample was reverse transcribed into cDNA using SYBR ® Green. All RT-qPCR assays were performed in duplicate. Reactions were carried out with SYBR *R* Premix Ex TaqTM kit (TaKaRa) and performed on Light Cycler ® 480 II System (Roche). For comparison of relative gene

expression, we analyzed RT-qPCR data by the ΔCt method and normalized the value to endogenous GAPDH control.

2.10. Statistical Analysis. The quantitative data are presented as the mean ± standard error of the mean (SEM) of at least three experimental repeats. Data are presented as mean ± SEM. SPSS 21.0 statistical software was used for all statistical analyses, and GraphPad Prism (GraphPad, San Diego, CA, USA) was used for mapping. The significance of the differences between groups was evaluated using Student's *t*-test for two groups and one-way analysis of variance (ANOVA) for multiple-group comparison. Kruskal–Wallis H was used for the distribution of ranked data. The statistical levels were all $\alpha = 0.05$, and $P < 0.05$ indicated that the difference was statistically significant.

3. Results

3.1. Observation of the Effect of Acupuncture and Moxibustion on UC Rats

3.1.1. Histopathological Observation of Colon Tissues from Rats in All Groups. In the rats in the NC group, NCHM group, and NCEA group, the mucous membrane of the colon was covered with intact epithelia, no ulcers were observed, the structures of all layers of tissues were clear, the crypts exhibited an orderly arrangement, only a small amount of inflammatory cell infiltration was noted in the mucosal layer, and no interstitial congestion or edema was evident. In the UC group, the epithelia covering the surface of the colon had fallen off, the number of crypts in the mucosal layer was decreased, large numbers of lymphocytes, plasma cells, neutrophils, and histiocytes had infiltrated the interstitial and submucosal layers, microvascular proliferation was evident, and lymphoid follicle formation was observed in some samples. Compared to the UC group, the number of inflammatory cells in rat colon tissues was significantly decreased, the tissue structure was normal, and healing ulcers were noted in the UCHM and UCEA groups (Figure 2).

The histopathological colon injury score was significantly higher in the UC group than that in the NC group ($P < 0.01$). The histopathological colon injury scores were significantly lower in the UCHM group and UCEA group than those in the UC group (both $P < 0.01$) (Figure 3).

3.1.2. Results of Serological Indicator Detection. The serum hs-CRP concentration in the rats in the UC group was significantly higher than that in the NC group ($P < 0.01$). The serum hs-CRP concentrations in the rats in the UCHM group and UCEA group were significantly lower than those in the UC group ($P < 0.01$). The serum hs-CRP concentration in the rats in the UCHM group was significantly lower than that in the UC group ($P < 0.05$). The serum hs-CRP concentration in the rats in the UCEA group was significantly lower than that in the UC group ($P < 0.05$) (Figure 4).

3.1.3. Results of Enzyme Activity of Myeloperoxidase Detection in Colon Tissues. The MPO concentration in rat colon tissues in the UC group was significantly higher than that in the NC group ($P < 0.01$). The MPO concentrations in rat colon tissues in the NCHM group, NCEA group, UCHM group, and UCEA group were significantly lower than those in the UC group (all $P < 0.01$). The MPO concentration in rat colon tissues in the NCHM group was significantly lower than that in the UCHM group ($P < 0.05$). The MPO concentration in rat colon tissues in the NCEA group was significantly lower than that in the UCEA group ($P < 0.05$) (Figure 5).

3.2. Effects of Acupuncture and Moxibustion on Gene Expression Profiles in Colon Tissues from UC Rats

3.2.1. The Differentially Expressed Gene Expression Profiles in All Groups. The colon tissues of three rats each from the NC group, UC group, UCHM group, and UCEA group were collected for extraction of total RNA. The RNA-seq sequencing method was performed to observe the effects of acupuncture and moxibustion on gene expression profiles in rat colon tissues. Compared with the NC group, 373 differentially expressed genes were identified in colon tissues from the UC group, including 206 upregulated genes and 167 downregulated genes. Compared with the UC group, 684 differentially expressed genes were identified in the UCHM group, including 380 upregulated genes and 304 downregulated genes (for top 10 regulated genes, see Tables 1 and 2), and 1182 differentially expressed genes were identified in the UCEA group, including 720 upregulated genes and 462 downregulated genes (for top 10 regulated genes, see Tables 3 and 4).

3.2.2. Overlap of Differentially Expressed Genes between Groups. Overlapping differentially expressed genes were analyzed and screened using the Venn diagram. Compared to the NC group, DSS-induced UC colon tissues had 206 upregulated genes, 38 of which overlapped with 304 downregulated differentially expressed genes in the UCHM group, while 19 differentially expressed genes overlapped with 462 downregulated genes in the UCEA group. In addition, a total of six overlapped genes were identified among these three groups (Figure 6(a)). Furthermore, compared to the NC group, 167 downregulated genes were identified in DSS-induced UC colon tissues, 21 of which overlapped with 380 upregulated genes in the UCHM group, while 28 genes overlapped with 720 upregulated genes in the UCEA group. In addition, a total of six overlapped genes were identified among these three groups (Figure 6(b)).

3.2.3. Cluster Analysis of Differentially Expressed Genes in All Groups. Cluster and heatmap analyses of differentially expressed mRNAs were performed using Cluster 3.0 and Tree view software to intuitively compare uniformity and differences in samples among the groups. Hierarchical cluster analysis was performed on a total of 12 samples from four groups to analyze 51 upregulated differentially expressed genes and 43

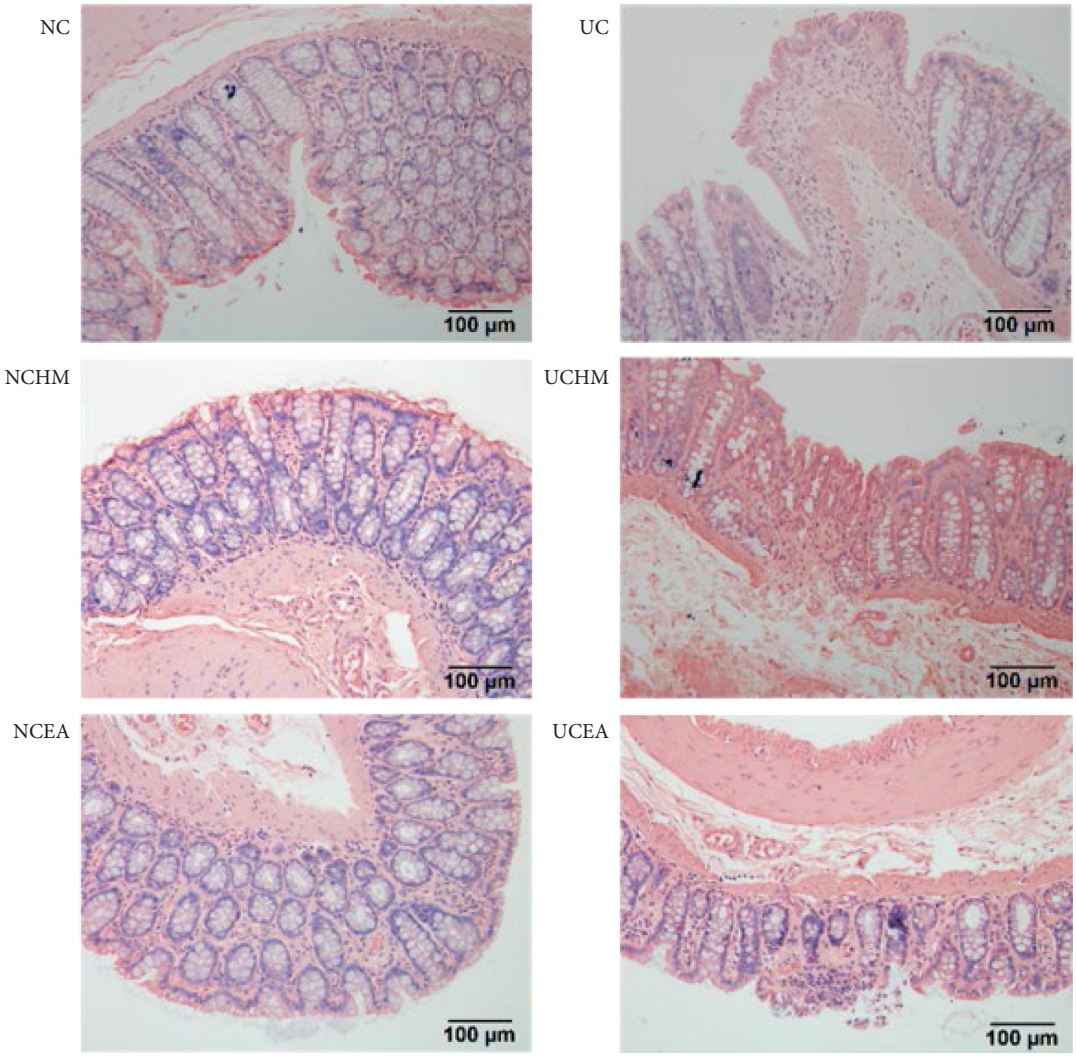

Figure 2: Histopathological observation of the colon. NC: normal control group; UC: model group; NCHM: control + herb-partitioned moxibustion group; UCHM: model + herb-partitioned moxibustion group; NCEA: control + electroacupuncture group; UCEA: model + electroacupuncture group.

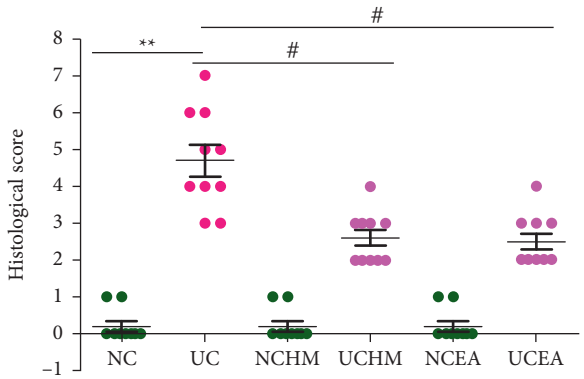

Figure 3: Histopathological colon injury score in each group. Compared with the NC group, $^{*}P < 0.01$; compared with the UC group, $^{\#}P < 0.01$ ($n = 10$).

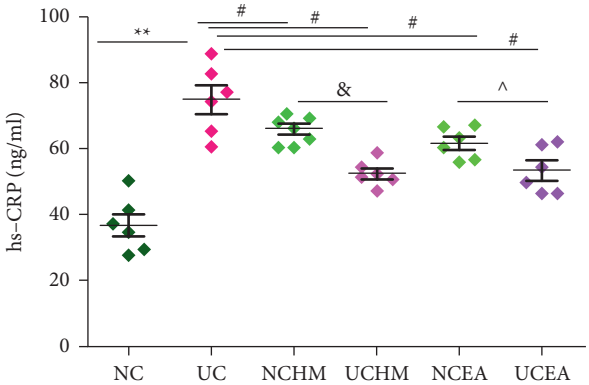

Figure 4: Serum hs-CRP concentration in each group. Compared to the NC group, $^{*}P < 0.01$; compared to the UC group, $^{\#}P < 0.01$; compared to the NCHM group, $^{\&}P < 0.05$; compared to the NCEA group, $^{\wedge}P < 0.05$ ($n = 6$).

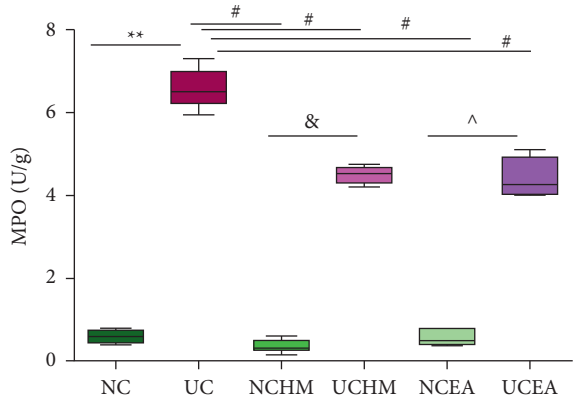

Figure 5: MPO concentration in each group. Compared to the NC group, $^{*}P < 0.01$; compared to the UC group, $^{\#}P < 0.01$; compared to the NCHM group, $^{\&}P < 0.05$; compared to the NCEA group, $\hat{}P < 0.05$ ($n = 6$).

Table 1: The top 10 downregulated genes in UCHM (compared with UC).

Gene name	Description	log2 (FC)	P
B4galnt2	β-1,4-N-Acetyl-galactosaminyltransferase 2	−4.2020411	<0.001
LOC103693426	Uncharacterized	−3.4374964	<0.001
Bpi	Bactericidal permeability increasing protein	−2.6558263	<0.001
Ildr2	Immunoglobulin-like domain-containing receptor 2	−2.2011603	<0.001
LOC102552725	Uncharacterized	−2.1239904	<0.001
Isx	Intestine-specific homeobox	−2.1092788	<0.001
Nfil3	Nuclear factor, interleukin-3 regulated	−2.0201916	<0.001
Aldob	Aldolase, fructose-bisphosphate B	−1.8416709	<0.001
LOC103693587	Uncharacterized	−1.6990522	<0.001
Acsm3	Acyl-CoA synthetase medium-chain family member 3	−1.6681228	<0.001

FC: fold change; UC: model group; NCHM: control + herb-partitioned moxibustion group.

Table 2: The top 10 upregulated genes in UCHM (compared with UC).

Gene name	Description	log2 (FC)	P
Ido1	Indoleamine 2,3-dioxygenase 1	7.028188	<0.001
RGD1305184	Similar to CDNA sequence BC023105	5.88236646	<0.001
LOC100909911	Uncharacterized	5.22976595	<0.001
LOC102556989	Uncharacterized	4.52584984	<0.001
Krt86	Keratin 86	3.90703757	<0.001
Cxcl10	C-X-C motif chemokine ligand 10	3.89489776	<0.001
Dbp	D-box binding PAR bZIP transcription factor	3.20964656	<0.001
MGC105567	Similar to cDNA sequence BC023105	3.1181265	<0.001
Igtp	Interferon-gamma-induced GTPase	3.00203997	<0.001
LOC681325	Uncharacterized	2.94009072	<0.001

FC: fold change; UC: model group; NCHM: control + herb-partitioned moxibustion group.

Table 3: The top 10 downregulated genes in UCEA (compared with UC).

Gene name	Description	log2 (FC)	P
Retnlg	Resistin-like gamma	−4.99819	<0.001
Pkd1l1	Polycystin 1 like 1, transient receptor potential channel interacting	−4.913304	<0.001
Rps10l1	Ribosomal protein S10-like 1	−4.6248477	<0.001
LOC100361240	Uncharacterized	−4.2525595	<0.001
Scgb1a1	Secretoglobin family 1A member 1	−3.2828908	<0.001
LOC102551811	Uncharacterized	−3.258879	<0.001
Crp	C-reactive protein	−3.0156217	<0.001
LOC102556038	Uncharacterized	−2.5977539	<0.001
Hoxd13	Homeobox D13	−2.5781291	<0.001
Evx2	Even-skipped homeobox 2	−2.539294	<0.001

FC: fold change; UC: model group; UCEA: model + electroacupuncture group.

Table 4: The top 10 upregulated genes in UCEA (compared with UC).

Gene name	Description	log2 (FC)	P
Ly49s6	Ly49 stimulatory receptor 6	5.56793974	<0.001
Klrd1	Killer cell lectin-like receptor D1	5.11232751	<0.001
Ccl4	C-C motif chemokine ligand 4	3.61234831	<0.001
Cd8b	CD8b molecule	3.1351152	<0.001
Phf11	PHD finger protein 11	2.95457726	<0.001
Lag3	Lymphocyte activating 3	2.93189218	<0.001
Cd8a	CD8a molecule	2.9117268	<0.001
Cd3e	CD3e molecule	2.90182201	<0.001
Gzma	Granzyme A	2.81778043	<0.001
LOC103693070	Uncharacterized	2.71738337	<0.001

FC: fold change; UC: model group; UCEA: model + electroacupuncture group.

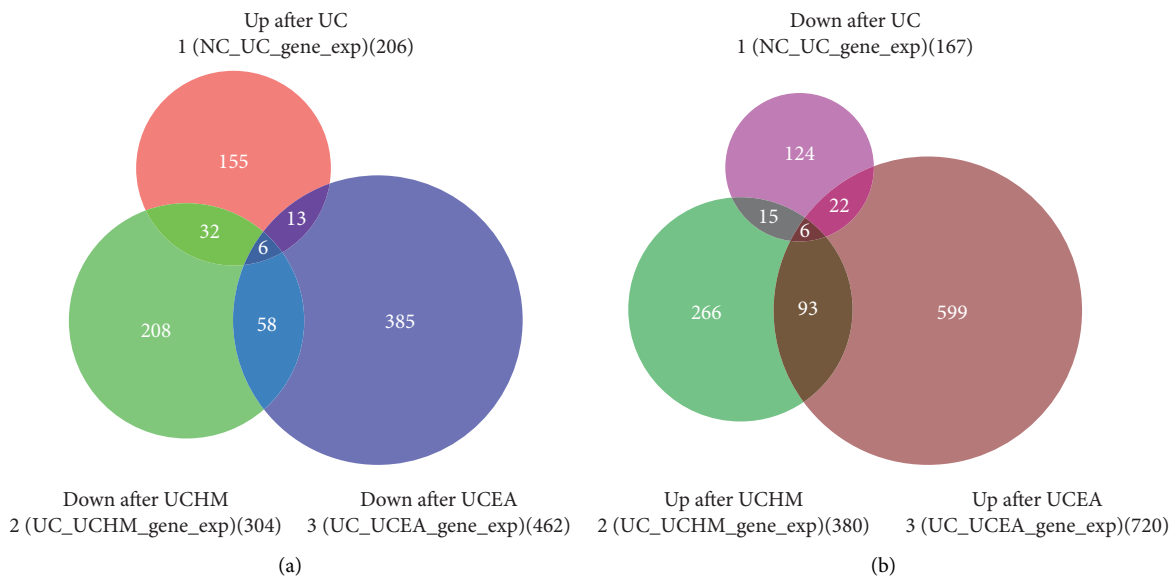

Figure 6: Number of overlapping differentially expressed genes between groups. (a) Overlap of differentially expressed genes in Up after UC, Down after UCHM, and Down after UCEA. (b) Overlap of differentially expressed genes in Down after UC, Up after UCHM, and Up after UCEA.

downregulated differentially expressed genes in the UC group that overlapped with genes in other groups. The results suggested that the genes in the UC group were all clustered together. In addition, the genes in the UCHM group and the UCEA group were also clustered together. The expression levels in three samples from each group were more consistent, a significant difference was found between the NC group and the UC group, and a significant difference was also found among the UCHM group, UCEA group, and UC group. Genes that were upregulated in the UC group were downregulated in the UCHM group and UCEA group, similar to observations in the NC group. In contrast, the results were the same (Figure 7).

3.2.4. Gene Ontology (GO) and Pathway Analyses of Differentially Expressed Genes in All Groups. The results of GO analyses of differentially expressed genes in colon tissues in the UCHM group suggested that the GO terms associated with 380 upregulated genes were mainly associated with biological functions of the nucleus, chromosome, and telomere regions, chromatin, and the major histocompatibility complex (MHC) class I protein complex. Only two GO terms were associated with downregulated genes, i.e., protein extracellular matrix and extracellular space (Figure 8(a)). Pathways that were associated with upregulated genes included DNA repair, the cell cycle, nucleotide excision repair, the JAK-STAT signaling pathway, cell adhesion molecule (CAM), miRNA function in cancer, and the phagosome. Furthermore, downregulated genes were closely associated with circadian rhythms, biosynthesis of antibiotics, and glycolysis/gluconeogenesis (Figure 8(b)).

The GO analysis results of differentially expressed genes in colon tissues in the UCEA group suggested that the GO terms associated with 720 upregulated genes were mainly associated with the nucleus, chromatin, chromosomes, the SMN-Sm protein complex, and mitochondrial proton transport. The GO terms associated with 380 downregulated genes were mainly closely associated with biological functions of the protein extracellular matrix, muscle fiber, basement membrane, collagen type IV (trimmer),

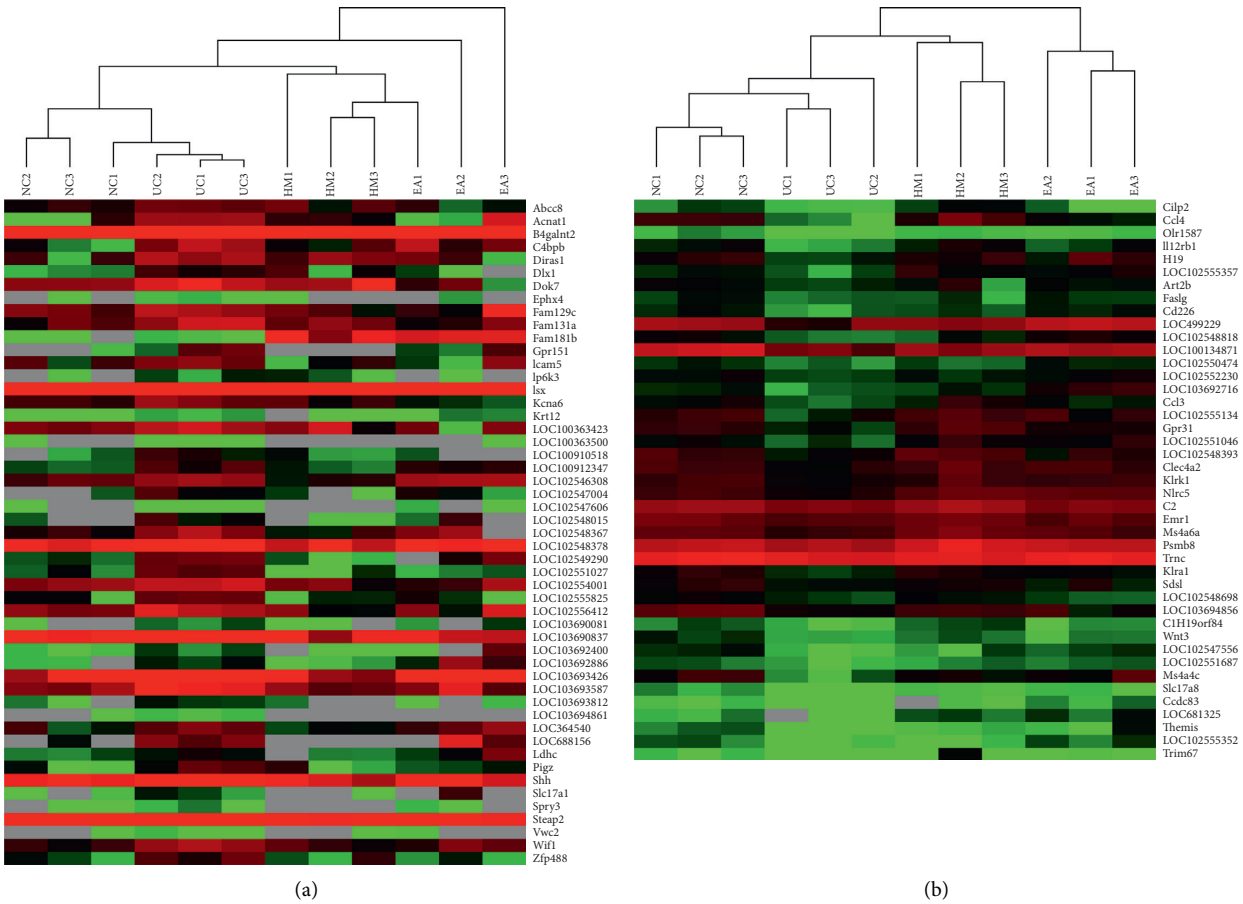

Figure 7: Heatmap of upregulated and downregulated differentially expressed genes. (a) Upregulated differentially expressed genes in UC. (b) Downregulated differentially expressed genes in UC. Bright red represents the highest expression, and the expression decreased with the darkening of red; black represents the expression of 0; dark green to bright green represents the decreased expression.

postsynaptic density, neuronal cell body, synapses, cell junction, basal layer, and contractile fibers in smooth muscle (Figure 9(a)). Pathways that were associated with upregulated genes were mainly associated with the biosynthesis of antibiotics, terpenoid skeleton biosynthesis, metabolic pathways, pyrimidine metabolism, steroid biosynthesis, RNA transport, DNA replication, the NF-κB signaling pathway, cytosolic DNA-sensing pathway, carbon metabolism, the cell cycle, the proteasome, the ribosome, and Toll-like receptor signaling pathways. Pathways that were associated with downregulated genes were mainly associated with adhesion, ECM-receptor interaction, the PI3K-Akt signaling pathway, protein digestion and absorption, the calcium signaling pathway, regulation of the actin cytoskeleton, vascular smooth muscle contraction, cancer pathways, cGMP-PKG signaling pathway, neuroactive ligand-receptor interaction, proteoglycan in cancer, the MAPK signaling pathway, the GABAergic synapse, the Wnt signaling pathway, and the cAMP signaling pathway (Figure 9(b)).

3.3. Validation of DEGs with RT-qPCR. To verify the reliability of RNA-seq results, 8 transcriptomic data were randomly selected from each group, and 3 DEGs expressions were tested following the results of RNA-seq data: c4bpb, ccl3, and il12rb1. It can be seen in Figure 10 that the RT-qPCR results of the three genes were consistent with RNA-seq analysis. The identification demonstrated the reliability of our RNA-seq results (Figure 10).

4. Discussion

The ST25 acupoint is an acupuncture point of the Stomach Meridian of Foot-Yangming. This acupoint is the front-mu point of the large intestine and mainly dredges and regulates the intestine. The ST25 acupoint was regarded as the key acupoint for the treatment of abdominal distension and diarrhea in ancient times. Many modern clinical studies have shown that the ST25 acupoint has excellent bidirectional regulatory effects on gastric and intestinal functions and significant efficacy in the treatment of gastric and intestinal diseases such as abdominal pain, diarrhea, constipation, and dysentery [16–18].

In this study, we found that the general condition of the rats with DSS-induced UC gene gradually improved after herb-partitioned moxibustion and electroacupuncture interventions. Microscopic scoring of colon tissue injury showed that colon tissues from DSS-induced UC rats

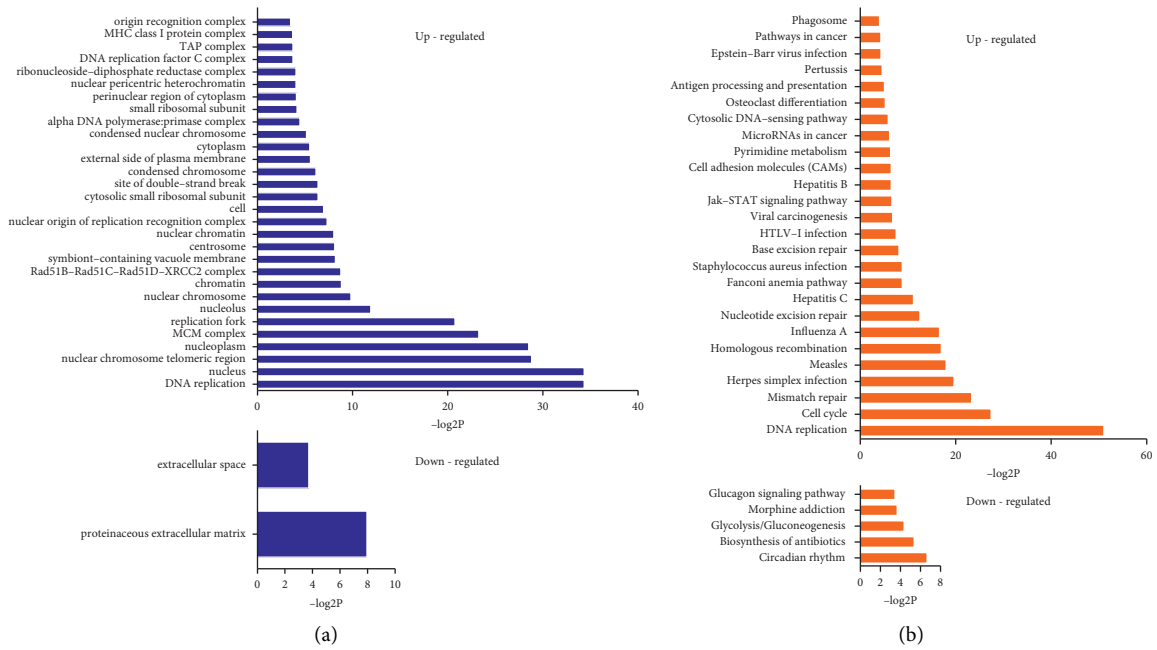

Figure 8: (a) GO analyses and (b) pathway analyses of differentially expressed genes of the UCHM group compared with the UC group.

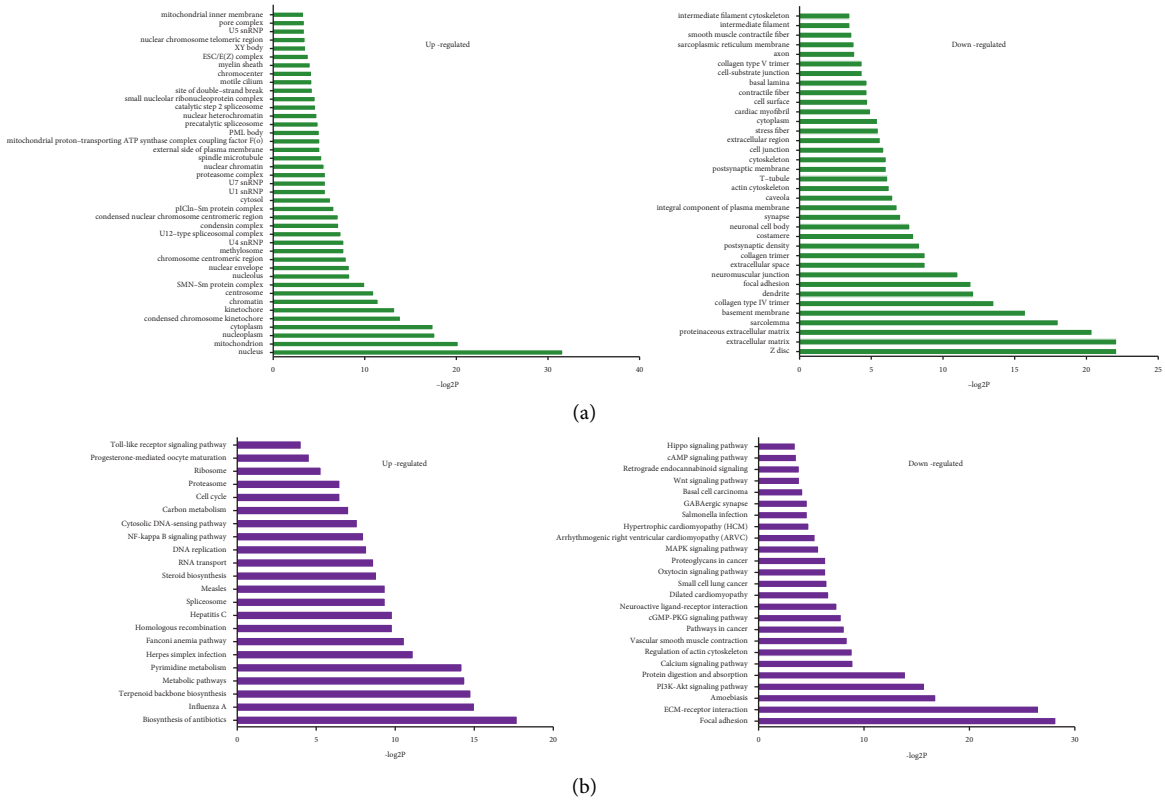

Figure 9: (a) GO analyses and (b) pathway analyses of differentially expressed genes of the UCEA group compared with the UC group.

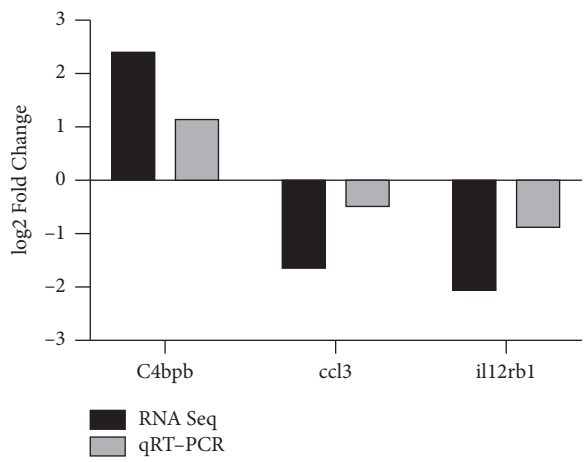

Figure 10: Validation of selected DEGs with RT-qPCR. The statistical graph showed the fold change (log2) of the mRNA expression of DEGs by RNA-seq (black) and RT-qPCR (grey), normalized to the GAPDH level.

exhibited obvious injury. After herb-partitioned moxibustion and electroacupuncture interventions, the UC rat tissues exhibited mild injury, less bleeding, and less feculent matter. In addition, histopathological features of the colon tissues included ulcer surface healing, mucosal epithelial hyperplasia and covering, and less lymphocyte and plasma cell infiltration. These results suggested that herb-partitioned moxibustion and electroacupuncture had protective effects on UC rat colon against DSS-induced injury.

The CRP level has an obvious correlation with the Mayo score of UC disease and moderate positive correlations with both the clinical classification and endoscopic classification of UC [19, 20]. Detection of the serum CRP level can objectively reflect changes in inflammation and disease conditions in UC patients and can be used as an indicator of colonic mucosal repair. In this study, the hs-CRP concentration in UC rats was higher than that in the NC group, indicating a large increase in CRP in the serum in UC inflammatory conditions; however, herb-partitioned moxibustion and electroacupuncture both significantly decreased the CRP level in rats with DSS-induced UC, thus controlling the inflammation in the colon. MPO activity in the colon shows a linear correlation with the level of neutrophil infiltration in tissues [21] and is a reliable indicator for evaluating the levels of neutrophil infiltration and inflammation in tissues [22]. An increased MPO level can promote the proliferation and activation of inflammatory effector cells, and effector cells more easily penetrate endothelial barriers to reach local inflammatory tissues and cause inflammation in the colon and the formation of ulcers [23]. This study showed that the MPO level in colon tissues from UC rats was significantly higher than that in the NC group rats, indicating that the level of neutrophil infiltration in colon tissues from UC rats was more severe, which is consistent with the histopathological results. The MPO levels in the UCHM and UCEA groups were both lower than those in the UC group, indicating that herb-partitioned moxibustion and electroacupuncture interventions can both effectively reduce the level of neutrophil infiltration in UC rats and reduce inflammatory responses in the colon.

The development of UC is considered caused by the joint actions of many factors, with genetic factors playing an important role. UC has been shown to exhibit the familial aggregation phenomenon. The risk of UC in family members of patients is significantly higher than that in the non-UC population [24]. To further elucidate the genetic features of UC and the specific mechanism underlying the effects of acupuncture and moxibustion in the treatment of UC, this study observed the effects of herb-partitioned moxibustion and electroacupuncture on gene expression profiles in colon tissues from UC model rats from a transcriptome perspective. This study showed that, compared to the NC group, the rats in the UC group had 373 differentially expressed genes, including 206 upregulated genes and 167 downregulated genes. Herb-partitioned moxibustion and electroacupuncture both affected gene expression profiles in colon tissues and could upregulate or downregulate the expression of some genes. The number of upregulated differentially expressed genes was higher than the number of downregulated differentially expressed genes. The heatmap and cluster analyses of differentially expressed genes in all groups showed a significant difference between the NC group and the UC group. The UCHM and UCEA groups also showed significant differences compared to the UC group. In addition, the upregulated genes in the UC group showed a trend of downregulation in the UCHM and UCEA groups similar to that in the NC group. Genes that were downregulated in the UC group showed a trend of upregulation in the UCHM and UCEA groups. The above results indicated that herb-partitioned moxibustion and electroacupuncture had a positive regulatory effect on gene expression profiles in colon tissues from UC rats and could orient them in a normal direction.

Furthermore, we performed GO and pathway functional enrichment analyses on differentially expressed genes. The results showed that 380 upregulated genes in the UCHM group were associated with many biological functions, including the nucleus, chromosome, and telomere regions, chromatin, and the MHC class I protein complex, the latter of which should receive special attention. MHC molecules participate in antigen presentation and are necessary for the differentiation and maturation of T cell immunity. They play important roles in the initiation and regulation of immune responses. MHC molecules are closely associated with immune responses, immune regulation, and the production of some pathological conditions in the body [25]. MHC class I molecules process and present endogenous antigens through the cytosolic pathway. At the gene level, the results confirmed that treatment of UC by herb-partitioned moxibustion was closely associated with enhanced immune responses and immune regulatory functions in the body. The GO terms associated with downregulated genes in the UCHM group included the protein extracellular matrix and extracellular space, which were associated with the colon tissue structure and cellular physiological activities of rats. The biological functions associated with upregulated genes in the UCEA group were similar to those in the UCHM group. The GO

terms associated with downregulated genes included protein extracellular matrix, muscle fiber, postsynaptic density, neuronal cell body, synapses, and cell junctions, which were mainly associated with the colon tissue structure and neuronal activities of rats. These differentially expressed genes regulated by herb-partitioned moxibustion and electroacupuncture are mainly involved in many signaling pathways related to inflammation and immune response, revealing to some extent the differential pathways of the anti-inflammatory effects of herb-partitioned moxibustion and electroacupuncture. Herb-partitioned moxibustion mainly regulates the expression of the JAK-STAT signaling pathway, cell adhesion molecule (CAM) related genes, while electroacupuncture can regulate NF-κB signaling pathway, the Toll-like receiver signaling pathways, the PI3K-Akt signaling pathway, the MAPK signaling pathway, and the Wnt signaling pathway. The IL and TNF superfamilies and many cytokines, including interferon, all participate in the development and progression of intestinal inflammation, and the above signal transduction pathways are closely associated with the regulation and release of these cytokines [26–28]. This study showed that electroacupuncture can downregulate many genes associated with the PI3K-Akt and Wnt signaling pathways. Previous studies have indicated that the PI3K-Akt signaling pathway mediates the development of UC by promoting inflammation and activating T cells [29]. In addition, abnormal activation of the Wnt signaling pathway was closely associated with canceration of UC [30, 31]. Modern experimental studies have indicated that acupuncture and moxibustion have obvious advantages for the adjustment of immune functions in the body [32], which is mainly achieved through the regulation of immune molecules and immune cells. The immune molecules regulated by acupuncture and moxibustion mainly include immunoglobulins, cytokines, and complements. The regulated immune cells mainly include neutrophils, red blood cells, T cells, macrophages, and natural killer cells [33–36]. Acupuncture and moxibustion can adjust immune system functions in the body, which is beneficial and bidirectional. Therefore, acupuncture and moxibustion may adjust disordered immune functions to normal status and enhance the antidisease ability of the body.

5. Conclusions

In summary, our study indicates that acupuncture and moxibustion at ST25 exerted the effects of anti-inflammation on UC rats and reversed the phenotypes by modulating abnormal gene profiles in the UC. Our results suggest that the anti-inflammatory effects of acupuncture and moxibustion may be achieved by pursuing multiple targets, which provide a clue for further investigation into the molecular mechanisms. We will provide more experimental evidence for the anti-inflammatory of acupuncture through further exploration in our next study.

Data Availability

The research data used to support the findings of this study are included within the article.

Conflicts of Interest

The authors declare no conflicts of interest.

Authors' Contributions

LW and YL designed the study. QQ, MG, and HZ performed the experiments. KL and ZM analyzed the data. ZW and RW wrote the manuscript. DW edited the manuscript. YH supervised the research. All authors read and approved the final version of the manuscript. ZW, YH, and DW contributed equally to this work.

Acknowledgments

This study was supported by the National Natural Science Foundation of China (Grant nos. 81774405, 81873372, and 81973955), Scientific Research Project of Shanghai Municipal Commission of Health and Family Planning (Grant no. 20184Y0038), Construction of Shanghai Key Specialties (Acupuncture and Moxibustion) (no. shslczdzk04701), and the Training Program for Excellent Young Medical Talents of Shanghai Municipal Population and Family Planning Commission (no. 2018YQ11).

References

[1] S. C. Ng, H. Y. Shi, N. Hamidi et al., "Worldwide incidence and prevalence of inflammatory bowel disease in the 21st century: a systematic review of population-based studies," *Lancet (London, England)*, vol. 390, no. 10114, pp. 2769–2778, 2018.

[2] G. Cui and A. Yuan, "A systematic review of epidemiology and risk factors associated with Chinese inflammatory bowel disease," *Frontiers in Medicine*, vol. 5, p. 183, 2018.

[3] N. T. Ventham, N. A. Kennedy, E. R. Nimmo, and J. Satsangi, "Beyond gene discovery in inflammatory bowel disease: the emerging role of epigenetics," *Gastroenterology*, vol. 145, no. 2, pp. 293–308, 2013.

[4] J. Ji, Y. Lu, and H. Liu, "Acupuncture and moxibustion for inflammatory bowel diseases: a systematic review and meta-analysis of randomized controlled trials," *Evidence Based Complement Alternative Medicine*, vol. 2013, Article ID 158352, 2013.

[5] J. P. Mu, H. G. Wu, and Z. Q. Zhang, "Meta-analysis on acupuncture and moxibustion for treatment of ulcerative colitis]," *Zhongguo Zhen Jiu*, vol. 27, no. 9, pp. 687–690, 2007.

[6] X. Wang, Y. Liu, and H. Dong, "Herb-partitioned moxibustion regulates the TLR2/NF-kappaB signaling pathway in a rat model of ulcerative colitis," *Evidence Based Complement Alternative Medicine*, vol. 2015, Article ID 949065, 2015.

[7] E.-H. Zhou, H.-R. Liu, H.-G. Wu et al., "Down-regulation of protein and mRNA expression of IL-8 and ICAM-1 in colon tissue of ulcerative colitis patients by partition-herb moxibustion," *Digestive Diseases and Sciences*, vol. 54, no. 10, pp. 2198–2206, 2009.

[8] S. Joos, N. Wildau, R. Kohnen et al., "Acupuncture and moxibustion in the treatment of ulcerative colitis: a randomized controlled study," *Scandinavian Journal of Gastroenterology*, vol. 41, no. 9, pp. 1056–1063, 2006.

[9] G. Song, C. Fiocchi, and J.-P. Achkar, "Acupuncture in inflammatory bowel disease," *Inflammatory Bowel Diseases*, vol. 25, no. 7, pp. 1129–1139, 2019.

[10] D. J. Stein, "Massage acupuncture, moxibustion, and other forms of complementary and alternative medicine in inflammatory bowel disease," *Gastroenterology Clinics of North America*, vol. 46, no. 4, pp. 875–880, 2017.

[11] H. G. Wu, S. Zheng, and Y. Zhu, "Clinical study on the treatment of ulcerative colitis with herb-partitioned moxibustion," *Shanghai Journal of Acupuncture and Moxibustion*, vol. 4, pp. 3-4, 2007.

[12] J. Ji, Y. Huang, and X. F. Wang, "Review of clinical studies of the treatment of ulcerative colitis using acupuncture and moxibustion," *Gastroenterology Research and Practice*, vol. 2016, Article ID 9248589, 2016.

[13] J. Fichna, M. Dicay, K. Lewellyn et al., "Salvinorin A has antiinflammatory and antinociceptive effects in experimental models of colitis in mice mediated by KOR and CB1 receptors," *Inflammatory Bowel Diseases*, vol. 18, no. 6, pp. 1137–1145, 2012.

[14] K. Y. Cheah, S. E. P. Bastian, T. M. V. Acott, S. M. Abimosleh, K. A. Lymn, and G. S. Howarth, "Grape seed extract reduces the severity of selected disease markers in the proximal colon of dextran sulphate sodium-induced colitis in rats," *Digestive Diseases and Sciences*, vol. 58, no. 4, pp. 970–977, 2013.

[15] J. D. Butzner, R. Parmar, C. J. Bell, and V. Dalal, "Butyrate enema therapy stimulates mucosal repair in experimental colitis in the rat," *Gut*, vol. 38, no. 4, pp. 568–573, 1996.

[16] H.-Y. Lee, O.-J. Kwon, J.-E. Kim et al., "Efficacy and safety of acupuncture for functional constipation: a randomised, sham-controlled pilot trial," *BMC Complementary and Alternative Medicine*, vol. 18, no. 1, p. 186, 2018.

[17] C. Y. Chen, M. D. Ke, C. D. Kuo, and C. H. Huang, "The influence of electro-acupuncture stimulation to female constipation patients," *The American Journal of Chinese Medicine*, vol. 41, no. 2, pp. 301–313, 2013.

[18] J. M. Zhao, J. H. Lu, and X. J. Yin, "Comparison of electroacupuncture and mild-warm moxibustion on brain-gut function in patients with constipation-predominant irritable bowel syndrome: a randomized controlled trial," *Chinese Journal of Integrative Medicine*, vol. 24, no. 5, pp. 328–335, 2018.

[19] J. Langhorst, J. Boone, R. Lauche, A. Rueffer, and G. Dobos, "Faecal lactoferrin, calprotectin, PMN-elastase, CRP, and white blood cell count as indicators for mucosal healing and clinical course of disease in patients with mild to moderate ulcerative colitis: post hoc analysis of a prospective clinical trial," *Journal of Crohn's & Colitis*, vol. 10, no. 7, pp. 786–794, 2016.

[20] A. P. S. Urbano, L. Y. Sassaki, and M. S. Dorna, "Associations among body composition, inflammatory profile and disease extent in ulcerative colitis patients," *Revista da Associacao Medica Brasileira*, vol. 64, no. 2, pp. 133–139, 1992.

[21] X. T. Yu, Y. F. Xu, and Y. F. Huang, "Berberrubine attenuates mucosal lesions and inflammation in dextran sodium sulfate-induced colitis in mice," *PLoS One*, vol. 13, no. 3, Article ID e0194069, 2018.

[22] D. El Kebir, L. Jozsef, W. Pan, and J. G. Filep, "Myeloperoxidase delays neutrophil apoptosis through CD11b/CD18 integrins and prolongs inflammation," *Circulationresearch*, vol. 103, no. 4, pp. 352–359, 2008.

[23] M. Barone, F. Chain, and H. Sokol, "A versatile new model of chemically induced chronic colitis using an outbred murine strain," *Front Microbiology*, vol. 9, p. 565, 2018.

[24] F. T. Moller, V. Andersen, J. Wohlfahrt, and T. Jess, "Familial risk of inflammatory bowel disease: a population-based cohort study 1977-2011," *The Americanjournal of Gastroenterology*, vol. 110, no. 4, pp. 564–571, 2015.

[25] D. S. M. Boulanger, R. C. Eccleston, A. Phillips, P. V. Coveney et al., "A mechanistic model for predicting cell surface presentation of competing peptides by MHC class I molecules," *Front Immunology*, vol. 9, p. 1538, 2018.

[26] S. Bank, P. S. Andersen, and J. Burisch, "Genetically determined high activity of IL-12 and IL-18 in ulcerative colitis and TLR5 in Crohns disease were associated with non-response to anti-TNF therapy," *The Pharmacogenomics Journal*, vol. 18, no. 1, pp. 87–97, 2018.

[27] H. S. Han, J. S. Shin, and S. B. Lee, "Cirsimarin, a flavone glucoside from the aerial part of Cirsium japonicum var. ussuriense (Regel) Kitam. ex Ohwi, suppresses the JAK/STAT and IRF-3 signaling pathway in LPS-stimulated RAW 264.7 macrophages," *Chemico-Biological Interactions*, vol. 293, pp. 38–47, 2018.

[28] L. Jiang, W. Xue, and Y. Wang, "Inhibition of miR-31a-5p decreases inflammation by down-regulating IL-25 expression in human dermal fibroblast cells (CC-2511 cells) under hyperthermic stress via Wnt/beta-catenin pathway," *Biomedicine & Pharmacother*, vol. 107, pp. 24–33, 2018.

[29] Q. Chen, X. Duan, and H. Fan, "Oxymatrine protects against DSS-induced colitis via inhibiting the PI3K/AKT signaling pathway," *International Immunopharmacology*, vol. 53, pp. 149–157, 2017.

[30] K. R. Hughes, F. Sablitzky, and Y. R. Mahida, "Expression profiling of Wnt family of genes in normal and inflammatory bowel disease primary human intestinal myofibroblasts and normal human colonic crypt epithelial cells," *Inflammatory Bowel Diseases*, vol. 17, no. 1, pp. 213–220, 2011.

[31] A. K. Shenoy, R. C. Fisher, and E. A. Butterworth, "Transition from colitis to cancer: high Wnt activity sustains the tumor-initiating potential of colon cancer stem cell precursors," *Cancer Research*, vol. 72, no. 19, pp. 5091–5100, 2012.

[32] Y. Gong, N. Li, and Z. Lv, "The neuro-immune microenvironment of acupoints-initiation of acupuncture effectiveness," *Journal of Leukocyte Biology*, vol. 08, no. 1, pp. 189–198, 2020.

[33] Y. Xu, S. Hong, and X. Zhao, "Acupuncture alleviates rheumatoid arthritis by immune-network modulation," *The American Journal of Chinese Medicine*, vol. 46, no. 5, pp. 997–1019, 2018.

[34] Y. Q. Yang, H. P. Chen, and Y. Wang, "Considerations for use of acupuncture as supplemental therapy for patients with allergic asthma," *Clinicalreviews in Allergy &Immunology*, vol. 44, no. 3, pp. 254–261, 2013.

[35] H. G. Wu, H. R. Liu, and L. Y. Tan, "Electroacupuncture and moxibustion promote neutrophil apoptosis and improve ulcerative colitis in rats," *Digestivediseasesand Sciences*, vol. 52, no. 2, pp. 379–384, 2007.

[36] M. L. Yu, R. D. Wei, and T. . Zhang, "Electroacupuncture relieves pain and attenuates inflammation progression through inducing IL-10 production in CFA-induced mice," *Inflammation*, vol. 43, no. 4, pp. 1233–1245, 2020.

Hindawi
Evidence-Based Complementary and Alternative Medicine
Volume 2021, Article ID 8137244, 10 pages
https://doi.org/10.1155/2021/8137244

Research Article

Electroacupuncture and Moxibustion Modulate the BDNF and TrkB Expression in the Colon and Dorsal Root Ganglia of IBS Rats with Visceral Hypersensitivity

Duiyin Jin,[1] **Yanan Liu**,[2,3] **Siyi Lv**,[1] **Qin Qi**,[1] **Mei Li**,[1] **Yuanyuan Wang**,[1] **Xiaomei Wang**,[2,3] **and Huangan Wu**[2,3]

[1]*Yueyang Clinical Medical College, Shanghai University of Traditional Chinese Medicine, Shanghai 200437, China*
[2]*Shanghai Research Institute of Acupuncture and Meridian, Shanghai University of Traditional Chinese Medicine, Shanghai 200030, China*
[3]*Key Laboratory of Acupuncture and Immunological Effects, Shanghai University of Traditional Chinese Medicine, Shanghai 200030, China*

Correspondence should be addressed to Xiaomei Wang; wxm123@vip.sina.com and Huangan Wu; wuhuangan@126.com

Received 8 July 2021; Accepted 11 September 2021; Published 28 September 2021

Academic Editor: Mi Liu

Objective. To evaluate the effects of electroacupuncture and moxibustion on brain-derived neurotrophic factor (BDNF) and its receptor tyrosine kinase receptor B (TrkB) protein and mRNA expressions in the colon and dorsal root ganglia of IBS rats with visceral hypersensitivity and to explore their underlying therapeutic mechanisms. *Method*. Forty Sprague Dawley rats were randomly divided into normal, model, model + mild moxibustion (MM), model + electroacupuncture (EA), and model + pinaverium bromide (PB) groups, with eight rats in each group. Chronic visceral hypersensitive IBS rat models were established by colorectal distension (CRD) with mustard oil clyster. Rats in the MM and EA groups, respectively, received moxibustion and electroacupuncture treatments on the Tianshu (ST25) and Shangjuxu (ST37) acupoints once daily for 7 days, and rats in the PB group received pinaverium bromide by oral gavage once daily for 7 consecutive days. After treatment, rats underwent abdominal withdrawal reflex (AWR) scoring under CRD and colon histopathological examination. Immunohistochemistry and real-time quantitative PCR (RT-qPCR) were used to study the protein and mRNA expressions of BDNF and TrkB in the rat colon and dorsal root ganglia. *Results*. Compared with the normal group, AWR scores and body weight were clearly increased in the model group rats (both $P < 0.01$). The body weights were significantly elevated ($P < 0.01$, $P < 0.05$), but the AWR scores were reduced ($P < 0.05$, $P < 0.01$), after electroacupuncture and mild moxibustion treatment. Compared with levels in normal rats, BDNF and TrkB protein and mRNA expressions were significantly elevated in the IBS model rats ($P < 0.01$) but were downregulated after mild moxibustion, electroacupuncture, and Western medicine treatment ($P < 0.01$). *Conclusion*. Electroacupuncture and moxibustion improved visceral hypersensitivity of IBS rats possibly by reducing BDNF and TrkB protein and mRNA expressions in the colon and dorsal root ganglia.

1. Introduction

Irritable bowel syndrome (IBS) is a chronic functional gastrointestinal disorder with a syndrome of persistent or recurrent episodes of intestinal disorder. It is characterized by abdominal pain, abdominal distension, altered bowel habits, and/or character of stool that severely affect the quality of patients' life. At present, the pathogenesis of IBS has not yet been fully elucidated. Most studies suggest that IBS is related to the interaction of various factors including genes, diet, psychosocial factors, mucosal immunity and inflammation, intestinal flora disorders, gastrointestinal motility abnormalities, and brain-gut axis dysfunction, causing visceral hypersensitivity and manifesting as the corresponding symptoms [1–3].

Brain-derived neurotrophic factor (BDNF) is a neurotrophic protein widely distributed in the nervous system and is involved in neuronal differentiation, development, and

repair and has the effect of causing pain and sensitivity in the nervous system [4, 5]. After being synthesized in primary sensory neurons, BDNF is transported to the primary afferent nerve terminals of the spinal cord dorsal horn, where it is involved in the regulation of pain hypersensitivity caused by different pain stimuli [6]. BDNF does not only present in the nervous system but also expresses in peripheral tissues, such as the intestine and pancreas [7, 8], and especially in the intestinal epithelium, myenteric plexus, and submucosal plexus of the colon. The fecal supernatants (FSN) from diarrhea-predominant IBS patients significantly increase BDNF mRNA and protein levels in colonic epithelial cells of humans and mice [9]. BDNF interacts with substance P (SP), nerve growth factor, and calcitonin gene-related peptide (CGRP) to regulate intestinal sensation and affect colon sensitivity [10]. Studies found that moderate amounts of BDNF can maintain the normal function of sensory nerves; however, abnormal elevation of BDNF can lead to a variety of pain-related sensations, such as chronic pain, inflammatory pain, and visceral pain [11].

A study has found that BDNF plays an important role in IBS pathogenesis and visceral sensitivity through binding with its high-affinity receptor of tyrosine receptor kinase B (TrkB) [12]. Currently, no effective Western medicine methods are available for IBS treatment. Although drugs such as pinaverium bromide and probiotics can relieve the symptoms, the long-term maintenance effect is unsatisfactory. Acupuncture and moxibustion are important parts of traditional Chinese medicine to alleviate visceral hypersensitivity and have good effects on improving the clinical symptoms of IBS patients, such as abdominal pain and bloating, as well as improving their quality of life [13–15]. However, the therapeutic mechanisms of acupuncture and moxibustion remain unclear. This study aimed to detect the expression of BDNF and TrkB in the colon and spinal cord of IBS rats and evaluate the regulatory effects and therapeutic mechanisms of acupuncture and moxibustion for visceral hypersensitivity in IBS.

2. Materials and Methods

2.1. Experimental Animals. 40 neonatal male Sprague Dawley (SD) rats aged five days of clean grade were provided by the Laboratory Animal Center of the Shanghai University of Traditional Chinese Medicine (Shanghai, China). Each litter of neonatal rats and a female lactating rat that had free access to water and food were housed in a cage. The animal housing environment provided a 12-hour light/dark cycle at $20 \pm 2^{\circ}$C room temperature and 50–70% indoor humidity. After adaptive feeding, experiments were conducted in neonatal SD rats 8 days after birth. All experiment procedures were performed in strict accordance with the guidelines provided by the National Institutes of Health for the Care and Use of Laboratory Animals, and the animal protocol was approved by the Animal Care and Use Committee of the Shanghai University of Traditional Chinese Medicine.

2.2. IBS Modeling and Identification. Colorectal distension (CRD) and intracolonic injection of mustard oil were used to establish the rat model of visceral hypersensitivity in IBS [16]. In this study, a hand-made saccule coated with a small amount of vaseline was slowly inserted from anus to the descending colon along the colorectal physiological curvature for approximately 2 cm. Saccule distension was made by inflating with 0.5 mL air for 1 minute followed by deflation. The same stimulation was repeated once after 30 min. The above procedures were conducted once a day for 14 consecutive days. Then, the rats continued feeding until postnatal week 6 and were intracolonically injected with 0.2 mL of 4% mustard oil daily for 14 consecutive days, with an injection depth of approximately 6–8 cm. Subsequently, abdominal withdrawal reflex (AWR) scoring under CRD was performed to evaluate their sensitivity to CRD stimulation to confirm successful modeling.

2.3. Abdominal Withdrawal Reflex (AWR) Scoring. AWR scoring was conducted by the method of Al-Chaer et al. [16] to evaluate behavioral changes in rats before and after treatment. All rats were fasted with free access to water for 8–12 hours before the AWR scoring. The balloon was connected to a desktop sphygmomanometer and syringe through a three-way valve to provide distension with constant pressure. The balloon was slowly inserted into the rectum from the anus and reached the descending colon of the rat. This was followed by inducing pain by colorectal distension at 20, 40, 60, and 80 mmHg. Each CRD scoring lasted approximately 20 seconds every 3 minutes, and each rat was evaluated 3 times to obtain the mean value as the final score for analysis. AWR scoring criteria were as follows: score 0, no behavioral response to CRD; score 1, brief head movement followed by immobility during CRD; score 2, mild contraction of the abdominal muscles but no lifting; score 3, strong contraction of the abdominal muscles and lifting of the abdomen without lifting of the pelvic structure and scrotum; and score 4, body was arched and lifting of the pelvis and scrotum [16].

2.4. Animal Grouping and Treatment. Laboratory animal treatments are in accordance with the International Association for the Study of Pain (IASP) guidelines. All 8-day-old neonatal rats were randomly divided into the normal group ($n = 8$) and IBS modeling group ($n = 32$). Rats in the normal group were routinely fed and housed without any stimulation; rats in the IBS modeling group were given CRD stimulation and intracolonically injected with mustard oil as described above. After the model was successfully established, 32 rats in the IBS modeling group were randomly divided into model group, mode + mild moxibustion (MM) group, model + electroacupuncture (EA) group, and model + pinaverium bromide (PB) group, 8 rats in each group.

In the MM group, rats were received moxibustion treatment on bilateral Tianshu (ST25) and Shangjuxu (ST37) acupoints [17]; special moxa sticks (Nanyang Hanyi Moxa Co., Ltd., Nanyang, Henan province, China) with a diameter of 0.5 cm were ignited and suspended at approximately

2–3 cm above the acupoints simultaneously for 10 minutes [18–20], once daily for 7 consecutive days. In the EA group, a disposable sterile acupuncture needle (0.25 mm × 25 mm; Suzhou Medical Appliance Factory, Jiangsu Province, China) was used for acupuncture at a depth of 5 mm on bilateral ST25 and ST37 acupoints and was connected to HANS-100A EA device (Nanjing Jisheng Medical Treatment Technology Co., Ltd., Jiangsu Province, China), with dilatational wave, 2/10 Hz frequency, and 1 mA intensity, 20 minutes for each time [19, 20], once daily for 7 consecutive days. Rats in the PB group received pinaverium bromide solution (State Food and Drug Administration, China, Approval number: H20120127) following the 1 : 0.018 of adult human (70 kg body weight)-to-rat (200 g body weight) ratio [21] by gavage daily for 7 consecutive days.

2.5. Sample Collection. After AWR scoring, all rats were weighed and anesthetized by intraperitoneal injection with 2% pentobarbital sodium (0.2 mL/100 g) and were then fixed on the dissection bench to open the abdominal cavity. Approximately 6–8 cm of colon tissue was collected 2 cm above the anus. The colon sample was cut longitudinally and rinsed with normal saline followed by fixing part of the colon sample in 4% paraformaldehyde solution and preserving the remaining sample at −80°C in a freezer for later experiments. Then, rats were sacrificed by cervical dislocation to reduce pain, and the spinal dorsal root ganglia at L6–S2 [17, 20, 22] were rapidly removed and preserved at −80°C in a freezer for later detection.

2.6. General Conditions in Rats. Mental state, fur appearance, dietary change, defecation, body weight, responsiveness, and activity of rats were monitored.

After IBS modeling was accomplished, AWR scoring was compared before and after each treatment to observe any behavioral changes in different groups of rats.

2.7. Histological Analysis. The colon tissues fixed in 4% paraformaldehyde solution were dehydrated, paraffin-embedded, and sectioned at a 4 μm thickness. The sections were deparaffinized in xylene I and II solutions for 15 min each and rehydrated from 100%, 95%, 90%, 80%, and 70% ethanol (5 min each) in double-distilled water (5 min each for 2 times on a shaker) followed by staining in hematoxylin solution for 3 min and rinsing in running water for 10 min. After differentiating in 1% hydrochloric acid alcohol for 3 s and bluing in running water for 10 min, the tissue section was stained in eosin solution for 2 min followed by dehydrating from 70%, 80%, 90%, 95% (2 min each) to 100% ethanol for 5 min each, clearing in xylene I and II solutions for 15 min each, and mounting coverslips on the glass slides using appropriate amounts of neutral gum. After drying, the histopathological changes of colon tissues in different group rats were observed under a light microscope (BH2; Olympus, Tokyo, Japan).

2.8. Immunohistochemistry to Detect BDNF and TrkB Protein Expression. The paraffin sections of colon and dorsal root ganglia tissue were deparaffinized in xylene I and II solutions for 10 min each and rehydration in 100%, 95%, 85%, and 75% ethanol for 5 min. After washing with PBS 5 min each for 2 times on a shaker, tissue sections were immersed in 0.01 M citrate buffer (pH 6.0) and heated in a microwave at 98°C for 2.5 min, 1.5 min, and 1 min, with 15-min intervals for antigen retrieval. After cooling down to room temperature, tissue sections were placed in 1% H_2O_2 for 10 min, washed 3 times in PBS for 3 min each, and blocked in 5% bovine serum albumin at 37°C for 20 min. The tissue sections were individually incubated with 20 μL primary antibodies (1 : 200 anti-BDNF antibodies, 1 : 25 anti-TrkB antibodies; Abcam, USA) overnight at 4°C. Next day, after 3 washes in PBS for 3 min each, the tissue sections were incubated with 20 μL biotin-labeled secondary antibody (goat anti-rabbit IgG, 1 : 100; Wuhan Boster Bio-Engineering Co., Ltd., Wuhan, China) at 37°C for 30 min followed by washing in PBS 3 times for 3 min each. After incubation with biotin-labeled avidin solution at 37°C for 30 min, the sections were washed with PBS 3 times for 3 min each and subsequently incubated with DAB for color development. The sections were rinsed in running water for 10 min, counterstained with hematoxylin solution for 30 s, rinsed in running water again, blued in hydrochloric acid alcohol for 2 s, followed by washing in water, and were dehydrated, cleared, and mounted with neutral gum. Immunohistochemistry of colon tissue was observed under a light microscope (BH2; Olympus, Tokyo, Japan).

2.9. RT-qPCR to Detect BDNF and TrkB mRNA Expression. Total RNAs were extracted from colon and dorsal root ganglia tissues using TRIzol reagent (Invitrogen) followed by pipetting 2 μL extracted RNA into a 1.5 mL centrifuge tube containing 8 μL DEPC water, 0.5 μL RNase inhibitor (50 U/μL), and 2 μL (50 pM/μL) random primers for reverse transcription and cDNA synthesis at 65°C in a water bath for 5 min. After standing at room temperature for 10 min, the mixtures were centrifuged at 5,000g for 5 s, then adding 0.5 μL RNase inhibitor (50 U/μL), 4 μL 5 × buffer (Invitrogen), 2 μL dNTP Mix (10 mM/each), and 1 μL reverse transcriptase (AMV) (200 U/μL) to the above reaction system to achieve a final reaction volume of 12.5 μL. The samples were allowed to reaction for 1 h at 40°C in a water bath followed by 90°C for 5–10 min, ice bath for 5 min, and high-speed centrifuging at 5,000g for 5 s before PCR amplification. The RT-qPCR reaction system contained 5 μL water, 8 μL 2 × SYBRGREEN PCR mix, 1 μL forward primer (10 pM/μL), 1 μL reverse primer (10 pM/μL), and 1 μL cDNA template. The RT-qPCR conditions were 95°C denaturation for 2 min, 40 cycles of 94°C denaturation for 10 s, 60°C annealing for 10 s, and 72°C elongation for 40 s. RT-qPCR was performed in a 7300 Real-Time PCR System (Applied Biosystems) to analyze the optical densities of the stripes, which were corrected by GAPDH to obtain the relative optical densities of the target genes.

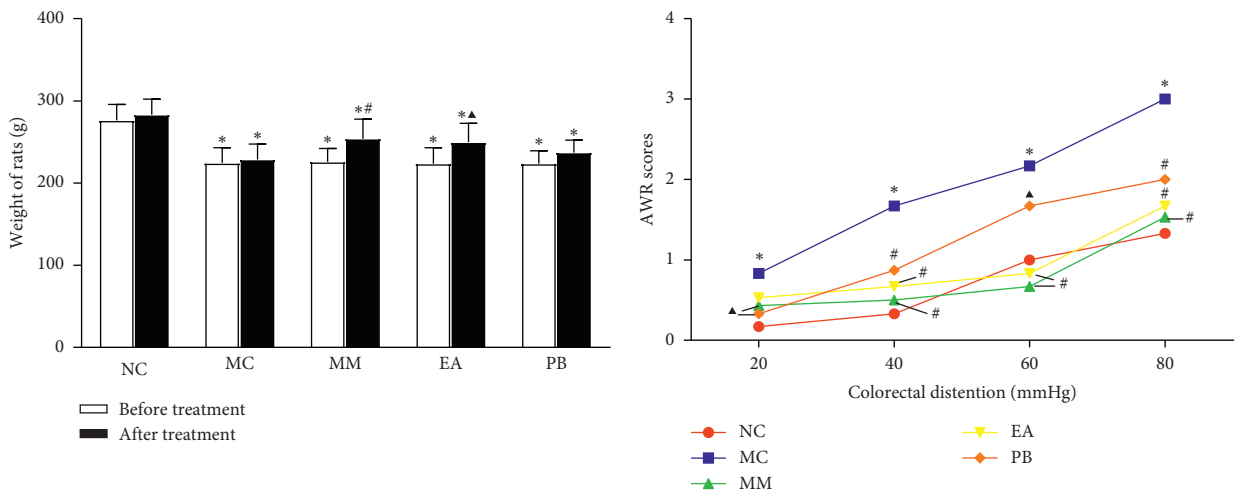

Figure 1: Change of body weight and AWR scores in rats of each group. (a) Weight changes of rats in each group before and after acupuncture and moxibustion treatment. Before treatment, $^{*}P < 0.01$ vs. NC; after treatment, $^{*}P < 0.01$ vs. NC, $^{\blacktriangle}P < 0.05$ vs. MC, and $^{\#}P < 0.01$ vs. MC. (b) AWR scores of rats in each group under different CRD stimulation. $^{*}P < 0.01$ vs. NC, $^{\blacktriangle}P < 0.05$ vs. MC, and $^{\#}P < 0.01$ vs. MC. NC: normal group; MC: model group; MM: model + mild moxibustion group; EA: model + electroacupuncture group; PB: model + pinaverium bromide group.

2.10. Statistical Analysis. SPSS 20.0 software (IBM SPSS Inc., Chicago, IL, USA) was used for data statistics and analysis. The normally distributed data were presented as mean ± standard deviation ($\bar{x} \pm s$), and one-way ANOVA was used for comparison among groups. The least significant difference (LSD) method was used for multiple comparisons if the variances were homogeneous, and Dunnett's T3 method was performed if the variances were not homogeneous. Non-normally distributed data were presented as median (minimum, maximum), and the nonparametric Kruskal–Wallis test was used for the comparison between groups. The test standard was $\alpha = 0.05$. $P < 0.05$ was considered a statistically significant difference.

3. Results

3.1. General Conditions of Rats in Each Group. Rats in the normal group were normal in food uptake and active and had white and well-groomed fur, stool with appropriate hardness, and clean perianal skin and fur. Rats in the model group were irritable and had poor appetite, reduced food uptake, slow movement, dry and sparse fur, watery stool, and dirty perianal skin. Rats in the MM, EA, and PB groups had different degrees of improvement in food uptake, grooming, responsiveness, and mobility, with most of the formed feces and occasionally contaminated perianal skin and fur, although the fur was relatively clear and shiny compared with the rats in the model group.

3.2. Changes in the Body Weight of Rats and Abdominal Withdrawal Reflex (AWR) Scoring. The body weights of IBS rats after modeling (before treatment) were significantly decreased compared with the body weights of rats in the normal group ($P < 0.01$). After treatment, the body weights of rats in the MM group ($P < 0.01$) and EA group ($P < 0.05$) were significantly higher than the body weights of rats in the model group. However, all IBS rats in different groups had lower body weight than rats in the normal group ($P < 0.01$) (Figure 1(a)). The AWR scores of rats in the model group were significantly elevated under all CRD pressures (20, 40, 60, and 80 mmHg) compared with the normal group (all $P < 0.01$). Compared with the model group, the AWR scores of rats in the MM and PB groups were significantly decreased under 20 mmHg CRD pressure ($P < 0.05$). AWR scores of rats in the MM, EA, and PB groups under 40, 60, and 80 mmHg CRD pressures were significantly decreased ($P < 0.05$ or $P < 0.01$) (Figure 1(b)).

3.3. Histological Observation. As shown in Figure 2, the morphology of the colonic mucosa in the normal rats was intact with clear structure, neatly arranged glands, and no inflammatory cell infiltration, congestion, or edema. In the model group, the colonic mucosa of IBS rats still demonstrated regular structure with regularly arranged colonic glands and only small numbers of infiltrated inflammatory cells in the submucosa, and no congestion or edema. Colonic structure of IBS rats in the MM, EA, and PB groups was intact, with relatively neatly arranged glands, few or no inflammatory cell infiltration in the mucosa and submucosa, and no obvious interstitial congestion and edema.

3.4. BDNF Protein and mRNA Expression in the Colon. As shown in Figure 3, BDNF protein and mRNA expressions in the colon of IBS rats in the model group were significantly higher than those in the healthy rats in the normal group ($P < 0.01$). Compared with the model

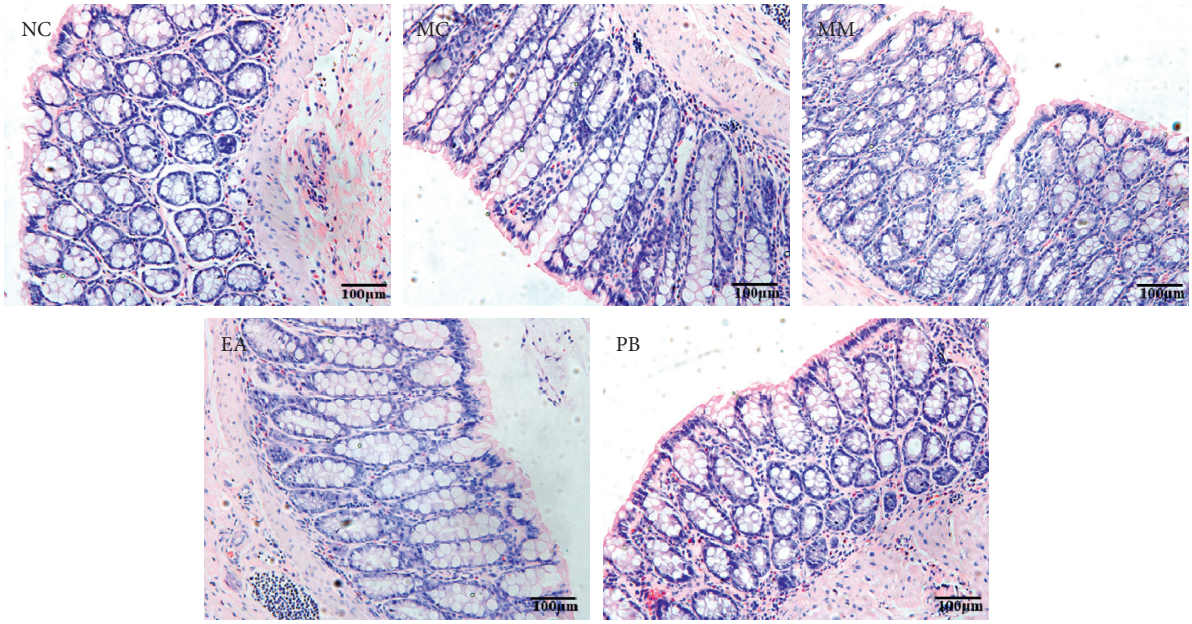

Figure 2: Pathological changes of colon tissue in rats. NC: normal group; MC: model group; MM: model + mild moxibustion group; EA: model + electroacupuncture group; PB: model + pinaverium bromide group (×200).

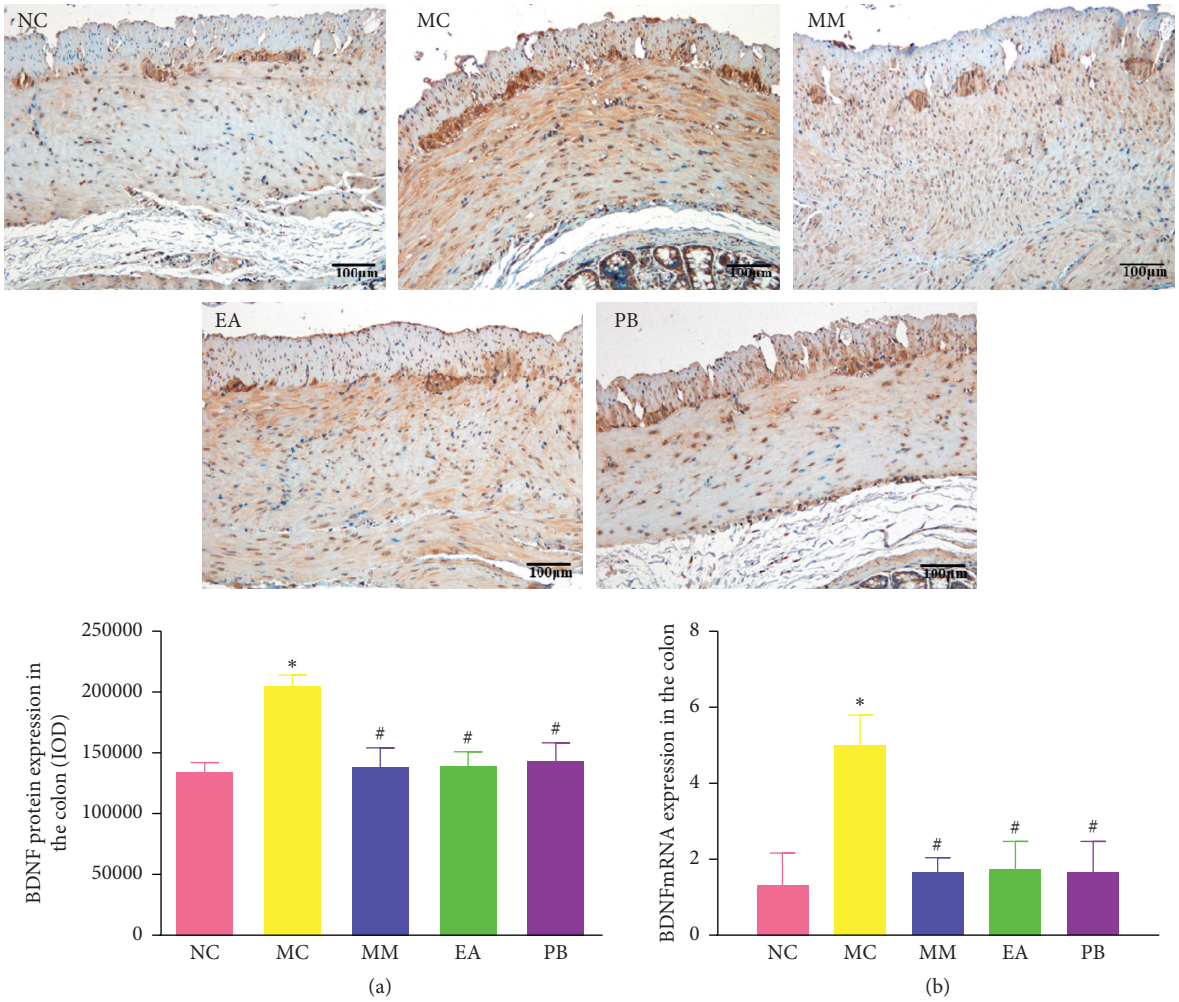

Figure 3: Expression of BDNF protein (×200) and relative expression of BDNF mRNA in rat colon tissue. (a) The expression of BDNF protein in rat colon tissue. (b): The relative expression of BDNF mRNA in rat colon tissue. NC: normal group; MC: model group; MM: model + mild moxibustion group; EA: model + electroacupuncture group; PB: model + pinaverium bromide group. The data were presented as mean ± SD. $^{*}P < 0.01$ vs. NC; $^{\#}P < 0.01$ vs. MC.

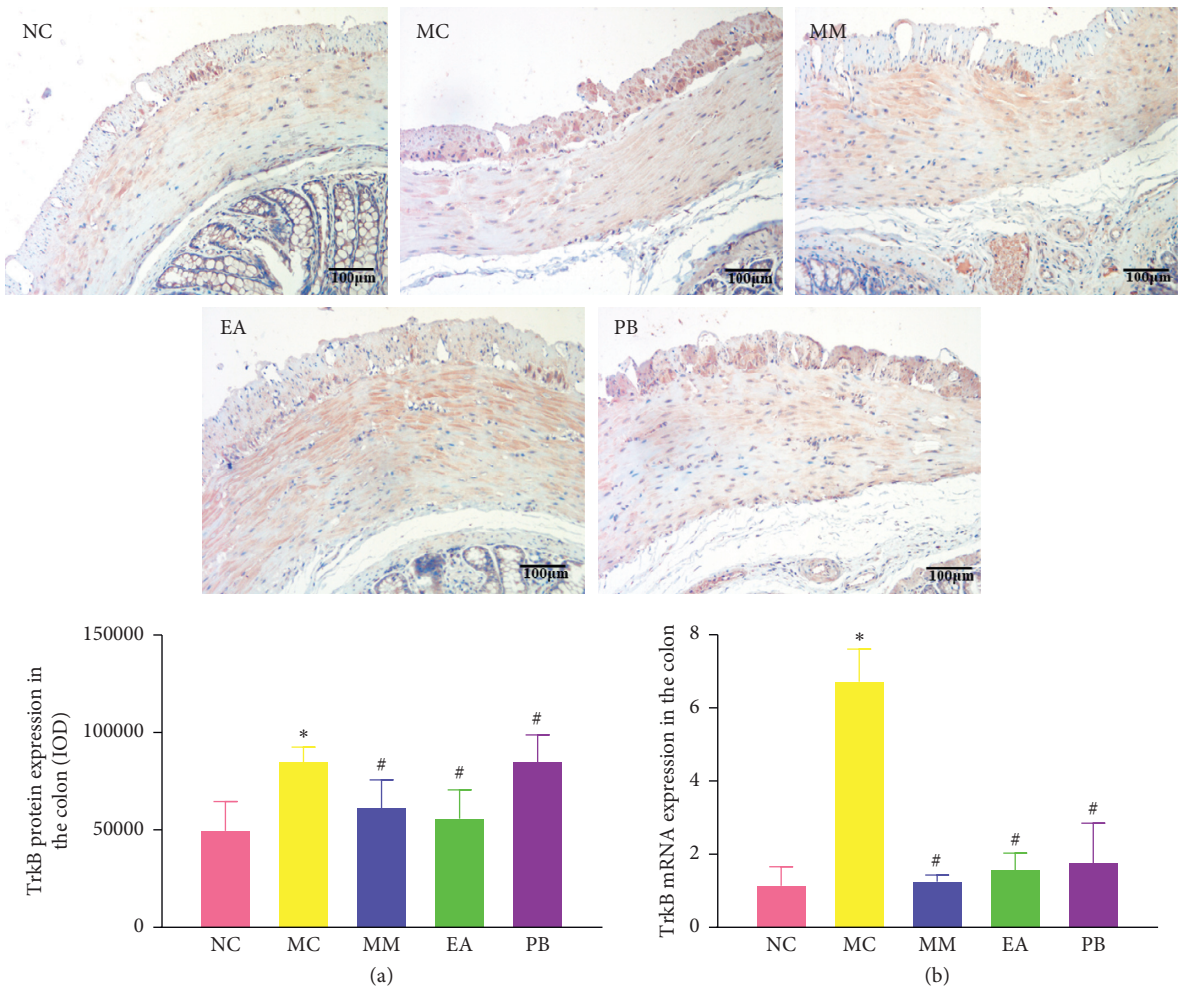

Figure 4: Expression of TrkB protein (×200) and relative expression of TrkB mRNA in the rat colon. (a) Expression of TrkB protein in rat colon tissue. (b) The relative expression of TrkB mRNA in rat colon tissue. NC: normal group; MC: model group; MM: model + mild moxibustion group; EA: model + electroacupuncture group; PB: model + pinaverium bromide group. The data were presented as mean ± SD. $^{*}P < 0.01$ vs. NC; $^{\#}P < 0.01$ vs. MC.

group, IBS rats in the MM, EA, and PB groups had significantly lower BDNF protein and mRNA expressions in the colon ($P < 0.01$).

3.5. TrkB Protein and mRNA Expression in the Colon. As shown in Figure 4, TrkB protein and mRNA expressions in the colon of IBS rats in the model group were significantly higher than those in the healthy rats in the normal group ($P < 0.01$). Compared with the model group, IBS rats in the MM, EA, and PB groups had significantly lower TrkB protein and mRNA expressions in the colon ($P < 0.01$). In addition, TrkB protein expression in the colon of the MM group was significantly lower than that of the MW group ($P < 0.01$).

3.6. BDNF Protein and mRNA Expression in the Dorsal Root Ganglia. As shown in Figure 5, the protein and mRNA expressions of BDNF in the dorsal root ganglia of IBS rats in the model group were significantly higher than those in the healthy rats in the normal group ($P < 0.01$). IBS rats in the MM, EA, and PB groups had significantly lower TrkB protein and mRNA expressions in the dorsal root ganglia than those in the model group ($P < 0.01$).

3.7. TrkB Protein and mRNA Expression in the Dorsal Root Ganglia. As shown in Figure 6, the protein and mRNA expressions of TrkB in the dorsal root ganglia of IBS rats in the model group were significantly higher than those in the healthy rats in the normal group ($P < 0.01$). IBS rats in the MM, EA, and PB groups had significantly lower TrkB protein and mRNA expressions in the dorsal root ganglia than those in the model group ($P < 0.01$).

4. Discussion

IBS is a chronic functional bowel disease with unclear pathogenesis. Based on the previous research methods, mechanical combined with chemical stimulation were used to simulate the visceral hypersensitivity of IBS in a rat model. Rats in the IBS model group had poor appetite and watery stool, indicating a change in bowel habits. Next, we observed the effect of acupuncture and moxibustion on IBS rats with

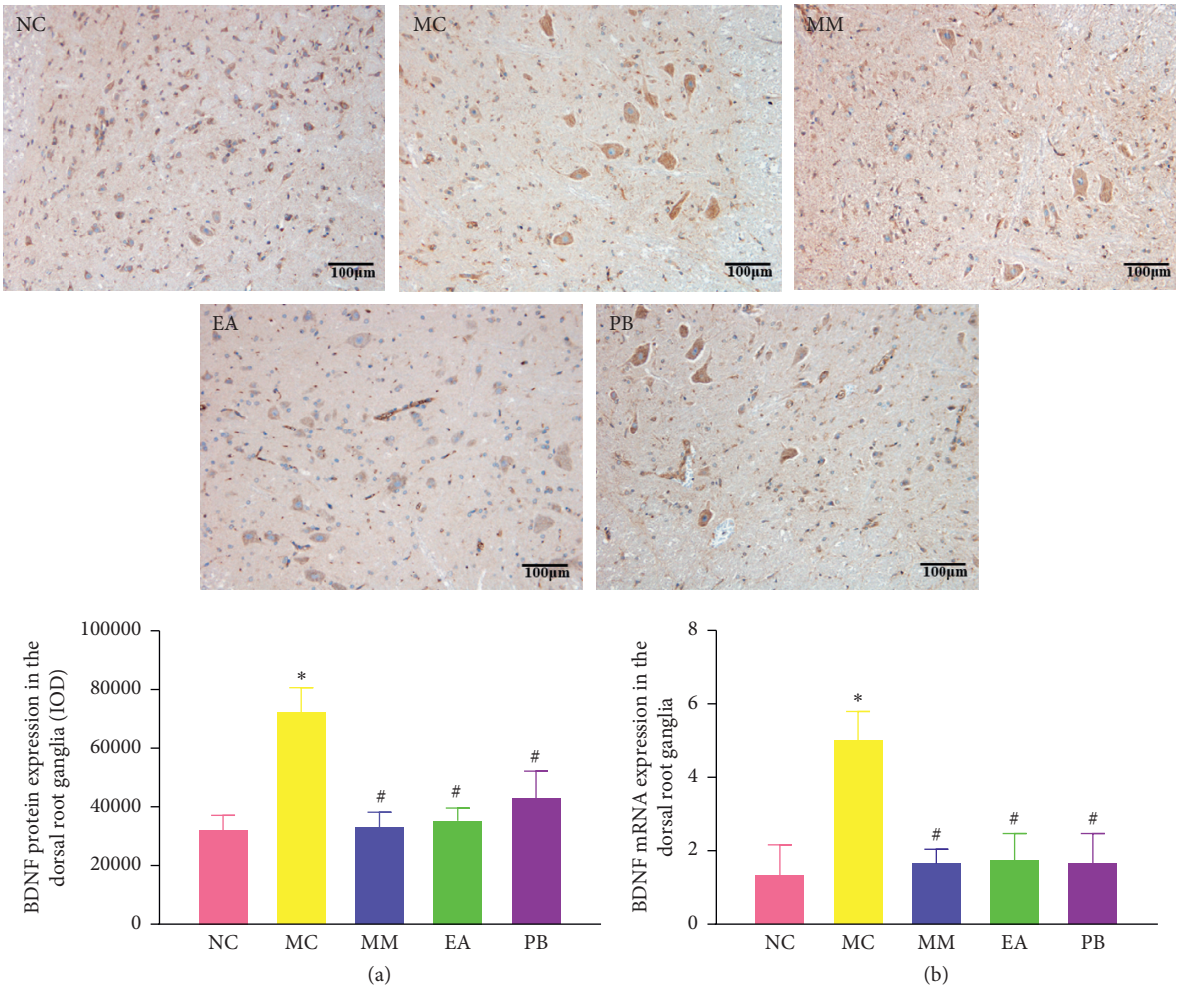

Figure 5: Expression of BDNF protein (×200) and relative expression of BDNF mRNA in the dorsal root ganglia of rats in each group. (a) Expression of BDNF protein in the dorsal root ganglia of rats. (b) The mRNA expression of BDNF in the dorsal root ganglia of rats. NC: normal group; MC: model group; MM: model + mild moxibustion group; EA: model + electroacupuncture group; PB: model + pinaverium bromide group. The data were presented as mean ± SD. $^{*}P < 0.01$ vs. NC; $^{\#}P < 0.01$ vs. MC.

visceral hypersensitivity and the possible therapeutic mechanism based on BDNF and TrkB. BDNF is one of the neurotrophic factors secreted by spinal microglia and mainly expressed in many brain regions including the cortex and hippocampus. It not only has beneficial effects by promoting the development, survival, and maintenance of neurons in the nervous system but also produces noxious stimuli in the central nervous system and is associated with pain regulation and central sensitization. In addition, BDNF is also abundantly expressed in peripheral gastrointestinal tissues and plays an important role in regulating gastrointestinal motility and visceral sensitivity [23]. Visceral hypersensitivity is an important physiopathological mechanism of IBS [24], and BDNF has been found to promote colon visceral hypersensitivity in animal experiments and clinical studies [25, 26]. The afferent nerves, which innervate intestinal sensation, are mainly distributed in the submucosal plexus and the myenteric plexus. Abnormal BDNF expression in these regions can influence the development of the endplate terminals of the gastrointestinal vagus nerve, thereby affecting the innervation of sensory neurons in the vagus nerve [27]. This allows BDNF to be involved in the modulation of inflammation, occurrence of neuropathic pain, and formation of hypersensitivity in chronic pain [23, 28]. Previous studies have shown that the expression of BDNF protein in the lumbosacral spinal dorsal horn was increased in young mice with visceral hypersensitivity induced by neonatal separation [29], and the mRNA expression of BDNF in the hippocampus of IBS rats with visceral hypersensitivity was significantly higher than that in the normal control rats [30]. After intrathecal injection of BDNF antibody in the dorsal root ganglia of rats with inflammatory pain, the body aches of rats were significantly reduced and the expression level of BDNF in the spinal dorsal horn and hippocampus was also reduced [31], indicating that high BDNF expression in the peripheral nervous system may be an important cause of visceral hypersensitive pain in IBS and other inflammatory pain. The main mechanisms of visceral hypersensitivity are the BDNF-mediated changes in gene expression and channel function in primary sensory neurons and the upregulation of spinal cord BDNF expression which were involved in the development of visceral hypersensitivity induced by prenatal

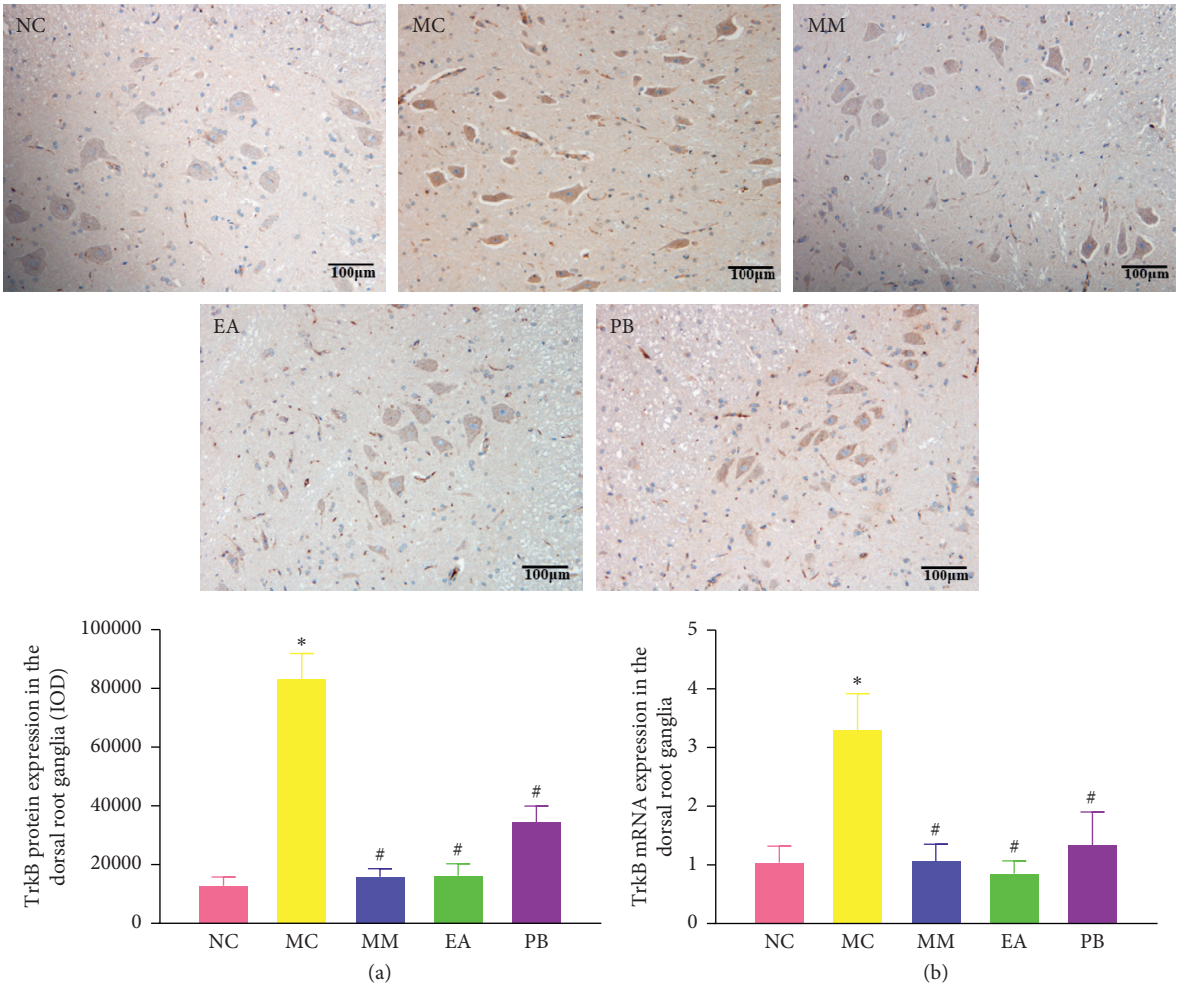

Figure 6: Expression of TrkB protein (×200) and relative expression of TrkB mRNA in the dorsal root ganglia of rats in each group. (a) Expression of TrkB protein in the dorsal root ganglia of rats. (b) The mRNA expression of TrkB in the dorsal root ganglia of rats in each group. NC: normal group; MC: model group; MM: model + mild moxibustion group; EA: model + electroacupuncture group; PB: model + pinaverium bromide group. The data were presented as mean ± SD. $^{*}P < 0.01$ vs. NC; $^{\#}P < 0.01$ vs. MC.

chronic stress [32, 33]. Furthermore, BDNF regulates the integrity of the intestinal epithelial mucosa barrier by affecting the expression of tight junction proteins in the intestinal epithelium, as well as alters the structure of intestinal flora, and is involved in the pathological process of IBS [34, 35].

TrkB, a high-affinity receptor for BDNF, is a tyrosine protein kinase encoded by the thymidine kinase (tdk) proto-oncogene family that can present in the myenteric plexus and submucosal plexus of intestinal tissues. BDNF acts as both an autocrine and a paracrine signal to activate presynaptic TrkB receptors, leading to the activation of tyrosine proteases. The activated tyrosine proteases are involved in the differentiation and development of nerve cells via TrkB-PI3K/AKT, TrkB-MEK/MAPK, and TrkB-PLC/IP3 signaling pathways, and these proteases regulate synaptic excitability in pain conduction and intestinal motility, and they also promote the development of hyperalgesia [36–38]. Binding between BDNF and its receptor TrkB also increases the release of the neurotransmitters serotonin, calcitonin gene-related peptide (CGRP), and P substance (SP) and then causes Ca^{2+} influx on target cell membranes, thereby increasing neuronal discharge activity and excitability in mesenteric afferent nerves and increasing muscle contraction intensity caused by SP and CGRP [39–41]. Studies have found that the expressions of BDNF and nerve fibers were significantly increased in the colon tissues of IBS patients, with damaged ultrastructure of axons in the colon mucosa. BDNF overexpression is also related to the severity and frequency of abdominal pain or discomfort of IBS patients. AWR scores of BDNF-knockout mice under CRD pressure were lower than those of normal mice. Intraperitoneal injection of BDNF in normal mice also induced a dose-dependent increase of postsynaptic TrkB expression and decreased threshold pressure in their dorsal root ganglia [12]. In addition, an IBS rat model induced by repeated water avoidance stress has increased BDNF and TrkB expression in the colon mucosa, submucosa, and myenteric plexus. In that model, BDNF preconditioning enhances the contraction of ring muscle induced by SP, and application of a TrkB antibody inhibited the contraction of colonic muscle. This also attenuates the excitatory effect of SP on the contraction of circular muscle strips, thereby reducing the

excessive movement and hypersensitivity of the colon in IBS rats [42]. The above reports suggest that the BDNF-TrkB signaling pathway is closely related to the IBS visceral hypersensitivity, and recent reports also confirmed that blocking BDNF/TrkB signal transduction in IBS model rats attenuated visceral hypersensitivity and synaptic activity [43].

Our results showed that the AWR scores of visceral hypersensitivity in IBS rats were significantly increased. MM and EA treatment reduced AWR scores of IBS rats, suggesting that acupuncture and moxibustion improved the visceral hypersensitivity of IBS rats. In addition, the protein and mRNA expressions of BDNF and TrkB were significantly increased in the submucosal plexus, myenteric plexus, and dorsal root ganglia of IBS rats. MM and EA treatments significantly reduced the AWR scores as well as the protein and mRNA expressions of BNDF and TrkB in the dorsal root ganglia and enteric nervous systems of IBS rats, suggesting that EA and moxibustion may weaken the noxious stimuli and reduce the hypersensitivity of the intestine, thereby achieving their therapeutic effects in IBS.

Data Availability

The data sets used to support the findings of this study are available from the corresponding author upon reasonable request.

Disclosure

Duiyin Jin, Yanan Liu, and Siyi Lv are the co-first authors.

Conflicts of Interest

The authors declare that there are no conflicts of interest.

Acknowledgments

The authors thank Dr. Huirong Liu for her advices in preparing this manuscript. This work was supported by the National Basic Research Program of China (973 Program, No. 2015CB554501) and the Natural Science Foundation of Shanghai (No. 14ZR1438700).

References

[1] A. Gupta, "Peripheral mechanisms in irritable bowel syndrome," *New England Journal of Medicine*, vol. 368, no. 6, p. 578, 2013.

[2] R. Wernersson and J. Carlsson, "Posttraumatic stress disorder is correlated to irritable bowel syndrome," *Ugeskrift for Laeger*, vol. 177, no. 26, pp. 1248–1252, 2015.

[3] R. Spiller and C. Lam, "An update on post-infectious irritable bowel syndrome: role of genetics, immune activation, serotonin and altered microbiome," *Journal of neurogastroenterology and motility*, vol. 18, no. 3, pp. 258–268, 2012.

[4] S. Cohen-Cory, A. H. Kidane, N. J. Shirkey, and S. Marshak, "Brain-derived neurotrophic factor and the development of structural neuronal connectivity," *Developmental neurobiology*, vol. 70, no. 5, pp. 271–288, 2010.

[5] L. Ulmann, J. P. Hatcher, J. P. Hughes et al., "Up-regulation of P2X4 receptors in spinal microglia after peripheral nerve injury mediates BDNF release and neuropathic pain," *Journal of Neuroscience*, vol. 28, no. 44, pp. 11263–11268, 2008.

[6] I. J. Lever, E. J. Bradbury, J. R. Cunningham et al., "Brain-derived neurotrophic factor is released in the dorsal horn by distinctive patterns of afferent fiber stimulation," *The Journal of Neuroscience*, vol. 21, no. 12, pp. 4469–4477, 2001.

[7] M. Steinkamp, N. Schulte, U. Spaniol, C. Pflüger, J. Kirsch, and G. B. von Boyen, "Apoptosis in enteric glia:Part of the puzzle in Crohn's disease?" *Medical Science Monitor*, vol. 18, no. 4, pp. BR117–BR122, 2012.

[8] C. Lucini, L. Maruccio, P. De Girolamo, and L. Castaldo, "Brain-derived neurotrophic factor in higher vertebrate pancreas: immunolocalization in glucagon cells," *Anatomy and Embryology*, vol. 206, no. 4, pp. 311–318, 2003.

[9] P. Wang, F.-X. Chen, C. Du et al., "Increased production of BDNF in colonic epithelial cells induced by fecal supernatants from diarrheic IBS patients," *Scientific Reports*, vol. 5, no. 1, Article ID 10121, 2015.

[10] R. D. Moloney, T. G. Dinan, and J. F. Cryan, "Strain-dependent variations in visceral sensitivity: relationship to stress, anxiety and spinal glutamate transporter expression," *Genes, Brain and Behavior*, vol. 14, no. 4, pp. 319–329, 2015.

[11] S. Sikandar, M. S. Minett, Q. Millet et al., "Brain-derived neurotrophic factor derived from sensory neurons plays a critical role in chronic pain," *Brain*, vol. 141, no. 4, pp. 1028–1039, 2018.

[12] Y.-B. Yu, X.-L. Zuo, Q.-J. Zhao et al., "Brain-derived neurotrophic factor contributes to abdominal pain in irritable bowel syndrome," *Gut*, vol. 61, no. 5, pp. 685–694, 2012.

[13] X. L. Wu, Y. L. Wang, J. H. Sun et al., "Clinical observation on acupuncture for diarrhea-predominant irritable bowel syndrome patients in syndrome of liver-stagnation and spleen-deficiency and its impact on Th1/Th2," *Zhongguo zhen jiu*, vol. 33, no. 12, pp. 1057–1060, 2013.

[14] J. K. Anastasi, D. J. McMahon, and G. H. Kim, "Symptom management for irritable bowel syndrome," *Gastroenterology Nursing*, vol. 32, no. 4, pp. 243–255, 2009.

[15] E. Manheimer, K. Cheng, L. S. Wieland et al., "Acupuncture for treatment of irritable bowel syndrome," *Cochrane Database of Systematic Reviews*, vol. 5, no. 5, Article ID CD005111, 2012.

[16] E. D. Al-Chaer, M. Kawasaki, and P. J. Pasricha, "A new model of chronic visceral hypersensitivity in adult rats induced by colon irritation during postnatal development," *Gastroenterology*, vol. 119, no. 5, pp. 1276–1285, 2000.

[17] L. D. Wang, J. M. Zhao, and R. J. Huang, "Study on the mechanism underlying the regulation of the NMDA receptor pathway in spinal dorsal horns of visceral hypersensitivity rats by moxibustion," *Evidence-Based Complementary and Alternative Medicine*, vol. 2016, Article ID 3174608, 11 pages, 2016.

[18] C.-H. Bao, C.-Y. Wang, G.-N. Li et al., "Effect of mild moxibustion on intestinal microbiota and NLRP6 inflammasome signaling in rats with post-inflammatory irritable bowel syndrome," *World Journal of Gastroenterology*, vol. 25, no. 32, pp. 4696–4714, 2019.

[19] X. Wang, H. Wu, X. Jin et al., "Gut microbiota was modulated by moxibustion stimulation in rats with irritable bowel syndrome," *Chinese Medicine*, vol. 13, no. 1, p. 63, 2018.

[20] Q. Qi, H. G. Wu, X. M. Jin et al., "Effect of moxibustion on the expression of GDNF and its receptor GFRα3 in the colon and spinal cord of rats with irritable bowel syndrome," *Acupuncture in Medicine*, vol. 37, no. 4, pp. 244–251, 2019.

[21] W. Wei, X. Wu, and Y. Li, *Experimental Methodology of Pharmacology*, People's Medical Publishing House, Beijing, China, 2010.

[22] Z.-Y. Li, Y. Huang, Y.-T. Yang et al., "Moxibustion eases chronic inflammatory visceral pain through regulating MEK, ERK and CREB in rats," *World Journal of Gastroenterology*, vol. 23, no. 34, pp. 6220–6230, 2017.

[23] J. A. M. Coull, S. Beggs, D. Boudreau et al., "BDNF from microglia causes the shift in neuronal anion gradient underlying neuropathic pain," *Nature*, vol. 438, no. 7070, pp. 1017–1021, 2005.

[24] L. Öhman and M. Simrén, "Pathogenesis of IBS: role of inflammation, immunity and neuroimmune interactions," *Nature Reviews Gastroenterology & Hepatology*, vol. 7, no. 3, pp. 163–173, 2010.

[25] Y. Fu, Y. M. Lin, J. H. Winston, R Radhakrishnan, L. M Huang, and X. Z Shi, "Role of brain-derived neurotrophic factor in the pathogenesis of distention-associated abdominal pain in bowel obstruction," *Neuro-Gastroenterology and Motility: The Official Journal of the European Gastrointestinal Motility Society*, vol. 30, no. 10, Article ID e13373, 2018.

[26] Y. Zhang, G. Qin, D.-R. Liu, Y. Wang, and S.-K. Yao, "Increased expression of brain-derived neurotrophic factor is correlated with visceral hypersensitivity in patients with diarrhea-predominant irritable bowel syndrome," *World Journal of Gastroenterology*, vol. 25, no. 2, pp. 269–281, 2019.

[27] J. E. Biddinger and E. A. Fox, "Reduced intestinal brain-derived neurotrophic factor increases vagal sensory innervation of the intestine and enhances satiation," *Journal of Neuroscience*, vol. 34, no. 31, pp. 10379–10393, 2014.

[28] M. Liu, J. C. Kay, S. Shen, and L.-Y. Qiao, "Endogenous BDNF augments NMDA receptor phosphorylation in the spinal cord via PLCγ, PKC, and PI3K/Akt pathways during colitis," *Journal of Neuroinflammation*, vol. 12, no. 1, p. 151, 2015.

[29] B. Wu, C. Xu, and H. Huang, "Expression profiles of brain-derived neurotrophic factor in the spinal dorsal horn of young rats with visceral hypersensitivity," *Chinese Journal of Contemporary Pediatrics*, vol. 18, no. 3, pp. 277–281, 2016.

[30] Y. Zhao, M. Su, and F. Wang, "Effect of chang'an No.I recipe on 5-hydroxytryptamine signal system and mRNA expression levels of hippocampal brain derived neurotrophic factor in visceral hypersensitivity rats with irritable bowel syndrome," *Chinese Journal of Integrated Traditional and Western Medicine*, vol. 35, no. 10, pp. 1228–1235, 2015.

[31] V. Duric and K. E. McCarson, "Neurokinin-1 (NK-1) receptor and brain-derived neurotrophic factor (BDNF) gene expression is differentially modulated in the rat spinal dorsal horn and hippocampus during inflammatory pain," *Molecular Pain*, vol. 3, no. 1, p. 32, 2007.

[32] X.-Z. Shi, Y.-M. Lin, and S. Hegde, "Novel insights into the mechanisms of abdominal pain in obstructive bowel disorders," *Frontiers in Integrative Neuroscience*, vol. 12, p. 23, 2018.

[33] J. H. Winston, Q. Li, and S. K. Sarna, "Chronic prenatal stress epigenetically modifies spinal cord BDNF expression to induce sex-specific visceral hypersensitivity in offspring," *Neuro-Gastroenterology and Motility*, vol. 26, no. 5, pp. 715–730, 2014.

[34] Y. B. Yu, D. Y. Zhao, Q. Q. Qi et al., "BDNF modulates intestinal barrier integrity through regulating the expression of tight junction proteins," *Neuro-Gastroenterology and Motility: The Official Journal of the European Gastrointestinal Motility Society*, vol. 29, no. 3, 2017.

[35] C. Li, Y.-Y. Cai, and Z.-X. Yan, "Brain-derived neurotrophic factor preserves intestinal mucosal barrier function and alters gut microbiota in mice," *The Kaohsiung Journal of Medical Sciences*, vol. 34, no. 3, pp. 134–141, 2018.

[36] J. Y. Lim, S. I. Park, J. H. Oh et al., "Brain-derived neurotrophic factor stimulates the neural differentiation of human umbilical cord blood-derived mesenchymal stem cells and survival of differentiated cells through MAPK/ERK and PI3K/Akt-dependent signaling pathways," *Journal of Neuroscience Research*, vol. 86, no. 10, pp. 2168–2178, 2008.

[37] F. Chen, Y. Yu, P. Wang et al., "Brain-derived neurotrophic factor accelerates gut motility in slow-transit constipation," *Acta Physiologica*, vol. 212, no. 3, pp. 226–238, 2014.

[38] Y.-T. Lin, L.-S. Ro, H.-L. Wang, and J.-C. Chen, "Up-regulation of dorsal root ganglia BDNF and trkB receptor in inflammatory pain: an in vivo and in vitrostudy," *Journal of Neuroinflammation*, vol. 8, no. 1, p. 126, 2011.

[39] W. Boesmans, P. Gomes, J. Janssens, J. Tack, and P. V. Berghe, "Brain-derived neurotrophic factor amplifies neurotransmitter responses and promotes synaptic communication in the enteric nervous system," *Gut*, vol. 57, no. 3, pp. 314–322, 2008.

[40] F. X. Chen, Y. B. Yu, X. M. Yuan, X. L Zuo, and Y. Q Li, "Brain-derived neurotrophic factor enhances the contraction of intestinal muscle strips induced by SP and CGRP in mice," *Regulatory Peptides*, vol. 178, no. 1-3, pp. 86–94, 2012.

[41] P. Wang, C. Du, F.-X. Chen et al., "BDNF contributes to IBS-like colonic hypersensitivity via activating the enteroglia-nerve unit," *Scientific Reports*, vol. 6, no. 1, p. 20320, 2016.

[42] X. Quan, H. Luo, H. Fan et al., "Brain-derived neurotrophic factor contributes to colonic hypermotility in a chronic stress rat model," *Digestive Diseases and Sciences*, vol. 60, no. 8, pp. 2316–2326, 2015.

[43] F. Fan, Y. Tang, H. Dai et al., "Blockade of BDNF signalling attenuates chronic visceral hypersensitivity in an IBS-like rat model," *European Journal of Pain*, vol. 24, no. 4, pp. 839–850, 2020.

Hindawi
Evidence-Based Complementary and Alternative Medicine
Volume 2021, Article ID 2771094, 14 pages
https://doi.org/10.1155/2021/2771094

Research Article

The Influence of Stomach Back-Shu and Front-Mu Points on Insular Functional Connectivity in Functional Dyspepsia Rat Models

Yuan Chen,[1] Ying Zhao,[1] Robert Yu-Sheng Tan,[1] Pu-yue Zhang,[1] Tao Long,[1] Yu Shi,[2] and Hua-bin Zheng[3]

[1]*Acupuncture and Tuina School, Chengdu University of Traditional Chinese Medicine, Chengdu, China*
[2]*Department of Oncology, Chongqing Beibei Traditional Chinese Medical Hospital, Chongqing, China*
[3]*Department of Acupuncture and Moxibustion, Affiliated Hospital of Chengdu University of Traditional Chinese Medicine, Chengdu 610072, China*

Correspondence should be addressed to Hua-bin Zheng; zhenghb@cdutcm.edu.cn

Received 4 June 2021; Revised 1 September 2021; Accepted 3 September 2021; Published 15 September 2021

Academic Editor: Mi Liu

Functional Dyspepsia (FD) is a common functional gastrointestinal disease, which can reduce the quality of life in patients. Prior research has indicated that insula is closely related to FD and that acupuncture can regulate the functional connectivity (FC) of FD. Therefore, we hypothesized that acupuncture on FD was effected through the insular pathway. To test our hypothesis, we performed electroacupuncture (EA) on FD rat models and then examined the FC between insula and other brain regions through resting-state functional magnetic resonance imaging (rs-fMRI). Seven-day-old male infant Sprague-Dawley (SD) rats were randomly divided into control group, FD model group, and FD acupuncture group, with twelve rats per group ($n = 36$). Upon establishing successful models, the FD acupuncture group was subjected to EA intervention using Stomach back-shu (BL-21) and front-mu (RN-12) points for ten consecutive days for durations of 20 minutes each day. After intervention, each group was subject to rs-fMRI. The digital image data obtained were analyzed using FC analysis methods. Subsequently, gastric ligation was performed to measure gastric emptying rates. Before EA intervention, the FD model group exhibited decreased functional connections between the insula and a number of brain regions. After EA intervention, FD acupuncture group exhibited increasing FC between insula and regions when compared to the FD model group, such as the primary somatosensory cortex (S1), hippocampal CA3 (CA3), polymorphic layer of dentate gyrus (PoDG), caudate putamen (CPu), and oral pontine reticular nuclei (PnO) ($P < 0.05$); decreasing FC was also exhibited between insula and regions such as the bilateral primary and secondary motor cortexes (M1/2), paraventricular hypothalamic nucleus (PVA), and limbic cortex (LC). These findings indicate that the effective treatment of FD using EA may be through regulating the abnormal FC between insula and several brain regions, in particular CA3, PoDG, and PVA.

1. Introduction

Functional Dyspepsia (FD) is a functional gastrointestinal disorder defined by the Rome IV consensus as the presence of symptoms thought to originate from the upper gastrointestinal region without organic causes; it can be divided into postprandial distress syndrome (PDS) and epigastric pain syndrome (EPS) [1]. Despite not being a life-threatening condition, it severely reduces quality of life for affected patients [2]. Current conventional allopathic treatment options exist for FD, such as *H. pylori* eradication, proton pump inhibitors (PPIs), and histamine-type-2-receptor antagonists (H2RAs); however, their efficacies are modest at best [3, 4], and they also result in negative side effects or negative long-term effects to the patient [5, 6]. For example, *H. pylori* eradication using antibiotics often produces gastrointestinal side effects such as diarrhea, nausea, taste distortion, stomatitis, and bloating, which reduce the

tolerability of treatment and lead to treatment withdrawal [5]; treatments using PPIs have been shown to potentially cause serious long-term adverse effects, such as pneumonia, *C. difficile* diarrhea, risk of fractures, and hypomagnesemia [6]. Studies on the effects of H2RAs have typically suffered from poor quality or have shown a small effect on FD at best [4].

As an alternative form of treatment for FD that does not result in the same long-term side effects and resistance as drugs [7], acupuncture and/or electroacupuncture (EA) has been used in China for thousands of years to help relieve its various symptoms [8]. Research in this area has focused on the mechanisms behind both the pathogenesis of the condition [9] and the therapeutic effects of acupuncture on human and animal subjects [10–12]. Such studies often use imaging technologies such as positron emission tomography-computed tomography (PET-CT) [8, 9, 12] and functional magnetic resonance imaging (fMRI) [13–15]. Regardless of the type of imaging study, results have consistently shown that the insula, a brain region in the deep cerebral hemisphere involved in processing emotional responses, visceral sensation, interoceptive awareness, cognitive and affective regulatory functions, and olfactory and gustatory stimulation processing [9, 16–18], is an important area in FD research, since it is involved in both the pathogenesis and treatment of FD [8, 9, 12]. Studies involving human subjects in this area have shown weakened structural changes and functional connections of the insula in patients with FD [9], correlation between these changes and severity of FD symptoms [12], and changes in functional connections occurring through acupuncture or EA treatment of FD [8]. However, there has been little research into the activation pathways and mechanisms that are triggered through the insula when treating FD with acupuncture or EA. Furthermore, modeling of FD using animals has become an emerging area of research due to ethical or economic considerations arising from use of human FD patients.

Rats have commonly been used to mimic some of the disease outcomes and conditions of FD, such as psychological distress, delayed gastric emptying, impaired gastric accommodation, and visceral hypersensitivity, as described by Ye et al. [11]. Acupuncture point combinations such as the pairing of Stomach back-shu (BL-21) and front-mu (RN-12) points are among those typically used in acupuncture or EA treatment modalities of animal models [19, 20]. This combination has been shown specifically to improve decreased gastric motility through the hippocampus [21], dorsal vagal complex (DVC) [19, 20], or the paraventricular hypothalamic nucleus (PVA) [20]. However, like similar studies involving human counterparts, there has been little research into the activation pathways and mechanisms involving the insula in acupuncture or EA treatment of FD [21]. Due to the importance of the insula in both the pathogenesis and treatment aspects of FD, we hypothesize that it occupies a major role in the central mechanisms in acupuncture or EA treatment of FD. Our study aims to explore this hypothesis by conducting a seed-based functional connectivity analysis of FD rat models with EA intervention, in which the insula is designated as the region of interest (ROI).

2. Materials and Methods

2.1. Ethical Approval. This study was approved by the Experimental Animal Welfare and Ethics Committee of Chengdu University of Traditional Chinese Medicine (no. 2016-10). All efforts were made to minimize suffering.

2.2. Materials. The materials used are as follows: 0.1% iodoacetamide (Sigma Corporation, USA), isoflurane (ISO) (RWD Living Science Technology Inc., Shenzhen, China), Safe 2010 Safety Cabinet (Heto-Holten A/S, Denmark), PF Hetotherm Heating circulator (Heto-Holten A/S, Denmark), G6805-II electroacupuncture pulse generator (Qingdao Xinsheng Medical Instrument Factory, Shandong, China), Bruker BioSpec 70/20 USR small animal 7T MRI scanner (600 MHz) (Bruker Corporation, Germany), SPSS 20.0 (SPSS Inc., Chicago, IL, USA), and spmratIHEP based on the statistical parametric mapping (SPM8) software (Welcome Department of Cognitive Neurology, London, UK).

2.3. Animals and Grouping. Thirty-six healthy Sprague-Dawley (SD) rat pups (7 days old, day of birth = day 0) were used in this study (Certificate no.: CXK [Sichuan] 2015-030). The rat pups were randomly divided into control group ($n = 12$), FD model group ($n = 12$), and FD acupuncture group ($n = 12$) and placed in three separate cages. Although neonatal maternal separation has been shown to be one of the commonly used methods in producing FD animal models [11], it has also been identified as a risk factor in irritable bowel syndrome (IBS) [22]. To prevent the possibility of creating IBS models as a confounding factor, we placed one lactating female rat in each cage with sufficient food and water to provide feeding for the pups. After seven days of nursing to help rat pups acclimatize, the first phase of FD modeling was commenced.

2.4. FD Modeling. A two-phase multiple-feature modeling method was used to create the FD model used in this study, including iodoacetamide-sucrose administration, tail clamping, and irregular feeding, which have been previously described [11, 21–24]. We aimed to produce FD rat models with the specific set of characteristics: presence of anxiety-like behaviour resulting in decreased appetite and water intake, reduction in activity, decrease of coat luster, increased knots in fur, and delayed gastric emptying. Phase one consisted of oral gavage administration of an iodoacetamide-sucrose solution, consisting of 0.1% iodoacetamide (IA) distilled water solution with a 2% sucrose distilled water solution, mixed at a ratio of 1 : 1 to induce neonatal gastric irritation [11]. The FD model and FD acupuncture groups received oral gavage administration of the IA-sucrose solution over 6 days, 0.2 mL per day, while the control group received oral gavage administration of 0.2 mL 2% sucrose distilled water solution over the same period, all alongside regular nursing [25]. After the six-day period, regular nursing was resumed until day 22, at which point the female

rats were separated from the litters. From day 22 onwards, feed pellets were introduced until the rat pups reached 7 weeks of age, and we commenced phase two of FD modeling. Phase two consisted of tail clamping to induce stress and delayed gastric emptying [11, 26] and irregular feeding to disrupt regular feeding cycles [21] over a period of 14 days. Tail clamping provocation was implemented in the FD model and FD acupuncture groups by clamping sponge forceps at the distal 1/3 region of rat tails, without injury to the skin, for 30 minutes at a time, four times per day [27]. Discomfort from tail clamping made the rats irritable and anxious and caused infighting. Irregular feeding was also administered to the FD model and FD acupuncture groups during this period by withholding food (but not water) on odd-numbered days and feeding normally on even-numbered days [21]. The control group was fed normally during phase two without tail clamping. At the end of phase two on day 63, successful FD modeling was confirmed by rats in the FD groups having exhibited the desired model characteristics prior to the beginning of EA intervention. EA intervention was then administered from day 63 to day 73, followed by subsequent fMRI scanning and gastric extraction. Indirect indication of successful FD modeling was also confirmed after gastric extraction, when delayed gastric emptying rates were measured in the FD model group and compared to the control group, after EA intervention. The workflow of the experimental protocol is shown in Figure 1.

2.5. Acupuncture Point Location. The Stomach front-mu Zhongwan (RN-12) and back-shu Weishu (BL-21) acupuncture points were located in the same manner as described by Wang et al. [19]. The location of Stomach front-mu point was established as being 20 mm above the umbilicus in the anterior centre line, needled at a depth of 2 mm [19]. The location of Stomach back-shu point was established as being 5 mm lateral to the twelfth thoracic vertebrae on both sides, needled at a depth of 4 mm [19]. Figure 2 shows the locations of RN-12 and BL-21 acupuncture points on our rat model [21].

2.6. Electroacupuncture Intervention. EA intervention commenced on day 63, when FD modeling had been successfully established. To prevent unnecessary struggle during the EA intervention, rats in all three groups were restrained, although only the FD acupuncture group received EA treatment. In addition, cotton cloth was used to cover the head of rats during the EA sessions to prevent unnecessary stress and to accommodate their preference for darkness, which better facilitated the EA procedures. The EA treatment administered to the FD acupuncture group consisted of needling both the RN-12 and one of BL-21 points (left and right sides, alternating on even and odd days) on rats sterilized with iodophor at the two point locations. Sterile one-time-use 0.25×13 mm needles were inserted at the previously indicated depth of 2 mm and monitored to avoid injury to the viscera. Due to the highly technical nature of EA treatment, all needle operators were licensed MDs who had been trained in acupuncture needling techniques. To avoid differences due to manual hand stimulation, needles were not stimulated by hand but were instead attached to an electroacupuncture apparatus (HANS-200A, Nanjing, China) to send controlled and uniformed stimulation to the needles (dilatational wave, frequency of 2/15 Hz, and output current of 1.5 mA). Treatment was administered for 20 minutes each day, beginning at 9 a.m. On rare occasions, rats who escaped from their restraints were rebound and had their treatments start from the beginning. The control and FD model groups, although also bound to eliminate differences in restraint-related stresses between the groups, were not subject to the EA treatment and were kept segregated from the FD acupuncture group to prevent undue stress triggered by noise from the FD acupuncture group.

2.7. fMRI Scanning, Observational Metrics, and Data Processing. At each phase of the study, metrics were collected with regard to changes in general observations, body weight, food intake, and water intake of the rats. The following criteria were observed and scored on a 20-point scale: coat color and luster, mental state, dexterity, body weight via digital scale, and amount of food and water intake [28]. Scoring was performed as follows and the changes were summarized using one-way analysis of variance (one-way ANOVA) as comparison:

(1) Rat coat color and luster: 5 points for bright and shiny coat, 3 points for mildly bright and shiny coat, and 1 point for dry and dull coats

(2) Rat dexterity: 5 points for extremely dexterous, 3 points for mildly dexterous, and 1 point for sluggish and not dexterous

(3) Rat food intake: 5 points for no change in food intake, 3 points for slight changes in food intake, and 1 point for significantly reduced food intake

(4) Rat body weight: 5 points for increased body weight, 3 points for unchanged body weight, and 1 point for significantly reduced body weight

After EA intervention, at least 6 rats were randomly chosen from each group according to the requirements of imaging research, and 7.0T animal rs-fMRI scans were performed on these selected rats. The scanning method was to extract 2-3 EPI sequences for each rat and 1 RARE sequence (EPI sequence: TE = 16 ms, TR = 1000 ms, segments = 2, average = 1, repetition = 300, FOV = 25×25 mm^2, Matrix = 80×80, slice = 18, and thickness = 0.75 mm; T2 structural image: RARE sequence, TE = 12 ms, TR = 4000 ms, average = 4, FOV = 25×25 mm 2, Matrix = 256×256, slice = 18, and thickness = 0.75 mm). The data obtained was processed using SPSS 20.0 statistical software package.

After data collection was completed, spmratIHEP toolkit based on the statistical parametric mapping (SPM8) software was used to sequentially perform image preprocessing, brain segmentation, data extraction, and functional connectivity calculation of the brain. Establishing the insula-related ROI as the seed in a similar manner as described by Nie et al. [29], its functional connections were compared to those of other

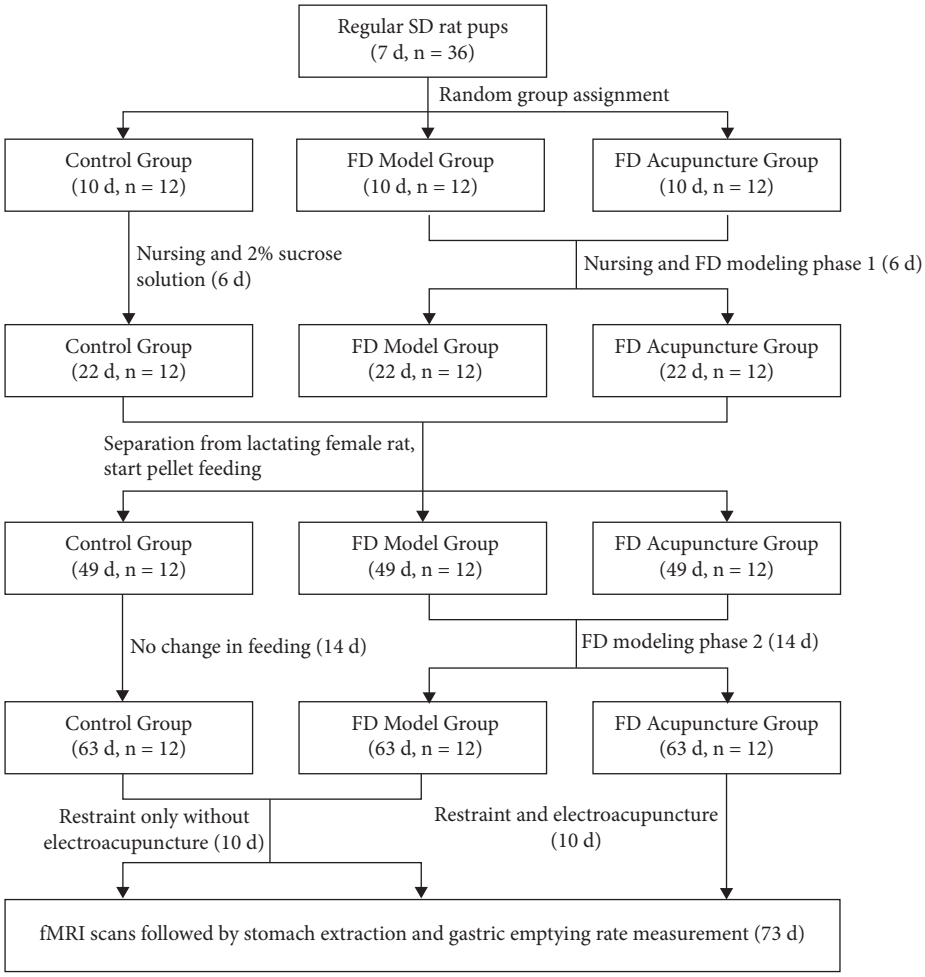

Figure 1: Experimental procedure.

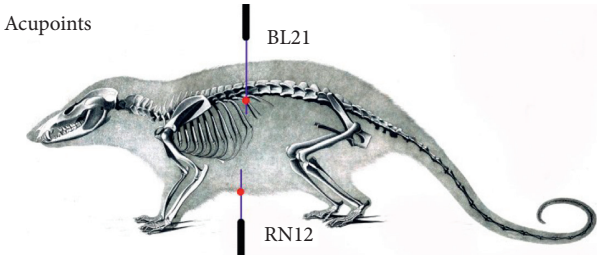

Figure 2: The locations of RN-12 and BL-21 acupuncture points on our rat model.

voxels of the entire brain in all three of the control, FD model, and FD acupuncture groups. Through nonparametric tests, it was found that when $P < 0.05$, clusters greater than 6 voxels were considered statistically significant. Permutation TFCE0.05 was used for correction. After correction, the statistically significant brain activation area image was superimposed onto the standard brain image. After statistical calculations were made, the positions, position coordinates, and signal types of the activated brain areas were recorded (see Figure 3 for an example of T2 structural phase).

2.8. Detection of Gastric Emptying Rate of Rats in Each Group after Intervention. Subsequent to fMRI scanning, gastric emptying rate was measured in the scanned rats, using methods similar to those described by Francis et al. and Asuzu and Njoku [30, 31]. On the last day of EA intervention, 6 rats from each group were randomly selected and placed into the anesthesia box, where a mixture of 5% isoflurane and 100% oxygen gas was administered through inhalation. 50 minutes prior to anesthesia, rats were also fed starch paste of 1 g/ml. Once anesthetized, the isoflurane concentration was reduced to 3% to maintain the anesthesia state. Then the rats were fixed, and a surgical scalpel was used to dissect the peritoneal cavity, which was opened gently using sterile gauze.

The cardia and pylorus were quickly ligated with surgical sutures, and the entire stomach was subsequently removed. The stomachs were weighed digitally after surface mucosa and excess tissue were removed and excess blood and fluids were wiped clean from the surface. After recording the gross stomach weights, small animal surgical shears were used to cut along the greater curvature of the stomach, with the remainder starch paste being washed out using a saline solution. The stomach was subsequently dried with gauze and weighed to determine net stomach weight. Upon

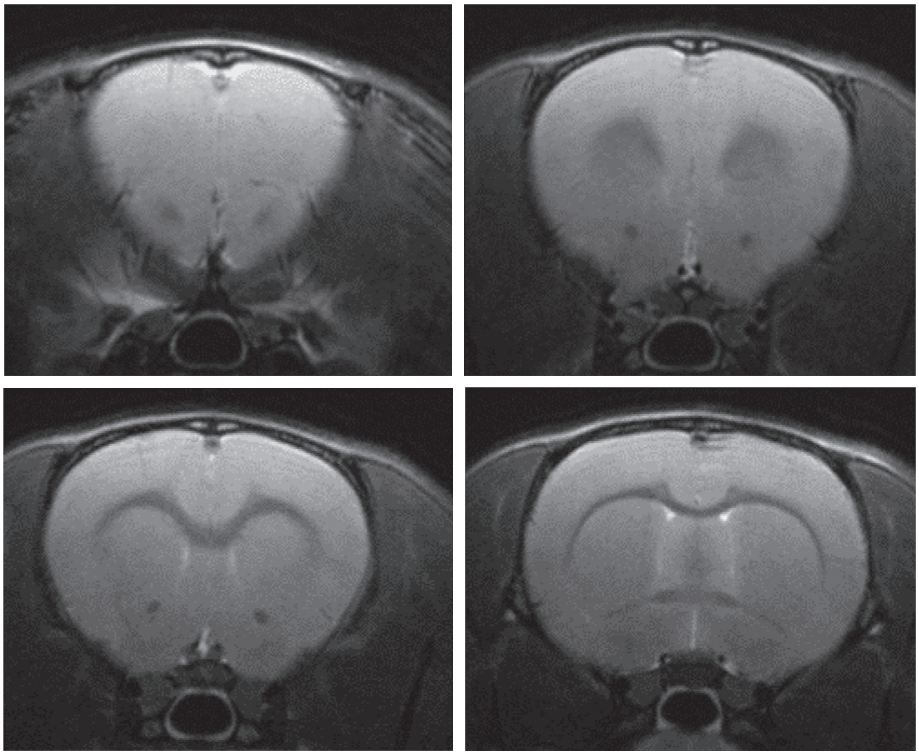

Figure 3: Example of T2 structural phases.

recording net stomach weight, the gastric emptying rate was calculated as follows: (1 − (gross stomach weight − net stomach weight)/starch weight) × 100%. Rats were then euthanized via anesthesia.

2.9. Statistical Analysis. Statistical analyses were performed using SPSS 20.0 software. Scoring of general observations, rat body weight, changes in food intake, changes in water intake, and gastric emptying rate are represented as the mean ± SD. The data of all three groups formed positive distributions, and the groups were compared using one-way analysis of variance (ANOVA) and Kruskal-Wallis H tests. Brain functional connection results were analyzed using nonparametric test. When the P value was less than 0.05 and the number of clusters was more than 6, the difference was considered statistically significant. Permutation TFCE 0.05 was used for correction.

3. Results and Discussion

3.1. Observations regarding General State. Changes in coat color and luster, mental state, dexterity, body weight, and amount of food and water intake are summarized in Figure 4 using one-way analysis of variance (one-way ANOVA) as comparison.

3.2. Body Changes in Rat Body Weight in Each Phase. Body weight for each rat was measured using a digital scale prior to FD modeling, during each phase of FD modeling, and after EA intervention. During phase-one oral gavage administration, weight was recorded on days 1, 3, and 6. The control group had statistically significantly higher body weight gain compared to both FD groups ($P < 0.05$). Both FD groups maintained similar weight throughout phase one ($P > 0.05$). Changes were compared using one-way ANOVA and are summarized in Figure 5(a).

During phase-two tail clamping, weight was recorded on days 1, 7, and 14. Throughout the tail clamping process, both FD model and FD acupuncture groups maintained similar increases ($P > 0.05$), which were significantly less compared to the control group ($P < 0.05$). Changes were compared using one-way ANOVA and are summarized in Figure 5(b).

During EA intervention, weight was recorded on the first day and last day. The FD acupuncture group had the highest increase in weight, followed by the FD model group and control group. The weight gain for FD acupuncture group was statistically significant compared separately to both the FD model and control groups ($P < 0.05$). The weight gain for FD model group was statistically significant compared to the control group ($P < 0.05$). Changes were compared using one-way ANOVA and are summarized in Figure 5(c).

3.3. Changes in Food and Water Intake of Rats in Each Group. Rats were fed each day at 9 a.m. with a fixed amount of feed that was weighed on a digital scale. The amount of remaining feed was measured at 9 a.m. the next morning, and the difference was taken as the change in daily food intake. Water intake was measured in a similar manner as the change in daily water intake.

Prior to EA intervention, both FD groups exhibited less food and water intake compared to the control group

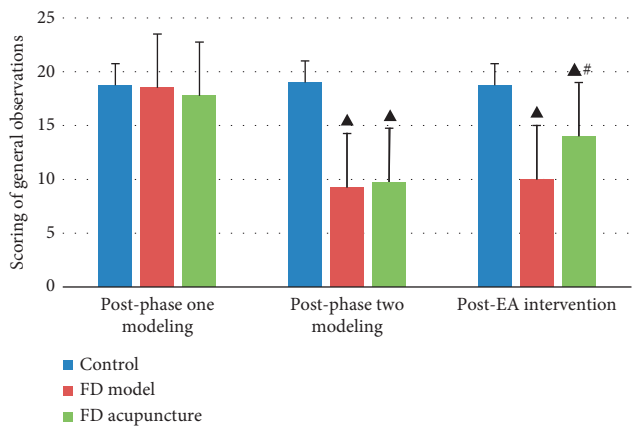

Figure 4: Scoring of general observations in different groups; data are presented as mean ± SD ($n = 6$). Note: ▲$P < 0.05$, versus control group; #$P < 0.05$, versus FD model group.

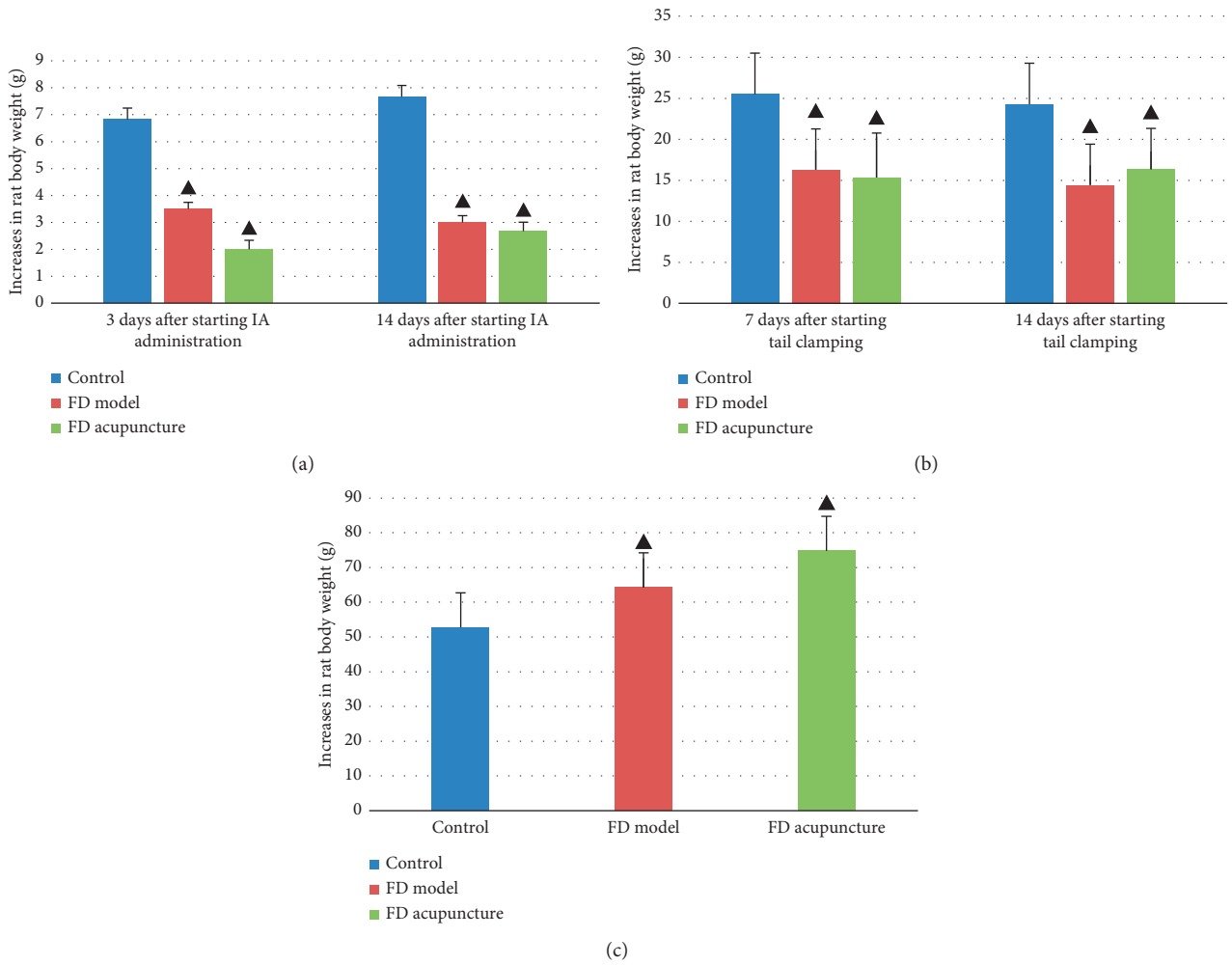

Figure 5: Increases in rat body weight in different groups. (a) During phase-one oral gavage administration; (b) during phase-two tail clamping; (c) during EA intervention. Data are presented as mean ± SD ($n = 6$). Note: ▲$P < 0.05$, versus control group.

($P < 0.05$). After EA intervention, both FD groups exhibited greater amounts of food and water intake, although FD model group was still less than that of FD acupuncture ($P < 0.05$). The results were compared using one-way ANOVA and are summarized in Figures 6(a) and 6(b).

3.4. Gastric Emptying Rate after EA Intervention. A summarized comparison of the gastric emptying rates between the groups after EA intervention is listed in Figure 7 with comparisons performed using the Kruskal-Wallis H test. The FD model group had a significant lower gastric emptying rate when compared to the control group ($P < 0.05$), while the FD acupuncture group had a significantly higher gastric emptying rate when compared to the FD model group ($P < 0.05$).

3.5. Rat fMRI Imaging Results. Six rats were chosen from each of the three groups, and rs-fMRI scanning was performed after EA intervention. The scans established the insula as the seed while exploring its functional connections with the rest of the brain:

(1) Compared to the control group, the FD model group contained regions which had significant functional connections with the insula, as seen in Table 1 and Figure 8. Compared with the control group, rats in the FD model group exhibited decreased functional connections in regions including the primary somatosensory cortex, hippocampal CA3, thalamus, ectorhinal cortex, polymorphic layer of dentate gyrus, medial parietal association cortex, primary visual cortex, and temporal association cortex ($P < 0.05$, cluster >6, differences are statistically significant).

(2) After EA intervention, when compared to the FD model group, the FD acupuncture group displayed regions which had significant functional connections to the insula, summarized in Table 2 and Figure 9. The regions which exhibited increased functional connections include caudate putamen, barrel field of primary somatosensory cortex, hippocampal CA3, oral pontine reticular nuclei, and polymorphic layer of dentate gyrus ($P < 0.05$, cluster >6, difference is statistically significant); some regions also exhibited decreased functional connections, including the paraventricular nucleus of hypothalamus, bilateral primary motor cortexes, and limbic cortex.

3.6. Discussion. Present explanations on the mechanism of acupuncture center around neural mechanisms or humoral mechanisms; thus our exploration focuses on the neural mechanism of acupuncture in the treatment of FD. There is increasing evidence in support of the presence of abnormal central changes of FD patients in addition to the peripheral changes in gastrointestinal tract. Previous results have suggested that the frontal cortex, somatosensory cortex, insula, ACC, thalamus, hippocampus, and amygdala were activated in FD patients prior to treatment, with the insula in particular occupying a key role [9, 32]. Interestingly, several studies have indicated that the brain regions activated in FD patients at baseline are different than those with acupuncture or EA intervention [8, 10]. This phenomenon suggests that the central mechanism involved in the pathogenesis of FD may be different than that of acupuncture treatment of FD patients and suggests the possibility of different pathway(s) in acupuncture treatment of FD patients, which we also explore in our results.

Our current rs-fMRI study involving seed-based functional connectivity analysis on EA treatment of FD rat models establishing the insula as ROI has revealed the following: (a) the combination of RN-12 and BL-21 acupoints can be used to improve gastric motility, which confirms the results of previous studies [19–21], and, more importantly, (b) specific patterns of increasing and decreasing functional connectivity not only exist with regard to the insula in FD rat models but also occur in EA intervention of FD.

Initially, we created a two-phase, multiple feature rat model of FD using methods previously established, including neonatal gastric irritation through oral gavage administration of iodoacetamide, tail clamping, and irregular feeding [11, 21, 23]. Successful models of both FD model and FD acupuncture groups were confirmed through monitoring of decreasing point measurements of general observations, increased anxiety-like behaviour, and infighting, resulting in decreased body weight and food and water intake, and through delayed gastric emptying rates which were measured subsequent to rs-fMRI scans. All measures that were recorded, except for gastric emptying rates, showed that statistically significant differences existed between the two FD groups and the control group. Our results also showed no statistically significant differences amongst the two FD groups prior to EA intervention, which confirmed successful FD modeling as reported in other studies [11, 21, 23]. Throughout the EA intervention phase of the study, the data collected regarding weight gain and food and water intake of the FD model group revealed two points of interest which seemed to contradict the initial effects of FD modeling to produce decreased weight gain, food intake, and water intake. First, the FD model group exhibited more weight gain than the control group throughout the EA intervention phase, even though FD model group was only restrained and not subject to EA intervention, as shown in Figure 5(c). Second, the FD model group also exhibited significant increases in food and water intake throughout the EA intervention phase, despite not being subject to EA intervention, as shown in Figures 6(a) and 6(b). These changes were unexpected because we initially believed that the FD modeling measures employed would produce permanent pathophysiological changes such as permanent increases in weight loss as noted by Wu et al. [23]. However, similar trends were shown in another study by Zhang et al. measuring the effects of Shen-Ling-Bai-Zhu-San on FD rat models [33], where the FD model group exhibited increases in food and water intake without intervention. Here, the data seemed to show other factors at work which decreased the effects of FD modeling on the FD model group, despite this group not being subject to EA intervention. Since no other

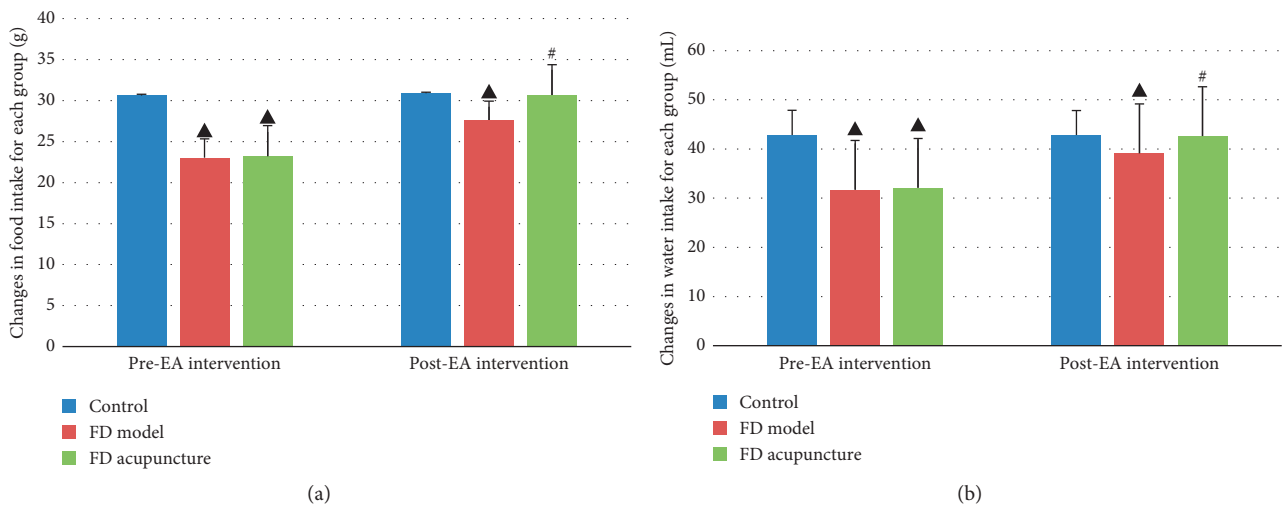

Figure 6: (a) Comparison of changes in food intake before and after EA intervention; (b) comparison of changes in water intake before and after EA intervention. Data are presented as mean ± SD ($n = 6$). Note: ▲$P < 0.05$, versus control group; #$P < 0.05$, versus FD model group.

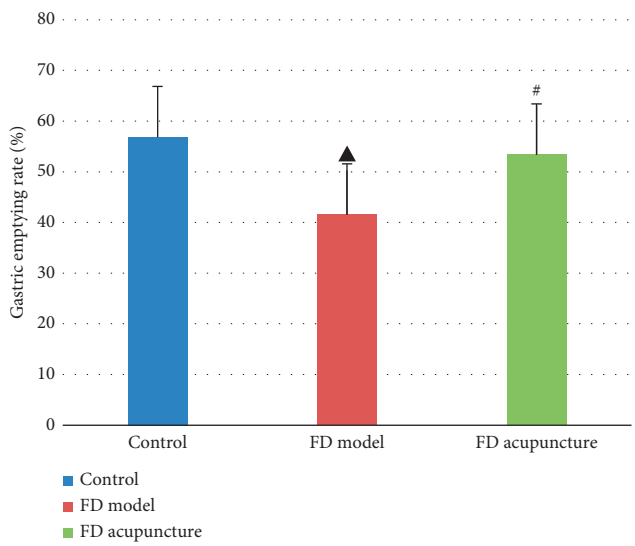

Figure 7: Comparison of gastric emptying rates between groups ($n = 6$). Note: ▲$P < 0.05$, versus control group; #$P < 0.05$, versus FD model group.

Table 1: FC results (control group versus FD model group).

Brain region	Brain functional connection results		Standard deviations	
	Voxel size	t value	Mean ± SD (control)	Mean ± SD (FD model)
Primary somatosensory cortex (S1)	133	−3.4199	0.16 ± 0.11	0.06 ± 0.06
Hippocampal CA3 (CA3)	>200	−4.9154	0.23 ± 0.09	0.10 ± 0.08
Thalamus (THa)	>100	−3.1142	0.10 ± 0.11	0.02 ± 0.06
Ectorhinal cortex (Ect)	35	−2.6699	0.25 ± 0.12	0.16 ± 0.09
Polymorphic layer of dentate gyrus (PoDG)	>100	−4.4994	0.13 ± 0.08	0.02 ± 0.06
Medial parietal association cortex (MPtA)	>100	−3.2009	0.22 ± 0.16	0.09 ± 0.09
Primary visual cortex (V1)	>100	−3.9261	0.16 ± 0.12	0.06 ± 0.08
Temporal association cortex (TeA)	>100	−4.4293	0.19 ± 0.11	0.07 ± 0.09

In the FD model group, regions exhibit significant functional connections to the insula. Negative t values denote weakening connection, while positive t values denote strengthening connections.

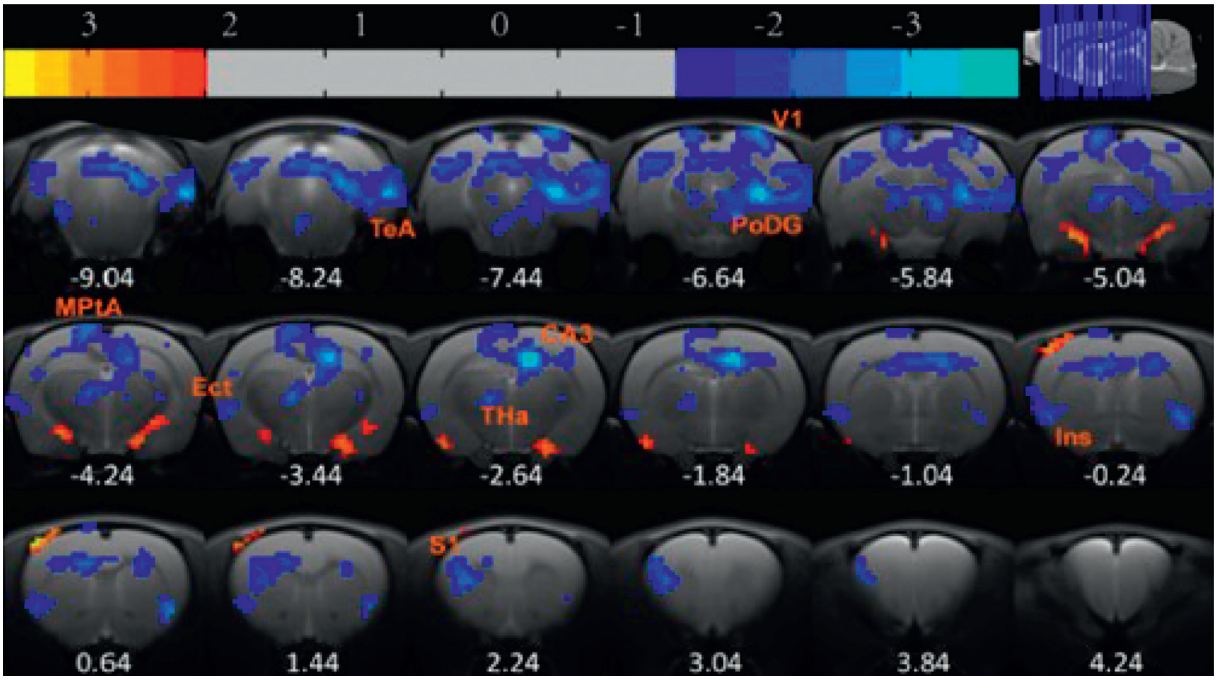

Figure 8: Regions exhibiting significant functional connections with the insula, FD model group after EA intervention.

Table 2: FC results (FD model group versus FD acupuncture group).

Brain region	Brain functional connection results		Standard deviations	
	Voxel size	t value	Mean ± SD (FD model)	Mean ± SD (FD acupuncture)
Right primary and secondary motor cortexes (M1/2)	44	−2.909	0.13 ± 0.09	0.05 ± 0.10
Left primary and secondary motor cortexes (M1/2)	23	−3.3159	0.09 ± 0.05	0.04 ± 0.07
Paraventricular nucleus of hypothalamus (PVA)	13	−2.7523	0.11 ± 0.08	0.05 ± 0.09
Caudate putamen (CPu)	9	2.56917	0.10 ± 0.05	0.14 ± 0.07
Barrel field of primary somatosensory cortex (S1BF)	29	2.0751	0.12 ± 0.07	0.19 ± 0.09
Hippocampal CA3 (CA3)	60	3.1749	0.07 ± 0.09	0.16 ± 0.11
Oral pontine reticular nuclei (PnO)	257	3.6603	−0.01 ± 0.06	0.09 ± 0.10
Polymorphic layer of dentate gyrus (PoDG)	62	3.5844	0.04 ± 0.07	0.11 ± 0.10

In the FD acupuncture group, regions exhibit significant functional connections to the insula. Negative t values denote weakening connection, while positive t values denote strengthening connections.

interfering measures were applied to the FD model group, we hypothesize that these improvements may have had to do with the natural healing functions of the body and take note of this as a point of interest to consider in future research.

After EA intervention and the rs-fMRI process, gastric ligation was performed to both indirectly confirm successful modeling and measure the effect of EA intervention on gastric emptying rates. We found that the control group had the highest gastric emptying rate (56.82%), followed by the FD acupuncture group (53.39%) and then followed by the FD model group (41.54%), which confirmed the results of previous research, indicating that EA treatment using the combination of RN-12 and BL-21 acupoints improves gastric motility [21]. Interestingly, despite previous research by Li et al., which showed that EA at RN-12 tended to suppress gastric motility in human subjects when used by itself [34], our results showed that the opposite was true. We hypothesize that the difference in outcome may be related to the synergistic effects of the BL-21 and RN-12 acupoint combination, as opposed to just using the RN-12 acupoint by itself.

In the brain imaging process, we conducted a seed-based functional connectivity analysis of the FD model and FD acupuncture groups after EA intervention, establishing the insula as ROI.

3.6.1. Functional Connections in FD Model Group and Comparisons to Previous Results. In the FD model group, significantly decreased functional connections were found only in the following brain regions: S1, CA3, THa, Ect, PoDG, MPtA, V1, and TeA, which bear both similarities and contrasts to previous results. Our results are similar to previous findings that indicate abnormal functional connections found between insula and S1, hippocampal CA3, and PoDG regions. In a systematic review of sixteen studies

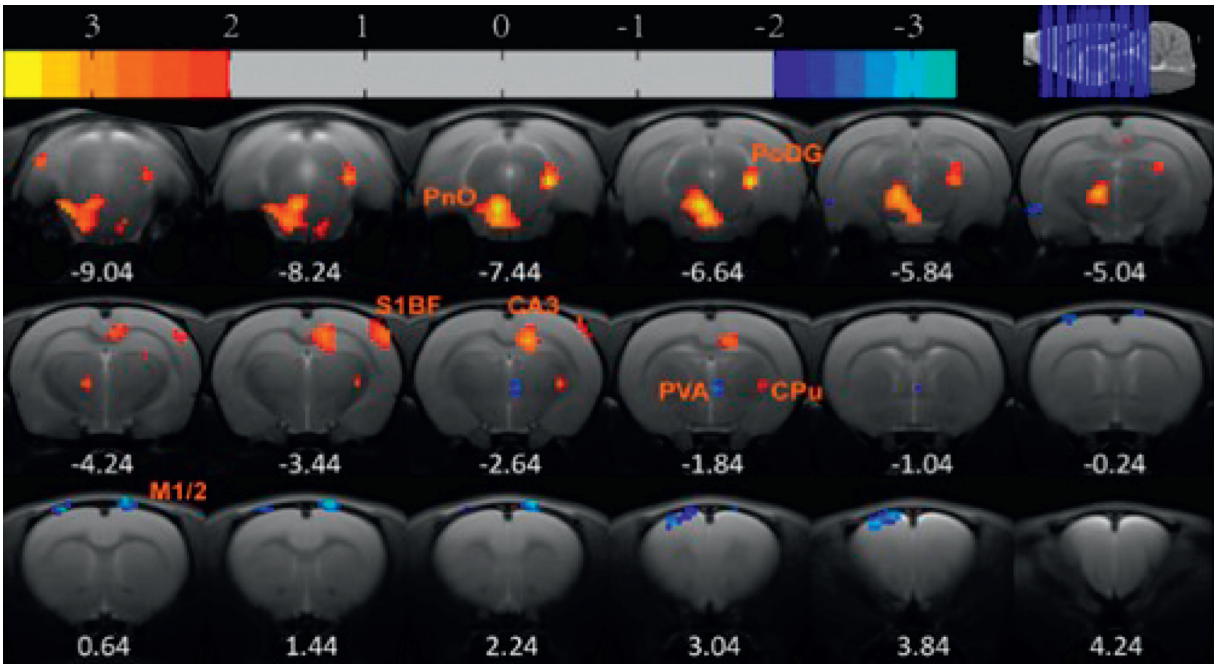

Figure 9: Regions exhibiting significant functional connections with the insula, FD model group after EA intervention.

of FD patient brain activity by Lee et al., abnormal brain activity was frequently found in several areas across resting-state FD patients, including the insula, hippocampus, S1, prefrontal cortex, anterior cingulate cortex, and amygdala [32].

Activation in S1 has been reported in the literature previously. In a PET-CT study on FD patients by Zeng et al., S1 activity was shown in FD patients treated with acupuncture, though not in FD model patients [10]. Similar results were observed in a review by Lee et al. in terms of functional abnormalities of FD patients in several brain regions including S1 [32]. Findings from the same review also indicate that the temporal lobe and S1 were commonly activated during simulated distension of FD rat models using balloons [32]. Since one of the main symptoms of FD is epigastric pain, which may be accompanied by distension, the activation of S1 in our results could be interpreted as another measure of FD modeling success.

Both CA3 and PoDG are located within the hippocampus, and previous results in an $H_2{}^{15}O$ PET study by Van et al. have shown that the hippocampus is activated in resting-state FD patients with history of physical abuse [35]. Another FD study reported that mRNA expression of GHS-R in hippocampus increased in the EA group compared with the model group [36]. In our study, the tail clamping and irregular feeding phases have been shown to create stress in rats and could have contributed to similar activation in the hippocampus.

Similar to the decreasing functional connections found between insula and THa within our results, a previous fMRI study of FD patients with acupuncture intervention by Liu et al. also found decreased functional connectivity in the right THa with the right anterior insula in resting-state FD patients [9]. An ^{18}F-FDG PET-CT study by Zeng et al. showed deactivating THa activity in FD patients treated with acupuncture but not in resting state [8]. However, the discrepancies in THa activity were also observed by Liu et al. in another study investigating neural patterns in FD patients without acupuncture intervention, while their explanation for the differences was that dysfunctions in visceral sensory pathway can affect the "switchboard" ability of the THa to coordinate multiple actions [14]. Likewise, similar discrepancies exist for the decreasing functional connections for the TeA region found in our study compared to results of previous studies. The aforementioned fMRI study with acupuncture intervention by Liu et al. found decreased functional connectivity of the right anterior insula with right THa, and FD patients had negative correlation between disease duration and the functional connectivity of right anterior insula with THa [9]. However, another fMRI study by Fang et al. showed activity in the inferior temporal gyrus in FD patients prior to acupuncture treatment [13], while the neural pattern study by Liu et al. found resting-state activity in both the THa and temporal pole [14]. The explanation of discrepancies by Liu et al. in their neural pattern study was that the temporal pole was related to the neuropsychological mechanism of emotion in FD patients and that patients with different disease durations could exhibit differing activity in this region [14]. In our study, the duration of disease was uniform among the FD model and FD acupuncture groups, leading us to reject the disease duration explanation for rat models. Instead, we believe that the activation of the TeA region in our results may be due to recall of fear in the rat models, as suggested by Cho et al. in their study on activation of the TeA from remote recall of fear [37].

Activities in V1, MPtA, and ectorhinal regions from our results were not observed in other studies. Increasing functional connectivity in V1 had been observed in a previous fMRI study of healthy subjects treated via acupuncture by Dhond et al., although their study did not focus on FD patients [38]. The MPtA region has been shown to be associated with the processing of spatial tasks in rats [39]. Furthermore, the ectorhinal complex has been shown to relate to the freezing of movements in conditioned fear in rats [40], and its activation may be due to similar reasons as our proposed explanation of TeA activation. Due to limited availability of research, further study of these brain regions is required.

3.6.2. Functional Connections in FD Acupuncture Group and Comparisons to Previous Results. In the FD acupuncture group, a different pattern of both significantly increasing and decreasing functional connections is seen in the following brain regions: left and right M1/2, PVA, CPu, S1BF, CA3, PRh, PnO, and PoDG.

In contrast to the FD model group, functional connections increased between the insula and the regions of S1, hippocampal CA3, and PoDG. Changes in these same regions were found in one study reviewed by Lee et al., indicating that brain activity increased in S1 but decreased in the insula and hippocampus in FD patients after 20 EA sessions [32]. Besides these similarities, we also noticed differences in comparison to results from another fMRI study by Zeng et al. [8], in which functional connectivity was measured between various ROIs in human FD patients before and after acupuncture treatment, in that they did not find functional connections between the anterior insula and hippocampus regions. The hippocampus brain region was previously shown by Wang et al. to be related to the regulation of gastric motility, as EA of RN-12 and BL-21 resulted in reduction of glutamate and subsequently improved gastric mobility [21]. The specific hippocampal CA3 and PoDG regions not only form part of the hippocampal formation [41] but also are involved in memory [38, 42, 43], production of new neurons after injury [44], the healing of physical trauma [45], and the remodeling of synapses after injury, all of which are functions that may help explain the treatment efficacies of EA or acupuncture towards FD. We attribute the discrepancies between our results and those of Fang et al. to differences in methodology, including different acupuncture points used, and differences in manual acupuncture versus EA. Furthermore, our findings would appear to suggest that abnormal functional connections between the insula and the hippocampal CA3 and PoDG regions form part of the mechanism which EA regulates in treating FD.

With regard to increased functional connectivity between the insula and CPu, S1BF, and PnO regions, research has shown that functional connections decreased between the insula and CPu in alcohol-dependent rats going through early withdrawal [46]. Both the insula and S1BF have also been shown to belong to the circuit which regulate gustatory information [47], and connections between the insula and PnO are yet to be explored, with more research required in these areas overall.

In contrast to the FD model group, functional connections decreased in the regions of left and right M1/M2, PVA, and PrH. PVA of the hypothalamus region is of particular interest, as previous studies, including a PET-CT brain imaging study by Zeng et al., have shown that the hypothalamus, insula, and ACC have been considered as key regions of the brain-gut axis [8] and that activations of these areas have been shown in studies for most gastrointestinal diseases [48]. The hypothalamus PVA has been shown in previous studies to play a role on its own in the regulation of appetite through the release of Neuropeptide Y (NPY) [49, 50], as well as in the regulation of thirst [51]. Functional connections between the insula and PVA were not exhibited in the FD model group but were exhibited in the FD acupuncture group. Therefore, the connection between insula and PVA may be part of the mechanism which improves food and water intake as part of acupuncture treatment of FD. Together with the results related to the hippocampus region discussed earlier in this paper, our results suggest that functional connections between the insula and the CA3, PoDG, and PVA regions are regulated through EA treatment in FD.

The functional connection results of the FD model (Table 1) and FD acupuncture groups (Table 2) indicate that different brain regions are activated in the two groups and that the only common active regions in the two groups are CA3 and PoDG of the hippocampus. Even though the importance of the CA3 and PoDG regions had been discussed earlier in this section, the observation of differing brain regions between two groups warrants attention. While it may be simple to hypothesize that the functional connections between the insula and brain regions in FD model patients would be reversed after EA intervention, both our results and those of prior studies have shown that this is not the case. One reason for this difference may be due to the way that compensatory strategies are used in healing of the brain. Hylin et al. examine the healing of brain injuries in their review and suggest that the brain is able to intrinsically react to change by inducing new growth pathways which help neurons near and distant from the affected area to survive, repair, and form new connections in order to achieve compensation or recovery [52]. Likewise, it is possible that EA intervention in our FD acupuncture group could contribute to a similar effect through compensation, thus resulting in the differences in brain regions, and this could be an area of research for future studies.

3.6.3. Limitations. With regard to limitations, although our results indicated functional connections between the insula and different brain areas in FD rats using fMRI technology, they do not provide insight into chemical composition of the definite pathways between the insula and these brain regions. This latter consideration was outside the scope of our current study, and so we did not include it in our submission but is part of ongoing trials in our research group. In order to further explore the key role of the insula in the central mechanism behind EA efficacy of gastrointestinal regulation, our research group used the same method of FD rat

modeling for analysis and concentrations of important metabolites in the insula between control, FD model, and FD acupuncture groups through magnetic resonance spectroscopy (MRS) instead of fMRI, so as to analyze the chemical composition of our suggested central mechanism [53]. The results from Long showed that, after EA treatment using stomach front-mu and back-shu points, concentrations of N-acetylaspartate (NAA), aspartic acid (Asp), and glycine (Gly) decreased significantly. These results suggest changes in chemical composition of the insula in FD rats after EA treatment and serve as a preliminary investigation into the chemical composition of the insular pathway in the treatment of FD.

4. Conclusions

In conclusion, our study aimed to explore the role of the insula in the EA treatment of FD through rs-fMRI seed-based functional connectivity analysis. The results showed the following: (a) in our two-phase multiple feature rat FD models created using iodoacetamide-sucrose administration, tail clamping, and irregular feeding, EA intervention using RN-12 and BL-21 successfully improved several measures in our rat FD models, including general observations, increased food and water intake, and improved gastric motility and, (b) after EA intervention, a number of both increasing and decreasing functional connections were seen between the insula and a number of brain regions, in particular the hippocampal CA3 and PoDG regions which are related to injury healing, and the hypothalamus PVA region which regulates thirst and appetite, and these may be parts of the central mechanism through which EA expresses its efficacy in the treatment of FD. One significant question raised in our study is that although the insula was shown to play a role in EA treatment of FD, both the magnitude and exclusiveness of its role are unknown. A potential subsequent step in this area of research would be to try and determine the magnitude and exclusivity of the role of the insula by blocking insular cortex function in rat FD models and then observing whether there are changes in the efficacy of EA intervention to see whether other action mechanisms are at work.

Data Availability

The data used to support the findings of this study are available from the corresponding author upon request.

Conflicts of Interest

The authors declare no conflicts of interest.

Authors' Contributions

Yuan Chen, Ying Zhao, and Robert Yu-Sheng Tan contributed equally to this work. Yuan Chen, Ying Zhao, and Robert Yu-Sheng Tan designed the study. Hua-bin Zheng was responsible for the planning of the statistical analysis. Yuan Chen, Ying Zhao, and Robert Yu-Sheng Tan wrote the first draft of the manuscript. Tao Long, Pu-yue Zhang, and Yu Shi designed and completed the whole animal experiment. All authors participated in the revision, reading, and approval of the submitted version.

Acknowledgments

This paper was financially supported by National Natural Science Fund of China Youth Foundation Project (no. 81603707) and Chengdu University of TCM "Xinglin Scholar" Disciplinary Talent Plan (no. 030041102) and the authors are grateful to them.

References

[1] Y. Guo, W. Wei, and J. D. Chen, "Effects and mechanisms of acupuncture and electroacupuncture for functional dyspepsia: a systematic review," *World Journal of Gastroenterology*, vol. 26, no. 19, pp. 2440–2457, 2020.

[2] S. Mahadeva and K.-L. Goh, "Epidemiology of functional dyspepsia: a global perspective," *World Journal of Gastroenterology*, vol. 12, no. 17, pp. 2661–2666, 2006.

[3] J. Tack, R. Bisschops, and G. Sarnelli, "Pathophysiology and treatment of functional dyspepsia," *Gastroenterology*, vol. 127, no. 4, pp. 1239–1255, 2004.

[4] B. E. Lacy, N. J. Talley, G. R. Locke et al., "Review article: current treatment options and management of functional dyspepsia," *Alimentary Pharmacology & Therapeutics*, vol. 36, no. 1, pp. 3–15, 2012.

[5] E. C. Nista, M. Candelli, F. Cremonini et al., "Bacillus clausii therapy to reduce side-effects of anti-helicobacter pylori treatment: randomized, double-blind, placebo controlled trial," *Alimentary Pharmacology & Therapeutics*, vol. 20, no. 10, pp. 1181–1188, 2004.

[6] S. M. Wilhelm, R. G. Rjater, and P. B. Kale-Pradhan, "Perils and pitfalls of long-term effects of proton pump inhibitors," *Expert Review of Clinical Pharmacology*, vol. 6, no. 4, pp. 443–451, 2013.

[7] B. Pang, T. Jiang, Y.-H. Du et al., "Acupuncture for functional dyspepsia: what strength does it have? A systematic review and meta-analysis of randomized controlled trials," *Evidence-based Complementary and Alternative Medicine*, vol. 2016, Article ID 3862916, 17 pages, 2016.

[8] F. Zeng, W. Qin, T. Ma et al., "Influence of acupuncture treatment on cerebral activity in functional dyspepsia patients and its relationship with efficacy," *American Journal of Gastroenterology*, vol. 107, no. 8, pp. 1236–1247, 2012.

[9] P. Liu, Y. Fan, Y. Wei et al., "Altered structural and functional connectivity of the insula in functional dyspepsia," *Neuro-Gastroenterology and Motility*, vol. 30, no. 9, Article ID e13345, 2018.

[10] F. Zeng, W. Z. Song, X. G. Liu et al., "Brain areas involved in acupuncture treatment on functional dyspepsia patients: a PET-CT study," *Neuroscience Letters*, vol. 456, no. 1, pp. 6–10, 2009.

[11] Y. Ye, X. R. Wang, Y. Zheng et al., "Choosing an animal model for the study of functional dyspepsia," *Canadian Journal of Gastroenterology & Hepatology*, vol. 2018, Article ID 1531958, 13 pages, 2018.

[12] F. Zeng, W. Qin, F. Liang et al., "Abnormal resting brain activity in patients with functional dyspepsia is related to symptom severity," *Gastroenterology*, vol. 141, no. 2, pp. 499–506, 2011.

[13] J. Fang, D. Wang, Q. Zhao et al., "Brain-gut axis modulation of acupuncture in functional dyspepsia: a preliminary resting-state fcMRI study," *Evidence-Based Complementary and Alternative Medicine*, vol. 2015, Article ID 860463, 11 pages, 2015.

[14] P. Liu, W. Qin, J. Wang et al., "Identifying neural patterns of functional dyspepsia using multivariate pattern analysis: a resting-state FMRI study," *PLoS One*, vol. 8, no. 7, Article ID e68205, 2013.

[15] G. Zhou, P. Liu, J. Wang et al., "Fractional amplitude of low-frequency fluctuation changes in functional dyspepsia: a resting-state fMRI study," *Magnetic Resonance Imaging*, vol. 31, no. 6, pp. 996–1000, 2013.

[16] L. Q. Uddin, J. S. Nomi, B. Hébert-Seropian, J. Ghaziri, and O. Boucher, "Structure and function of the human insula," *Journal of Clinical Neurophysiology*, vol. 34, no. 4, pp. 300–306, 2017.

[17] L. Yi, H. Sun, C. Ge et al., "Role of insular cortex in visceral hypersensitivity model in rats subjected to chronic stress," *Psychiatry Research*, vol. 220, no. 3, pp. 1138–1143, 2014.

[18] S.-I. Ito, "Visceral region in the rat primary somatosensory cortex identified by vagal evoked potential," *The Journal of Comparative Neurology*, vol. 444, no. 1, pp. 10–24, 2002.

[19] H. Wang, G.-M. Shen, W.-J. Liu, S. Huang, and M.-T. Zhang, "The neural mechanism by which the dorsal vagal complex mediates the regulation of the gastric motility by Weishu (RN12) and zhongwan (BL21) stimulation," *Evidence-Based Complementary and Alternative Medicine*, vol. 2013, Article ID 291764, 7 pages, 2013.

[20] H. Wang, W.-J. Liu, G.-M. Shen, M.-T. Zhang, S. Huang, and Y. He, "Neural mechanism of gastric motility regulation by electroacupuncture at RN12 and BL21: a paraventricular hypothalamic nucleus-dorsal vagal complex-vagus nerve-gastric channel pathway," *World Journal of Gastroenterology*, vol. 21, no. 48, pp. 13480–13489, 2015.

[21] H. Wang, W.-J. Liu, M.-J. Hu, M.-T. Zhang, and G.-M. Shen, "Acupuncture at gastric back-shu and front-mu acupoints enhances gastric motility via the inhibition of the glutamatergic system in the Hippocampus," *Evidence-Based Complementary and Alternative Medicine*, vol. 2020, Article ID 3524641, 10 pages, 2020.

[22] T.-H. Ren, J. Wu, D. Yew et al., "Effects of neonatal maternal separation on neurochemical and sensory response to colonic distension in a rat model of irritable bowel syndrome," *American Journal of Physiology-Gastrointestinal and Liver Physiology*, vol. 292, no. 3, pp. G849–G856, 2007.

[23] Z. Wu, X. Lu, S. Zhang, and C. Zhu, "Sini-san regulates the NO-cGMP-PKG pathway in the spinal dorsal horn in a modified rat model of functional dyspepsia," *Evidence-Based Complementary and Alternative Medicine*, vol. 2020, Article ID 3575231, 11 pages, 2020.

[24] C. Zhu, L. Zhao, and J. Zhao, "Sini San ameliorates duodenal mucosal barrier injury and low-grade inflammation via the CRF pathway in a rat model of functional dyspepsia," *International Journal of Molecular Medicine*, vol. 45, no. 1, pp. 53–60, 2020.

[25] L. S. Liu, J. H. Winston, M. M. Shenoy, G. Q. Song, J. D. Z. Chen, and P. J. Pasricha, "A rat model of chronic gastric sensorimotor dysfunction resulting from transient neonatal gastric irritation," *Gastroenterology*, vol. 134, no. 7, pp. 2070–2079, 2008.

[26] H. Li, Q. Liang, Y. Yan et al., "Evaluation of a modified rat model for functional dyspepsia," *Saudi Journal of Gastroenterology*, vol. 24, no. 4, pp. 228–235, 2018.

[27] Y. Yang, P. Xu, Y. Xin, Z. Kang, H. Zhang, and L. Zhou, "Involvement of neurotensin-mediated brain-gut Axis in electroacupuncture intervention induced improvement of functional dyspepsia in rats," *Zhenciyanjiu*, vol. 41, no. 1, pp. 35–39+50, 2016.

[28] M. Ling, C. Li, and Y. Ba, "Effect of Baoshen No.1 cataplasm on ET-1 in rats with chronic renal failure," *Hubei Journal of traditional Chinese medicine*, vol. 35, no. 1, pp. 22-23, 2013.

[29] B. Nie, J. Hui, L. Wang et al., "Automatic method for tracing regions of interest in rat brain magnetic resonance imaging studies," *Journal of Magnetic Resonance Imaging*, vol. 32, no. 4, pp. 830–835, 2010.

[30] J. Francis, D. Critchley, C. T. Dourish, and S. J. Cooper, "Comparisons between the effects of 5-HT and DL-fenfluramine on food intake and gastric emptying in the rat," *Pharmacology, Biochemistry, and Behavior*, vol. 50, no. 4, pp. 581–585, 1995.

[31] I. U. Asuzu and J. C. Njoku, "The pharmacological properties of the ethanolic root extract of Combretum dolichopetalum," *Phytotherapy Research*, vol. 6, no. 3, pp. 125–128, 2010.

[32] I.-S. Lee, H. Wang, Y. Chae, H. Preissl, and P. Enck, "Functional neuroimaging studies in functional dyspepsia patients: a systematic review," *Neuro-Gastroenterology and Motility*, vol. 28, no. 6, pp. 793–805, 2016.

[33] S. Zhang, L. Lin, W. Liu et al., "Shen-Ling-Bai-Zhu-San alleviates functional dyspepsia in rats and modulates the composition of the gut microbiota," *Nutrition Research*, vol. 71, pp. 89–99, 2019.

[34] H. Li, T. He, Q. Xu et al., "Acupuncture and regulation of gastrointestinal function," *World Journal of Gastroenterology*, vol. 21, no. 27, pp. 8304–8313, 2015.

[35] L. Van Oudenhove, J. Vandenberghe, P. Dupont et al., "Regional brain activity in functional dyspepsia: a H215O-PET study on the role of gastric sensitivity and abuse history," *Gastroenterology*, vol. 139, no. 1, pp. 36–47, 2010.

[36] L. Zhou and Y.-p. Cheng, "Effect of electroacupuncture on expression of ghrelin and mRNA expression of its receptor in functional dyspesia rats," *Zhongguo Zhong Xi Yi Jie He Za Zhi*, vol. 36, no. 3, pp. 322–326, 2016.

[37] J.-H. Cho, B. S. Huang, and J. M. Gray, "RNA sequencing from neural ensembles activated during fear conditioning in the mouse temporal association cortex," *Scientific Reports*, vol. 6, no. 1, Article ID 31753, 2016.

[38] R. P. Dhond, C. Yeh, K. Park, N. Kettner, and V. Napadow, "Acupuncture modulates resting state connectivity in default and sensorimotor brain networks," *Pain*, vol. 136, no. 3, pp. 407–418, 2008.

[39] F. Torrealba and J. L. Valdés, "The parietal association cortex of the rat," *Biological Research*, vol. 41, no. 4, pp. 369–377, 2008.

[40] L. Albrechet-Souza, K. G. Borelli, R. C. Almada, and M. L. Brandão, "Midazolam reduces the selective activation of the rhinal cortex by contextual fear stimuli," *Behavioural Brain Research*, vol. 216, no. 2, pp. 631–638, 2011.

[41] D. G. Amaral, H. E. Scharfman, and P. Lavenex, "The dentate gyrus: fundamental neuroanatomical organization (dentate gyrus for dummies)," *Progress in Brain Research*, vol. 163, pp. 3–22, 2007.

[42] M. W. Brown and J. P. Aggleton, "Recognition memory: what are the roles of the perirhinal cortex and hippocampus?" *Nature Reviews Neuroscience*, vol. 2, no. 1, pp. 51–61, 2001.

[43] J. Jin and S. Maren, "Prefrontal-hippocampal interactions in memory and emotion," *Frontiers in Systems Neuroscience*, vol. 9, p. 170, 2015.

[44] A. K. Shetty, M. S. Rao, B. Hattiangady, V. Zaman, and G. A. Shetty, "Hippocampal neurotrophin levels after injury: relationship to the age of the hippocampus at the time of injury," *Journal of Neuroscience Research*, vol. 78, no. 4, pp. 520–532, 2004.

[45] Y. Song, G. X. Han, L. Chen et al., "The role of the hippocampus and the function of calcitonin gene-related peptide in the mechanism of traumatic brain injury accelerating fracture-healing," *European Review for Medical and Pharmacological Sciences*, vol. 21, no. 7, pp. 1522–1531, 2017.

[46] G. Scuppa, S. Tambalo, S. Pfarr, W. H. Sommer, and A. Bifone, "Aberrant insular cortex connectivity in abstinent alcohol-dependent rats is reversed by dopamine D3 receptor blockade," *Addiction Biology*, vol. 25, no. 3, Article ID e12744, 2020.

[47] A. Maffei, M. Haley, and A. Fontanini, "Neural processing of gustatory information in insular circuits," *Current Opinion in Neurobiology*, vol. 22, no. 4, pp. 709–716, 2012.

[48] E. A. Mayer and K. Tillisch, "The brain-gut axis in abdominal pain syndromes," *Annual Review of Medicine*, vol. 62, no. 1, pp. 381–396, 2011.

[49] S. P. Kalra, M. G. Dube, A. Sahu, C. P. Phelps, and P. S. Kalra, "Neuropeptide Y secretion increases in the paraventricular nucleus in association with increased appetite for food," *Proceedings of the National Academy of Sciences*, vol. 88, no. 23, pp. 10931–10935, 1991.

[50] B. A. Newmyer, W. Nandar, R. I. Webster, E. Gilbert, P. B. Siegel, and M. A. Cline, "Neuropeptide Y is associated with changes in appetite-associated hypothalamic nuclei but not food intake in a hypophagic avian model," *Behavioural Brain Research*, vol. 236, no. 1, pp. 327–331, 2013.

[51] D. E. Leib, C. A. Zimmerman, and Z. A. Knight, "Thirst," *Current Biology*, vol. 26, no. 24, pp. R1260–R1265, 2016.

[52] M. J. Hylin, A. L. Kerr, and R. Holden, "Understanding the mechanisms of recovery and/or compensation following injury," *Neural Plasticity*, vol. 2017, Article ID 7125057, 12 pages, 2017.

[53] T. Long, "The study on the metabolites in insula of rats with functional dyspepsia upon the impact of acupuncture," Masters dissertation, Chengdu University of Traditional Chinese Medicine, Acupuncture and Tuina School, Chengdu, China, 2019.